



University of
Stavanger

Faculty of Science and Technology

BACHELOR'S THESIS

Study program/Specialization: Control Engineering and Circuit Design - Bachelor's Degree Programme	Spring semester, 2021 Open
Writers: Gent Luta John Håvard Aarvåg	<i>Gent Luta</i> <i>John Håvard Aarvåg</i> (Writer's signature)
Faculty supervisor: Damiano Rotondo	
Thesis title: <i>Study on the applicability of the Carleman embedding to the control of the water level in a tank.</i>	
Credits (ECTS): 20	
Key words: Control theory Modelling Simulation Programming	Pages: <i>80</i> + enclosure: <i>84</i> Stavanger, <i>15/05-2021</i> Date/year

Acknowledgements

We would like to express our utmost gratitude to our faculty supervisor Assoc.Prof. Damiano Rotondo for his guidance throughout this project. He has been incredibly helpful, always available and very patient with us. We are very lucky to have had such a good supervisor.

Unë do të doja të shprehja mirënjohjen time të sinqertë për familjen time për dashurinë dhe mbështetjen e tyre të pakushtëzuar. Jam i mirënjohës motrës time që ishte gjithmonë aty për mua dhe më brohoriti. Jam i mirënjohës vëllait tim që më dha mësim të vlefshme për jetë. Jam i mirënjohës prindërve të mi që më dhanë mua dhe vëllaut dhe motrës time një jetë të mirë, edhe pse kjo nënkuptonte sakrificat të panumërta. Unë do të jem përgjithmonë mirënjohës.

- Gent Luta

Jeg ønsker å dedikere denne oppgaven til mine nieser og nevøer. Takk til alle mine nærmeste for enorm støtte. En spesiell takk til Ida Marita og Mons, for gode arbeidsforhold under arbeidet med oppgaven.

- John Håvard Aarvåg

Abstract

This thesis presents control design of an approximated dynamical model, which is derived by using the Carleman embedding technique. To perform the Carleman embedding, the nonlinear dynamical model should be expressed in a polynomial form. By using the higher order Taylor approximation, a nonlinear system, if analytical, can be expressed in such a form. Carleman embedding of the *cubic* two-tank model proves to give a compromise between accuracy and computational labour. However, Carleman linearization of this model results in an uncontrollable system. Therefore, controller design for the quadratic Carleman approximation is considered. This controller is a state feedback controller. The process of finding the controller gain \mathcal{K} , can be expressed as an optimization problem in terms of *linear matrix inequalities*. A quadratic controller has to fulfil some necessary constraints to be operational. The main benefit of this type of controller design, is that it ensures stability in the given region that the controller was designed for. However, this controller design leads to poor feasibility, which limits its usefulness in a practical setting.

Sammendrag

Denne avhandlingen presenterer kontrollert design av en estimert dynamisk modell, hvor modellen er utledet ved bruk av teknikken *Carleman embedding*. For å utføre denne teknikken, burde den ikkelineære dynamiske modellen være uttrykt på polynom form. Hvis et ikkelineært system er analytisk, kan det uttrykkes som et polynom ved hjelp av Taylor approksimasjon av høyere orden. Taylor approksimasjonen av orden tre, også kalt *cubic* modell, viser seg å være den best egnede modellen for utføringen av Carleman embedding teknikken. *Carleman linearisering* av denne cubic modellen resulterer i et ukontrollerbart system. Derfor vil kontrollert design for *quadratic Carleman approksimasjonen* bli vurdert. Kontrolleren for dette systemet er basert på tilbakekobling. Prosessen i å finne kontrollert forsterkningen \mathcal{K} kan uttrykkes som et optimaliseringsproblem i form av *linear matrix inequalities*. En slik kontrollert er nødt til å tilfredsstille visse kriterier for å være operasjonell. Hovedfordelen i en slik kontrollert er at den garanterer stabilitet i den regionen som kontrollert ble designet for. Ulempen med denne typen kontrollert design er at numeriske problemer oppstår, som begrenser dens praktiske nytte.

Table of Contents

List of Figures	VI
List of Tables	VII
I Introduction	1
1 Motivation	2
1.1 Introduction	2
1.2 The history of Carleman embedding	3
1.3 Objective	3
2 The two-tank system	5
2.1 Description	5
2.2 Nonlinear model of tank 1	9
2.3 Nonlinear model of tank 2	10
II Modelling using Taylor and Carleman approximations	14
3 Taylor approximations	15
3.1 Taylor series	15
3.1.1 Taylor series in several variables	16
3.2 Taylor models	17
3.2.1 Linear model	17
3.2.2 Quadratic model	19
3.2.3 Partially quadratic models	20
3.2.4 Cubic model	21
3.2.5 Higher order models	22
3.3 Taylor model comparison	23

4	Modelling using the Carleman embedding	33
4.1	Carleman embedding	33
4.1.1	Carleman embedding technique	34
4.1.2	Truncation	34
4.2	Carleman approximation of the cubic tank model	36
4.3	Carleman approximation comparison	38
III	Control	43
5	State feedback control using the linear Carleman approximation	44
5.1	Control	44
5.2	Controllability of the linear Carleman approximation	46
6	State feedback control using the quadratic Carleman approximation	48
6.1	Supplemental theory	48
6.1.1	Polytopes	48
6.1.2	Lyapunov stability criterion	50
6.1.3	State feedback control of nonlinear quadratic systems	52
6.2	Controller for the quadratic Carleman approximation	54
6.3	Controller for the quadratic Carleman approximation using two input variables	58
7	Experimental results	62
7.1	Application of the quadratic controller on to the two-tank system	62
7.2	Analysis of the experimental results	63
IV	Conclusions and future work	65
8	Conclusions	66
9	Future work	67
	Bibliography	69
V	Appendices	71
A	Taylor model comparison for Scenario 2	72

B	Carleman approximation comparison for Scenario 2	77
C	Controller of the quadratic Carleman approximation for Scenario 2	80
D	Experimental results for Scenario 2	85
E	Simulation of the controller designed with a reduced polytope	87
F	MATLAB code and Simulink schemes	89
F.1	<i>totank_main.m</i>	89
F.2	<i>Carleman_lin_ss.m</i>	112
F.3	<i>Carleman_Linearized_func.m</i>	116
F.4	<i>Carleman_NonLinearized_func_2Var.m</i>	117
F.5	<i>Carleman_NonLinearized_func.m</i>	118
F.6	<i>carleman_statespace_2Var.m</i>	118
F.7	<i>carleman_statespace.m</i>	119
F.8	<i>example_file_solver.m</i>	119
F.9	<i>Quadratic_controller.m</i>	119
F.10	<i>Quadratic_system.m</i>	120
F.11	<i>Polytope_figures.m</i>	121
F.12	<i>vert2con.m</i> [11]	121
F.13	<i>EKSEMPEL_CARLEMAN.m</i>	122
F.14	Simulink schemes	124

List of Figures

2.1	This is a schematic sketch of the two-tank processing plant [7].	6
2.2	Simplified version of the schematic sketch with limited functionality [7].	7
2.3	The relation between the control signal and the relative flow through the valve with respect to the maximum capacity [7].	8
2.4	The relation between the control signal and the flow through the pump [7].	9
2.5	Schematic sketch of tank 2 for area calculation [7].	11
2.6	Triangle similarity.	12
3.1	Calculating $\frac{\delta f_1}{\delta u_{LV001}}$ in Simulink.	18
3.2	3-D plot of the nonlinear model.	25
3.3	Level curve representing the operating points of the nonlinear model.	25
3.4	Comparisons between the nonlinear and the Taylor approximation models.	26
3.5	Contour plots of the Taylor models and the nonlinear model, where ζ is given by (3.32).	28
3.6	Color maps comparing the different Taylor models.	29
3.7	Model comparison in Simulink.	31
4.1	Carleman approximations of (4.4) compared to the nonlinear system.	35
4.2	Utilising the State-Space block in Simulink.	38
4.3	Step response with an increment in $u_{LV001}(t)$ of 0.02 at 10 seconds.	39
4.4	$\delta = 0.05m$ gives a starting point of 0.3m.	40
4.5	$\delta = 0.2m$ gives a initial condition of 0.45m.	41
4.6	Simulation of the quadratic Carleman approximations.	42
4.7	Simulation of the quadratic Carleman approximations with a larger step.	42
5.1	Feedback control system [1].	44
6.1	Polytope \mathcal{P} is contained by the blue half-spaces, and represented by the green region.	50

6.2	Polytope for the 2nd order quadratic Carleman approximation.	55
6.3	Simulation of Eq. (6.29), with initial condition equal to $0.05m$	57
6.4	Signal $\delta u_{LV001}(t)$, calculated by $\mathcal{K}z(t)$	57
6.5	4th order quadratic Carleman approximation with two actuator.	59
6.6	Signal $u(t)$, calculated by $\mathcal{K}z(t)$	59
6.7	4th order quadratic Carleman approximation with two actuator and implemented convergence rate.	60
6.8	Signal $u(t)$, calculated by $\mathcal{K}z(t)$ with implemented convergence rate.	61
7.1	Experimental results from the quadratic controller.	63
7.2	Experimental results from the quadratic controller.	64
9.1	Modified polytope.	67
A.1	3-D plots of the Taylor models and the nonlinear model as reference.	73
A.2	Contour plots of the Taylor models and the nonlinear model, where ζ is given by (3.32).	74
A.3	Color maps comparing the different Taylor models.	75
A.4	Model comparison in Simulink.	76
B.1	Step response with an increment in $u_{LV001}(t)$ of 0.02 at 10 seconds.	77
B.2	$\delta = 0.05m$ gives a starting point of 0.8m.	78
B.3	$\delta = 0.2m$ gives a starting point of 0.95m.	78
B.4	Simulation of the quadratic Carleman approximations.	79
B.5	Simulation of the quadratic Carleman approximations with a larger step.	79
C.1	Simulation of Eq. (6.29), with initial condition equal to $0.05m$	80
C.2	Signal $\delta u_{LV001}(t)$, calculated by $\mathcal{K}z(t)$	81
C.3	4th order quadratic Carleman approximation with two actuator.	82
C.4	Signal $u(t)$, calculated by $\mathcal{K}z(t)$	82
C.5	4th order quadratic Carleman approximation with two actuator and implemented convergence rate.	83
C.6	Signal $u(t)$, calculated by $\mathcal{K}z(t)$ with implemented convergence rate.	84
D.1	Experimental results from the quadratic controller.	85
D.2	Experimental results from the quadratic controller.	86

E.1	Simulation of the state $z_1(t)$ for the reduced polytope.	87
E.2	Simulation of the input variables $\delta u_{LV001}(t)$ and $\delta u_{PA001}(t)$ for the reduced polytope.	88

List of Tables

2.1	System instrumentation.	5
2.2	Variables regarding tank 1.	10
2.3	Variables regarding tank 2.	10
2.4	The dimensions of tank 2.	12
3.1	Table presenting the <i>2nd</i> order partial derivatives of the nonlinear function.	19
3.2	Table presenting the <i>3rd</i> order partial derivatives of the nonlinear function.	21
3.3	Operating values for <i>Scenario 1</i> and <i>2</i>	23
3.4	Labels for the different values of ψ	27
3.5	Definition of not applicable points.	27
3.6	Numerical interpretation of the area within the hollow rectangles in Figure 3.6.	30
3.7	Integral performance criteria.	32
4.1	Integral performance criteria of the linearized Carleman approximations, with $\delta = 0.05m$	40
4.2	Integral performance criteria of the linearized Carleman approximations, with $\delta = 0.2m$	41
7.1	Experiment procedure.	63
A.1	Numerical interpretation of the area within the hollow rectangles in Figure A.3	75
A.2	Integral performance criteria.	76

Part I

Introduction

Chapter 1

Motivation

1.1 Introduction

A mathematical model for a system is the equation or the equations that describes the system's behaviour. Based on a mathematical model for a given system, it becomes possible to predict how the system will behave at a given state. A mathematical model that describes the system's *dynamics* is the basis for development of simulations, analysis of the system's stability properties, and the design of processes such as signal filtering and regulatory systems.

Unfortunately, a mathematical model, though very useful, can never describe a physical system with absolute certainty. There will always be aspects of a physical system which cannot be modelled. However, a model that only describes parts of the physical system is still useful, if those parts are the dominant parts of the system's dynamical properties [10].

If a physical system is to be described as accurately as possible by mathematical equations, it is highly probable that one or more of these equations will be nonlinear (differential) equations. Linearizing these nonlinear (differential) equations is a key concept in engineering. This is often done by performing the Taylor linearization on the nonlinear equations.

Transforming a nonlinear system into a linear system enables the applications of simple yet effective design techniques for fulfilling a wide number of tasks. One of these tasks includes controlling the system about an equilibrium point. It is also known, and often stressed, that the quality of the approximation fades the more the nonlinear system steers away from the equilibrium point. The reason for this is that the higher order terms in the Taylor series stop being negligible.

Including higher order terms in the approximated model would provide more precision, in the sense of achieving a better approximation of the nonlinear dynamics. However, this increases the complexity of the control design approach, i.e. Laplace transform and frequency response stop being useful tools. Hence, whether there is any practical advantage in using a nonlinear model, although less nonlinear than the original model, is dubious. The advantages, if any, would probably depend on the system under consideration and the nonlinearities therein included.

A way of mimicking the higher order terms, while still keeping linearity, is to utilize the *Carleman linearization*. This may allow for linear design approaches for the controller design of the system including higher order terms. Whether this method of controller design proves advantageous or not, will be explored in this thesis.

1.2 The history of Carleman embedding

In 1932 Torsten Carleman showed that a finite dimensional system of nonlinear differential equations can be embedded into an infinite system of linear differential equations, an embedding technique known as Carleman embedding. Since then it has been applied to several fields in the last 89 years. The most notable works are mentioned:

- In **1963 Bellman and Richardson** [6] discussed the use of Carleman embedding for approximate solutions of nonlinear differential equations.
- In **1980 Steeb and Wilhelm** [18] explored approximate solutions of Lotka-Volterra models using Carleman embedding.
- In **1989 Steeb** [17] discussed the correspondence between solutions of nonlinear systems and the infinite linear system resulting from the Carleman embedding.
- In **1991 Steeb and Kowalski** [12] wrote the book *Nonlinear Dynamical Systems And Carleman Linearization*, discussing several methods of using the Carleman embedding on nonlinear systems.
- In **2008 Mozyrska and Bartosiewicz** [14] talked about the Carleman embedding of linearly observable polynomial systems.
- In **2009 Rauh and Minisini and Aschemann** [16] discussed the use of Carleman embedding in *Carleman Linearization for Control and for State and Disturbance Estimation of Nonlinear Dynamical Processes*.
- In **2019 Amini, Sun and Motee** [5] discussed another approach for optimizing a controller for a nonlinear system approximated with use of the truncated Carleman embedding.

1.3 Objective

The main objectives in this thesis can be segmented into the following parts:

- Develop a mathematical model that describes the two-tank system's dynamics.
- Develop multiple Taylor approximations of the mathematical model. The Taylor approximations differ in the sense of including a different amount of higher order terms.
- Compare the different Taylor approximations, and select the model that is best suited for the Carleman embedding.
- Perform the Carleman embedding on the best suited Taylor approximation, which results in a *infinite* dimensional nonlinear system. Approximating this system as a *finite* dimensional nonlinear system is deemed as the quadratic Carleman approximation.
- Linearize the quadratic Carleman approximation, resulting in the linearized Carleman approximation.
- Design a controller for the linearized Carleman approximation.
- Design a controller for the quadratic Carleman approximation.

The above-mentioned objectives will be reached by using the model of the two-tank process available in the room KE E-459, and some results will be obtained using extensive simulations in MATLAB and, possibly, experimental validation.

The *learning objectives* related to this thesis are:

- Learn how to perform the Carleman linearization of a nonlinear system.
- Get a first contact with design approaches for nonlinear systems.
- Learn how available toolboxes/solvers for linear matrix inequalities can be applied to control problems.

Chapter 2

The two-tank system

The theoretical results described in this report are applied to the two-tank process plant located at the University of Stavanger in the room KE E-459. In Section 2.1, the two-tank processing plant is described in detail. Section 2.2 and 2.3 derive the mathematical expressions of the dynamical models for tank 1 and tank 2.

2.1 Description

The process plant consists of two containers, tank 1 and tank 2. Tank 1 has a rectangular shape, whereas tank 2 has a conical shape. Tank 1 has two inlets, one from the pump PA001, and one from the mixer tap LV003, and two outlets, one which goes to the valve FV001 via a hose coil, and one which goes to tank 2 via the valve LV001. There is also a 2kW heating flask HE001 mounted in tank 1, in order to heat up the liquid.

Tank 2 has only one inlet, which is the one that comes from tank 1 via valve LV001. Tank 2 has two outlets, one via the valve FV002, and one via the valve LV002. Both of these outlets lead to the same collection vessel. The liquid in this vessel is the same liquid that gets pumped back into tank 1 by the pump PA001.

The plant is equipped with a variety of instrumentation. Table 2.1 describes the type of instrument, its name code, and purpose. Figure 2.1 shows a schematic sketch of the processing plant.

Type	Code	Purpose
Pressure gauge	PT001	Measures the pressure in the tap water
Temperature meter	TT003	Measures the temperature of the tap water
Temperature meter	TT001	Measures the temperature of tank 1
Level meter	LT001	Measures the level of tank 1
Temperature meter	TT002	Measures the temperature of the water from tank 1 which is delayed through the hose coil
Level meter	LT002	Measures the level of tank 2
Flow meter	FT001	Measures the water flow from the pump PA001

Table 2.1: System instrumentation.

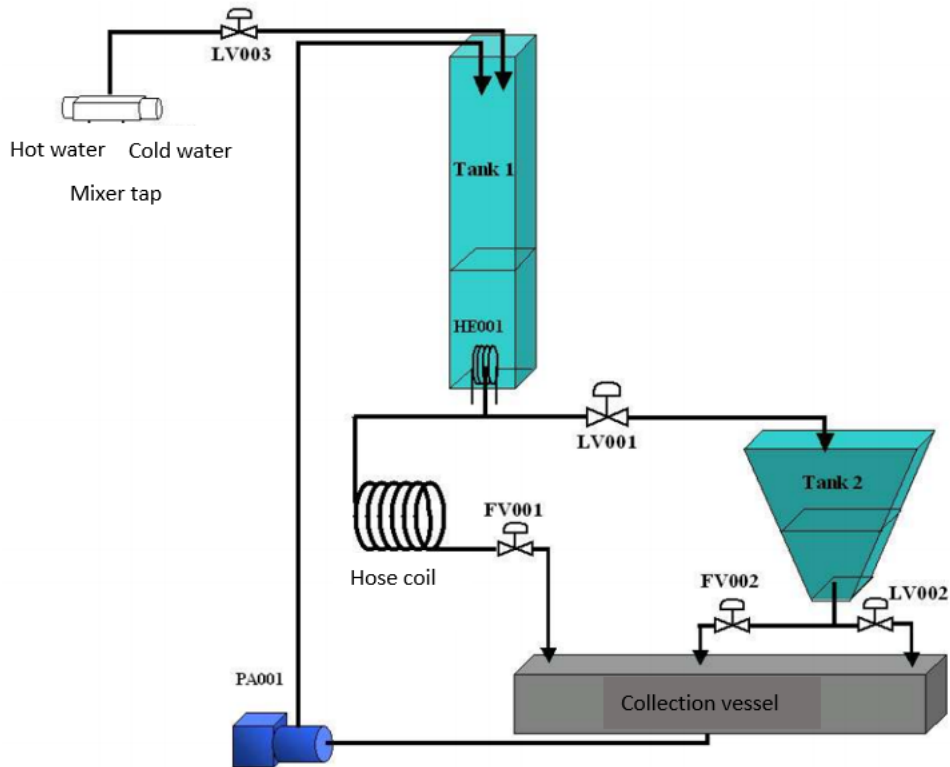


Figure 2.1: This is a schematic sketch of the two-tank processing plant [7].

The processing plant can be used to simulate a number of different industrial scenarios, but this report will use only a setting with limited functions. This means that some of the available functionalities will not be taken into account. This is done such that the complexity of the system is reduced, while the integrity of the verifiability and testing performed on the system is maintained.

The system that is taken into account when calculating a dynamical model, contains tank 1 and 2, the pump PA001, valve LV001, valve LV002 and the collection vessel. The instruments that will be used are FT001, LT001 and LT002. Figure 2.2 shows a simplified version of the schematic sketch that only includes the parts and instruments that are relevant.

With this configuration, one is able to control the water level of tank 1 via the LV001-valve, and the water level of tank 2 via the LV002-valve. The water pumped into tank 1 via the pump PA001 can also be regulated.

With a defined system and its boundaries, it becomes possible to create a mathematical model of the system. In order to make this mathematical model as accurate as possible, the characteristics of the valves and the pump must be considered. (2.1) is the mathematical model of the valves, it describes the volume flow q [m^3/h] through the valves as a function of the valve constant $K_v[\frac{m^3/h}{\sqrt{bar}}]$, valve opening x and the pressure drop across the valve $\Delta p[bar]$.

$$q(t) = K_v x(t) \sqrt{\Delta p(t)} \quad (2.1)$$

As evident from (2.1), the results have the unit [m^3/h] instead of [m^3/s] for the volume flow. The results from (2.1) will be used later in other calculations, therefore, it is more convenient to have the units in SI format. This means dividing equation (2.1) by 3600.

The system uses compressed air in order to make the valves move. The compressed air enters the lower side of the diaphragm, which opens the valve as the control signal $u(t)$ is increased. This applies for valve LV001 and LV002, and they are therefore regarded as normally closed valves. However,

In other words, these valves will close if the compressed air disappears. This type of actuator usually has 1st order dynamics. However, this can be neglected due to the slower dynamic of the processing plant. The control signal will be the same as the actual valve opening, hence (2.5) can be rewritten as (2.6). The relation between $f(u(t))$ and $u(t)$ is shown in Figure 2.3.

$$f(u(t)) = \frac{e^{u(t)^{1.2}} - 1}{e - 1} \quad (2.6)$$

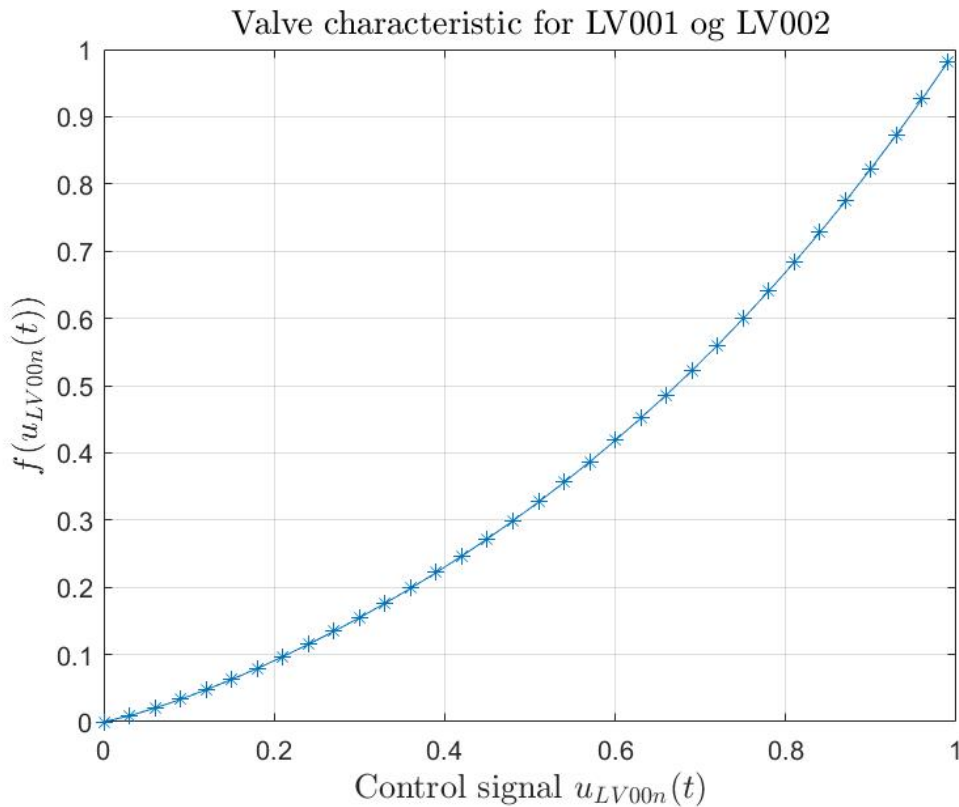


Figure 2.3: The relation between the control signal and the relative flow through the valve with respect to the maximum capacity [7].

With this relation defined, (2.4) can be rewritten as follows:

$$q = \frac{K_v f_n(u_{LV00n}(t))}{3600} \sqrt{\frac{\rho g h(t)}{100000}} \quad (2.7)$$

where $n \in \{1, 2\}$, depending on which valve is considered.

As with the valves, the pump also has nonlinearities between the control signal $u_{PA001}(t)$ and the volume flow through the pump $q_{PA001}(t)$. The characteristics are usually provided by the supplier, but may vary depending on where and how the pump functions under operation. Variables such as pipe resistance and lifting height may affect the characteristics of the pump. Therefore, after the pump is installed, it is required to find the characteristics that apply for the pump in the processing plant. This is done by increasing the control signal incrementally, while also measuring the flow through the pump. Figure 2.4 presents the results of such a work process. The flow through the pump, with respect to the control signal, will be denoted as $f_3(u_{PA001}(t))$.

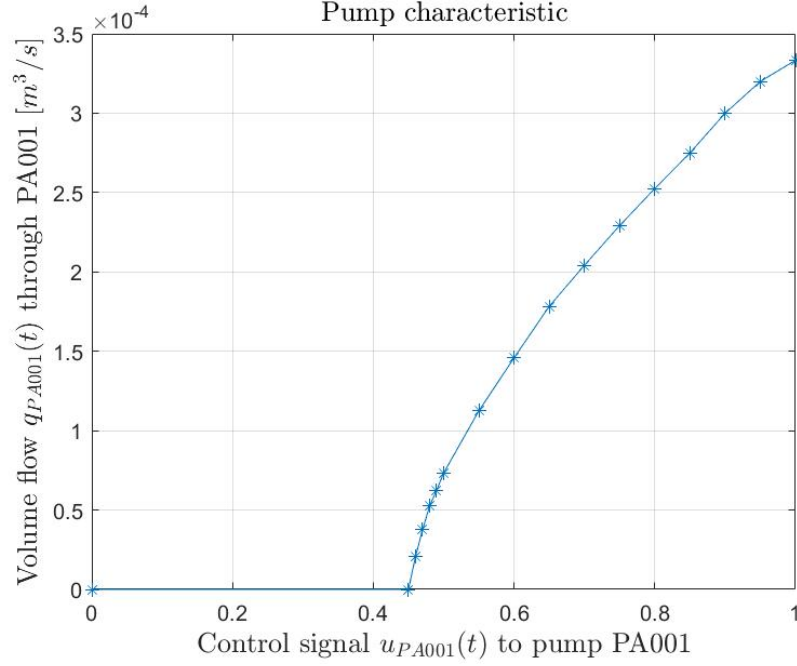


Figure 2.4: The relation between the control signal and the flow through the pump [7].

2.2 Nonlinear model of tank 1

With a restricted system, and the assumptions concerning the dynamics for the valves and the pump, it becomes fairly straightforward to create a dynamical model for the processing plant. The first step in achieving this is to use the balance law, which states the following:

A change in the amount per time in any system is equal to the net amount flow of the system.

The *amount* can be regarded as energy, mass, momentum, charge and also population. Net flow means the sum of all the inflows minus the sum of all the outflows plus the generated amount within the system:

$$\frac{d(\text{amount})}{dt} = \sum In - \sum Out + \sum Generated \quad (2.8)$$

(2.8) results in one or more differential equations. In this case, the *amount* in the balance law is regarded as mass. The following part will derive the dynamical model for tank 1. Table 2.2 provides the relevant information regarding tank 1.

Since the *amount* in this case is mass, (2.8) can be written as (2.9), where m [kg] is the mass, w_i [$\frac{kg}{s}$] is the mass flow, i denotes the different mass flows and t [s] is the time.

$$\frac{dm(t)}{dt} = \sum w_i(t) \quad (2.9)$$

where $m(t) = \rho V(t) = \rho A h(t)$. The mass flows are expressed as:

$$w_{IN}(t) = \rho q_{PA001}(t) = \rho f_3(u_{PA001}(t)) \quad (2.10)$$

$$w_{OUT}(t) = \rho q_{LV001}(t) \quad (2.11)$$

By substituting (2.7) into (2.11), we obtain the following equation:

$$w_{OUT}(t) = \rho \frac{K_v f_1(u_{LV001}(t))}{3600} \sqrt{\frac{\rho g (h_1(t) + h_{LV001})}{100000}} \quad (2.12)$$

where the actual height $h(t)$ in (2.7) is the sum of h_{LV001} and $h_1(t)$.

Given this information the differential equation for the height of tank 1 can be expressed as:

$$\frac{dh_1(t)}{dt} = \frac{1}{A_1} \left(f_3(u_{PA001}(t)) - \frac{K_v f_1(u_{LV001}(t))}{3600} \sqrt{\frac{\rho g (h_1(t) + h_{LV001})}{100000}} \right) \quad (2.13)$$

The reason why the term w_{OUT} is subtracted, is because it represents the mass flow *out* of the system. With (2.13), it becomes possible to describe the behaviour of the system. A mathematical model of any dynamical system is the basis for developing simulations and for analysing the characteristics of the system.

Name	Description	Unit	Value
$h_1(t)$	Water level in tank 1 measured with LT001	m	0-1
A_1	Area for tank 1	m^2	0.0096
ρ	Density of water	$\frac{kg}{m^3}$	1000
$q_{PA001}(t)$	Volume flow from pump PA001	$\frac{m^3}{min}$	0 - 12
$u_{PA001}(t)$	Control signal to pump PA001	-	0 - 1
$q_{LV001}(t)$	Volume flow through LV001	$\frac{l}{min}$	0 - 17
$u_{LV001}(t)$	Control signal to valve LV001	-	0 - 1
$K_{v,LV001}$	Valve constant for valve LV001	$\frac{m^3}{time \sqrt{bar}}$	11.25
h_{LV001}	Height from the bottom of tank 1 down to LV001	m	0.05
$h_{1,utlop}$	Height from the bottom of tank 1 up to the tank outlet	m	0.14
g	Acceleration of gravity	$\frac{m}{s^2}$	9.81

Table 2.2: Variables regarding tank 1.

2.3 Nonlinear model of tank 2

This section will show how to obtain the mathematical model for tank 2. As for tank 1, Table 2.3 is a helpful tool which explains the variables seen in Figure 2.2. Since the procedure is more or less the same as for tank 1, this section will mostly present the mathematical expressions which leads to the differential equation.

Name	Description	Unit	Value
$h_2(t)$	Water level in tank 2 measured with LT002	m	0-0.4
$A_2(h_2(t))$	Area for tank 2 (function of $h_2(t)$)	m^2	0.025 - 0.07
$q_{LV002}(t)$	Volume flow through LV002	$\frac{l}{min}$	0 - 17
$u_{LV002}(t)$	Control signal to valve LV002	-	0 - 1
$K_{v,LV002}$	Valve constant for valve LV002	$\frac{m^3}{time \sqrt{bar}}$	11.25
h_{LV002}	Height from the bottom of tank 2 down to LV002	m	0.25
$h_{2,utlop}$	Height from the bottom of tank 2 up to the tank outlet	m	0.03

Table 2.3: Variables regarding tank 2.

As before, the first step is to set up the balance law, with mass as the amount. The structure is still identical to equation (2.9). As seen in Figure 2.2, the inflow comes from the valve LV001, and the outflow goes to the valve LV002. Recall that these in and outflows need to be regarded as

mass flows in order to fit in (2.9). Equation (2.14) and (2.15) shows the corresponding mass flows to and from the system.

$$w_{IN}(t) = \rho q_{LV001}(t) = \rho \frac{K_v f_1(u_{LV001}(t))}{3600} \sqrt{\frac{\rho g (h_1(t) + h_{LV001})}{100000}} \quad (2.14)$$

$$w_{OUT}(t) = \rho q_{LV002}(t) = \rho \frac{K_v f_2(u_{LV002}(t))}{3600} \sqrt{\frac{\rho g (h_2(t) + h_{LV002})}{100000}} \quad (2.15)$$

Before inserting (2.14) and (2.15) into (2.9), recall also that the mass can be rewritten as a product between the density of the liquid, the area of the tank at a certain height, and the height of the liquid. Doing this results in the following equation:

$$\frac{dh_2(t)}{dt} = \frac{1}{A_2(h_2(t))} \left(\frac{K_v f_1(u_{LV001}(t))}{3600} \sqrt{\frac{\rho g (h_1(t) + h_{LV001})}{100000}} - \frac{K_v f_2(u_{LV002}(t))}{3600} \sqrt{\frac{\rho g (h_2(t) + h_{LV002})}{100000}} \right) \quad (2.16)$$

Note that the area, $A_2(h_2(t))$, is a function of the height $h_2(t)$ due to the conical shape of tank 2. In order to find this function, it is helpful to use the information presented in Figure 2.5 and Table 2.4.

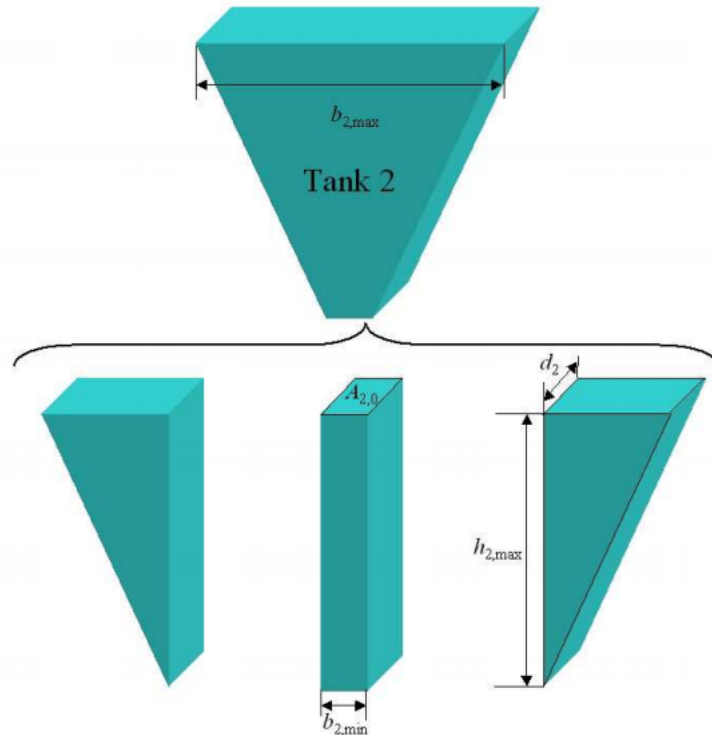


Figure 2.5: Schematic sketch of tank 2 for area calculation [7].

$A_{2,0}$	The area at the bottom of tank 2	0.004 m^2
d_2	Depth of tank 2	0.08 m
$b_{2,max}$	Upper width of tank 2	0.4 m
$b_{2,min}$	Lower width of tank 2	0.05 m
$h_{2,max}$	The height of tank 2	0.4 m

Table 2.4: The dimensions of tank 2.

As shown in Figure 2.5, the conical tank can be segmented into three parts, which consists of two identical right angled prisms and one rectangle shaped prism. The area of the conical tank is given by summing the area of these three segmented parts.

The area of the rectangle shaped prism is already stated in Table 2.3, and it is calculated by multiplying the lower width $b_{2,min}$ and the depth d_2 . This area is always constant and independent of the water level.

The area of the two right angled prisms can be calculated by using the triangle similarity theorem. This theorem entails that if two triangles of different sizes have the same shape, then the ratio between two sides of triangle A is equal to the ratio between the same two sides of triangle B. This is illustrated in Figure 2.6.

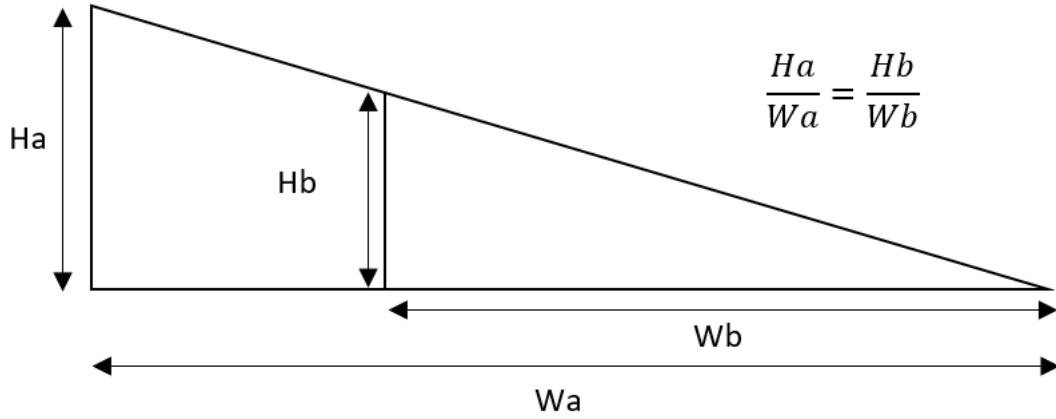


Figure 2.6: Triangle similarity.

In the case of the conical tank, W_a is $h_{2,max}$, W_b is $h_2(t)$ and H_a is given by:

$$H_a = \frac{b_{2,max} - b_{2,min}}{2} \quad (2.17)$$

In order to calculate the area of the right angled prisms, it is desired to multiply the current width H_b with the tanks depth d_2 . However, it is evident from Figure 2.5 that H_b is a function of the height $h_2(t)$. By using the triangular similarities, H_b can be expressed as:

$$H_b(t) = \frac{H_a W_b}{W_a} = \frac{\left(\frac{b_{2,max} - b_{2,min}}{2}\right) h_2(t)}{h_{2,max}} \quad (2.18)$$

which leads to:

$$A_p(t) = \frac{\left(\frac{b_{2,max} - b_{2,min}}{2}\right) h_2(t)}{h_{2,max}} d_2 \quad (2.19)$$

The total area for the conical tank is finally given by:

$$\begin{aligned}
A_2(t) &= 2 A_p + A_{2,0} \\
&= 2 \frac{\left(\frac{b_{2,max} - b_{2,min}}{2}\right) h_2(t)}{h_{2,max}} d_2 + A_{2,0} \\
&= \frac{(b_{2,max} - b_{2,min}) h_2(t)}{h_{2,max}} d_2 + A_{2,0} \\
&= 0.07 h_2(t) + 0.004
\end{aligned} \tag{2.20}$$

Inserting (2.20) into (2.16) gives the final differential equation for tank 2:

$$\begin{aligned}
\frac{dh_2(t)}{dt} &= \frac{1}{0.07 h_2(t) + 0.004} \left(\frac{K_v f_1(u_{LV001}(t))}{3600} \sqrt{\frac{\rho g (h_1(t) + h_{LV001})}{100000}} \right. \\
&\quad \left. - \frac{K_v f_2(u_{LV002}(t))}{3600} \sqrt{\frac{\rho g (h_2(t) + h_{LV002})}{100000}} \right)
\end{aligned} \tag{2.21}$$

This report will focus on the dynamical model for tank 1, see (2.13). Tank 2 will not be considered, however, the dynamical model (2.21) is included as an example and for possible use in future work.

Part II

Modelling using Taylor and Carleman approximations

Chapter 3

Taylor approximations

In this chapter, the nonlinear model:

$$\begin{aligned} \dot{h}_1(t) &= f\left(h_1(t), u_{LV001}(t), u_{PA001}(t)\right) \\ &= \frac{1}{A_1} \left(f_3(u_{PA001}(t)) - \frac{K_v f_1(u_{LV001}(t))}{3600} \sqrt{\frac{\rho g (h_1(t) + h_{LV001})}{100000}} \right) \end{aligned} \quad (3.1)$$

is used as a starting point to obtain approximated models using the truncated Taylor series. This chapter is structured as follows. Section 3.1 summarises the key theoretical concepts related to the Taylor series and its use in approximating nonlinear differential equations. Section 3.2 derives and presents the Taylor approximations of the nonlinear tank model. Section 3.3 compares the obtained models so that a model can be chosen as a starting point for Chapter 4.

3.1 Taylor series

A mathematical pattern of summations can be expressed as a series. For instance $1 + 2 + \dots + n$ can be expressed in the form of the summation $\sum_{i=1}^n i$. The *Taylor series* is indeed based upon the same principles, however, it is an infinite sum of the derivatives of a function at a single point. The definition of a single variable Taylor series is as follows:

$$\sum_{n=0}^{\infty} \frac{f^{(n)}(a)}{n!} (x - a)^n = f(a) + \frac{f'(a)}{1!} (x - a) + \dots \quad (3.2)$$

given that $f(x)$ is infinitely differentiable at a [24].

The Taylor series of an analytic function¹ will be equal to the function itself in the defined area around the point a .

As calculating the infinite sum of a series is not always feasible, an approximation using the finite partial sum is commonly utilised instead. The partial sum of the $n + 1$ first terms of the Taylor series forms the *nth Taylor polynomial* of the function, hereafter referred to as the *nth order Taylor approximation*. It is an approximation which will generally become better as n increases.

¹A function where its Taylor series converges to the function itself at every point in a defined area around the working point.

The Taylor series has several uses in mathematics, with the most relevant to this report being the approximation of the nonlinear differential equation (3.1). Using an approximation can make an otherwise unsolvable, or hard to solve problem, solvable "near" a working point². The n th order Taylor approximation of a n -times differentiable function allows for an approximation, which can be used to compute the functions value numerically. For the Taylor series, the function has to be infinitely differentiable at a , while the truncated version at n only requires that the function is n -times differentiable.

3.1.1 Taylor series in several variables

As we step into multivariable calculus, the Taylor series still applies and is described by:

$$\begin{aligned}
 f(x_1, x_2, \dots, x_d) = & \\
 & f(a_1, \dots, a_d) + \sum_{j=1}^d \frac{\partial f(a_1, \dots, a_d)}{\partial x_j} (x_j - a_j) \\
 & + \frac{1}{2!} \sum_{j=1}^d \sum_{k=1}^d \frac{\partial^2 f(a_1, \dots, a_d)}{\partial x_j \partial x_k} (x_j - a_j)(x_k - a_k) \\
 & + \frac{1}{3!} \sum_{j=1}^d \sum_{k=1}^d \sum_{l=1}^d \frac{\partial^3 f(a_1, \dots, a_d)}{\partial x_j \partial x_k \partial x_l} (x_j - a_j)(x_k - a_k)(x_l - a_l) + \dots
 \end{aligned} \tag{3.3}$$

Consider the following nonlinear differential equation:

$$\frac{dx}{dt} = e^x \sqrt{y}$$

Calculate the 2nd order Taylor approximation around (0,1).

Compute all the necessary partial derivatives:

$$\begin{aligned}
 f_x &= e^x \sqrt{y} \\
 f_y &= \frac{e^x}{2\sqrt{y}} \\
 f_{xx} &= e^x \sqrt{y} \\
 f_{yy} &= -\frac{e^x}{4y^{3/2}} \\
 f_{xy} &= \frac{e^x}{2\sqrt{y}}
 \end{aligned}$$

Evaluate the partial derivatives at (0,1):

$$\begin{aligned}
 f_x(0, 1) &= 1 \\
 f_y(0, 1) &= \frac{1}{2} \\
 f_{xx}(0, 1) &= 1 \\
 f_{yy}(0, 1) &= -\frac{1}{4} \\
 f_{xy}(0, 1) &= \frac{1}{2}
 \end{aligned}$$

²In this context "near a working point" means the operating range around the approximated function where the approximation is adequate.

Inserting the partial derivatives into (3.3) truncated at the 2nd order gives:

$$T(0, 1) = \frac{1}{2}x^2 - \frac{1}{8}y^2 + \frac{1}{2}xy + \frac{1}{2}x + \frac{3}{4}y + \frac{3}{8}$$

3.2 Taylor models

The dynamical model (3.1) will be the starting point for developing the following models. It is easier to perform the *Carleman linearization*, discussed in the next chapter, if the function under consideration is a polynomial. It is evident that (3.1) is not a polynomial. However, by means of the Taylor series, (3.1) can be rewritten as an infinite amount of terms which are polynomials as explained in Section 3.1.

This leads to an intermediate step where (3.1) must be transformed, via the Taylor series, into an equation involving polynomials.

Since the Taylor series describes a function with an infinite amount of terms, it becomes impossible to compute this in any numerical way. A practical solution is to truncate terms at a certain point. This truncation will lead to a numerically computable approximation at the expense of precision.

This section will focus on using the *Taylor approximation* on (3.1), and develop a variety of models where the amount of terms that get truncated will differ. In Section 3.3, these models will be compared to each other, and the most successful³ approximation will become the starting point for the Carleman linearization.

3.2.1 Linear model

As described in Chapter 1, the 1st order Taylor approximation is the most common method used to linearize a system. By applying the concepts presented in Section 3.1, the linearized model can be written as:

$$\delta \dot{h}_1(t) \approx \left. \frac{\partial f}{\partial h_1} \right|_O \delta h_1(t) + \left. \frac{\partial f}{\partial u_{LV001}} \right|_O \delta u_{LV001}(t) + \left. \frac{\partial f}{\partial u_{PA001}} \right|_O \delta u_{PA001}(t) \quad (3.4)$$

where O indicates the partial derivatives in the operating point.

(3.4) is a general equation, where the values of the partial derivatives are yet to be determined. Their values will differ depending on which operating point is selected. Therefore, they will be presented as symbolic functions.

Note that u_{LV001} and u_{PA001} are both independent variables in the functions f_1 and f_3 . Due to this fact, in order to find the partial derivatives $\frac{\partial f}{\partial u_{LV001}}$ and $\frac{\partial f}{\partial u_{PA001}}$, one must take into account the chain rule for derivatives, as follows:

$$\frac{\partial f}{\partial u_{LV001}} = \frac{\partial f}{\partial f_1} \frac{\partial f_1}{\partial u_{LV001}} \quad (3.5)$$

$$\frac{\partial f}{\partial u_{PA001}} = \frac{\partial f}{\partial f_3} \frac{\partial f_3}{\partial u_{PA001}} \quad (3.6)$$

³This report will define a 'successful approximation' as a trade-off between precision and computational labour. If a model is slightly more accurate, but it requires substantially more calculations, then it will be discarded.

The partial derivatives $\frac{\partial f}{\partial f_1}$ and $\frac{\partial f}{\partial f_3}$ are found by straight forward differentiation of the non-linear function (3.1) at the operating point:

$$\left. \frac{\partial f}{\partial f_1} \right|_O = \frac{-K_{v,LV001} \sqrt{\frac{g \rho (h_{1,O} + h_{LV001})}{10^5}}}{3600 A_1} \quad (3.7)$$

$$\frac{\partial f}{\partial f_3} = \frac{1}{A_1} \quad (3.8)$$

The next step is finding the partial derivatives $\frac{\partial f_1}{\partial u_{LV001}}$ and $\frac{\partial f_3}{\partial u_{PA001}}$. These can be found by using the definition of the derivative on the valve and pump characteristics. Note that these will also vary depending on the selected operating point:

$$\left. \frac{\partial f_1}{\partial u_{LV001}} \right|_O = \lim_{\Delta \rightarrow 0} \frac{f_1(u_{LV001,O} + \Delta) - f_1(u_{LV001,O})}{\Delta} \approx \frac{\Delta f_1}{\Delta u_{LV001}} \quad (3.9)$$

$$\left. \frac{\partial f_3}{\partial u_{PA001}} \right|_O = \lim_{\Delta \rightarrow 0} \frac{f_3(u_{PA001,O} + \Delta) - f_3(u_{PA001,O})}{\Delta} \approx \frac{\Delta f_3}{\Delta u_{PA001}} \quad (3.10)$$

Figure 3.1 shows a schematic sketch on how (3.9) is calculated manually, using the valve characteristics in Simulink. The exact same concept applies for (3.10), but the pump characteristics and the input variable u_{PA001} are used instead. In a practical setting, $\Delta \rightarrow 0.01$, instead of $\Delta \rightarrow 0$.

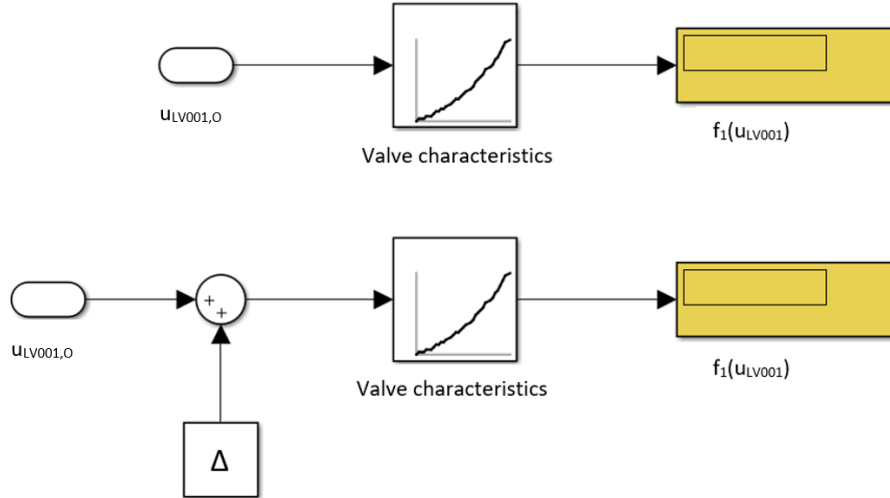


Figure 3.1: Calculating $\frac{\delta f_1}{\delta u_{LV001}}$ in Simulink.

Inserting (3.7)-(3.10) into (3.5)-(3.6) results in the final expressions for the partial derivatives regarding the inputs $u_{LV001}(t)$ and $u_{PA001}(t)$:

$$\left. \frac{\partial f}{\partial u_{LV001}} \right|_O = \frac{-K_{v,LV001} \sqrt{\frac{g \rho (h_{1,O} + h_{LV001})}{10^5}}}{3600 A_1} \frac{\delta f_1}{\delta u_{LV001}} \quad (3.11)$$

$$\left. \frac{\partial f}{\partial u_{PA001}} \right|_O = \frac{1}{A_1} \frac{\delta f_3}{\delta u_{PA001}} \quad (3.12)$$

while the partial derivative $\frac{\partial f}{\partial h_1}$ is given by:

$$\left. \frac{\partial f}{\partial h_1} \right|_O = -\frac{K_{v,LV001} g \rho f_1(u_{LV001,O})}{7.2 \cdot 10^8 A_1 \sqrt{\frac{g \rho (h_{1,O} + h_{LV001})}{10^5}}} \quad (3.13)$$

3.2.2 Quadratic model

Performing the *2nd* order Taylor approximation on the nonlinear function (3.1), results in another approximated model which will be referred to as the *quadratic model*:

$$\begin{aligned} \delta \dot{h}_1(t) = & \left. \frac{\partial f}{\partial h_1} \right|_O \delta h_1(t) + \left. \frac{\partial f}{\partial u_{LV001}} \right|_O \delta u_{LV001}(t) + \left. \frac{\partial f}{\partial u_{PA001}} \right|_O \delta u_{PA001}(t) \\ & + \frac{1}{2} \left. \frac{\partial^2 f}{\partial h_1^2} \right|_O \delta h_1^2(t) + \frac{1}{2} \left. \frac{\partial^2 f}{\partial u_{LV001}^2} \right|_O \delta u_{LV001}^2(t) + \frac{1}{2} \left. \frac{\partial^2 f}{\partial u_{PA001}^2} \right|_O \delta u_{PA001}^2(t) \\ & + \left. \frac{\partial^2 f}{\partial h_1 \partial u_{LV001}} \right|_O \delta h_1(t) \delta u_{LV001}(t) + \left. \frac{\partial^2 f}{\partial h_1 \partial u_{PA001}} \right|_O \delta h_1(t) \delta u_{PA001}(t) \\ & + \left. \frac{\partial^2 f}{\partial u_{LV001} \partial u_{PA001}} \right|_O \delta u_{LV001}(t) \delta u_{PA001}(t) \end{aligned} \quad (3.14)$$

As evident by (3.14), the number of partial derivatives in the *n*th order Taylor approximation increases rapidly. Expanding beyond the quadratic model with a multivariable function results in lengthy equations. Therefore, one can opt to present the same partial derivatives using tables. This is simply done in order to have a more compact notation.

Table 3.1 illustrates this form of notation for the quadratic model. The *f* in each cell is the function that is being derived. In this case, *f* represents the nonlinear function. The subscripts represents what the nonlinear function *f* is being derived with respect to. In this case, $x = h_1$, $y = u_{LV001}$ and $z = u_{PA001}$. Note that Table 3.1 only shows the *2nd* order terms. For the complete quadratic model, these terms comes as an *addition to* the terms found in the linear model.

f_{xx}	f_{xy}	f_{xz}
f_{yx}	f_{yy}	f_{yz}
f_{zx}	f_{zy}	f_{zz}

Table 3.1: Table presenting the *2nd* order partial derivatives of the nonlinear function.

The red cells in Table 3.1 represents the non-zero partial derivatives. The non-zero *2nd* order partial derivatives are as follows:

$$\begin{aligned} & \frac{1}{2!} \left(\left. \frac{\partial^2 f}{\partial h_1^2} \right|_O \delta h_1^2(t) + 2 \left. \frac{\partial^2 f}{\partial h_1 \partial u_{LV001}} \right|_O \delta h_1(t) \delta u_{LV001}(t) \right) = \\ & \frac{1}{2} \left. \frac{\partial^2 f}{\partial h_1^2} \right|_O \delta h_1^2(t) + \left. \frac{\partial^2 f}{\partial h_1 \partial u_{LV001}} \right|_O \delta h_1(t) \delta u_{LV001}(t) \end{aligned} \quad (3.15)$$

Note that $f_{xy} = f_{yx}$.

Since the partial derivatives in (3.15) are only the 2nd order partials, these need to be added to the linear model in order to complete the quadratic model:

$$\begin{aligned} \delta \dot{h}_1(t) = & \frac{\partial f}{\partial h_1} \Big|_O \delta h_1(t) + \frac{\partial f}{\partial u_{LV001}} \Big|_O \delta u_{LV001}(t) + \frac{\partial f}{\partial u_{PA001}} \Big|_O \delta u_{PA001}(t) \\ & + \frac{1}{2} \frac{\partial^2 f}{\partial h_1^2} \Big|_O \delta h_1^2(t) + \frac{\partial^2 f}{\partial h_1 \partial u_{LV001}} \Big|_O \delta h_1(t) \delta u_{LV001}(t) \end{aligned} \quad (3.16)$$

As with the linear model, the following equations only shows the symbolic functions of the 2nd order partial derivatives:

$$\begin{aligned} \frac{\partial^2 f}{\partial h_1^2} \Big|_O &= \frac{K_{V_{LV001}} f_1(u_{LV001}, O) g^2 \rho^2}{1.44 \cdot 10^{14} A_1 \left(\frac{g \rho (h_{1,O} + h_{LV001})}{10^5} \right)^{3/2}} \\ \frac{\partial^2 f}{\partial h_1 \partial f_1} \Big|_O &= - \frac{K_{V_{LV001}} g \rho}{7.2 \cdot 10^8 A_1 \sqrt{\frac{g \rho (h_{1,O} + h_{LV001})}{10^5}}} \\ \frac{\partial^2 f}{\partial h_1 \partial u_{LV001}} \Big|_O &= \frac{\partial^2 f}{\partial h_1 \partial f_1} \frac{\delta f_1}{\delta u_{LV001}} = - \frac{K_{V_{LV001}} g \rho}{7.2 \cdot 10^8 A_1 \sqrt{\frac{g \rho (h_{1,O} + h_{LV001})}{10^5}}} \frac{\delta f_1}{\delta u_{LV001}} \\ \frac{\partial^2 f}{\partial f_1^2} &= \frac{\partial^2 f}{\partial f_3^2} = \frac{\partial^2 f}{\partial h_1 \partial f_3} = \frac{\partial^2 f}{\partial f_1 \partial f_3} = 0 \end{aligned}$$

3.2.3 Partially quadratic models

Before performing the 3rd order Taylor approximation on the nonlinear function, it may be of interest to inspect further the quadratic model. A question that arises is what are the consequences of excluding certain 2nd order terms from the quadratic model. Doing this, will result in a so-called *Partially Quadratic (PQ)* model. As evident by (3.16), there are only two 2nd order terms. This gives the opportunity to create two different *PQ* models.

These two *PQ* models will be referenced using subscripts throughout this report. The subscript A means that the 2nd order term that was *included* is $\frac{\partial^2 f}{\partial h_1^2}$. The subscript B implies that the 2nd order term that was *included* is $\frac{\partial^2 f}{\partial h_1 \partial u_{LV001}}$.

PQ_A :

$$\begin{aligned} \delta \dot{h}_1(t) = & \frac{\partial f}{\partial h_1} \Big|_O \delta h_1(t) + \frac{\partial f}{\partial u_{LV001}} \Big|_O \delta u_{LV001}(t) + \frac{\partial f}{\partial u_{PA001}} \Big|_O \delta u_{PA001}(t) \\ & + \frac{1}{2} \frac{\partial^2 f}{\partial h_1^2} \Big|_O \delta h_1^2(t) \end{aligned} \quad (3.17)$$

PQ_B :

$$\begin{aligned} \delta \dot{h}_1(t) = & \frac{\partial f}{\partial h_1} \Big|_O \delta h_1(t) + \frac{\partial f}{\partial u_{LV001}} \Big|_O \delta u_{LV001}(t) + \frac{\partial f}{\partial u_{PA001}} \Big|_O \delta u_{PA001}(t) \\ & + \frac{\partial^2 f}{\partial h_1 \partial u_{LV001}} \Big|_O \delta h_1(t) \delta u_{LV001}(t) \end{aligned} \quad (3.18)$$

3.2.4 Cubic model

Performing the 3rd order Taylor approximation on the nonlinear function (3.1), results in the following model referred to as the *cubic model*:

$$\begin{aligned} \delta \dot{h}_1(t) = & \frac{\partial f}{\partial h_1} \Big|_O \delta h_1(t) + \frac{\partial f}{\partial u_{LV001}} \Big|_O \delta u_{LV001}(t) + \frac{\partial f}{\partial u_{PA001}} \Big|_O \delta u_{PA001}(t) \\ & + \frac{1}{2} \frac{\partial^2 f}{\partial h_1^2} \Big|_O \delta h_1^2(t) + \frac{\partial^2 f}{\partial h_1 \partial u_{LV001}} \Big|_O \delta h_1(t) \delta u_{LV001}(t) \\ & + \frac{1}{6} \frac{\partial^3 f}{\partial h_1^3} \Big|_O \delta h_1^3(t) + \frac{1}{2} \frac{\partial^3 f}{\partial h_1^2 \partial u_{LV001}} \Big|_O \delta h_1^2(t) \delta u_{LV001}(t) \end{aligned} \quad (3.19)$$

As stated earlier, the amount of partial derivatives in a multivariable n th order Taylor approximation increases rapidly as n increases. The amount of partial derivatives that are *added* to a $(n-1)$ th order Taylor approximation as the order increases to n , is given by d^n , where d is the amount of variables and n is the order of the Taylor approximation of $f(x_1, x_2, \dots, x_d)$.

This implies that increasing the order of the Taylor approximation from 2 to 3 would require $d^n = 3^3 = 27$ partial derivatives, in addition to those calculated for the 2nd order Taylor approximation. This is the case for the nonlinear system, since the amount of variables are equal to three. These *additional* partial derivatives are presented in Table 3.2.

f_{xxx}	f_{xxy}	f_{xxz}	f_{xyx}	f_{xyy}	f_{xyz}	f_{zxx}	f_{zxy}	f_{xzz}
f_{yxx}	f_{yyx}	f_{yxz}	f_{yyx}	f_{yyy}	f_{yyz}	f_{yzx}	f_{yzy}	f_{yzz}
f_{zxx}	f_{zxy}	f_{zxz}	f_{zyx}	f_{zyy}	f_{zyz}	f_{zxx}	f_{zxy}	f_{zxx}

Table 3.2: Table presenting the 3rd order partial derivatives of the nonlinear function.

Note that Table 3.2 only shows the 3rd order partials. As with the quadratic model, the red cells in Table 3.2 represent the non-zero partial derivatives, given by:

$$\begin{aligned} & \frac{1}{3!} \left(\frac{\partial^3 f}{\partial h_1^3} \delta h_1^3(t) + 3 \frac{\partial^3 f}{\partial h_1^2 \partial u_{LV001}} \delta h_1^2(t) \delta u_{LV001}(t) \right) = \\ & \frac{1}{6} \frac{\partial^3 f}{\partial h_1^3} \delta h_1^3(t) + \frac{1}{2} \frac{\partial^3 f}{\partial h_1^2 \partial u_{LV001}} \delta h_1^2(t) \delta u_{LV001}(t) \end{aligned} \quad (3.20)$$

Note that $f_{xxy} = f_{xyx} = f_{yxx}$.

Adding (3.20) to the quadratic model (3.16), results in the cubic model presented in (3.19).

The following equations show the symbolic functions of the non-zero 3rd order partial derivatives:

$$\left. \frac{\partial^3 f}{\partial h_1^3} \right|_O = - \frac{K_{V_{LV001}} f_1(u_{LV001,O}) g^3 \rho^3}{9.6 \cdot 10^{18} A_1 \left(\frac{g \rho (h_{1,O} + h_{LV001})}{100000} \right)^{5/2}} \quad (3.21)$$

$$\left. \frac{\partial^3 f}{\partial h_1^2 \partial u_{LV001}} \right|_O = \left. \frac{\partial^3 f}{\partial h_1^2 \partial f_1} \right|_O \frac{\delta f_1}{\delta u_{LV001}} = \frac{K_{V_{LV001}} g^2 \rho^2}{1.44 \cdot 10^{14} A_1 \left(\frac{g \rho (h_{1,O} + h_{LV001})}{100000} \right)^{3/2}} \frac{\delta f_1}{\delta u_{LV001}} \quad (3.22)$$

3.2.5 Higher order models

The 4th and 5th order Taylor approximations of the nonlinear function proves rather tedious to calculate. For the 5th order approximation, it includes a total of 363 partial derivatives. Presenting these in detail will add little to no value to this report. Therefore, only the final equation for the 4th and 5th order models are presented. The 4th order model is given by:

$$\begin{aligned} \delta \dot{h}_1(t) = & \left. \frac{\partial f}{\partial h_1} \right|_O \delta h_1(t) + \left. \frac{\partial f}{\partial u_{LV001}} \right|_O \delta u_{LV001}(t) + \left. \frac{\partial f}{\partial u_{PA001}} \right|_O \delta u_{PA001}(t) \\ & + \frac{1}{2} \left. \frac{\partial^2 f}{\partial h_1^2} \right|_O \delta h_1^2(t) + \left. \frac{\partial^2 f}{\partial h_1 \partial u_{LV001}} \right|_O \delta h_1(t) \delta u_{LV001}(t) + \frac{1}{6} \left. \frac{\partial^3 f}{\partial h_1^3} \right|_O \delta h_1^3(t) \\ & + \frac{1}{2} \left. \frac{\partial^3 f}{\partial h_1^2 \partial u_{LV001}} \right|_O \delta h_1^2(t) \delta u_{LV001}(t) + \frac{1}{24} \left. \frac{\partial^4 f}{\partial h_1^4} \right|_O \delta h_1^4(t) + \frac{1}{6} \left. \frac{\partial^4 f}{\partial h_1^3 \partial u_{LV001}} \right|_O \delta h_1^3(t) \delta u_{LV001}(t) \end{aligned} \quad (3.23)$$

The 5th order model is given by:

$$\begin{aligned} \delta \dot{h}_1(t) = & \left. \frac{\partial f}{\partial h_1} \right|_O \delta h_1(t) + \left. \frac{\partial f}{\partial u_{LV001}} \right|_O \delta u_{LV001}(t) + \left. \frac{\partial f}{\partial u_{PA001}} \right|_O \delta u_{PA001}(t) \\ & + \frac{1}{2} \left. \frac{\partial^2 f}{\partial h_1^2} \right|_O \delta h_1^2(t) + \left. \frac{\partial^2 f}{\partial h_1 \partial u_{LV001}} \right|_O \delta h_1(t) \delta u_{LV001}(t) + \frac{1}{6} \left. \frac{\partial^3 f}{\partial h_1^3} \right|_O \delta h_1^3(t) \\ & + \frac{1}{2} \left. \frac{\partial^3 f}{\partial h_1^2 \partial u_{LV001}} \right|_O \delta h_1^2(t) \delta u_{LV001}(t) + \frac{1}{24} \left. \frac{\partial^4 f}{\partial h_1^4} \right|_O \delta h_1^4(t) + \frac{1}{6} \left. \frac{\partial^4 f}{\partial h_1^3 \partial u_{LV001}} \right|_O \delta h_1^3(t) \delta u_{LV001}(t) \\ & + \frac{1}{120} \left. \frac{\partial^5 f}{\partial h_1^5} \right|_O \delta h_1^5(t) + \frac{1}{24} \left. \frac{\partial^5 f}{\partial h_1^4 \partial u_{LV001}} \right|_O \delta h_1^4(t) \delta u_{LV001}(t) \end{aligned} \quad (3.24)$$

The reason why the 5th order model has a noticeably lower amount of terms than 363, is because the majority of these partial derivatives result in zero. Whether it is appropriate to consider this model in further research, will be discussed in the next section. The 4th order model is presented for completeness, but will not be further considered.

3.3 Taylor model comparison

This section will analyse the different models obtained in Section 3.2. The models will be compared to each other, and the results of these comparisons will help determine which model is to be used as a starting point for the *Carleman linearization*.

Before we can start the different comparisons, we have to make some general assumptions regarding the different models. As stated in Section 3.2, the different models will vary depending on the chosen operating point. The degree of nonlinearity of tank 1 will differ with the water level, therefore, it makes sense to choose two operating points that are at the lower- and higher end of the tank. By doing this, we can also see if the degree of nonlinearity will have an impact on the results. The operating points for the height are set at $0.25m$ and $0.75 m$. $h_{1,O} = 0.25m$ will be referred to as *Scenario 1*, and $h_{1,O} = 0.75m$ as *Scenario 2*. In order to keep this section tidy, we have decided to present only the results regarding *Scenario 1*. The corresponding results obtained from *Scenario 2* will be presented in Appendix A.

The next assumption is that the pump's behaviour is constant. The control signal $u_{PA001,O} = 0.65$ is therefore set for both *Scenario 1* and *2*. Reading Figure 2.4 at $u_{PA001,O} = 0.65$ gives $f_{3,O} = 0.0001783$. It will be stated explicitly when this assumption is no longer true. Otherwise, the reader can safely assume that the pump is constant at $u_{PA001,O} = 0.65$.

To find the operating point for the valve LV001, we follow this four step process:

1. Set the nonlinear equation (3.1) equal to zero.
2. Insert the chosen operating points $h_{1,O}$ and $f_{3,O}$.
3. Solve the equation with respect to $f_{1,O}$.
4. Insert $f_{1,O}$ into Figure 2.3 in order to find $u_{LV001,O}$.

Obviously, since we are considering two different operating points for the height, this process is done once for each scenario. These results are presented in Table 3.3.

	<i>Scenario 1</i>	<i>Scenario 2</i>
$f_{1,O}$	0.3326	0.2037
$u_{LV001,O}$	0.5159	0.3666
$f_{3,O}$	0.0001783	0.0001783
$u_{PA001,O}$	0.65	0.65
$h_{1,O} [m]$	0.25	0.75

Table 3.3: Operating values for *Scenario 1* and *2*.

The equations and the methods for calculating the different partials are explained in Section 3.2. With these operating points, it becomes possible to write down the corresponding models. The only modification to the nonlinear model (3.1) is that $f_3(u_{PA001}(t))$ is replaced by $f_{3,O} = 0.0001783$:

$$\dot{h}_1(t) = \frac{1}{A_1} \left(0.0001783 - \frac{K_v f_1(u_{LV001}(t))}{3600} \sqrt{\frac{\rho g (h_1(t) + h_{LV001})}{100000}} \right) \quad (3.25)$$

The Taylor models for *Scenario 1* are as follows:

Linear model:

$$\delta \dot{h}_1(t) = -0.0297 (h_1(t) - 0.25) - 0.0525 (u_{LV001}(t) - 0.5159) \quad (3.26)$$

Quadratic model:

$$\begin{aligned} \delta \dot{h}_1(t) = & -0.0297 (h_1(t) - 0.25) - 0.0525 (u_{LV001}(t) - 0.5159) \\ & + 0.0248 (h_1(t) - 0.25)^2 - 0.0876 (h_1(t) - 0.25) (u_{LV001}(t) - 0.5159) \end{aligned} \quad (3.27)$$

PQ_A model:

$$\begin{aligned} \delta \dot{h}_1(t) = & -0.0297 (h_1(t) - 0.25) - 0.0525 (u_{LV001}(t) - 0.5159) \\ & + 0.0248 (h_1(t) - 0.25)^2 \end{aligned} \quad (3.28)$$

PQ_B model:

$$\begin{aligned} \delta \dot{h}_1(t) = & -0.0297 (h_1(t) - 0.25) - 0.0525 (u_{LV001}(t) - 0.5159) \\ & - 0.0876 (h_1(t) - 0.25) (u_{LV001}(t) - 0.5159) \end{aligned} \quad (3.29)$$

Cubic model:

$$\begin{aligned} \delta \dot{h}_1(t) = & -0.0297 (h_1(t) - 0.25) - 0.0525 (u_{LV001}(t) - 0.5159) \\ & + 0.0248 (h_1(t) - 0.25)^2 - 0.0876 (h_1(t) - 0.25) (u_{LV001}(t) - 0.5159) \\ & - 0.0413 (h_1(t) - 0.25)^3 + 0.0730 (h_1(t) - 0.25)^2 (u_{LV001}(t) - 0.5159) \end{aligned} \quad (3.30)$$

5th order model:

$$\begin{aligned} \delta \dot{h}_1(t) = & -0.0297 (h_1(t) - 0.25) - 0.0525 (u_{LV001}(t) - 0.5159) \\ & + 0.0248 (h_1(t) - 0.25)^2 - 0.0876 (h_1(t) - 0.25) (u_{LV001}(t) - 0.5159) \\ & - 0.0413 (h_1(t) - 0.25)^3 + 0.0730 (h_1(t) - 0.25)^2 (u_{LV001}(t) - 0.5159) \\ & + 0.0860 (h_1(t) - 0.25)^4 - 0.1216 (h_1(t) - 0.25)^3 (u_{LV001}(t) - 0.5159) \\ & - 0.2006 (h_1(t) - 0.25)^5 + 0.2534 (h_1(t) - 0.25)^4 (u_{LV001}(t) - 0.5159) \end{aligned} \quad (3.31)$$

Note that every term regarding the pump will result in zero, as $u_{PA001}(t)$ is constant at the operating point. This is given by:

$$\delta u_{PA001}(t) = u_{PA001}(t) - u_{PA001,O} = u_{PA001,O} - u_{PA001,O} = 0$$

Given that Eqs. (3.25)-(3.31) only depend on two variables, it becomes possible to create a 3-D plot that shows combinations of $h_1(t)$ and $u_{LV001}(t)$, and the resulting $\delta \dot{h}_1(t)$. In order to create a 2-D grid with uniformly spaced u_{LV001} -coordinates and h_1 -coordinates in the interval $[0,1]$, we use the `meshgrid`⁴ MATLAB function. Using this 2-D grid as an input in the Eqs. (3.25)-(3.31) results in the matrix ξ for each model. The elements in ξ represent $\delta \dot{h}_1(t)$, while the indices of the columns and rows represent u_{LV001} and h_1 , respectively. Figure 3.2 shows such a 3-D plot for the nonlinear model.

The intersection between the nonlinear model and the u_{LV001} - h_1 plane forms a level curve at $\delta \dot{h}_1(t) = 0$. It represents the operating points of the system. This level curve shows every combination of $h_1(t)$ and $u_{LV001}(t)$, where the system is at an equilibrium point (see Figure 3.3).

⁴Meshgrid

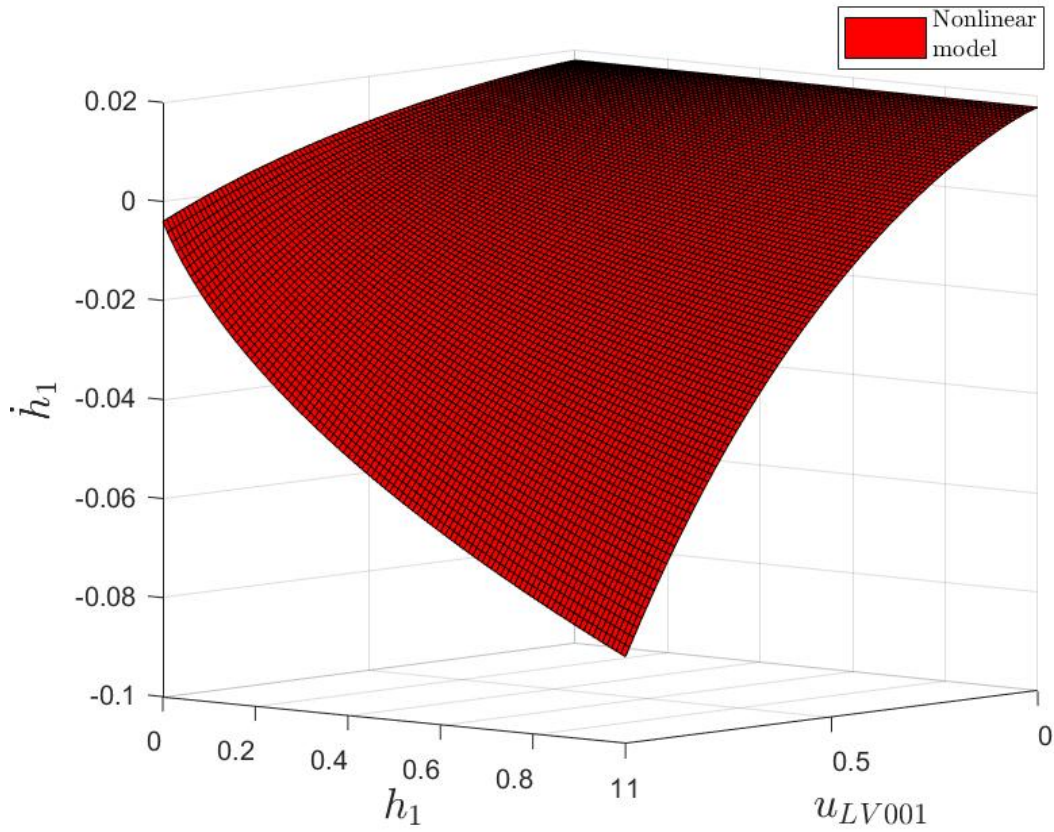


Figure 3.2: 3-D plot of the nonlinear model.

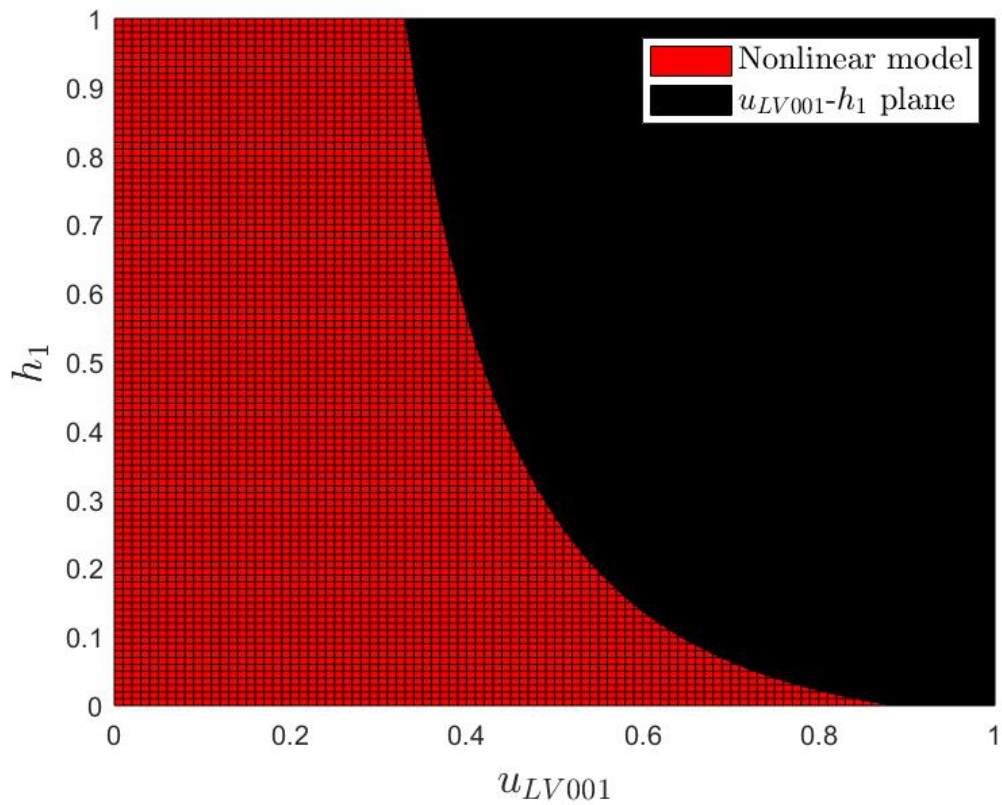
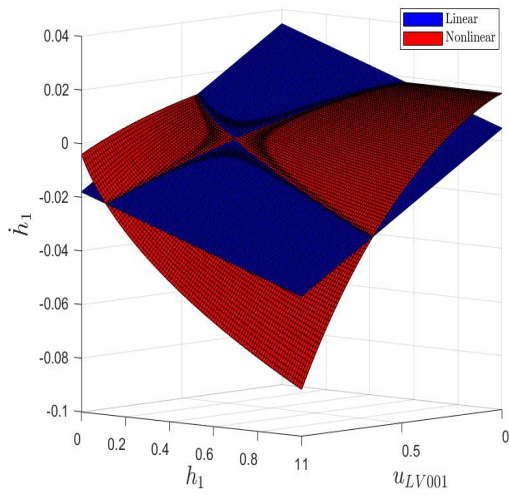
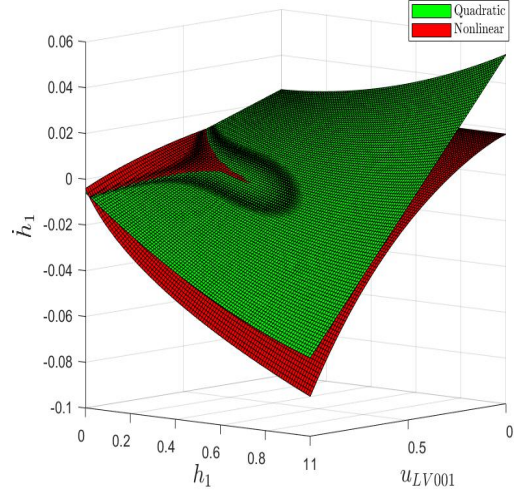


Figure 3.3: Level curve representing the operating points of the nonlinear model.

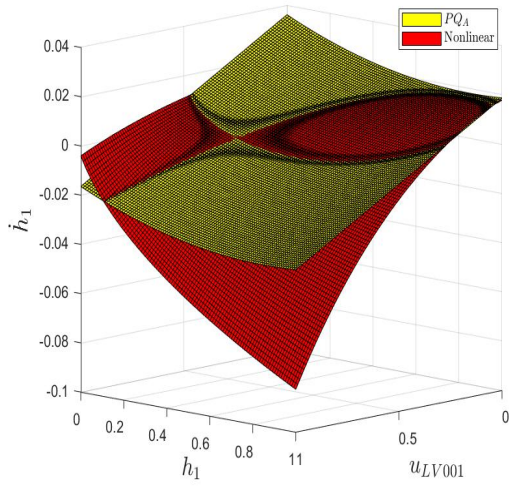
Figure 3.4 shows 3-D plots of the obtained Taylor models, with the nonlinear model as reference.



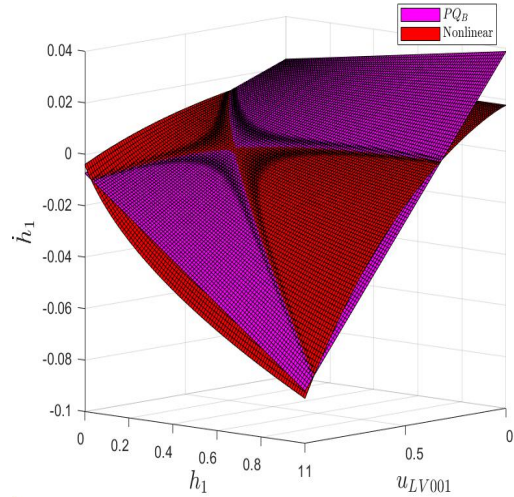
(a) Linear and nonlinear model.



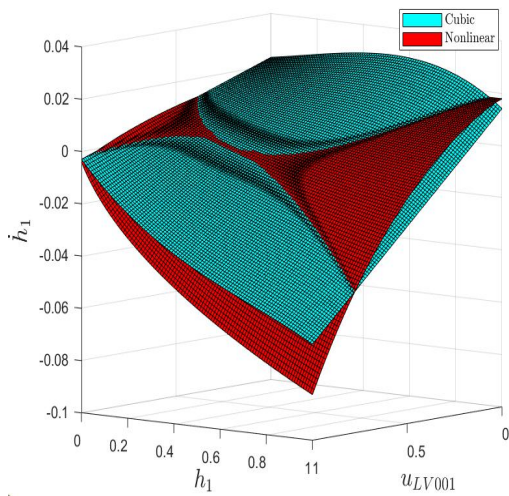
(b) Quadratic and nonlinear model.



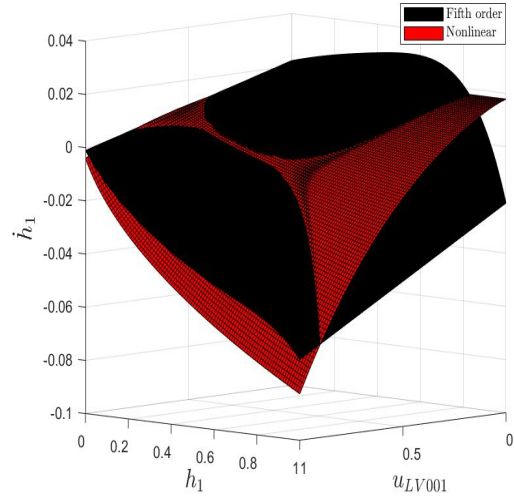
(c) PQ_A and nonlinear model.



(d) PQ_B and nonlinear model.



(e) Cubic and nonlinear model.



(f) 5th order and nonlinear model.

Figure 3.4: Comparisons between the nonlinear and the Taylor approximation models.

The series of Figures 3.4a through 3.4f shows that the Taylor models become more similar to the nonlinear model as the order n of the Taylor approximation increases.

The 3-D plots gives a general idea of how well the models are performing. To be able to quantify the performance of the Taylor models, we use contour plots ⁵, where the height values on the $u_{LV001} - h_1$ plane are given by:

$$\zeta = |\xi_{Nonlinear_model} - \xi_{Taylor_model}| \quad (3.32)$$

Contour plotting ζ provides an intuitive comparison between the nonlinear model and the Taylor model in question. Whether the Taylor models approximates a higher or lower value for $\delta h_1(t)$ than the nonlinear model may be useful information in some cases. However, in this case, we are only interested in the magnitude of the error between our approximations and the nonlinear model. Figure 3.5 presents the contour plots for the different Taylor models.

Figures 3.5a- 3.5f show that the *region* where ζ is close to zero, which means that the Taylor approximation and the nonlinear model are similar, increases as we consider higher order Taylor approximations.

The presented 3-D and contour plot gives the general notion on how a Taylor series approximation represents its original function more accurately as the order of the approximation increases. However, the definition of a successful model in this report was not based on accuracy alone. It is also of interest to know the *degree of improvement* as the Taylor model goes from an n th order to an $(n + 1)$ th order approximation. If this *degree of improvement* is not considered significant enough, then it leads to selecting the final truncation to happen at n .

In order to see how well the models compare, we calculate the difference in the obtained ζ -value for each model, given by:

$$\psi = \zeta_A - \zeta_B \quad (3.33)$$

where the subscripts A and B are used to separate the ζ -value for the models in question. The sign and magnitude of ψ will indicate which model provides a better approximation. Table 3.4 shows how the values of ψ have been considered.

ψ value	Result	Color code
$\psi > 0.005$	B >>	Green
$0.005 > \psi > 0$	B >	Light green
$0 > \psi > -0.005$	A >	Light Blue
$-0.005 > \psi$	A >>	Blue

Table 3.4: Labels for the different values of ψ .

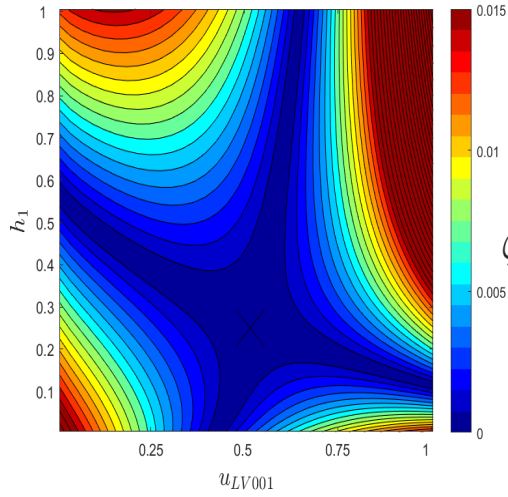
Certain points where both models approximate the nonlinear model poorly are considered non-relevant for the comparison. These occurrences are identified as shown in Table 3.5.

Criteria	Result	Color code
$ \zeta_A > 0.005$ & $ \zeta_B > 0.005$	Not applicable (N/A)	Red

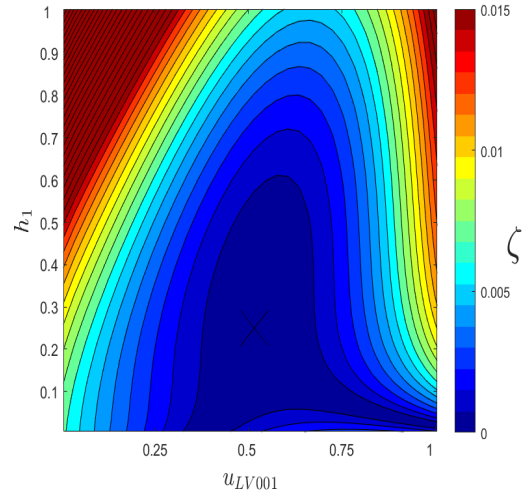
Table 3.5: Definition of not applicable points.

Figure 3.6 shows color maps which uses the color codes given in Table 3.4 and 3.5.

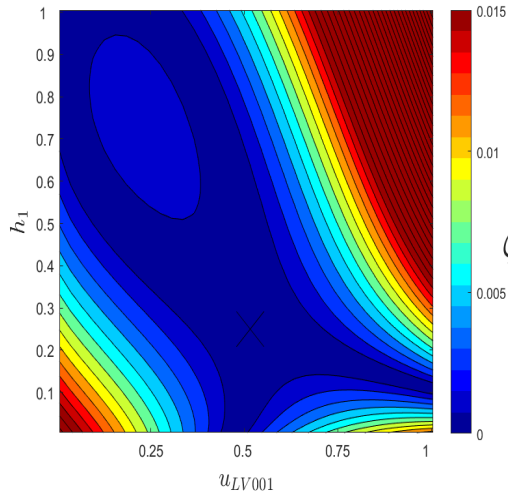
⁵In order to make these plots, the MATLAB function *contourf* is utilised: [Contourf](#)



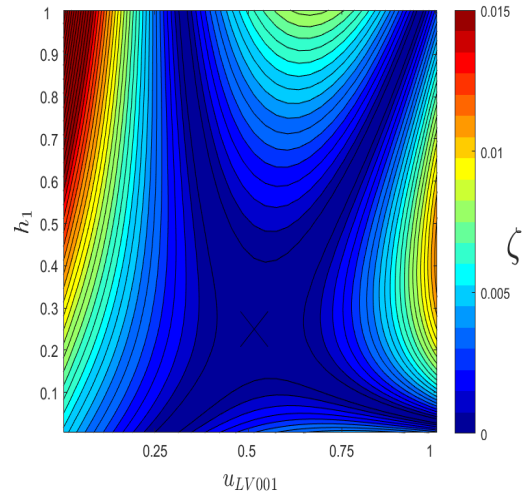
(a) Linear and nonlinear model.



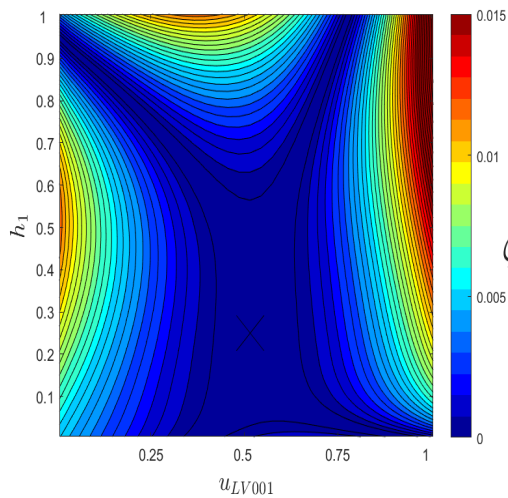
(b) Quadratic and nonlinear model.



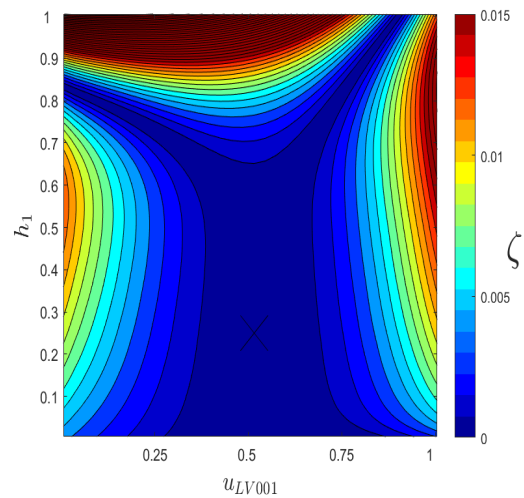
(c) PQ_A and nonlinear model.



(d) PQ_B and nonlinear model.



(e) Cubic and nonlinear model.



(f) 5th order and nonlinear model.

Figure 3.5: Contour plots of the Taylor models and the nonlinear model, where ζ is given by (3.32).

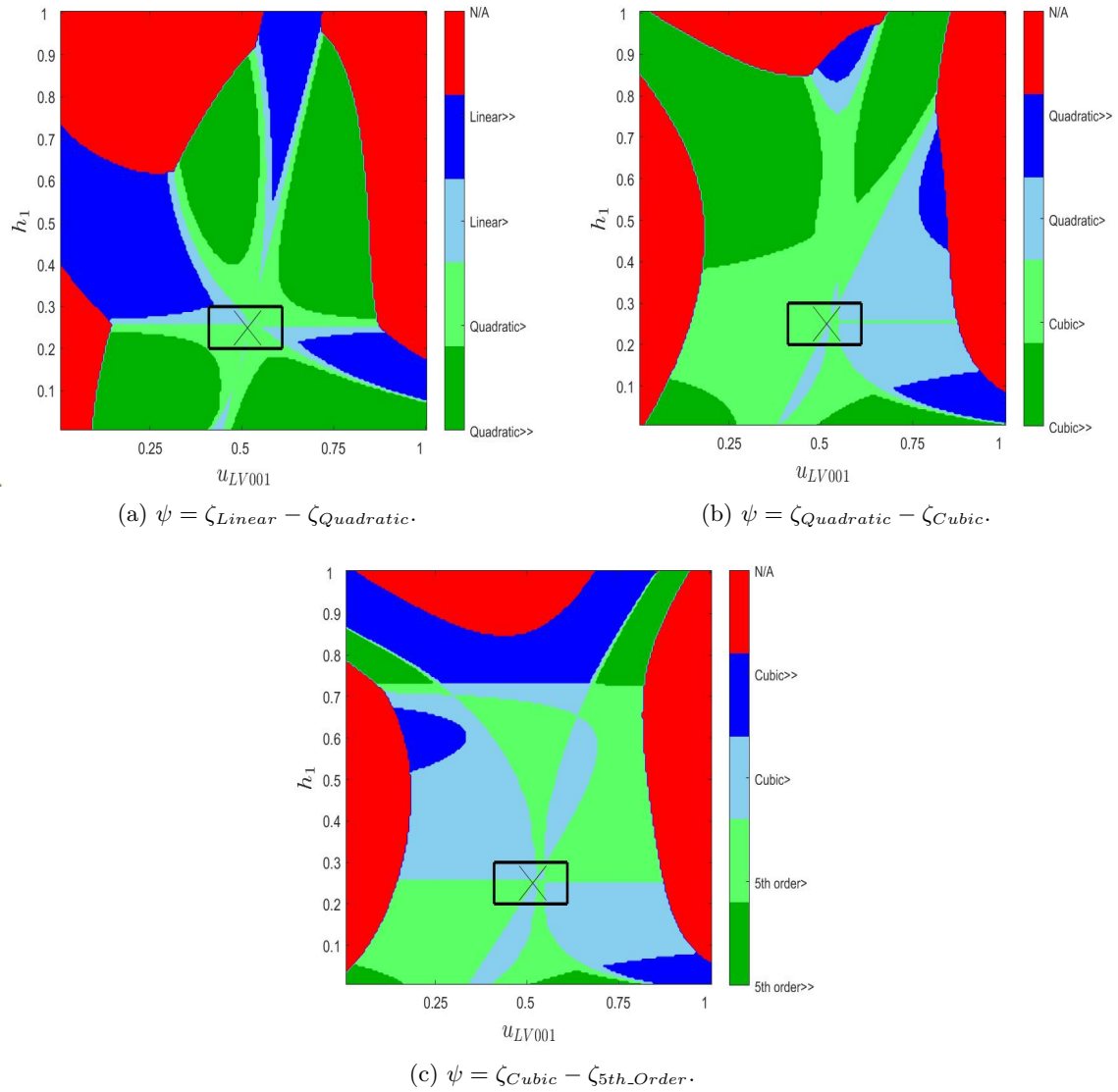


Figure 3.6: Color maps comparing the different Taylor models.

It is important to note that the Taylor models only approximates the nonlinear model *around the operating point*. Therefore, to test the *degree of improvement* from an n th order to an $(n+1)$ th order approximation, only the intervals $[0.2m, 0.3m]$ for h_1 and $[0.41, 0.61]$ for u_{LV001} will be considered. These intervals are represented by the hollow rectangle. The large cross indicates the operating point, where $h_1 = 0.25m$ and $u_{LV001} = 0.5159$.

By extracting a sub matrix from the matrix ψ , which corresponds to the data points within the hollow rectangle, we can find the amount of data points representing the different color codes in that interval. This gives a numerical interpretation of how the area within the hollow rectangle for the figures in Figure 3.6 is divided. These results are presented in Table 3.6.

Case	Data points	Case	Data points	Case	Data points
Quadratic >>	0	Cubic >>	0	5th order >>	0
Quadratic >	579	Cubic>	509	5th order>	388
Linear >	241	Quadratic>	311	Cubic>	432
Linear >>>	0	Quadratic>>>	0	Cubic>>>	0
N/A	0	N/A	0	N/A	0

(a) Data points in sub matrix of ψ from Figure 3.6a.

(b) Data points in sub matrix of ψ from Figure 3.6b.

(c) Data points in sub matrix of ψ from Figure 3.6c.

Table 3.6: Numerical interpretation of the area within the hollow rectangles in Figure 3.6.

Table 3.6a shows that the quadratic model approximates the nonlinear model slightly better than the linear model at 579 different data points, which is 338 points more than the other way around. The entire hollow rectangle under consideration consists of 820 individual data points. This means that the quadratic model covers a total of $\frac{579 \cdot 100\%}{820} = 70.61\%$ of the area around the operating point. Given the fact that it requires an additional $3^2 = 9$ partial derivatives to obtain the 2nd order approximation from the 1st order approximation, it makes sense to discard the linear model for the more improved quadratic model.

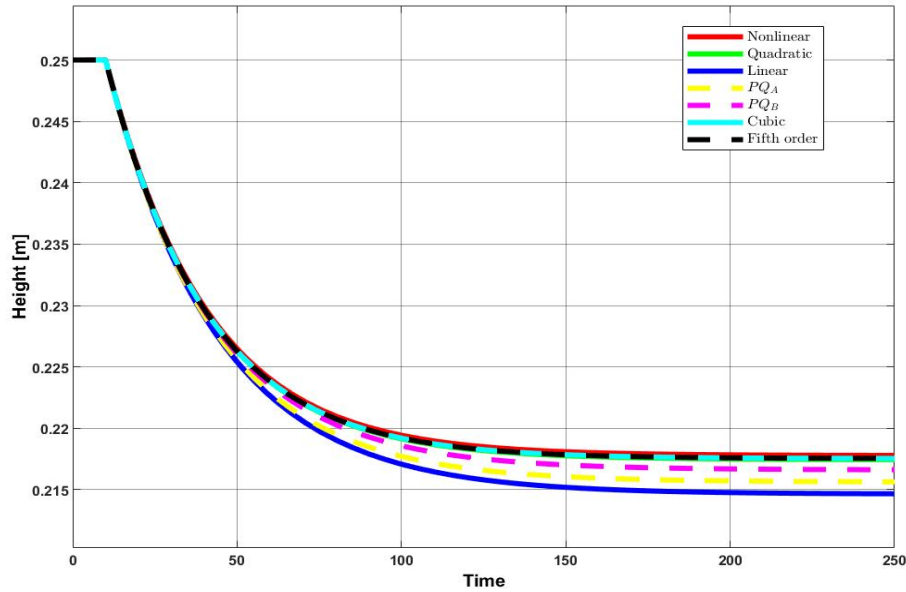
Following the same logic, the cubic model is slightly better than the quadratic model at 198 different data points more than the other way around. This can be calculated by the information in Table 3.6b. The cubic model covers a total of $\frac{509 \cdot 100\%}{820} = 62.07\%$ of the area within the hollow rectangle. This improvement is significant enough to discard the quadratic model for the cubic model, even though it requires an additional $3^3 = 27$ partial derivatives to obtain.

From Table 3.6c we see that, in contrast to the previous comparisons, the accuracy of the higher order Taylor approximation was not improved. The cubic model is actually slightly better than the 5th order approximation at 44 different data points more than the other way around. In this case, the cubic model covers $\frac{432 \cdot 100\%}{820} = 52.68\%$ of the area within the hollow rectangle. Given this information, it does *not* make sense to discard the cubic model for the higher order approximation.

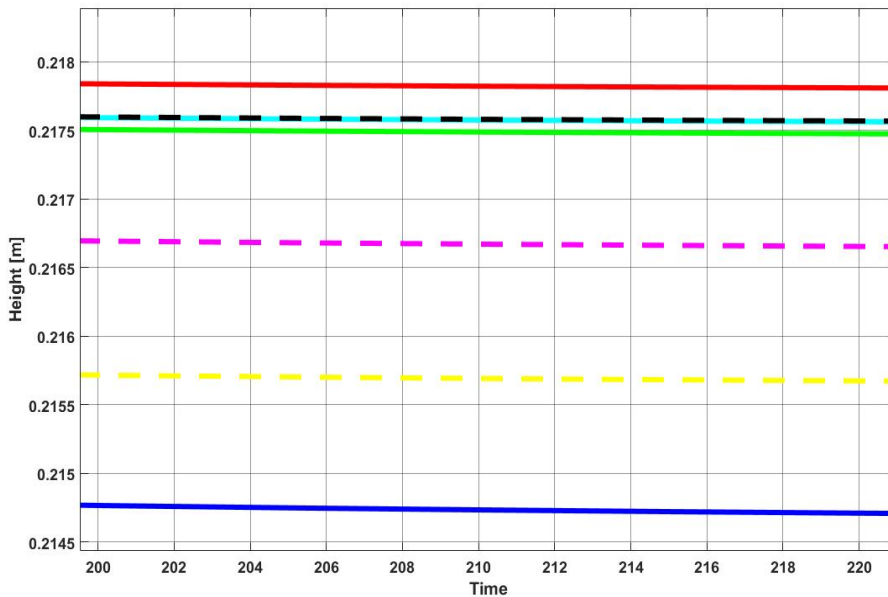
Note that none of the models were significantly better or worse in the immediate surroundings of the operating point. Every single data point within the hollow rectangle was either slightly in favour or slightly in disfavour of the models. There were also no cases where both models approximated the nonlinear model poorly in the set area around the operating point. Given these results, we can temporarily conclude that the cubic model is the best suited approximation of the nonlinear model.

It is possible to simulate the different Taylor models, and see how they respond to different input signals. In order to perform the simulations, the software Simulink and MATLAB are used. These simulations will be based on a *step response*, where the control signal $u_{LV001}(t)$ changes stepwisely. The control signal $u_{PA001}(t)$ will be constant at the operating point 0.65.

Figure 3.7 shows the step response of the different Taylor models together with the nonlinear model. The simulation lasted for a total of 250 seconds, and the step in $u_{LV001}(t)$ happened at 10 seconds. The control signal $u_{LV001}(t)$ went from its operating point of 0.5159 to 0.5359, which is an increment of 0.02.



(a) Step response with an increment in u_{LV001} of 0.02 at 10 seconds.



(b) Close up of 3.7a.

Figure 3.7: Model comparison in Simulink.

A standardised method to compare the performance of models and controllers is integrating the error over a time period. The *Integral performance criteria* is a set of commonly used integrals which quantify the error in a model or controller. The different integrals emphasise on different aspects of the error, for instance **ITAE** penalises errors more as time passes.

IAE - Integral Absolute Error: **IAE** is a commonly used error integral to compare errors over an interval.

$$IAE = \int_0^t |e(t)| dt$$

It integrates the absolute value of the error to make sure that positive and negative error do not cancel out. **IAE** does not add weight to any of the errors, it penalises small and large errors equally.

ISE - Integral Square Error:

$$ISE = \int_0^t e(t)^2 dt$$

The **ISE** penalises larger errors more than small errors.

ITAE- Integral Time Absolute Error:

$$ITAE = \int_0^t t|e(t)| dt$$

The **ITAE** penalises errors occurring at a later time more than at the start.

ITSE - Integral Time Square Error:

$$ITSE = \int_0^t te(t)^2 dt$$

The **ITSE** penalises large errors more than small, it also penalises errors at a later time more than at the start.

ISTE- Integral Square Time Error:

$$ISTE = \int_0^t t^2 e(t)^2 dt$$

The **ISTE** penalises large errors more than small, it also penalises errors at a later time more than at the start and it penalises more as time passes.

Table 3.7 quantifies the performance of the different models in the step response.

	IAE	ISE	ITAE	ITSE	ISTE
Linear	0.54638	0.001469	85.6911	0.24681	45.4302
PQ_A	0.39043	0.00073252	60.1709	0.12058	21.9437
PQ_B	0.20247	0.00020149	31.7901	0.034027	6.2837
Quadratic	0.066824	2.001e-05	9.7707	0.0031159	0.5532
Cubic	0.052571	1.2066e-05	7.4364	0.0017891	0.30999
5th order	0.051707	1.1652e-05	7.2912	0.0017189	0.29703

Table 3.7: Integral performance criteria.

It is evident that the cubic model, alongside with the 5th order model, are the approximations describing the nonlinear function the best. This agrees with previous results. Applying the same comparisons to *Scenario 2* leads to the same conclusion, for which reason the cubic model is chosen as the starting point for the *Carleman linearization*, which is described in the following chapter.

An important remark regarding the two scenarios, is that the approximations behave more similarly among them for *Scenario 2* than for *Scenario 1*. From Figure 3.3, we can see that the degree of nonlinearity for the nonlinear model is bigger at 0.25m than at 0.75m. This means that the nonlinear properties arising as the order of the approximation increases have a smaller impact on the results.

Chapter 4

Modelling using the Carleman embedding

In the previous chapter, it was shown that the following model:

$$\begin{aligned} \delta \dot{h}_1(t) = & \frac{\partial f}{\partial h_1} \Big|_O \delta h_1(t) + \frac{\partial f}{\partial u_{LV001}} \Big|_O \delta u_{LV001}(t) + \frac{\partial f}{\partial u_{PA001}} \Big|_O \delta u_{PA001}(t) \\ & + \frac{1}{2} \frac{\partial^2 f}{\partial h_1^2} \Big|_O \delta h_1^2(t) + \frac{\partial^2 f}{\partial h_1 \partial u_{LV001}} \Big|_O \delta h_1(t) \delta u_{LV001}(t) \\ & + \frac{1}{6} \frac{\partial^3 f}{\partial h_1^3} \Big|_O \delta h_1^3(t) + \frac{1}{2} \frac{\partial^3 f}{\partial h_1^2 \partial u_{LV001}} \Big|_O \delta h_1^2(t) \delta u_{LV001}(t) \end{aligned} \quad (4.1)$$

was the best approximation of the nonlinear tank model. This approximation will be the starting point of the *Carleman embedding* presented in this chapter. Section 4.1 introduces the key theoretical concepts related to the Carleman embedding and its practical use. Section 4.2 derives a general expression for the *Carleman approximation* of the cubic model. Section 4.3 presents the results of the Carleman approximation of the cubic model truncated at different n .

4.1 Carleman embedding

The general idea of Carleman embedding is that a finite dimensional set of nonlinear differential equations, can be embedded into an infinite dimensional set of linear differential equations. More specifically, a polynomial or analytical ¹ model defined on a finite dimensional space, can be transformed into a linear or bilinear model on an infinite dimensional space [12] [16].

The following finite dimensional nonlinear differential equation (4.2), with V consisting of polynomials in x , can be embedded into the infinite dimensional linear differential equation (4.3):

$$\dot{x}(t) = V(x(t)) \quad (4.2)$$

¹By analytical model we mean a model where its Taylor series converges to the model itself at every point in a defined area around the working point. This means that we can make a non-polynomial model into a polynomial by means of *Taylor approximation* as seen in Section 3.2.

$$\dot{z}(t) = A z(t) \tag{4.3}$$

by using an infinite vector of state variables: $z(t) = (z_1(t), z_2(t), \dots)^T$.

(4.3) is the infinite linear model associated to the finite nonlinear model given in (4.2). This is further explained in [14].

4.1.1 Carleman embedding technique

The Carleman embedding technique is introduced with an example.

Consider the following system:

$$\dot{x}(t) = x(t) + x^2(t) + x^3(t) \tag{4.4}$$

The goal is to describe this system with a linear state-space representation, where the state variables are defined as the infinite sequence of functions $z = (z_1, z_2, \dots)^T$. This can be achieved by expanding the state vector with the monomials corresponding to the state variable z :

$$\begin{aligned} z_1(t) &= x(t) \\ z_2(t) &= x^2(t) \\ z_3(t) &= x^3(t) \\ &\vdots \\ z_n(t) &= x^n(t) \\ &\vdots \end{aligned}$$

By differentiating the expanded state variables, we obtain:

$$\begin{aligned} \dot{z}_1(t) &= \dot{x}(t) = x(t) + x^2(t) + x^3(t) = z_1(t) + z_2(t) + z_3(t) \\ \dot{z}_2(t) &= 2x(t)\dot{x}(t) = 2x^2(t) + 2x^3(t) + 2x^4(t) = 2z_2(t) + 2z_3(t) + 2z_4(t) \\ \dot{z}_3(t) &= 3x^2(t)\dot{x}(t) = 3x^3(t) + 3x^4(t) + 3x^5(t) = 3z_3(t) + 3z_4(t) + 3z_5(t) \\ &\vdots \\ \dot{z}_n(t) &= nx^{n-1}(t)\dot{x}(t) = nx^n(t) + nx^{n+1}(t) + nx^{n+2}(t) = nz_n(t) + nz_{n+1}(t) + nz_{n+2}(t) \end{aligned}$$

which can be put into the compact form (4.3) with state matrix A given by:

$$A = \begin{bmatrix} 1 & 1 & 1 & 0 & \dots & & \\ 0 & 2 & 2 & 2 & 0 & \dots & \\ \vdots & 0 & 3 & 3 & 3 & 0 & \dots \\ \vdots & \vdots & 0 & 4 & 4 & 4 & 0 & \dots \\ \vdots & \vdots & \vdots & \vdots & \vdots & \vdots & \vdots & \ddots \end{bmatrix} \tag{4.5}$$

4.1.2 Truncation

As (4.3) is an infinite set of linear differential equations, numerical calculations using the result become nontrivial. A common take on this problem is truncating the Carleman embedding at the

n th state variable. This results in the *Carleman approximation*, which will become more accurate as n increases, disregarding computational errors.

Truncating (4.5) at $n = 3$ results in:

$$A = \begin{bmatrix} 1 & 1 & 1 \\ 0 & 2 & 2 \\ 0 & 0 & 3 \end{bmatrix}$$

Truncating (4.5) at $n = 5$ results in:

$$A = \begin{bmatrix} 1 & 1 & 1 & 0 & 0 \\ 0 & 2 & 2 & 2 & 0 \\ 0 & 0 & 3 & 3 & 3 \\ 0 & 0 & 0 & 4 & 4 \\ 0 & 0 & 0 & 0 & 5 \end{bmatrix}$$

while truncating at a generic n results in the $n \times n$ -matrix:

$$A = \begin{bmatrix} 1 & 1 & 1 & 0 & \dots & 0 \\ 0 & 2 & 2 & 2 & \dots & \vdots \\ \vdots & \vdots & \ddots & \ddots & \ddots & \vdots \\ \vdots & \vdots & \ddots & \ddots & n-1 & n-1 \\ \vdots & \vdots & \ddots & \ddots & 0 & n \end{bmatrix}$$

The truncation leads to approximations that become more accurate as n increases. A comparison between the nonlinear system (4.4) and some Carleman approximations are presented in Figure 4.1. The comparison shows that in this case, the Carleman approximation leads to an adequate approximation at $n = 3$.

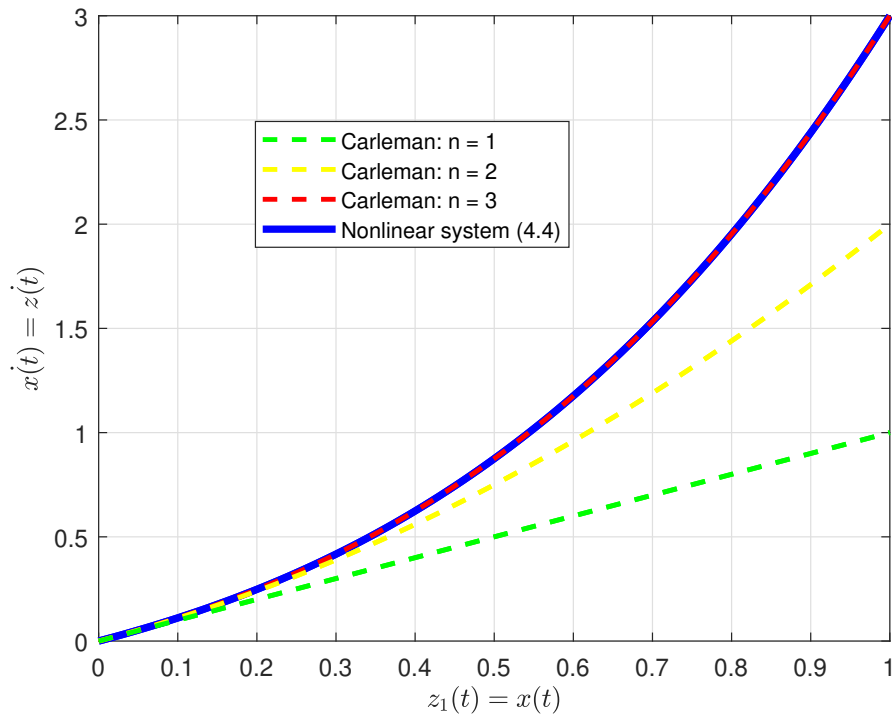


Figure 4.1: Carleman approximations of (4.4) compared to the nonlinear system.

4.2 Carleman approximation of the cubic tank model

The cubic tank model (4.1) is the starting point of the Carleman approximation. Applying the Carleman embedding technique shown in the previous section to (4.1), results in a nonlinear quadratic system. By means of the 1st order Taylor approximation, the nonlinear quadratic system is linearized. The *linearized Carleman approximation* is the state-space representation truncated at the n th state variable.

Let us introduce the following compact notation for the partial derivatives appearing in (4.1):

$$\begin{aligned}
 a &= \left. \frac{\partial f}{\partial h_1} \right|_O \\
 b &= \left. \frac{\partial f}{\partial u_{LV001}} \right|_O \\
 c &= \left. \frac{1}{2} \frac{\partial^2 f}{\partial h_1^2} \right|_O \\
 d &= \left. \frac{\partial^2 f}{\partial h_1 \partial u_{LV001}} \right|_O \\
 e &= \left. \frac{1}{6} \frac{\partial^3 f}{\partial h_1^3} \right|_O \\
 f &= \left. \frac{1}{2} \frac{\partial^3 f}{\partial h_1^2 \partial u_{LV001}} \right|_O
 \end{aligned} \tag{4.6}$$

The Carleman embedding of (4.1) is derived from the following steps:

- Expand the state vector with the monomials corresponding to the state variable

$$z(t) = (z_1(t), z_2(t), \dots)^T:$$

$$\begin{aligned}
 z_1(t) &= \delta h_1(t) \\
 z_2(t) &= \delta h_1^2(t) \\
 z_3(t) &= \delta h_1^3(t) \\
 &\vdots \\
 z_n(t) &= \delta h_1^n(t) \\
 &\vdots
 \end{aligned}$$

- Differentiate the expanded state variables:

$$\begin{aligned}
 \dot{z}_1(t) &= \delta \dot{h}_1(t) = a \delta h_1(t) + b \delta u_{LV001}(t) + c \delta h_1^2(t) + d \delta h_1(t) \delta u_{LV001}(t) + e \delta h_1^3(t) \\
 &\quad + f \delta h_1^2(t) \delta u_{LV001}(t) = \\
 &= a z_1(t) + b \delta u_{LV001}(t) + c z_2(t) + d z_1(t) \delta u_{LV001}(t) + e z_3(t) + f z_2(t) \delta u_{LV001}(t) \\
 \\
 \dot{z}_2(t) &= 2 \delta h_1(t) \delta \dot{h}_1(t) = 2 a \delta h_1^2(t) + 2 b \delta h_1(t) \delta u_{LV001}(t) + 2 c \delta h_1^3(t) \\
 &\quad + 2 d \delta h_1^2(t) \delta u_{LV001}(t) + 2 e \delta h_1^4(t) + 2 f \delta h_1^3(t) \delta u_{LV001}(t) = \\
 &= 2 a z_2(t) + 2 b z_1(t) \delta u_{LV001}(t) + 2 c z_3(t) + 2 d z_2(t) \delta u_{LV001}(t) + 2 e z_4(t) \\
 &\quad + 2 f z_3(t) \delta u_{LV001}(t)
 \end{aligned}$$

$$\begin{aligned}
 \dot{z}_3(t) &= 3 \delta h_1^2(t) \delta \dot{h}_1(t) = \\
 &= 3 a z_3(t) + 3 b z_2(t) \delta u_{LV001}(t) + 3 c z_4(t) + 3 d z_3(t) \delta u_{LV001}(t) + 3 e z_5(t) \\
 &\quad + 3 f z_4(t) \delta u_{LV001}(t) \\
 &\quad \vdots \\
 \dot{z}_n(t) &= n \delta h_1^{n-1}(t) \delta \dot{h}_1(t) = \\
 &= n a z_n(t) + n b z_{n-1}(t) \delta u_{LV001}(t) + n c z_{n+1}(t) + n d z_n(t) \delta u_{LV001}(t) + n e z_{n+2}(t) \\
 &\quad + n f z_{n+1}(t) \delta u_{LV001}(t)
 \end{aligned}$$

The Carleman embedding results in a nonlinear quadratic system in the form:

$$\dot{z}(t) = A z(t) + B \delta u_{LV001}(t) + \begin{bmatrix} z(t)^T E_1 \\ z(t)^T E_2 \\ \vdots \\ z(t)^T E_n \end{bmatrix} \delta u_{LV001}(t) \quad (4.7)$$

where $z(t)$ is the system state, $\delta u_{LV001}(t)$ is the control input and:

$$A = \begin{bmatrix} a & c & e & 0 & \cdots & & \\ 0 & 2a & 2c & 2e & 0 & \ddots & \\ \vdots & 0 & 3a & 3c & 3e & 0 & \ddots \\ \vdots & \vdots & 0 & 4a & 4c & 4e & 0 \\ \vdots & \vdots & \vdots & \vdots & \vdots & \vdots & \ddots \end{bmatrix}$$

$$B = \begin{bmatrix} b & 0 & \cdots \\ 0 & 0 & \cdots \\ \vdots & \vdots & \cdots \end{bmatrix}$$

$$E_1 = \begin{bmatrix} d \\ f \\ 0 \\ \vdots \end{bmatrix} \quad E_2 = \begin{bmatrix} 2b \\ 2d \\ 2f \\ 0 \\ \vdots \end{bmatrix} \quad E_3 = \begin{bmatrix} 0 \\ 3b \\ 3d \\ 3f \\ 0 \\ \vdots \end{bmatrix} \cdots$$

The linearized version of the embedded cubic model can be found by neglecting the nonlinear term $[z(t)^T E_1, \dots, z(t)^T E_n]^T \delta u_{LV001}(t)$. If the approximation is truncated at $n = 1$, then this corresponds to the *Taylor linearization* about the equilibrium point. This leads to the *Linear Time Invariant*(LTI) state-space representation:

$$\begin{aligned}
 \dot{z}(t) &= A z(t) + B \delta u_{LV001}(t) \\
 y(t) &= C z(t)
 \end{aligned}$$

where the *output matrix* is given by:

$$C = \begin{bmatrix} 1 & 0 & \dots & \dots \\ 0 & 0 & \dots & \dots \\ \vdots & \vdots & \dots & \ddots \end{bmatrix}$$

This representation is the *infinite linear model associated to the finite nonlinear cubic model* (4.1).

The linearized Carleman approximation is the state-space representation truncated at the n th state variable. Comparison between models truncated at different values of n will be discussed in the next section.

4.3 Carleman approximation comparison

In Section 4.2, we derived a general expression for the n th order linearized Carleman approximation of the cubic model. In this section, the goal is to determine the accuracy of this approximation and to find a value of n at which the truncation can happen without losing relevant information about the process' dynamics. In order to do this, we will use Simulink as a tool to simulate different linearized Carleman approximations of the cubic model, where n will differ. As with the previous chapter, we consider the two operating points named *Scenario 1* and *Scenario 2*. This section will present and discuss the results related to *Scenario 1*. The reader is referred to Appendix B for the results related to *Scenario 2*.

In the Simulink library browser, there is a block named *State-Space*, which will be used to simulate the different linearized Carleman approximations. This block uses the state matrix A , the input matrix B , the output matrix C and the feedthrough matrix D as parameters. How to obtain these matrices was explained in Section 4.2. The input is $\delta u_{LV001}(t)$ and the output is $\delta h_1(t)$. Figure 4.2 shows how this block is used in Simulink.

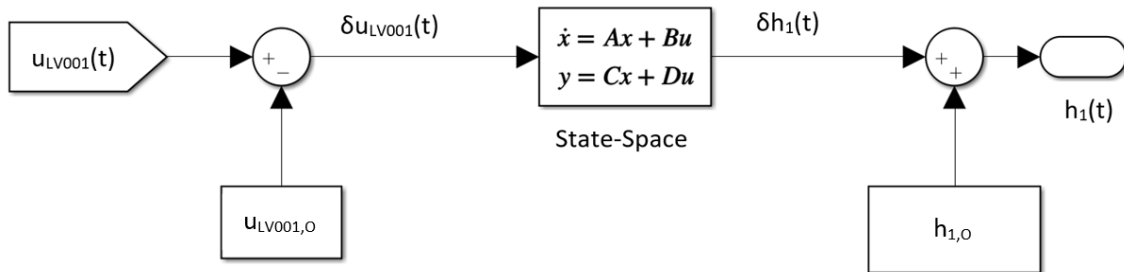


Figure 4.2: Utilising the State-Space block in Simulink.

This first simulation will be based on a *forced response*, where the control signal $u_{LV001}(t)$ changes stepwisely, and the initial condition is set to zero. The signal $u_{PA001}(t)$ will be kept constant at the value 0.65, which corresponds to the equilibrium point, as explained in Section 3.3. The total length of each simulation is 250 seconds. There will be a total of six different linearized Carleman approximations, where $n \in \{1, 2, 3, 4, 5, 10\}$. Figure 4.3 presents the results of this simulation.

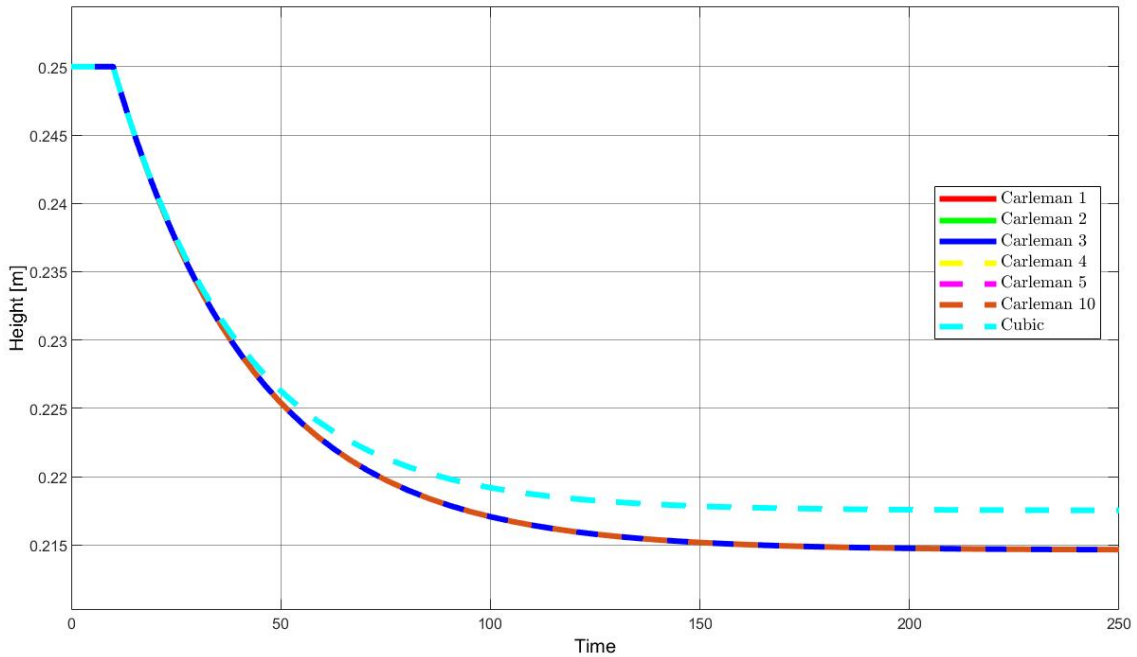


Figure 4.3: Step response with an increment in $u_{LV001}(t)$ of 0.02 at 10 seconds.

Figure 4.3 shows that all of the linearized Carleman approximations are exactly the same, and that they do not follow the cubic model. Upon further inspection, the linearized Carleman approximations actually follow the 1st order Taylor approximation. This can be seen by comparing the results from Figure 3.7a with the results from Figure 4.3. This comparison tells us that, when considering the contribution of the input signal to the overall response, the linearized Carleman approximations behave exactly as the linearized model obtained using a 1st order Taylor approximation, and that the order n is irrelevant. The cause for this behaviour will be further discussed in the next chapter.

Another way to observe the linearized Carleman approximations, is by simulating the *free response* of the models, where the input signal $u_{LV001}(t)$ is constant and the initial conditions are altered. If the initial condition is different from the operating point, the model will eventually converge to the operating point because the system is open-loop stable, otherwise it would not. By studying this convergence, it becomes possible to compare the cubic model with the linearized Carleman approximations. Note that the operating point for the cubic model is $h_{1,O} = 0.25m$ for *Scenario 1*. However, since the elements in the state vector $z(t)$ for the Carleman approximations is defined as $\delta h_1(t)^n$, the operating point is $0m$ when defined with respect to $\delta h_1(t)$ and its powers. This means that if the cubic model and the linearized Carleman approximations are meant to start from the same initial water level, they need to have an initial condition of $0.25m + \delta m$ and δm , respectively, where δm is the offset from the equilibrium points. Since the Carleman approximations consists of n states, it needs a $n \times 1$ matrix which includes the initial condition for each state:

$$\delta_matrix = \begin{bmatrix} \delta^1 \\ \delta^2 \\ \vdots \\ \delta^n \end{bmatrix} \quad (4.8)$$

Defining the δ variable as $0.05m$, means that the models will start at $0.25m + 0.05m = 0.3m$.

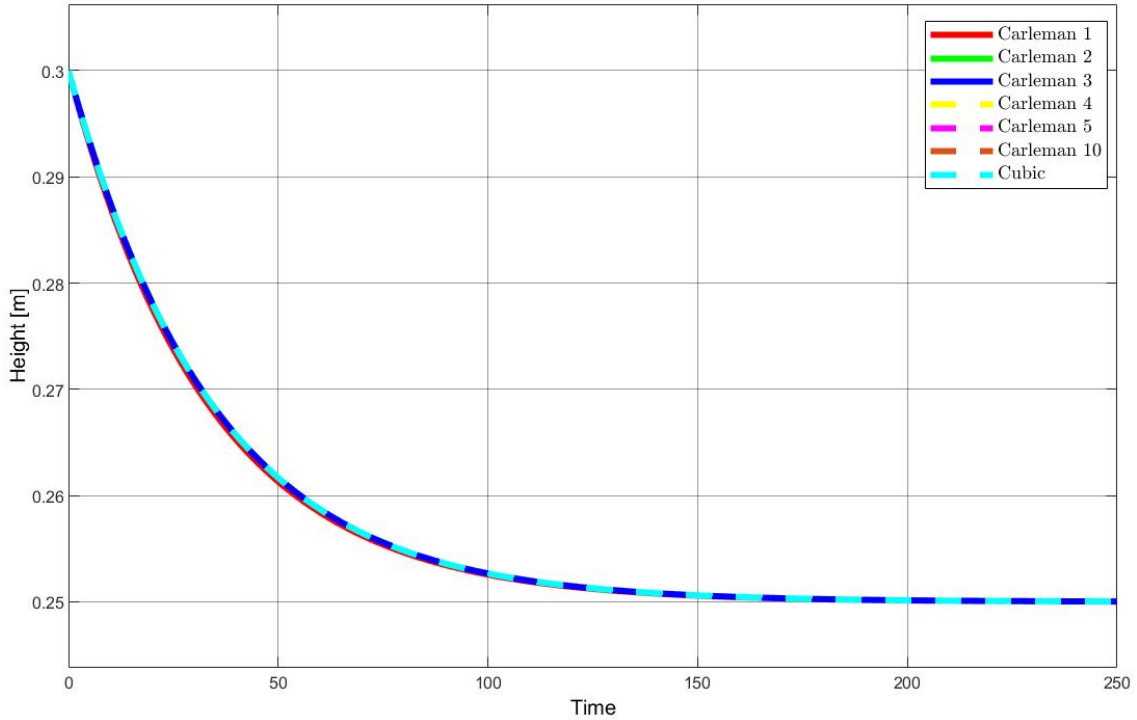


Figure 4.4: $\delta = 0.05m$ gives a starting point of 0.3m.

From Figure 4.4, it is evident that the linearized Carleman approximations do indeed follow the cubic model, and that they converge to the operating point at 0.25m. Section 3.3 introduced *integral performance criteria* as a method to compare the different Taylor approximations. Applying that same concept here, results in Table 4.1².

	IAE	ISE	ITAE	ITSE	ISTE
<i>Carleman 1</i>	0.033946	1.1314e-05	1.7255	0.00042025	0.021141
<i>Carleman 2</i>	0.0010657	1.9028e-08	0.032067	4.1273e-07	1.2094e-05
<i>Carleman 3</i>	9.2014e-05	8.8891e-11	0.0047623	3.4878e-09	1.7297e-07
<i>Carleman 4</i>	1.6684e-06	2.1323e-14	0.00010913	1.143e-12	8.1992e-11
<i>Carleman 5</i>	1.8461e-07	-1.0709e-15	8.7203e-06	-1.0774e-14	-1.2033e-13
<i>Carleman 10</i>	3.0644e-12	-1.4964e-15	1.5481e-10	-2.6411e-14	-8.1151e-13

Table 4.1: Integral performance criteria of the linearized Carleman approximations, with $\delta = 0.05m$.

Table 4.1 shows that around $n = 2$, the linearized Carleman approximation approximates the cubic model with small discrepancies. However, since the starting point only has a 0.05m deviation from the operating point, the behaviour required in order to follow the cubic model is less nonlinear. This allows a low order linearized Carleman approximation to have a high accuracy. Increasing the δ variable to 0.2m, gives a starting point of 0.45m.

²Due to the precision of numerical calculations in MATLAB, some values that are small appear as negative values. These values can be regarded as zero.

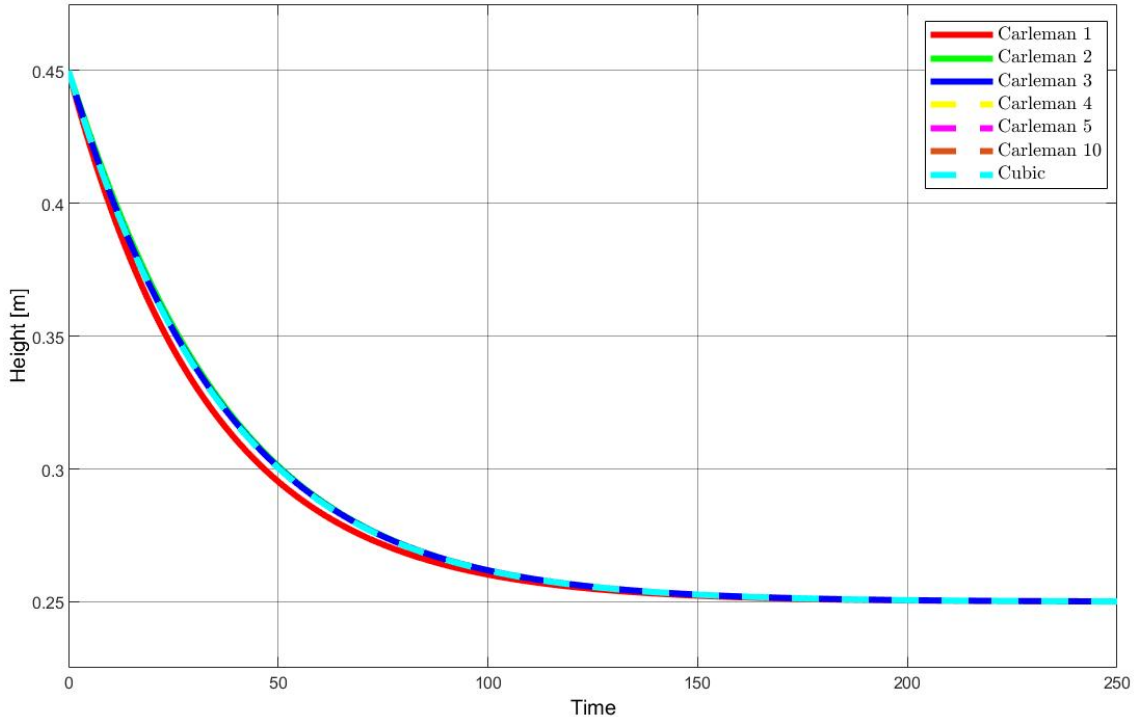


Figure 4.5: $\delta = 0.2m$ gives a initial condition of 0.45m.

From Figure 4.5 we see that the 1st order linearized Carleman approximation is not able to follow the cubic model as well as the other models. Table 4.2 also expresses this notion.

	IAE	ISE	ITAE	ITSE	ISTE
<i>Carleman 1</i>	0.47434	0.0021312	25.1139	0.084099	4.4267
<i>Carleman 2</i>	0.085848	0.00010673	3.0072	0.0026045	0.087056
<i>Carleman 3</i>	0.023531	5.6366e-06	1.2597	0.00023117	0.011911
<i>Carleman 4</i>	0.0015259	2.259e-08	0.089447	8.2185e-07	5.1763e-05
<i>Carleman 5</i>	0.00084781	8.4265e-09	0.0425	3.2894e-07	1.5478e-05
<i>Carleman 10</i>	2.9821e-07	-8.067e-15	1.5674e-05	-1.8252e-13	-5.7072e-12

Table 4.2: Integral performance criteria of the linearized Carleman approximations, with $\delta = 0.2m$.

Table 4.2 shows that the linearized Carleman approximations of lower order, are significantly less accurate. In this case, the preferred models are Carleman 4, 5 and 10. Obviously, increasing the order above 10 will make the approximation more accurate. However, since the level of improvement from $n = 5$ to $n = 10$ is so small, considering $n > 10$ is redundant with respect to this project.

It was shown that the linearized Carleman approximation only follows the 1st order Taylor approximation when there is a change in the control signal $u_{LV001}(t)$. This behaviour makes the linearized Carleman approximation inadequate for the cubic model. Because of this, the quadratic Carleman approximation (4.7), obtained in Section 4.2 will be considered.

To simulate the quadratic Carleman approximations, we use the same settings as in the previous step response shown in Figure 4.3. $u_{LV001}(t)$ changes stepwisely with an increment of 0.02 at 10 seconds, $u_{PA001}(t)$ is kept constant at 0.65 and the total simulation length is 250 seconds. There will be a total of six different quadratic Carleman approximations, where $n \in \{1, 2, 3, 4, 5, 10\}$.

Figure 4.6 shows that the quadratic Carleman approximations follow the cubic model to a great extent, with an exception of the 1st order quadratic Carleman approximation. Given that the change in $u_{LV001}(t)$ is only 0.02 away from the operating point, it is expected that the order n required to follow the cubic model is small. However, if the step in $u_{LV001}(t)$ is bigger in

magnitude, it will be harder for the quadratic Carleman approximations of lower order to follow the cubic model. Figure 4.7 shows an equivalent simulation, but the step in $u_{LV001}(t)$ is now -0.1 .

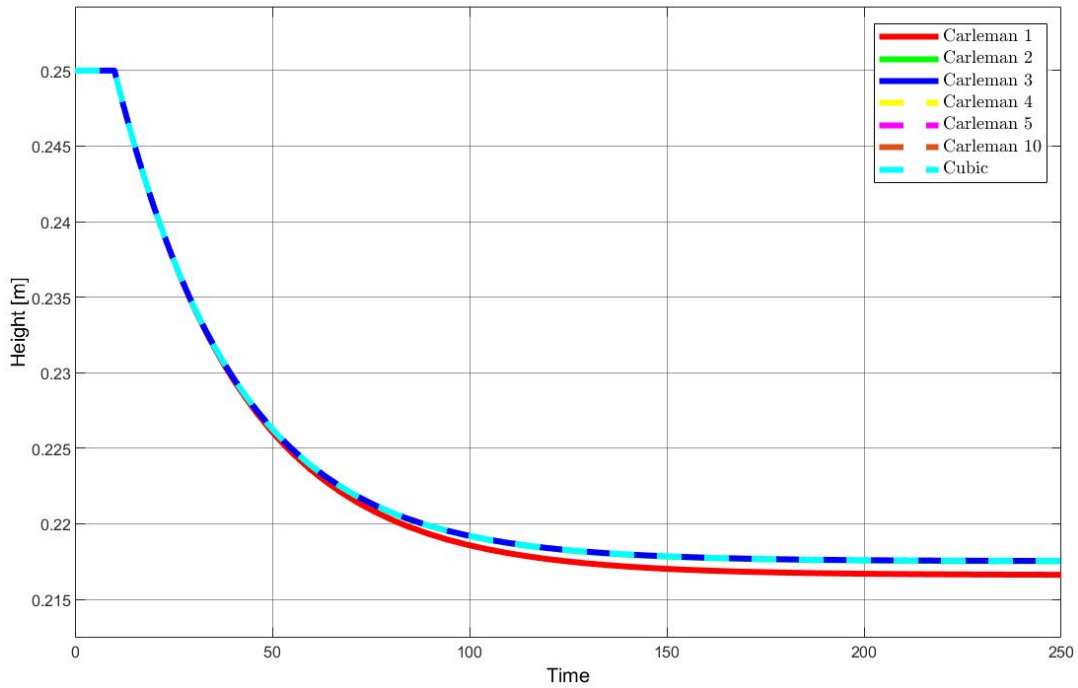


Figure 4.6: Simulation of the quadratic Carleman approximations.

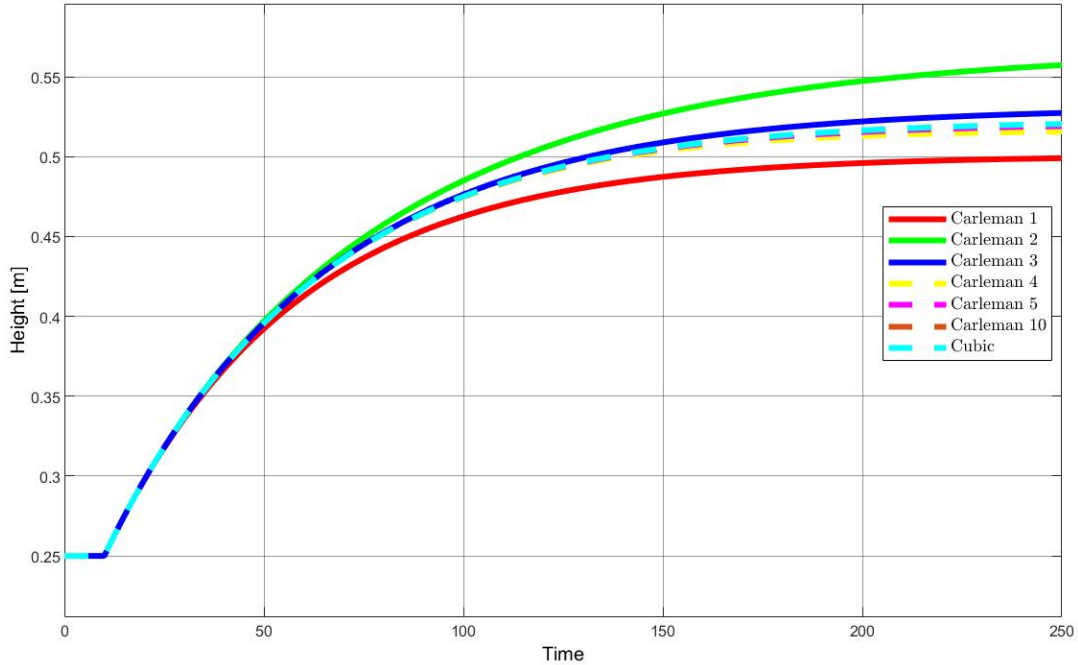


Figure 4.7: Simulation of the quadratic Carleman approximations with a larger step.

From Figure 4.7, we see again that the preferred order for the quadratic Carleman approximations are $n \in \{4, 5, 10\}$. This shows that the Carleman embedding technique from Section 4.2 works as intended, and that the nonlinear quadratic system, truncated at $n \in \{4, 5, 10\}$, gives an accurate representation of the cubic model.

Part III

Control

Chapter 5

State feedback control using the linear Carleman approximation

In the previous chapter, we saw that the linearized Carleman approximation did not follow the cubic model when a forced response was applied. This behaviour will be further investigated in this chapter. Section 5.1 gives a brief introduction to some relevant elements from control theory, while Section 5.2 further investigates the *controllability* of the linearized Carleman approximation.

5.1 Control

Control of a dynamical system involves using the system inputs to drive it to a desired state with some prescribed performance [20]. The controller for the Carleman approximations will be a state feedback controller. This means that the control input is dependent on the current value of the state, which is "fed back" to the controller. The current state is compared to the reference as the goal is to move the system back to the equilibrium point. This gives the measured error that the controller has to correct.

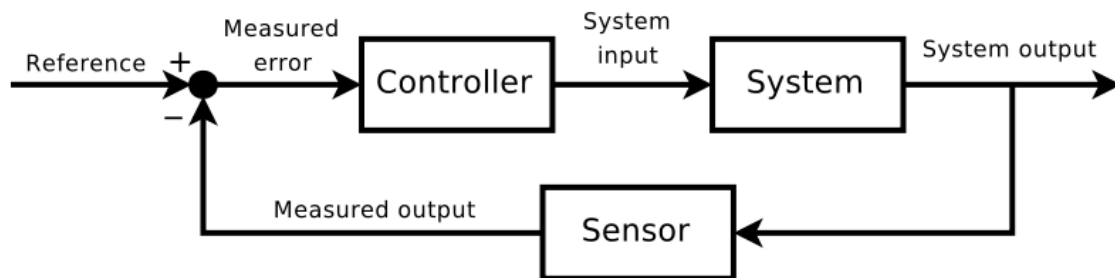


Figure 5.1: Feedback control system [1].

Controllability is a key property of a system which describes its ability to reach any point in the state-space by applying the correct sequence of control inputs.

Theorem 1 *The LTI system:*

$$\dot{x}(t) = Ax(t) + Bu(t) \tag{5.1}$$

is controllable if and only if the controllability matrix:

$$\mathcal{C} = [B, AB, A^2B, \dots, A^{n-1}B] \tag{5.2}$$

has full row rank.

The column rank of a matrix is determined by the number of linearly independent columns of the matrix. Equivalently the row rank is the number of dimensions of the vector space spanned by its rows. A fundamental result in linear algebra shows that the column rank and row rank are always equal [23]. Therefore, either can be calculated to check the rank of the controllability matrix.

Theorem 2 *The $n \times nm$ matrix \mathcal{C} has full row rank if and only if:*

$$\text{rank}(\mathcal{C}) = \min(n, nm) = n \tag{5.3}$$

Consider the following system:

$$A = \begin{bmatrix} 1 & 1 & 1 \\ 0 & 2 & 2 \\ 1 & 0 & 3 \end{bmatrix}, B = \begin{bmatrix} 1 \\ 1 \\ 0 \end{bmatrix}$$

then the controllability matrix is given by:

$$\mathcal{C} = \begin{bmatrix} 1 & 2 & 5 \\ 0 & 2 & 6 \\ 0 & 1 & 5 \end{bmatrix}$$

To examine the rank of the controllability matrix, we first have to make sure that the columns are *linearly independent*. Therefore, a common approach to finding the rank is to perform *Gaussian elimination* on the matrix to get it in a simple *row echelon form*. This way, all the dependent rows become 0 and the *rank* is equal to the number of non-zero rows remaining.

The \mathcal{C} matrix in *row echelon* form:

$$\mathcal{C} = \begin{bmatrix} 1 & 0 & 0 \\ 0 & 1 & 0 \\ 0 & 0 & 1 \end{bmatrix}$$

clearly shows that there are 3 non-zero rows giving it *rank* = 3, revealing that the system is controllable.

5.2 Controllability of the linear Carleman approximation

In order to find the controllability property of the linearized Carleman approximation, the state matrix A , and the input matrix B is required. The general expression for these matrices was derived in Section 4.2, and are presented below:

$$A = \begin{bmatrix} a & c & e & 0 & \cdots \\ 0 & 2a & 2c & 2e & 0 & \ddots \\ \vdots & 0 & 3a & 3c & 3e & 0 & \ddots \\ \vdots & \vdots & 0 & 4a & 4c & 4e & 0 \\ \vdots & \vdots & \vdots & \vdots & \vdots & \vdots & \ddots \end{bmatrix}, B = \begin{bmatrix} b & 0 & \cdots \\ 0 & 0 & \cdots \\ \vdots & \vdots & \cdots \end{bmatrix} \quad (5.4)$$

With the equations (5.2) and (5.4), the controllability matrix for the linearized Carleman approximation can be calculated. As an example, we can truncate the linearized Carleman approximation at $n = 3$, which gives the following A and B matrices:

$$A = \begin{bmatrix} a & c & e \\ 0 & 2a & 2c \\ 0 & 0 & 3a \end{bmatrix}, B = \begin{bmatrix} b \\ 0 \\ 0 \end{bmatrix} \quad (5.5)$$

Inserting the A and B matrices from (5.5) into (5.2) yields:

$$C = \begin{bmatrix} \begin{bmatrix} b \\ 0 \\ 0 \end{bmatrix} & \begin{bmatrix} a & c & e \\ 0 & 2a & 2c \\ 0 & 0 & 3a \end{bmatrix} \begin{bmatrix} b \\ 0 \\ 0 \end{bmatrix} & \begin{bmatrix} a & c & e \\ 0 & 2a & 2c \\ 0 & 0 & 3a \end{bmatrix}^2 \begin{bmatrix} b \\ 0 \\ 0 \end{bmatrix} \end{bmatrix} = \begin{bmatrix} b & ab & a^2b \\ 0 & 0 & 0 \\ 0 & 0 & 0 \end{bmatrix} \quad (5.6)$$

If the calculations are repeated for a higher order system, e.g., for $n = 6$, one gets:

$$A = \begin{bmatrix} a & c & e & 0 & 0 & 0 \\ 0 & 2a & 2c & 2e & 0 & 0 \\ 0 & 0 & 3a & 3c & 3e & 0 \\ 0 & 0 & 0 & 4a & 4c & 4e \\ 0 & 0 & 0 & 0 & 5a & 5c \\ 0 & 0 & 0 & 0 & 0 & 6a \end{bmatrix}, B = \begin{bmatrix} b \\ 0 \\ 0 \\ 0 \\ 0 \\ 0 \end{bmatrix} \quad (5.7)$$

As in the previous example, the matrices in (5.7) are inserted into Eq. (5.2):

$$C = [B \quad AB \quad A^2B \quad A^3B \quad A^4B \quad A^5B] = \begin{bmatrix} b & ab & a^2b & a^3b & a^4b & a^5b \\ 0 & 0 & 0 & 0 & 0 & 0 \\ 0 & 0 & 0 & 0 & 0 & 0 \\ 0 & 0 & 0 & 0 & 0 & 0 \\ 0 & 0 & 0 & 0 & 0 & 0 \\ 0 & 0 & 0 & 0 & 0 & 0 \end{bmatrix} \quad (5.8)$$

It is clear that for a generic n th order linearized Carleman approximation, the controllability

matrix is given by:

$$\mathcal{C} = \begin{bmatrix} b & ab & a^2b & \dots & a^{n-1}b \\ 0 & 0 & 0 & \dots & 0 \\ \vdots & \vdots & \vdots & \dots & \vdots \\ 0 & 0 & 0 & \dots & 0 \end{bmatrix} \quad (5.9)$$

Note that all of the elements $[A_{2,1}, A_{3,1}, \dots, A_{n,1}]$ in the A^{n-1} matrix are all equal to zero, with the exception of $A_{1,1}$ which is equal a^{n-1} . Note also that the only non-zero element in the B matrix is $B_{1,1}$, which is equal to b . This explains why the multiplication $A^{n-1}B$ always results in a column vector, where the only non-zero element is the first entry. This is the reason why the first row in (5.9) is the only non-zero row of the controllability matrix.

Given (5.9), it is evident that the order of the linearized Carleman approximation will not affect the fact that the first row is the only non-zero row of the controllability matrix. In Section 5.1, it was stated that the rank of the controllability matrix needed to be equal to n , in order for the system to be controllable. It is evident from (5.9) that the rank of the controllability matrix will always be equal to 1, regardless of the order n of the linearized Carleman approximation. This means that the linearized Carleman approximation will not be controllable unless the order $n = 1$, which is equal to the 1st order Taylor approximation of the nonlinear system. The lack of controllability means that the system's eigenvalues can not be arbitrarily located in the complex plane, which means that some eigenvalues can not be reached [26]. This explains the behaviour observed in Figure 4.3, and why all of the linearized Carleman approximations follow the 1st order Taylor approximation.

Chapter 6

State feedback control using the quadratic Carleman approximation

In the previous chapter we saw that the linearized Carleman approximation was not controllable and that the forced response followed the 1st order Taylor linearization, regardless of the order n . In this chapter, we will consider the quadratic system arising from the Carleman approximation of the cubic model. In Section 6.1, some introductory theory is presented to better grasp the process of making a state feedback controller for a quadratic system. Section 6.2 describes the design of the controller gain \mathcal{K} for the *quadratic Carleman approximation*. In Section 6.3, necessary modifications of LMIs are implemented to include the pump *PA001* as an actuator, in addition to the valve *LV001*, resulting in a new controller gain \mathcal{K} . The results presented in this chapter are related to *Scenario 1*. For the results related to *Scenario 2*, the reader is referred to Appendix C.

6.1 Supplemental theory

6.1.1 Polytopes

A *polytope* is a geometric object, with flat surfaces and straight edges. Convex polytopes are the simplest kind of polytopes, and they are defined as the intersection of a set of half-spaces [22]. The actual points at which these half-spaces intersect and form the corners of the convex polytopes are defined as the *vertices* of the polytope [25].

It is possible to create a convex polytope by applying the *convex hull* on a finite set of points. A convex hull is defined as the minimal convex set that contains all of the points [21]. This hull creates a convex polytope, where each extreme point of the hull is a vertex. It is also possible to express the half-spaces, containing the polytope, if the vertices are known. In this project, this was done by using the `vert2con` MATLAB function, which requires the vertices as an input argument, and returns a set of constraints such that $Ax \leq b$ defines the region of space enclosing the convex hull of the given points [11].

A convex polytope, in \mathbb{R}^2 , in the shape of a box is given by: $\mathcal{P} = [-1, 2] \times [-1, 3]$. The points at which these four half-spaces intersect are:

$$x_{(1)} = (2, -1)^T, x_{(2)} = (2, 3)^T, x_{(3)} = (-1, 3)^T, x_{(4)} = (-1, -1)^T \quad (6.1)$$

which are the vertices of the convex polytope.

Using the vertices from (6.1) as an input argument in the `vert2con` function, gives the following inequalities:

$$Ax \leq b, A = \begin{bmatrix} 0 & 0.5000 \\ 0 & -0.5000 \\ 0.6667 & 0 \\ -0.6667 & 0 \end{bmatrix}, b = \begin{bmatrix} 1.5000 \\ 0.5000 \\ 1.3333 \\ 0.6667 \end{bmatrix} \quad (6.2)$$

Usually, the constraints that expresses the region of the polytope are described as:

$$Ax \leq 1 \quad (6.3)$$

Therefore, we divide both sides of (6.2) by b . This results in a matrix denoted as A_k :

$$A_k = A \oslash b = \begin{bmatrix} 0 & 0.3333 \\ 0 & -1.0000 \\ 0.5000 & 0 \\ -1.0000 & 0 \end{bmatrix} \rightarrow A_k x \leq 1 \quad (6.4)$$

where each *row vector* in A_k represents the transposed of the half-space vector that contains the polytope. These vectors can be written as:

$$a_1^T = (0, \frac{1}{3}), a_2^T = (0, -1), a_3^T = (\frac{1}{2}, 0), a_4^T = (-1, 0) \quad (6.5)$$

Plotting these half-spaces shows the points at which they intersect, and the region in which they cut off. This contained region is known as the polytope \mathcal{P} . Figure 6.1 illustrates this notion.

In fact, the inequality in (6.4) can be segmented into the following inequalities:

$$a_1^T x \leq 1 \rightarrow \begin{bmatrix} 0 & \frac{1}{3} \end{bmatrix} \begin{bmatrix} x_1 \\ x_2 \end{bmatrix} \leq 1 \quad (6.6)$$

$$a_2^T x \leq 1 \rightarrow \begin{bmatrix} 0 & -1 \end{bmatrix} \begin{bmatrix} x_1 \\ x_2 \end{bmatrix} \leq 1 \quad (6.7)$$

$$a_3^T x \leq 1 \rightarrow \begin{bmatrix} \frac{1}{2} & 0 \end{bmatrix} \begin{bmatrix} x_1 \\ x_2 \end{bmatrix} \leq 1 \quad (6.8)$$

$$a_4^T x \leq 1 \rightarrow \begin{bmatrix} -1 & 0 \end{bmatrix} \begin{bmatrix} x_1 \\ x_2 \end{bmatrix} \leq 1 \quad (6.9)$$

In order for the inequalities (6.6) and (6.7) to be true, the variable x_2 must be confined within the range $-1 \leq x_2 \leq 3$, regardless of what x_1 is.

For the inequalities (6.8) and (6.9) to be true, the variable x_1 must be confined within the range $-1 \leq x_1 \leq 2$, regardless of what x_2 is.

This confirms the confined region that is contained by the half-spaces, defined as the polytope \mathcal{P} , is as shown in Figure 6.1.

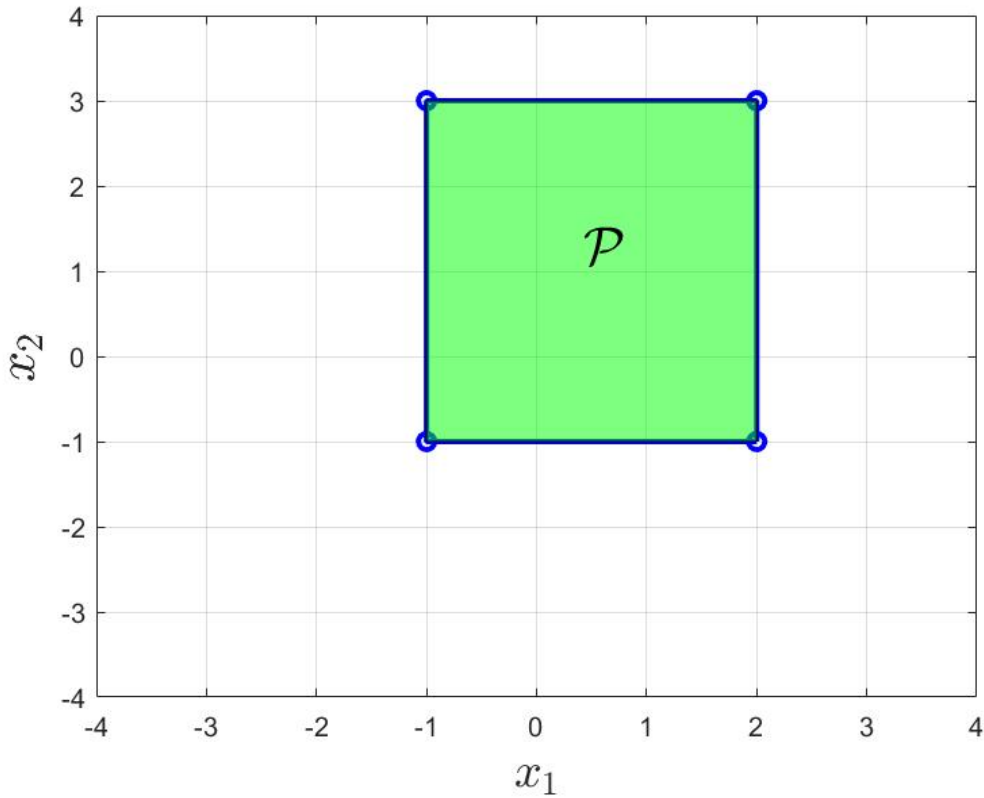


Figure 6.1: Polytope \mathcal{P} is contained by the blue half-spaces, and represented by the green region.

6.1.2 Lyapunov stability criterion

To ensure stability of a dynamical system, stability theory is explored. We saw that the linear Carleman approximation was uncontrollable, therefore, some of its eigenvalues could not be moved to make it follow the cubic model. If an LTI-system is controllable, then the closed-loop eigenvalues can be assigned at arbitrary desired locations of the complex plane. The stability of a nonlinear dynamical system *around* an equilibrium point of the solution can be proven using the *Lyapunov stability criterion*.

Theorem 3 *An equilibrium is said to be locally asymptotically stable if the Lyapunov function is locally positive definite for $x \neq x_{equilibrium}$:*

$$V(x) > 0 \tag{6.10}$$

and its derivative is locally negative definite for $x \neq x_{equilibrium}$:

$$\dot{V}(x) < 0 \tag{6.11}$$

These criteria are often explained using $V(x)$ as a general energy function. If a system $V(x)$ has positive definite energy and a negative definite derivative in some neighbourhood around the equilibrium point, then this point is said to be *locally asymptotically stable* (L.A.S).

Finding the *Lyapunov function* $V(x)$ can be hard in some cases, but for a linear system $\dot{x} = Ax$ it can be done as follows [2]:

$$V(x) = x^T P x \quad (6.12)$$

where $P = P^T > 0$ ensures that (6.12) is positive definite as required in (6.10).

From this, the derivative can also be found:

$$\dot{V}(x) = \frac{\partial V}{\partial x} \frac{dx}{dt} = x^T (A^T P + P A) x \quad (6.13)$$

where $A^T P + P A < 0$ ensures that (6.13) is negative definite as required in (6.11).

The linear system is *Lyapunov stable* if there exists some positive definite symmetrical matrix P with a negative definite derivative in some neighbourhood around the equilibrium point.

Region of attraction

For any Lyapunov function satisfying the stability criterion, there exists a *region of attraction* (RA)¹. This is a firmly stated region which describes the renowned "around the equilibrium", however, it is hard or even impossible to find the RA except for in some simple cases. An estimate of the RA can be found by using *linear matrix inequalities* (LMI's) as described in [4]. The idea is that given the nonlinear system corresponding to the quadratic Carleman model (4.7):

$$\dot{x}(t) = Ax(t) + \begin{bmatrix} x^T(t)B_1x \\ x^T(t)B_2x \\ \vdots \\ x^T(t)B_nx \end{bmatrix}$$

a quadratic Lyapunov function satisfying the stability criterion over an *invariant set*² is built using an LMI-based optimization problem[27]. If solveable, these inequalities ensure that the polytope \mathcal{P} belongs to the RA.

¹ "...given an asymptotically stable system, the RA is defined as the largest connected set Ω containing the origin and such that every solution starting in Ω converges to 0" [4].

²If, for all solutions of a system starting in a set remains in the set as $t \rightarrow \infty$, then the set is said to be invariant.

6.1.3 State feedback control of nonlinear quadratic systems

The goal of this section is to explore a method of finding a L.A.S state feedback controller in the form:

$$u(t) = \mathcal{K}x(t) \quad (6.14)$$

for the nonlinear system ³:

$$\dot{x} = Ax(t) + Bu(t) + \begin{bmatrix} x^T(t)E_1 \\ x^T(t)E_2 \\ \vdots \\ x^T(t)E_n \end{bmatrix} u(t) \quad (6.15)$$

which is L.A.S on the polytope \mathcal{P} enclosed by the RA.

Theorem 4 *Given system (6.15), with $A \in n \times n$ and $B \in m \times n$ and the polytope \mathcal{P} , a controller gain \mathcal{K} can be found by solving:*

$$0 < \gamma < 1 \quad (6.16a)$$

$$P > 0 \quad (6.16b)$$

$$\begin{bmatrix} 1 & \gamma a_k^T P \\ Pa_k \gamma & P \end{bmatrix} \geq 0, \quad k = 1, 2, \dots, q \quad (6.16c)$$

$$\begin{bmatrix} 1 & x_{(i)}^T \\ x_{(i)} & P \end{bmatrix} \geq 0, \quad i = 1, 2, \dots, p \quad (6.16d)$$

$$\gamma(AP + PA^T) + \gamma(BL + L^T B^T) + \begin{bmatrix} x_{(i)}^T E_1 L \\ x_{(i)}^T E_2 L \\ \vdots \\ x_{(i)}^T E_n L \end{bmatrix} + \left((L^T E_1^T) x_{(i)} \cdots (L^T E_n^T) x_{(i)} \right) \quad (6.16e)$$

$$< 0 \quad i = 1, 2, \dots, p$$

with a symmetric matrix $P \in \mathbb{R}^{n \times n}$ and a matrix $L \in \mathbb{R}^{m \times n}$, where p is the amount of vertices and q is the amount of constraints a_k . Then, the controller gain in (6.14) can then be calculated as $\mathcal{K} = LP^{-1}$.

In (6.16) we can see that (6.16b) is the positive definite Lyapunov function, $V(x)$ shown in (6.10) and (6.16e) is the negative definite $\dot{V}(x)$ shown in (6.11) with a given polytope \mathcal{P} . (6.16a) is a scalar that can be set to a fixed value, an optimal value can be found through parameter searches if necessary [3].

Condition (6.16c) ensures that the upscaled polytope $\frac{1}{\gamma}\mathcal{P}$ contains a level curve of the Lyapunov function, $\frac{1}{\gamma}\mathcal{P} \supset \mathcal{E}$, which is a subset of the RA. The level curve is expressed by the ellipsoid:

³Corresponding to the quadratic Carleman model (4.7).

$$\mathcal{E} := \{x \in \mathbb{R}^n : x^T P^{-1} x \leq 1\}$$

(6.16c) ensures therefore that the ellipsoid \mathcal{E} is invariant.

Condition (6.16d) ensures that the polytope \mathcal{P} is a subset of the ellipsoid \mathcal{E} , $\mathcal{E} \supset \mathcal{P}$. This, alongside with (6.16c), ensures that \mathcal{P} is in the RA.

Given the Lyapunov function:

$$V(x) = x^T P^{-1} x$$

with $P > 0$, find $\dot{V}(x) < 0$.

$$\begin{aligned} \dot{V}(x) &= \dot{x}^T P^{-1} x + x^T P^{-1} \dot{x} \\ &= x^T \left\{ (A + BK)^T + ((E_1 \mathcal{K})^T x_{(i)} \cdots (E_n \mathcal{K})^T x_{(i)}) \right\} P^{-1} \\ &\quad + P^{-1} \left[A + BK + \begin{bmatrix} x_{(i)}^T E_1 \mathcal{K} \\ \vdots \\ x_{(i)}^T E_n \mathcal{K} \end{bmatrix} \right] \} x \end{aligned}$$

Pre- and post-multiply by P .

$$\begin{aligned} x^T \left\{ \left[PA^T + PK^T B^T + (PK^T E_1^T x_{(i)} \cdots PK^T E_n^T x_{(i)}) \right] \right. \\ \left. + \left[AP + BKP + \begin{bmatrix} x_{(i)}^T E_1 \mathcal{K} P \\ \vdots \\ x_{(i)}^T E_n \mathcal{K} P \end{bmatrix} \right] \right\} x \end{aligned}$$

Introduce $L = \mathcal{K}P$.

$$\begin{aligned} x^T \left\{ \left[PA^T + L^T B^T + (L^T E_1^T x_{(i)} \cdots L^T E_n^T x_{(i)}) \right] \right. \\ \left. + \left[AP + BL + \begin{bmatrix} x_{(i)}^T E_1 L \\ \vdots \\ x_{(i)}^T E_n L \end{bmatrix} \right] \right\} x \end{aligned}$$

This results in the inequality:

$$PA^T + L^T B^T + (L^T E_1^T x_{(i)} \cdots L^T E_n^T x_{(i)}) + AP + BL + \begin{bmatrix} x_{(i)}^T E_1 L \\ \vdots \\ x_{(i)}^T E_n L \end{bmatrix} < 0 \quad (6.17)$$

By introducing γ we get (6.16e).

Solvers

The LMIs presented are solved using the MATLAB LMI toolboxes YALMIP [13] and SEDUMI [19]. The steps for solving LMIs are:

- The A and B matrices must be available for the solvers.

- Create symbolic decision variables⁴ for the symmetric matrix P and the *full* matrix L .
- Create a list of LMIs/constraints.
- Optimize the LMIs.
- If the problem has a feasible solution, then values for the matrices P and L are found.
- The controller gain is $\mathcal{K} = LP^{-1}$

6.2 Controller for the quadratic Carleman approximation

In Section 6.1, we introduced several concepts that are related to finding the controller gain \mathcal{K} . In this section, those concepts will be applied to the quadratic Carleman approximation. The goal is to create a state feedback controller for this system.

Before applying the constraints introduced in 6.1.3, it is important to identify certain limitations of the system. These limitations are included as additional constraints to those shown in 6.1.3, they ensure that the controller operates within its capabilities. The main limitation of our system is the range at which the valve $LV001$ can operate. It is not possible for the valve to open more than its max capacity, and it is not possible to close the valve more than when it is shut tight. For the signal $u_{LV001}(t)$, these limitations are defined as:

$$0 \leq u_{LV001}(t) \leq 1 \quad (6.18)$$

Recall that for the quadratic Carleman approximation, the state is defined as:

$$z_n(t) = (h_1(t) - h_{1,O})^n \quad (6.19)$$

which means that the input is calculated as:

$$\delta u_{LV001}(t) = u_{LV001}(t) - u_{LV001,O} \quad (6.20)$$

For *Scenario 1*, this means that the signal $\delta u_{LV001}(t)$ cannot exceed the following boundaries:

$$-0.5159 \leq \delta u_{LV001}(t) \leq 0.4841 \quad (6.21)$$

Due to this, we define the upper and lower bound of $\delta u_{LV001}(t)$ to ± 0.45 .

The constraints that ensures that the controller does not exceed these boundaries are defined as:

$$\begin{bmatrix} P & L^T \\ L & \gamma_*^2 \end{bmatrix} > 0 \quad (6.22)$$

where $\gamma_*^2 = 0.45$ is the boundary for the signal $\delta u_{LV001}(t)$ [15].

In Chapter 4, Section 4.3, we concluded that the quadratic Carleman approximation of order $n \geq 4$ was an accurate approximation of the cubic model. Therefore, for the remaining part of this project, the 4th order quadratic Carleman approximation will be considered. The state vector

⁴*sdpvar* in MATLAB.

$z(t)$, state matrix A , input matrix B and the matrices regarding the nonlinear parts E_1, \dots, E_4 for the 4th order quadratic Carleman approximation are reiterated below:

$$z(t) = \begin{bmatrix} z_1(t) \\ z_2(t) \\ z_3(t) \\ z_4(t) \end{bmatrix}, A = \begin{bmatrix} a & c & e & 0 \\ 0 & 2a & 2c & 2e \\ 0 & 0 & 3a & 3c \\ 0 & 0 & 0 & 4a \end{bmatrix}, B = \begin{bmatrix} b \\ 0 \\ 0 \\ 0 \end{bmatrix}, E_1 = \begin{bmatrix} d \\ f \\ 0 \\ 0 \end{bmatrix}, E_2 = \begin{bmatrix} 2b \\ 2d \\ 2f \\ 0 \end{bmatrix}, E_3 = \begin{bmatrix} 0 \\ 3b \\ 3d \\ 3f \end{bmatrix}, E_4 = \begin{bmatrix} 0 \\ 0 \\ 4b \\ 4d \end{bmatrix} \quad (6.23)$$

where a, b, \dots, f are defined as in Section 4.2, Eq.(4.6).

The vertices of the polytope \mathcal{P} are yet to be defined. Since the order of the quadratic Carleman approximation is $n = 4$, this means that the vertices will exist in the 4th dimensional space, where the axes are $[z_1, z_2, z_3, z_4]$. Given equation (6.19), the *value* on the z_1 -axis for each vertex will determine how far the polytope \mathcal{P} reaches from the operating point. A desired range for the controller is $\pm 0.05m$ from the operating point. By defining the *values* for each state at which a vertex lies, we can use the MATLAB function `combvec`⁵ to express the actual coordinates of the vertices.

Consider the following example for a 2nd order quadratic Carleman approximation:

The desired range of our controller is $\pm 0.05m$. Recall that:

$$z_1(t) = h_1(t) - h_{1,O} \quad (6.24)$$

Thus, the two *values* for this state are $[-0.05, 0.05]$. Given equation (6.19), we can see that the *values* for z_2 are $[(-0.05)^2, (0.05)^2]$. However, this action loses the lower bound for z_2 , due to the exponent being an even number. This is why the lower bound is manually set to 0. If the exponent is odd, say for z_3 , then the lower bound is just -0.05^3 . This gives the actual values for z_2 to be $[0, 0.05^2]$. Using the `combvec` function, with these values as inputs, gives the following coordinates:

$$\text{combvec}([-0.05, 0.05], [0, 0.05^2]) = \begin{bmatrix} -0.0500 & 0.0500 & -0.0500 & 0.0500 \\ 0 & 0 & 0.0025 & 0.0025 \end{bmatrix} \quad (6.25)$$

where each column is the coordinates of a vertex. Inserting these vertices in the `vert2con` function gives the half-spaces that contain the polytope. Figure 6.2 shows the plot of this polytope.

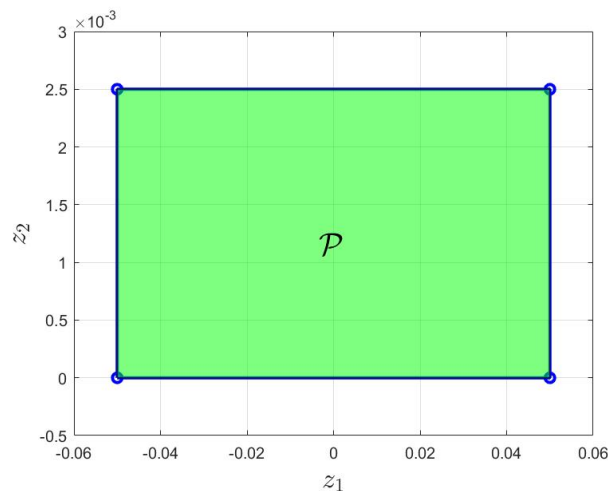


Figure 6.2: Polytope for the 2nd order quadratic Carleman approximation.

⁵`combvec`.

Following the same logic as in the example above, the *values* of the states for the 4th order quadratic Carleman approximation are⁶:

$$\begin{aligned} z_{1,V} &= [-0.05, 0.05], \quad z_{2,V} = [\approx 0, 0.0025], \\ z_{3,V} &= [-0.000125, 0.000125], \quad z_{4,V} = [\approx 0, 0.00000625] \end{aligned} \quad (6.26)$$

Inserting these values in the `combvec` function yields the following vertices:

$$\begin{aligned} x_1 &= \begin{bmatrix} -0.0500 \\ -0.0003 \\ -0.0001 \\ -0.0000 \end{bmatrix}, \quad x_2 = \begin{bmatrix} 0.0500 \\ -0.0003 \\ -0.0001 \\ -0.0000 \end{bmatrix}, \quad x_3 = \begin{bmatrix} -0.0500 \\ 0.0025 \\ -0.0001 \\ -0.0000 \end{bmatrix}, \quad x_4 = \begin{bmatrix} 0.0500 \\ 0.0025 \\ -0.0001 \\ -0.0000 \end{bmatrix} \\ x_5 &= \begin{bmatrix} -0.0500 \\ -0.0003 \\ 0.0001 \\ -0.0000 \end{bmatrix}, \quad x_6 = \begin{bmatrix} 0.0500 \\ -0.0003 \\ 0.0001 \\ -0.0000 \end{bmatrix}, \quad x_7 = \begin{bmatrix} -0.0500 \\ 0.0025 \\ 0.0001 \\ -0.0000 \end{bmatrix}, \quad x_8 = \begin{bmatrix} 0.0500 \\ 0.0025 \\ 0.0001 \\ -0.0000 \end{bmatrix} \\ x_9 &= \begin{bmatrix} -0.0500 \\ -0.0003 \\ -0.0001 \\ 0.0000 \end{bmatrix}, \quad x_{10} = \begin{bmatrix} 0.0500 \\ -0.0003 \\ -0.0001 \\ 0.0000 \end{bmatrix}, \quad x_{11} = \begin{bmatrix} -0.0500 \\ 0.0025 \\ -0.0001 \\ 0.0000 \end{bmatrix}, \quad x_{12} = \begin{bmatrix} 0.0500 \\ 0.0025 \\ -0.0001 \\ 0.0000 \end{bmatrix} \\ x_{13} &= \begin{bmatrix} -0.0500 \\ -0.0003 \\ 0.0001 \\ 0.0000 \end{bmatrix}, \quad x_{14} = \begin{bmatrix} 0.0500 \\ -0.0003 \\ 0.0001 \\ 0.0000 \end{bmatrix}, \quad x_{15} = \begin{bmatrix} -0.0500 \\ 0.0025 \\ 0.0001 \\ 0.0000 \end{bmatrix}, \quad x_{16} = \begin{bmatrix} 0.0500 \\ 0.0025 \\ 0.0001 \\ 0.0000 \end{bmatrix} \end{aligned} \quad (6.27)$$

The scalar γ is set to:

$$\gamma = 0.1$$

When solving the constraints shown in 6.1.3, Eq. (6.16c) will be excluded from these calculations. The reason for this will be further discussed in Chapter 9. This implies that the solved controller can not guarantee that \mathcal{E} is invariant.⁷ Since (6.16c) will not be included in this part, this means that there is no need to present the half-spaces a_k . With that, all of the variables that are required in order to solve the constrains for \mathcal{K} are now defined.

Solving the constrains (6.16a)-(6.16e), with the exclusion of (6.16c), together with the additional constraint (6.22), results in the following controller gain⁸:

$$\mathcal{K} = [0.2345 \quad 0.0129 \quad -0.0464 \quad -0.0325] \quad (6.28)$$

With the \mathcal{K} matrix defined, it is now possible to rewrite the quadratic Carleman approximation, by replacing $\delta u_{LV001}(t)$ with $\mathcal{K}z(t)$:

$$\dot{z}(t) = Az(t) + BKz(t) + \begin{bmatrix} z^T(t)E_1 \\ z^T(t)E_2 \\ z^T(t)E_3 \\ z^T(t)E_4 \end{bmatrix} \mathcal{K}z(t) \quad (6.29)$$

⁶Due to numerical issues, the lower bound of the states $z_n(t)$ where n is an even number, are set to small negative numbers that are approximately zero.

⁷The consequences of \mathcal{E} not being invariant is that it cannot be guaranteed that a solution of the inequalities starting inside \mathcal{E} stays inside \mathcal{E} as $t \rightarrow \infty$, which can lead to instability/divergence.

⁸The procedure of how to solve the different constraints are explained in 6.1.3.

To verify that the state feedback controller works, Equation (6.29) is simulated. The system will start with an initial condition of $0.05m$, which is the same as:

$$h_1(t) = z_1(t) + h_{1,O} = 0.05m + 0.25m = 0.3m \quad (6.30)$$

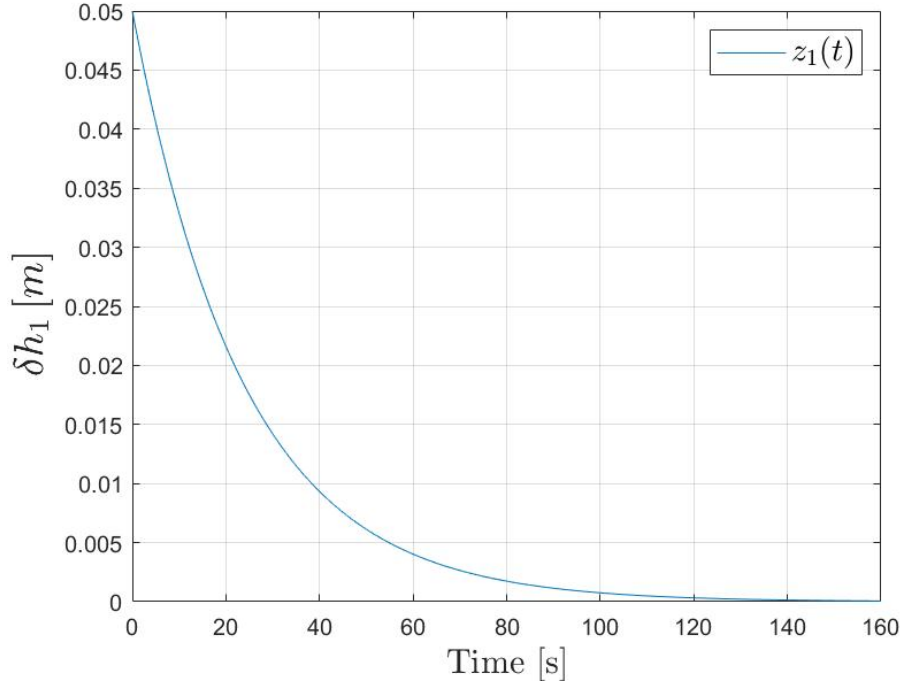


Figure 6.3: Simulation of Eq. (6.29), with initial condition equal to $0.05m$.

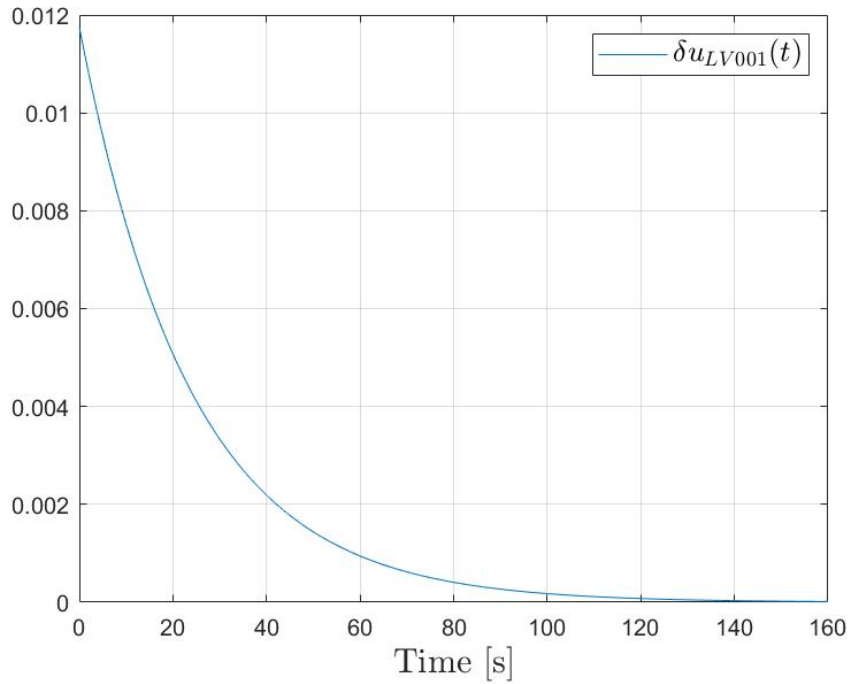


Figure 6.4: Signal $\delta u_{LV001}(t)$, calculated by $\mathcal{K}z(t)$.

Figure 6.3 shows that the state $z_1(t)$ converges to zero, which is equivalent to the water level converging to its operating point of $0.25m$. Figure 6.4 shows that the signal $\delta u_{LV001}(t)$ also converges to zero, which means that the signal $u_{LV001}(t)$ converges to its operating point of 0.5159 .

6.3 Controller for the quadratic Carleman approximation using two input variables

Up until now, this project has only considered the valve $LV001$ as an actuator. However, the system does have the option of regulating the contribution of the pump $PA001$ as well. Introducing the pump into the quadratic Carleman approximation leads to small adjustments in the input vector $u(t)$, input matrix B and the matrices regarding the nonlinear parts E_1, E_2, \dots, E_n . These adjusted variables are now defined as⁹:

$$u(t) = \begin{bmatrix} u_{LV001}(t) \\ u_{PA001}(t) \end{bmatrix}, B = \begin{bmatrix} b & g \\ 0 & 0 \\ 0 & 0 \\ 0 & 0 \end{bmatrix}, E_1 = \begin{bmatrix} d & 0 \\ f & 0 \\ 0 & 0 \\ 0 & 0 \end{bmatrix}, E_2 = \begin{bmatrix} 2b & 2g \\ 2d & 0 \\ 2f & 0 \\ 0 & 0 \end{bmatrix}, E_3 = \begin{bmatrix} 0 & 0 \\ 3b & 3g \\ 3d & 0 \\ 3f & 0 \end{bmatrix}, E_4 = \begin{bmatrix} 0 & 0 \\ 0 & 0 \\ 4b & 4g \\ 4d & 0 \end{bmatrix} \quad (6.31)$$

where:

$$g = \left. \frac{\partial f}{\partial u_{PA001}} \right|_O \quad (6.32)$$

All of the other variables that were defined in Section 6.2 remain unchanged.

With this new actuator, it is again necessary to identify the limitation of the system. After introducing the pump to the controller, it is now important to define certain constraints such that the controller operates within its capability. It is not possible for the pump to supply the tank with more than a certain amount of water. The least amount of water that the pump can supply the tank with is zero. The pump cannot extract water from the tank. Given the pump characteristics, shown in Figure 2.4, one can see that the pump stops adding water to the tank at $u_{PA001}(t) = 0.45$ ¹⁰. The maximum water that the pump can supply occurs at $u_{PA001}(t) = 1$. This gives the following constraint:

$$0.45 \leq u_{PA001}(t) \leq 1 \quad (6.33)$$

The quadratic Carleman approximation works with the signal:

$$\delta u_{PA001}(t) = u_{PA001}(t) - u_{PA001,O} \quad (6.34)$$

where $u_{PA001,O} = 0.65$. For this reason, we define the upper and lower bound of $\delta u_{PA001}(t)$ to ± 0.2 ¹¹. This gives another additional constraint, (6.22), where $\gamma_*^2 = 0.2$.

To find the controller gain \mathcal{K} , we solve the same constraints as in Section 6.2, with the addition of the saturation constraint for the pump. This results in the following:

$$\mathcal{K} = \begin{bmatrix} 0.2345 & -0.0076 & -0.0446 & -0.0227 \\ -0.1029 & -0.0223 & 0.0178 & 0.0177 \end{bmatrix} \quad (6.35)$$

Replacing the input vector $u(t)$ with $\mathcal{K}z(t)$, results in a quadratic system, as shown by (6.29). Verification of the controller is done by simulating this system. The initial level is set to $0.05m$.

⁹Note that these matrices only apply for the 4th order quadratic Carleman approximation, which is still being regarded from the previous section.

¹⁰The pump needs a value of at least 0.45 to pump water up to the tank, any lower values and the pump will not be able to pump water up to the intake of the tank.

¹¹As (6.22) only works in symmetrical ranges.

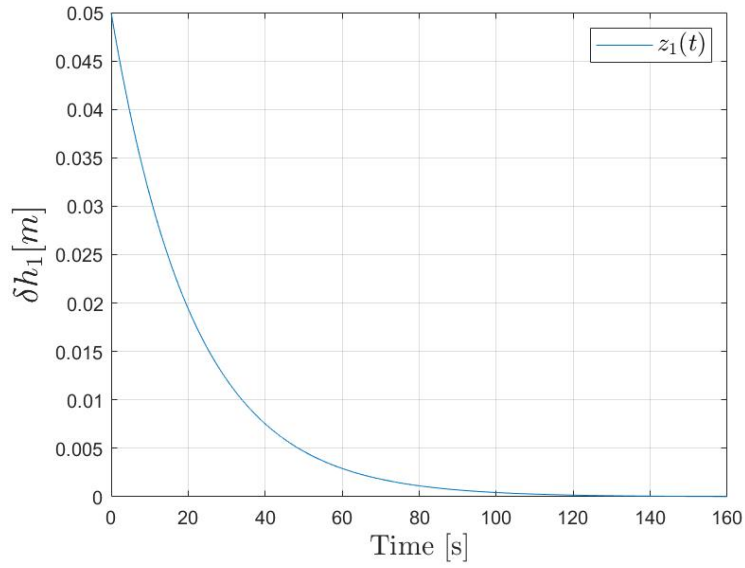


Figure 6.5: 4th order quadratic Carleman approximation with two actuator.

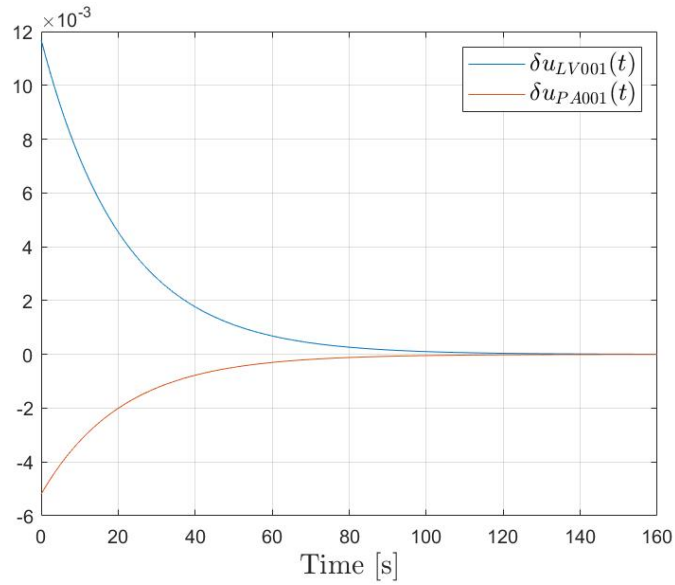


Figure 6.6: Signal $u(t)$, calculated by $\mathcal{K}z(t)$.

Note that the response in Figure 6.5 is slightly faster than the response in Figure 6.3. However, the main benefit of creating the controller gain \mathcal{K} with two actuators, is that the degree of freedom is increased. This means that the probability of finding a solution to the constraints in (6.16) is higher.

The rate of convergence can be added as an additional constraint. By introducing an α , we can make the controller less conservative, leading in faster responses. In [3], it is introduced with:

$$2\alpha P + AP + PA^T + BL + L^T B^T < 0$$

This implementation of α amplifies the linear part of the quadratic Carleman approximation, which makes the quadratic parts of the system negligible. This is the equivalent to the linearized Carleman approximation, which was proven to be uncontrollable in the previous chapter. Therefore, we include α to the vertex that corresponds to the maximum positive deviation from the

equilibrium point. This makes the linear part impact the system the least, allowing for a bigger α and more feasible solutions.

$$\begin{aligned} & \gamma(AP + PA^T + BL + L^T B^T) + (L^T G_1^T x_{(i)} \cdots L^T G_n^T x_{(i)}) \\ & + \begin{bmatrix} x_{(i)}^T G_1 L \\ \vdots \\ x_{(i)}^T G_n L \end{bmatrix} + 2\gamma P\alpha < 0 \end{aligned} \quad (6.36)$$

$$i = 1, 2, \dots, p$$

Equation (6.36) shows the additional constraint that includes α for the maximum positive vertex. By further inspecting the vertices in (6.27), it is possible to see that x_{16} is the vertex that corresponds to the maximum positive deviation from the equilibrium point. The biggest α that allows for a feasible solution is:

$$\alpha = 0.096 \quad (6.37)$$

The constraints are solved as usual, with the addition of (6.36), which results in the following controller gain:

$$\mathcal{K} = \begin{bmatrix} 1.3312 & -0.3827 & -1.4645 & 0.2560 \\ -0.0861 & -0.2364 & -0.0611 & 0.5122 \end{bmatrix} \quad (6.38)$$

The input vector $u(t)$ is replaced by $Kz(t)$, which gives the quadratic Carleman approximation the same form as (6.29). To verify the quadratic controller, the quadratic Carleman approximation is simulated with an initial condition of $0.05m$.

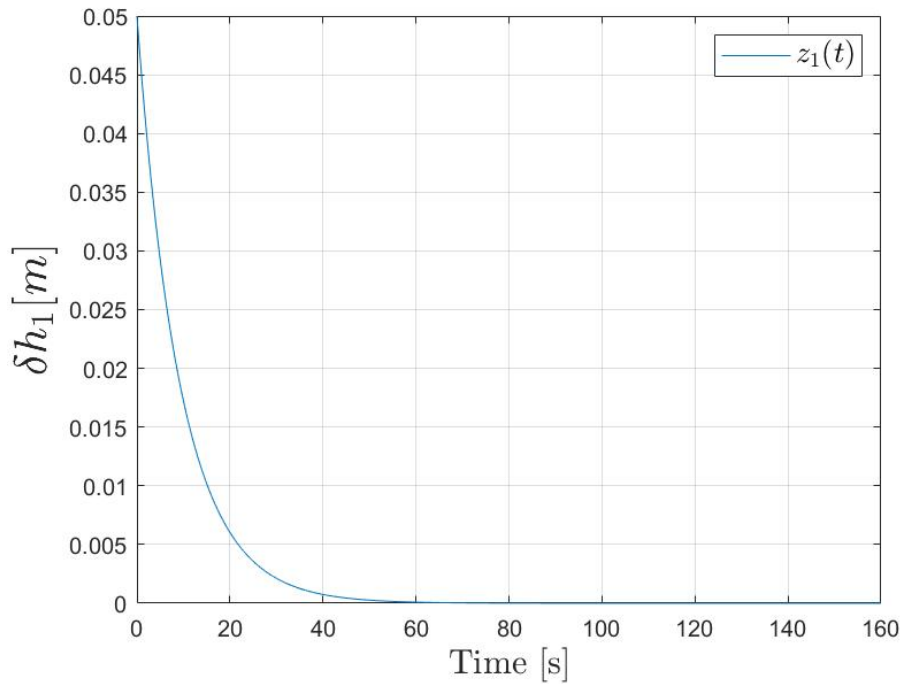


Figure 6.7: 4th order quadratic Carleman approximation with two actuator and implemented convergence rate.

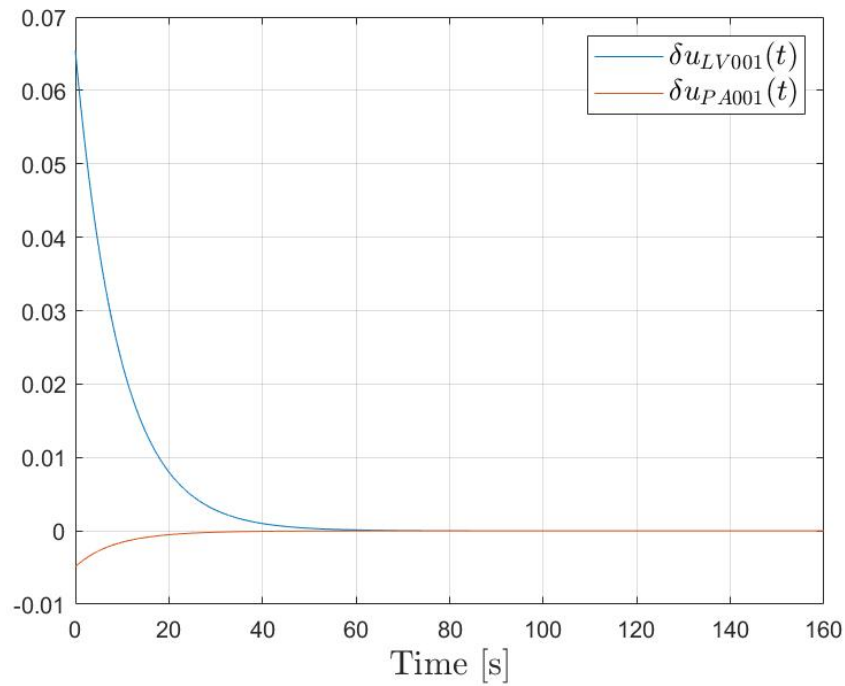


Figure 6.8: Signal $u(t)$, calculated by $\mathcal{K}z(t)$ with implemented convergence rate.

Comparing the response of Figure 6.7 with the response of Figure 6.5, we see that the time it takes for the system to converge to its operating point is greatly reduced. The signal $\delta u_{LV001}(t)$ is also less conservative with its contribution. These improvements makes for this final iteration of the quadratic controller to be considered further in the next chapter.

Chapter 7

Experimental results

In Chapter 6, a quadratic controller was calculated for the 4th order quadratic Carleman approximation. There were presented several results, regarding different iterations of the controller. The conclusion was that the controller that took into account two input variables and the convergence rate α was the superior controller. This chapter will look to apply this controller to the two-tank system, and observe how well the controller works in a practical setting. Section 7.1 will describe the approach to implementing the controller to the system, and describe the procedure of how the data was collected. Section 7.2 will analyze and discuss the obtained results from the experiments. This chapter will only include results from *Scenario 1*. For the results regarding *Scenario 2*, see Appendix D.

7.1 Application of the quadratic controller on to the two-tank system

In this project, the Simulink file that connects to the system was made accessible by [8]. This file is slightly modified, such that the input vector $u(t)$ follows the quadratic controller. In Chapter 6, the controller gain was calculated to be:

$$\mathcal{K} = \begin{bmatrix} 1.3312 & -0.3827 & -1.4645 & 0.2560 \\ -0.0861 & -0.2364 & -0.0611 & 0.5122 \end{bmatrix} \quad (7.1)$$

This gives the following δ input vector:

$$\delta u(t) = \begin{bmatrix} \delta u_{LV001}(t) \\ \delta u_{PA001}(t) \end{bmatrix} = \mathcal{K}z(t) = \mathcal{K} \begin{bmatrix} z_1(t) \\ z_2(t) \\ z_3(t) \\ z_4(t) \end{bmatrix} = \mathcal{K} \begin{bmatrix} h_1(t) - h_{1,O} \\ (h_1(t) - h_{1,O})^2 \\ (h_1(t) - h_{1,O})^3 \\ (h_1(t) - h_{1,O})^4 \end{bmatrix} \quad (7.2)$$

Note that the quadratic controller was made with respect to the quadratic Carleman approximation, which works with δ -variables, i.e. $\delta u_{LV001}(t) = u_{LV001}(t) - u_{LV001,O}$ and $\delta u_{PA001}(t) = u_{PA001}(t) - u_{PA001,O}$. Therefore, the input vector $u(t)$ of the *two-tank system*, is calculated as:

$$u(t) = u_O + \delta u(t) = \begin{bmatrix} u_{LV001,O} \\ u_{PA001,O} \end{bmatrix} + \begin{bmatrix} -\delta u_{LV001}(t) \\ \delta u_{PA001}(t) \end{bmatrix} \quad (7.3)$$

Note that the variable $\delta u_{LV001}(t)$ is inverted when calculating the input vector $u(t)$. The reason for this is that the signal $u_{LV001}(t)$ has an inverse correlation with the water level $h_1(t)$. If

the signal $u_{LV001}(t)$ is increased, then the valve $LV001$ will open more, which leads to a reduction in the water level $h_1(t)$.

The procedure of the experiments is as shown in Table 7.1¹. The two first periods of the procedure are used to drive the system to some desired initial condition before the quadratic controller is implemented.

Period [s]	$u_{PA001}(t)$	$u_{LV001}(t)$	Description
$0 \leq t \leq 10$	0	1	Empty the tank by turning off $PA001$ and opening $LV001$ to the max.
$10 \leq t \leq 30$	$0 \leq \lambda \leq 1$	0	Fill up the tank manually by closing $LV001$ and turning $PA001$ on.
$30 \leq t$	$u_{PA001,O} + \delta u_{PA001}(t)$	$u_{LV001,O} - \delta u_{LV001}(t)$	Introduce the quadratic controller to the system.

Table 7.1: Experiment procedure.

7.2 Analysis of the experimental results

Following the procedure from Table 7.1, and introducing the controller when $h_1(t) \approx 0.3m$ resulted in the data presented in Figure 7.1.

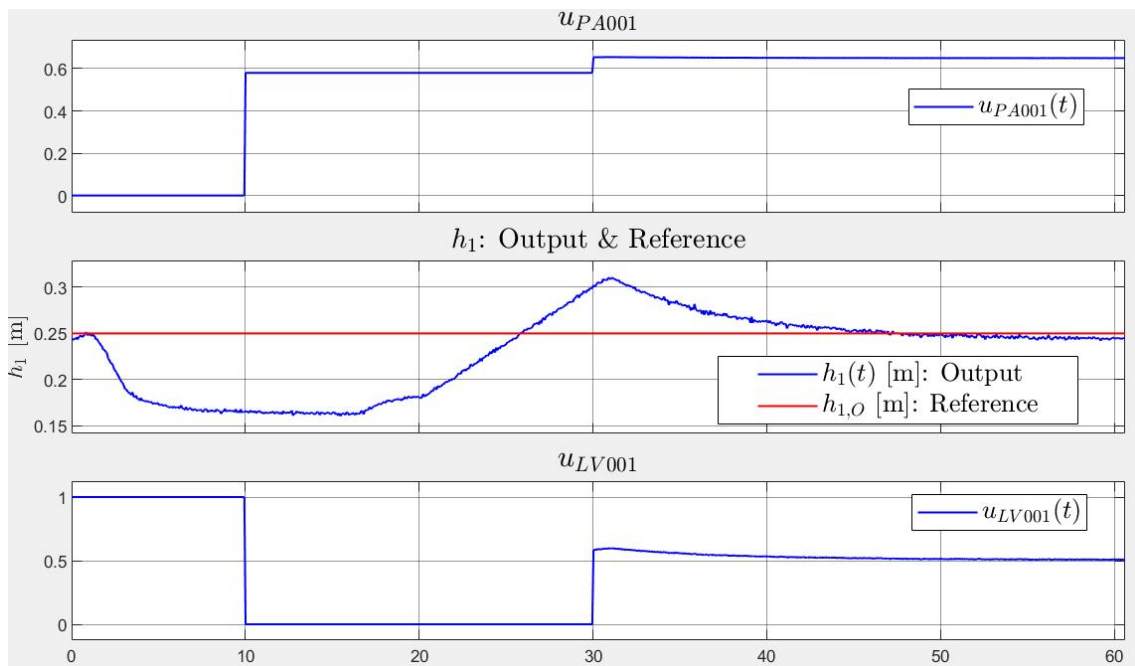


Figure 7.1: Experimental results from the quadratic controller.

Figure 7.1 shows that the system, with the introduced controller, converges to the operating point of $0.25m$. The controller is introduced to the system when the water level is $h_1(t) \approx 0.3m$, which is within the polytope \mathcal{P} that the controller was designed for. It looks as if the signal $u_{PA001}(t)$ is constant, however, this is not the case. The explanation to this can be found by further analysing the controller gain (7.1). The 2nd row vector in (7.1), which is the gain for $\delta u_{PA001}(t)$, consists mostly of values that are of the order 10^{-1} or smaller. This is why the contribution of $\delta u_{PA001}(t)$ is so small when compared to $\delta u_{LV001}(t)$, which explains why it looks as if $u_{PA001}(t)$ is constant at $u_{PA001,O}$.

¹ λ is an arbitrary value, depending on the desired water level before the quadratic controller is implemented.

An additional experiment is performed, where the goal is to test the controller when the water level $h_1(t)$ is outside of the polytope \mathcal{P} . In this case, the controller is introduced to the system when $h_1(t) \approx 0.5m$, which is $0.2m$ outside of the reach of the polytope \mathcal{P} that the controller was designed for. This means that it is not possible to guarantee that the controller will work within its capabilities and not saturate the input variables. Figure 7.2 shows the results of this experiment.

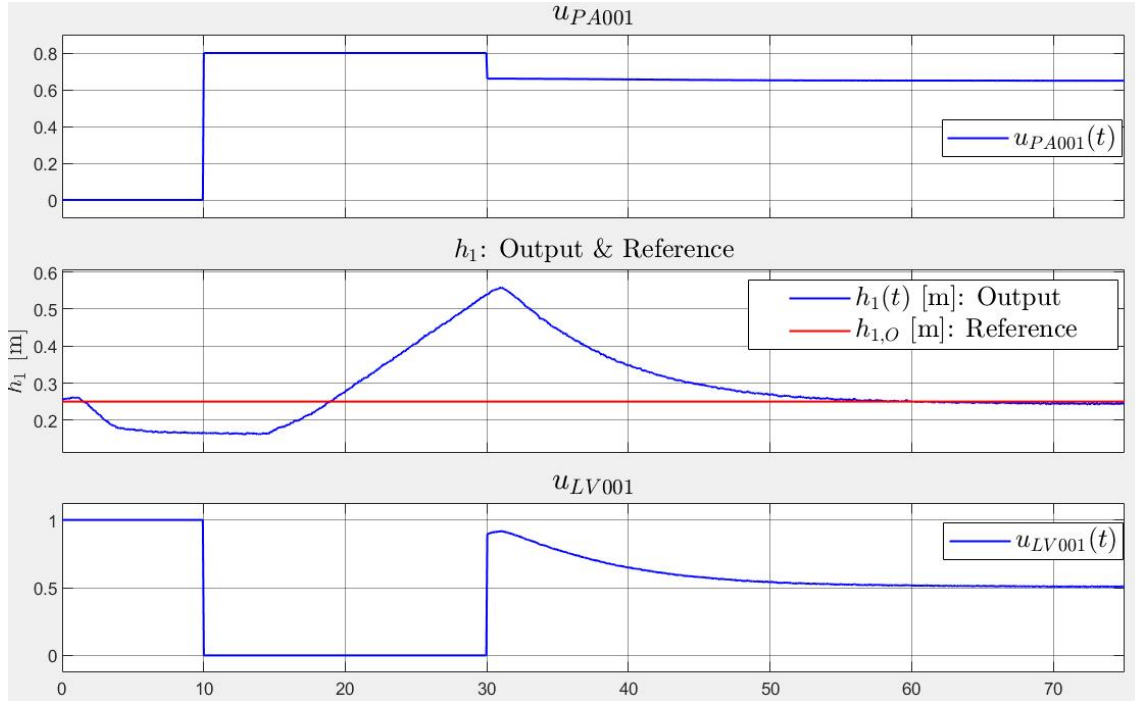


Figure 7.2: Experimental results from the quadratic controller.

Figure 7.2 shows that, even though the controller is working outside of its designed region, the system still converges to its operating point. In this case, the controller does not saturate the input variables. However, an equivalent experiment was performed for *Scenario 2*², where the controller demanded that $u_{LV001}(t) < 0$, which is not possible.

Figure 7.1, together with Figure D.1, shows that the controller works symmetrically, and that the desired output is achieved in both cases.

²See Figure D.2.

Part IV

Conclusions and future work

Chapter 8

Conclusions

The main goal of this thesis was to design controllers for the two-tank process, using models derived with the Carleman embedding technique. A hypothesis is that designing a controller based upon the linearized Carleman approximation, derived from a higher order Taylor approximation, would lead to a better controller than one based upon the Taylor linearization.

The conclusions obtained in this thesis are the following:

- Among the higher order Taylor approximations, the cubic model was concluded to be best suited for the Carleman approximation when applied to the two-tank system.

- The Carleman embedding technique was applied to the cubic model, resulting in a quadratic Carleman approximation. Linearizing this approximation resulted in an uncontrollable system. Designing a controller for this system would be the equivalent of designing a controller for the Taylor linearized model. Therefore, design of a controller for the quadratic Carleman approximation was explored instead.

- The most successful controller design included two input variables, which resulted in a wider feasibility of the linear matrix inequalities. The convergence rate α was also included in the control design, which made the response of the system faster.

- The main drawback in this controller design was numerical issues related to solving the LMIs. Therefore, an exclusion of the condition (6.16c) ensuring invariancy had to be considered. However, this could lead to divergence in some cases. It is also worth mentioning that in order to prevent saturation in the input variables, symmetrical ranges must be considered. This limits the input variables, leading to a slower response.

- There is not necessarily a clear advantage in designing a controller for the quadratic Carleman approximation, but this approach has some potential. A quadratic controller fulfilling the criterions in (6.16), will ensure stability in a given region that the controller was designed for.

Chapter 9

Future work

Further improvements and interesting aspects to be pursued:

- Improvements on the design of the polytopes could be explored further in [9]. Better constructed polytopes would lead to a more feasible controller design.
- The controller input limitations (6.22) on $u_{PA001}(t)$ and $u_{LV001}(t)$ only work in symmetrical ranges. This means that it does not use the whole range of the inputs available, leading to a potentially slower response and less feasible controller design.
- Numerical issues lead to poor feasibility especially when including condition (6.16c). Scaling the variables from meters to centimeters could have a positive effect on the feasibility of the controller design, leading to less numerical issues.
- An interesting scenario for the controller design was briefly investigated, where the quadratic Carleman approximation is truncated at $n = 2$. The polytope \mathcal{P} is modified to be strictly positive.

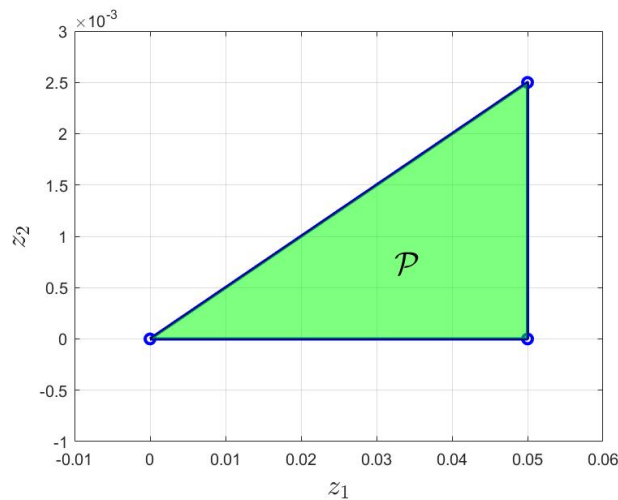


Figure 9.1: Modified polytope.

α is introduced to the vertex with the maximum positive deviation from the equilibrium point. This controller results in a faster response and a bigger controller gain, in addition to being feasible when including constraint (6.16c)¹. The drawbacks of this is that it only works for positive δh_1 . A suggested workaround would be to introduce a type of switching which has one controller for positive and one for negative δh_1 . This would require some modifications of the Lyapunov theory to ensure that stability is preserved in spite of the switching.

¹See Appendix E.

- The tank system is open-loop stable, therefore, the benefits of a quadratic controller become unclear. Testing a quadratic Carleman approximation on a system that is not open-loop stable could be explored. The benefit would be that the quadratic controller would ensure stability in a given region around the equilibrium point.

- A parameter search for optimal γ could be conducted to more easily find feasible solutions and a bigger α [3].

- The nonlinear dynamical model of tank 2 was derived in Chapter 2. However, this model was not considered. It would be interesting to see if the linearized Carleman approximation of this dynamical model is controllable.

Bibliography

- [1] *Open-loop-and-closed-loop-feedback-control*. Read: 27.04.2021, [Available here](#).
- [2] *Quadratic Lyapunov function*. Read: 02.05.2021, [Available here](#).
- [3] F. Amato, R. Ambrosino, M. Ariola, C. Cosentino, and A. Merola. State feedback control of nonlinear quadratic systems. In *2007 46th IEEE Conference on Decision and Control*, pages 1699–1703, 2007.
- [4] F. Amato, C. Cosentino, and A. Merola. On the region of attraction of nonlinear quadratic systems. *Automatica*, 43(12):2119–2123, 2007.
- [5] Arash Amini, Qiyu Sun, and Nader Motee. Carleman state feedback control design of a class of nonlinear control systems. *IFAC-PapersOnLine*, 52(20):229–234, 2019. 8th IFAC Workshop on Distributed Estimation and Control in Networked Systems NECSYS 2019.
- [6] Bellman and Richardson. *On some questions arising in the approximate solution of nonlinear differential equations*, 1963. Read: 11.05.2021, [Available here](#).
- [7] Tormod Drenngstig. *ELE320 totank1 motivasjon modellering*, 2020.
- [8] Tormod Drenngstig. *ELE320 Totankøving 4: Bestemmelse av regulatorparametre og regulering av totankprosessen*, 2020.
- [9] Christoph Fünfzig, Dominique Michelucci, and Sebti Foufou. Polytope-based computation of polynomial ranges. *Computer Aided Geometric Design*, 29:18–29, 01 2012.
- [10] Finn Haugen. *Dynamiske systemer, modellering, analyse og simulering*. Vigmostad & Bjørke AS, 2016.
- [11] Michael Kleder. *VERT2CON - vertices to constraints*, 2021. Read: 06.05.2021, [Available here](#).
- [12] Willi-hans Kowalski, Krzysztof Steeb. *Nonlinear Dynamical Systems And Carleman Linearization*. World Scientific, 1991.
- [13] J. Löfberg. Yalmip : A toolbox for modeling and optimization in matlab. In *In Proceedings of the CACSD Conference*, Taipei, Taiwan, 2004.
- [14] Dorota Mozyska and Zbigniew Bartosiewicz. On carleman linearization of linearly observable polynomial systems. *Mathematical Control Theory and Finance*, 01 2008.
- [15] T Nguyen and Faryar Jabbari. Output feedback controllers for disturbance attenuation with actuator amplitude and rate saturation. *Automatica*, 36(9):1339–1346, 2000.
- [16] Andreas Rauh, Johanna Minisini, and Harald Aschemann. Carleman linearization for control and for state and disturbance estimation of nonlinear dynamical processes. *IFAC Proceedings Volumes*, 42(13):455–460, 2009. 14th IFAC Conference on Methods and Models in Automation and Robotics.
- [17] W.-H. Steeb. A note on carleman linearization. *Physics Letters A*, 140(6):336–338, 1989.
- [18] W.-H Steeb and F Wilhelm. Non-linear autonomous systems of differential equations and carleman linearization procedure. *Journal of Mathematical Analysis and Applications*, 77(2):601–611, 1980.

- [19] Jos F. Sturm. *SEDUMI-Coral lab*, 2021. Read: 06.05.2021, [Available here](#).
- [20] Wikipedia. *Control Theory*. Read: 25.04.2021, [Available here](#).
- [21] Wikipedia. *Convex hull*. Read: 06.05.2021, [Available here](#).
- [22] Wikipedia. *Polytope*. Read: 06.05.2021, [Available here](#).
- [23] Wikipedia. *Rank linear algebra*. Read: 25.04.2021, [Available here](#).
- [24] Wikipedia. *Taylor series*. Read: 20.03.2021, [Available here](#).
- [25] Wikipedia. *Vertex (geometry)*. Read: 06.05.2021, [Available here](#).
- [26] Wikipedia. *Controllability and observability*, 2021. Read: 07.05.2021, [Available here](#).
- [27] Wikipedia. *Optimization problem*, 2021. Read: 11.05.2021, [Available here](#).

Part V

Appendices

Appendix A

Taylor model comparison for Scenario 2

Intervals under consideration for *Scenario 2*:

[0.70, 0.80] for $h_1(t)$ and [0.26, 0.46] for $u_{LV001}(t)$

The Taylor models for *Scenario 2* are as follows:

Linear model:

$$\delta\dot{h}_1(t) = -0.0111 (h_1(t) - 0.75) - 0.0683 (u_{LV001}(t) - 0.3666) \quad (\text{A.1})$$

Quadratic model:

$$\begin{aligned} \delta\dot{h}_1(t) = & -0.0111 (h_1(t) - 0.75) - 0.0683 (u_{LV001}(t) - 0.3666) \\ & + 0.0035 (h_1(t) - 0.75)^2 - 0.0427 (h_1(t) - 0.75) (u_{LV001}(t) - 0.3666) \end{aligned} \quad (\text{A.2})$$

PQ_A model:

$$\begin{aligned} \delta\dot{h}_1(t) = & -0.0111 (h_1(t) - 0.75) - 0.0683 (u_{LV001}(t) - 0.3666) \\ & + 0.0035 (h_1(t) - 0.75)^2 \end{aligned} \quad (\text{A.3})$$

PQ_B model:

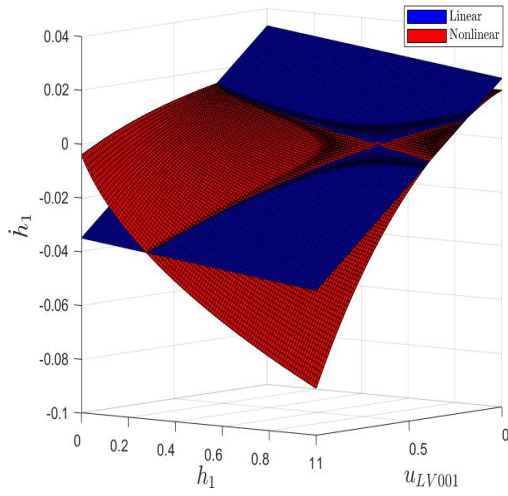
$$\begin{aligned} \delta\dot{h}_1(t) = & -0.0111 (h_1(t) - 0.75) - 0.0683 (u_{LV001}(t) - 0.3666) \\ & - 0.0427 (h_1(t) - 0.75) (u_{LV001}(t) - 0.3666) \end{aligned} \quad (\text{A.4})$$

Cubic model:

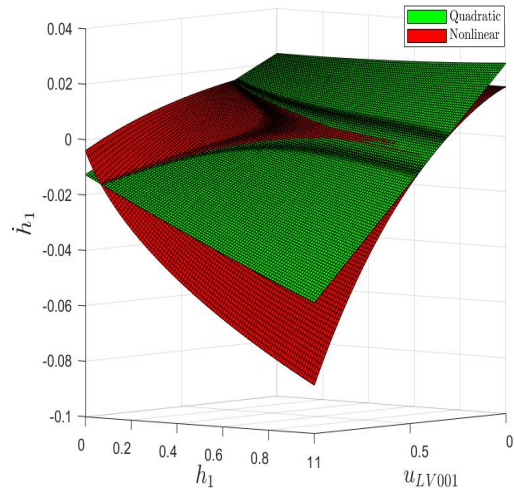
$$\begin{aligned} \delta\dot{h}_1(t) = & -0.0111 (h_1(t) - 0.75) - 0.0683 (u_{LV001}(t) - 0.3666) \\ & + 0.0035 (h_1(t) - 0.75)^2 - 0.0427 (h_1(t) - 0.75) (u_{LV001}(t) - 0.3666) \\ & - 0.0022 (h_1(t) - 0.75)^3 + 0.0133 (h_1(t) - 0.75)^2 (u_{LV001}(t) - 0.3666) \end{aligned} \quad (\text{A.5})$$

5th order model:

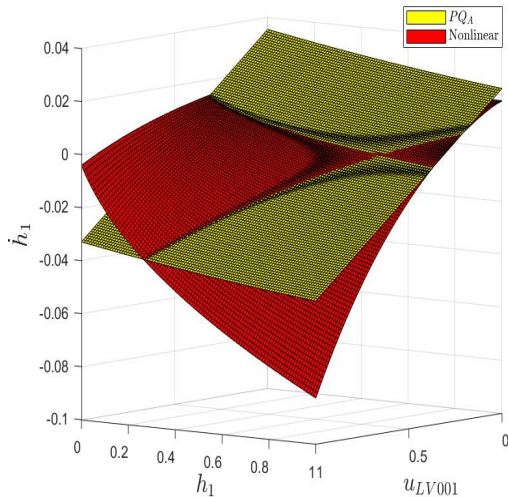
$$\begin{aligned} \delta\dot{h}_1(t) = & -0.0111 (h_1(t) - 0.75) - 0.0525 (u_{LV001}(t) - 0.3666) \\ & + 0.0035 (h_1(t) - 0.75)^2 - 0.0427 (h_1(t) - 0.75) (u_{LV001}(t) - 0.3666) \\ & - 0.0022 (h_1(t) - 0.75)^3 + 0.0133 (h_1(t) - 0.75)^2 (u_{LV001}(t) - 0.3666) \\ & + 0.0017 (h_1(t) - 0.75)^4 - 0.0083 (h_1(t) - 0.75)^3 (u_{LV001}(t) - 0.3666) \\ & - 0.0015 (h_1(t) - 0.75)^5 + 0.0065 (h_1(t) - 0.75)^4 (u_{LV001}(t) - 0.3666) \end{aligned} \quad (\text{A.6})$$



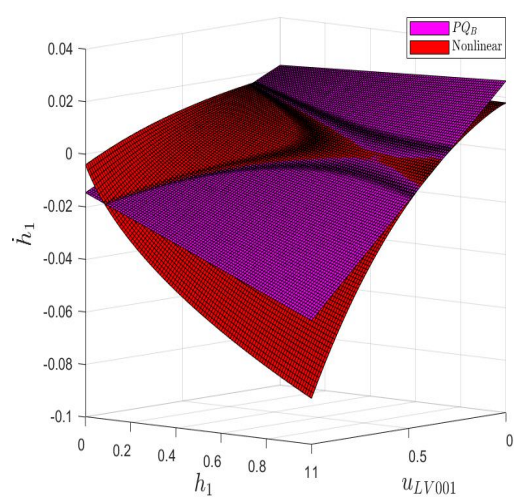
(a) Linear and nonlinear model.



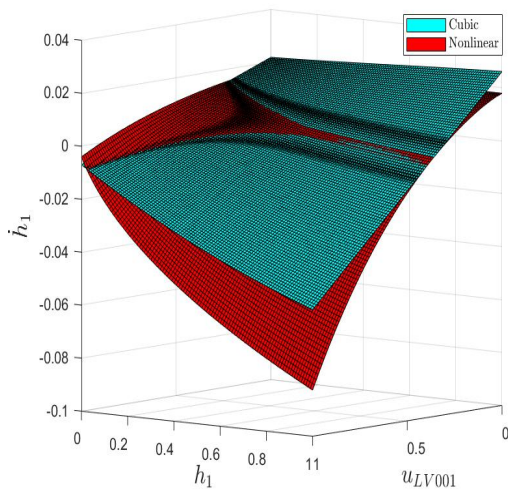
(b) Quadratic and nonlinear model.



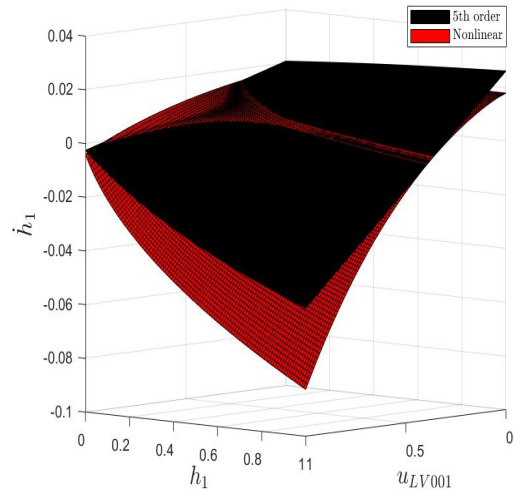
(c) PQ_A and nonlinear model.



(d) PQ_B and nonlinear model.

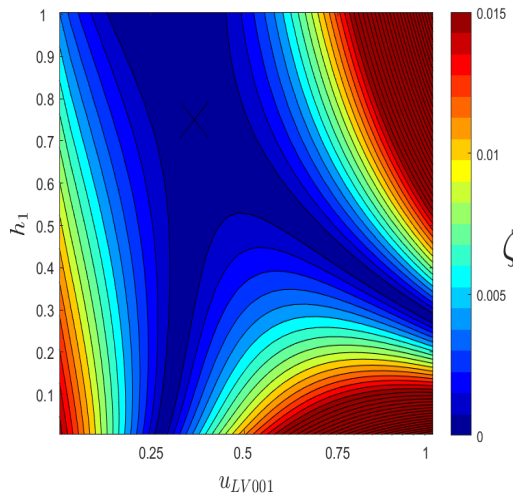


(e) Cubic and nonlinear model.

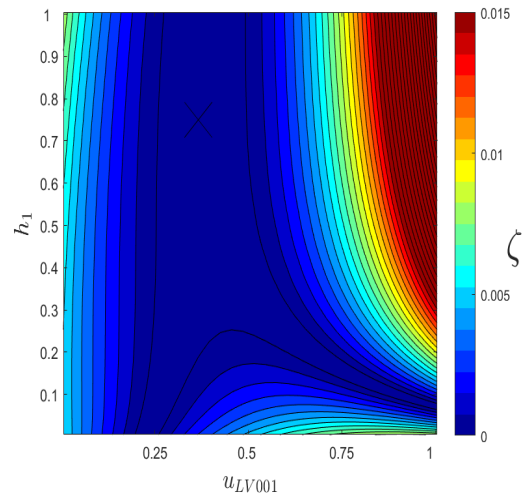


(f) 5th order and nonlinear model.

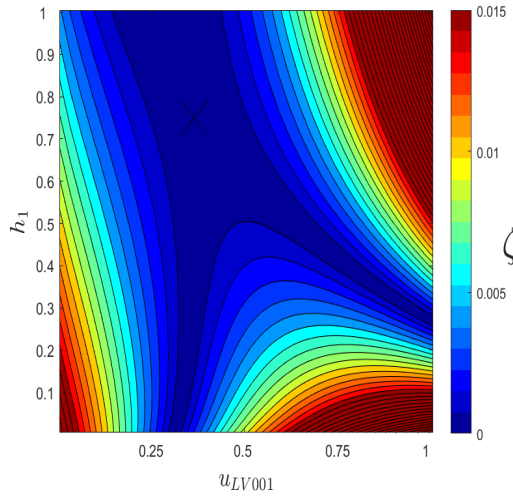
Figure A.1: 3-D plots of the Taylor models and the nonlinear model as reference.



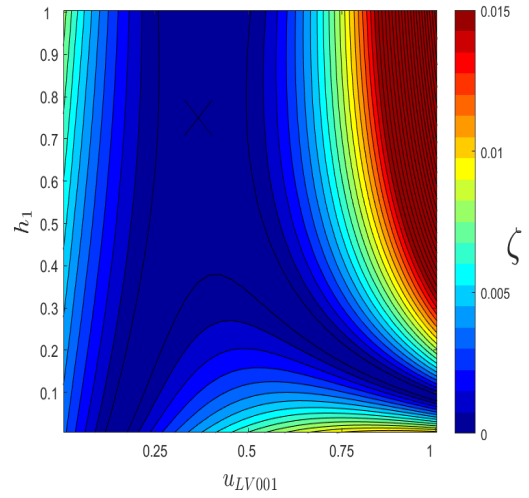
(a) Linear and nonlinear model.



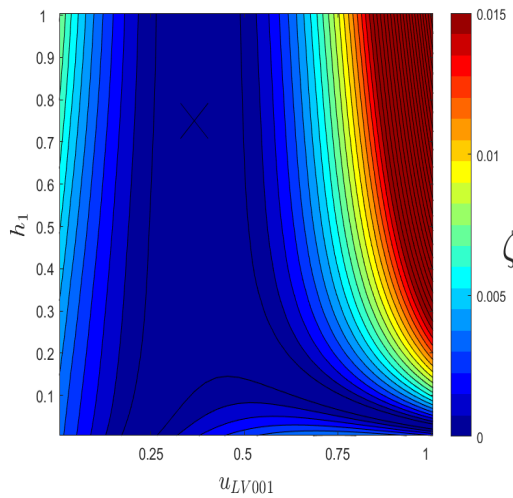
(b) Quadratic and nonlinear model.



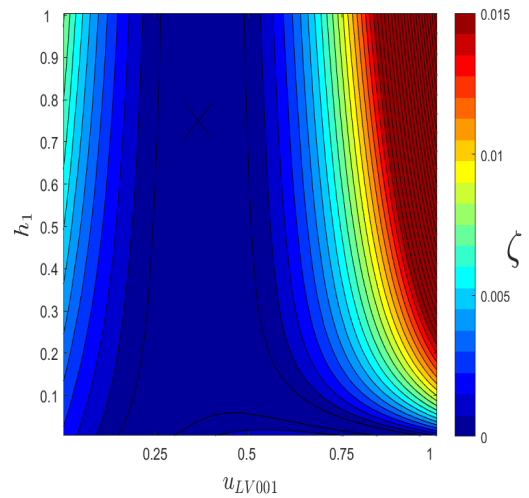
(c) P_{Q_A} and nonlinear model.



(d) P_{Q_B} and nonlinear model.



(e) Cubic and nonlinear model.



(f) 5th order and nonlinear model.

Figure A.2: Contour plots of the Taylor models and the nonlinear model, where ζ is given by (3.32).

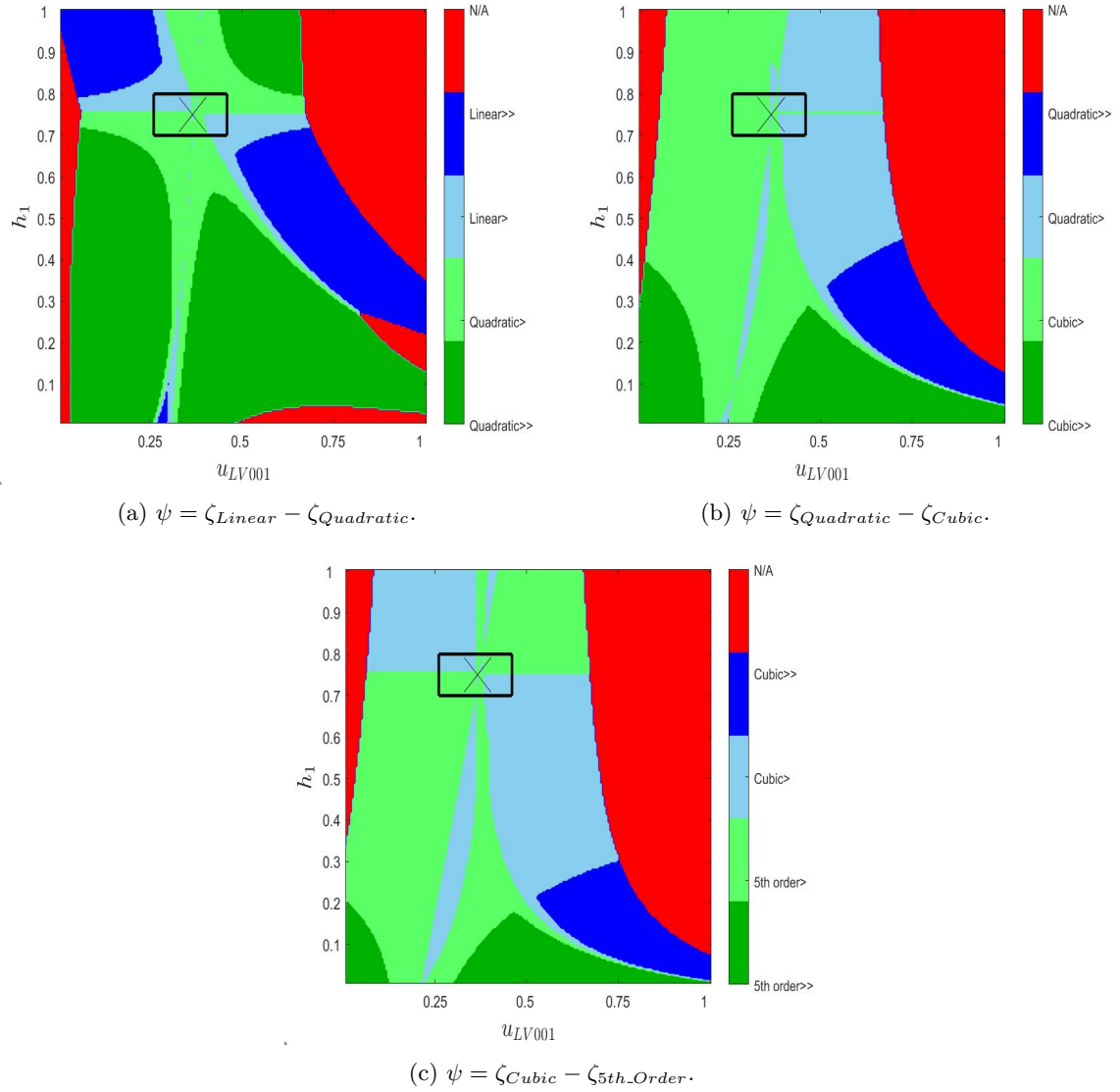


Figure A.3: Color maps comparing the different Taylor models.

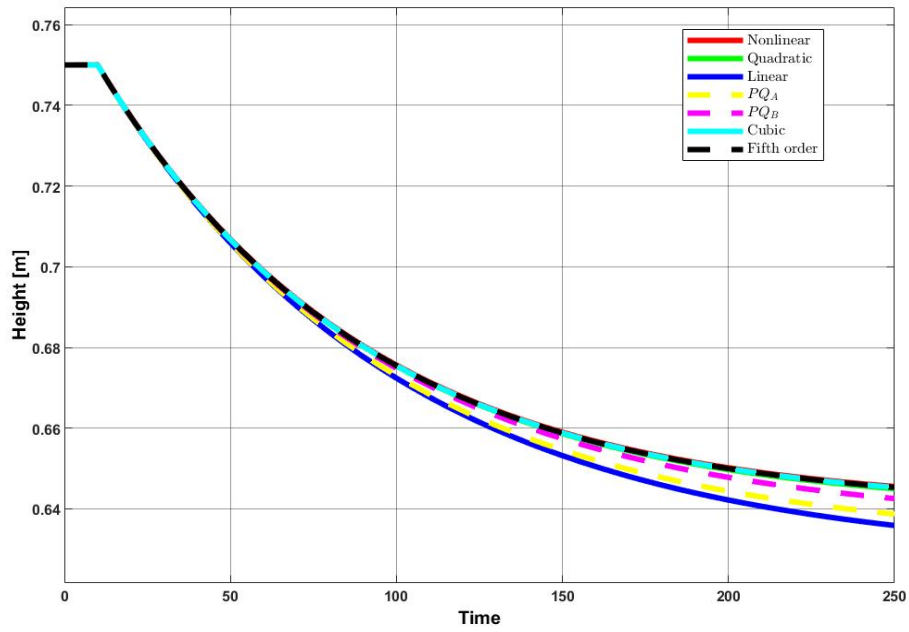
Case	Data points	Case	Data points	Case	Data points
Quadratic >>	0	Cubic >>	0	5th order >>	0
Quadratic >	458	Cubic>	478	5th order>	437
Linear >	335	Quadratic>	342	Cubic>	383
Linear >>	0	Quadratic>>	0	Cubic>>	0
N/A	0	N/A	0	N/A	0

(a) Data points in sub matrix of ψ from Figure A.3a.

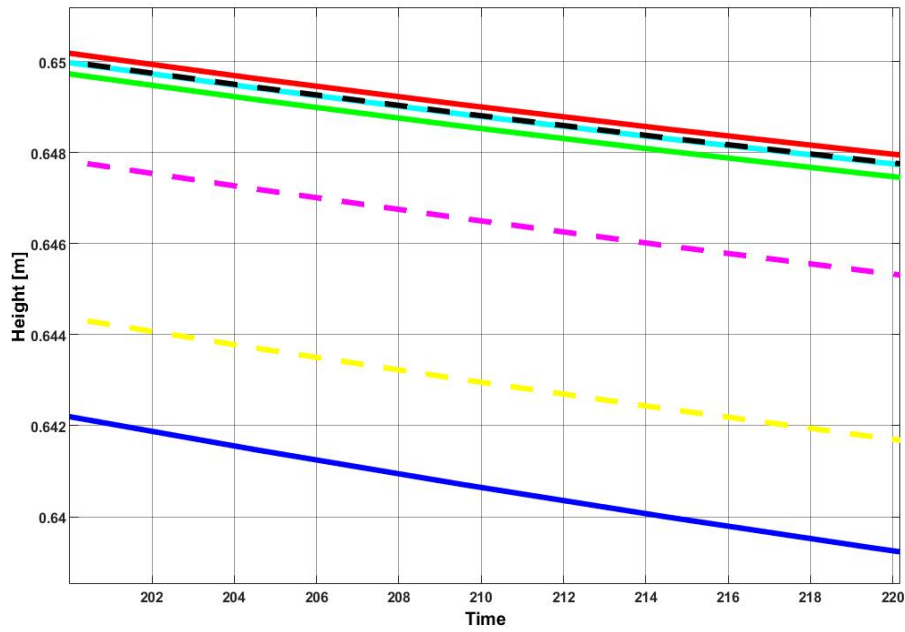
(b) Data points in sub matrix of ψ from Figure A.3b.

(c) Data points in sub matrix of ψ from Figure A.3c.

Table A.1: Numerical interpretation of the area within the hollow rectangles in Figure A.3



(a) Step response with an increment of 0.02 at 10 seconds.



(b) Close up of A.4a.

Figure A.4: Model comparison in Simulink.

	IAE	ISE	ITAE	ITSE	ISTE
Linear	1.1293	0.0076354	198.3931	1.4769	299.2148
PQ_A	0.84907	0.0041538	146.6415	0.7893	157.9692
PQ_B	0.32071	0.00064944	57.5376	0.12877	26.5431
Quadratic	0.071009	2.6413e-05	11.7253	0.0049235	0.98053
Cubic	0.039517	6.9896e-06	5.8743	0.0011394	0.20972
5th order	0.03751	6.2086e-06	5.488	0.00098663	0.17856

Table A.2: Integral performance criteria.

Appendix B

Carleman approximation comparison for Scenario 2

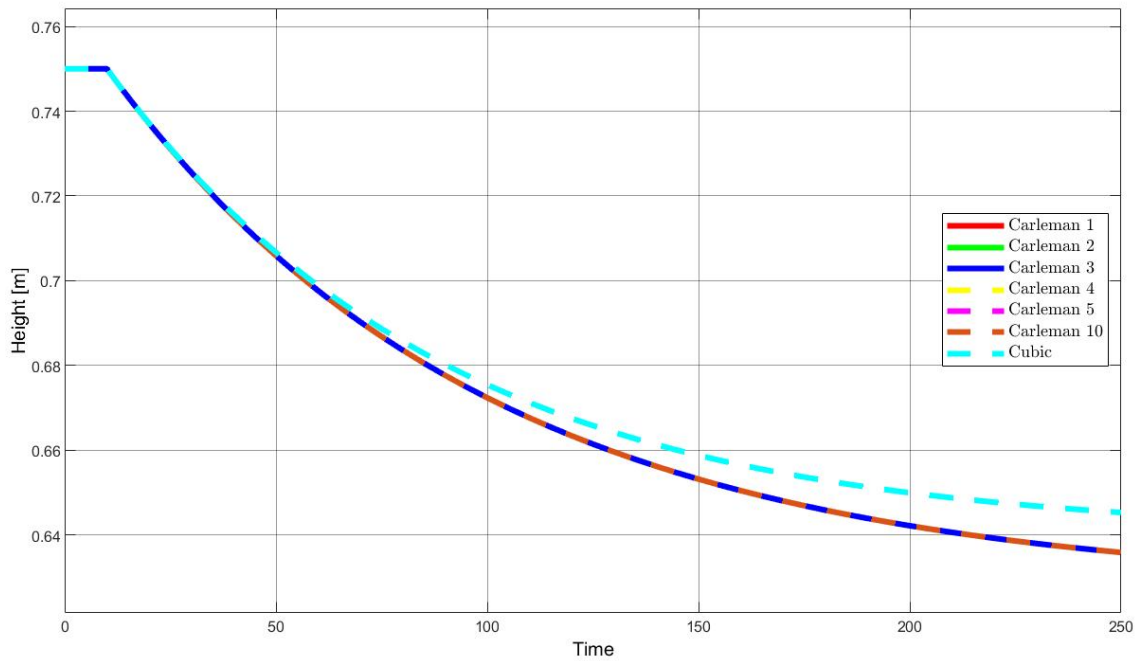


Figure B.1: Step response with an increment in $u_{LV001}(t)$ of 0.02 at 10 seconds.

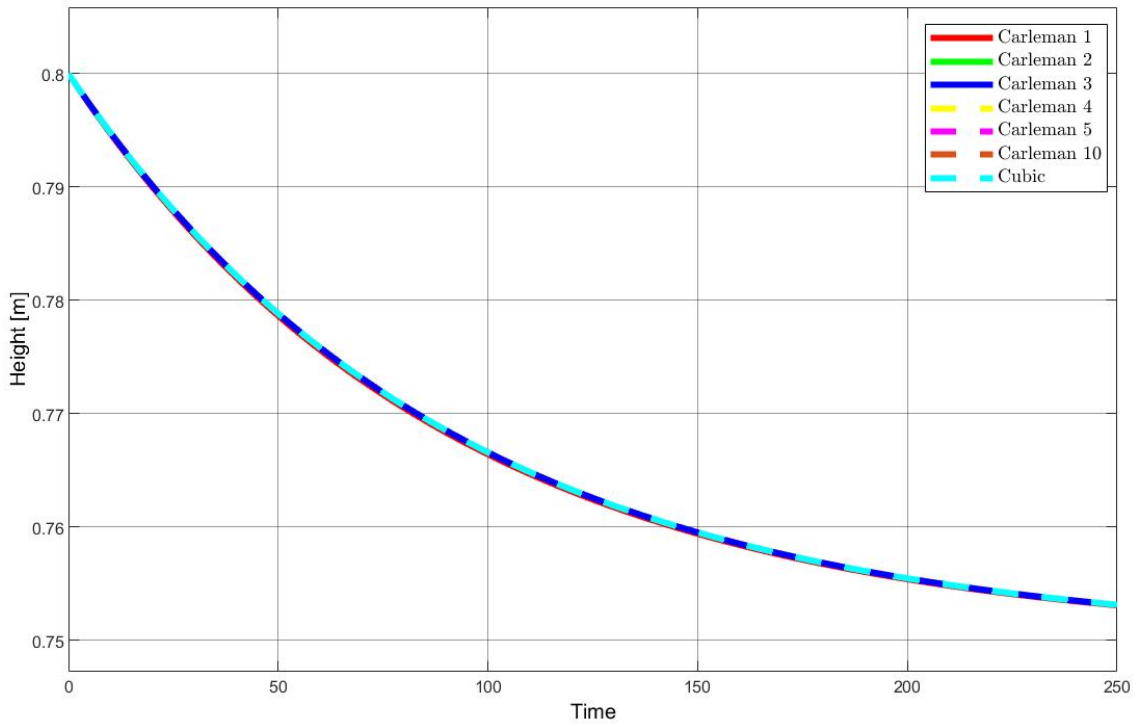


Figure B.2: $\delta = 0.05m$ gives a starting point of 0.8m.

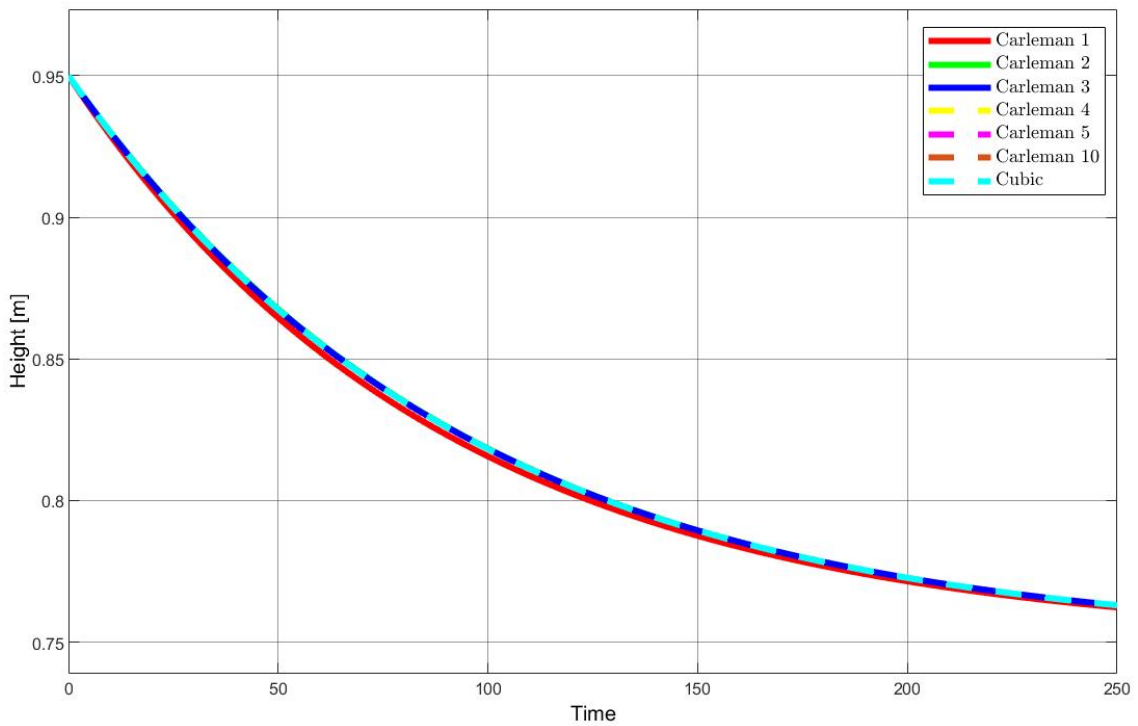


Figure B.3: $\delta = 0.2m$ gives a starting point of 0.95m.

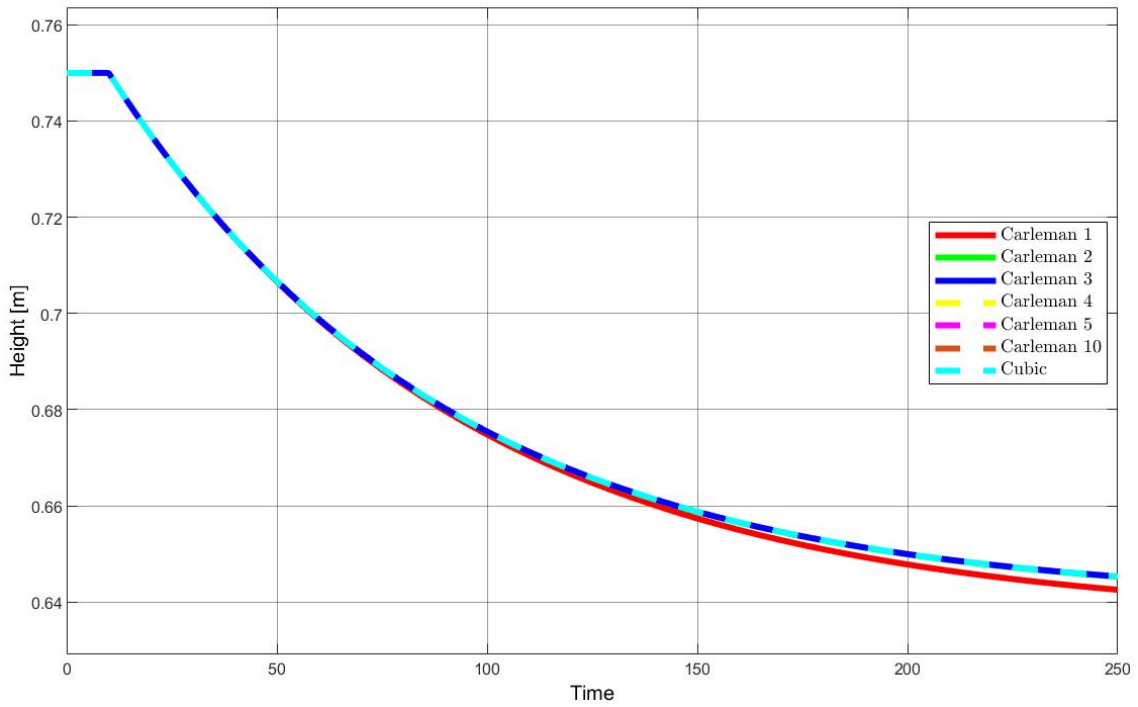
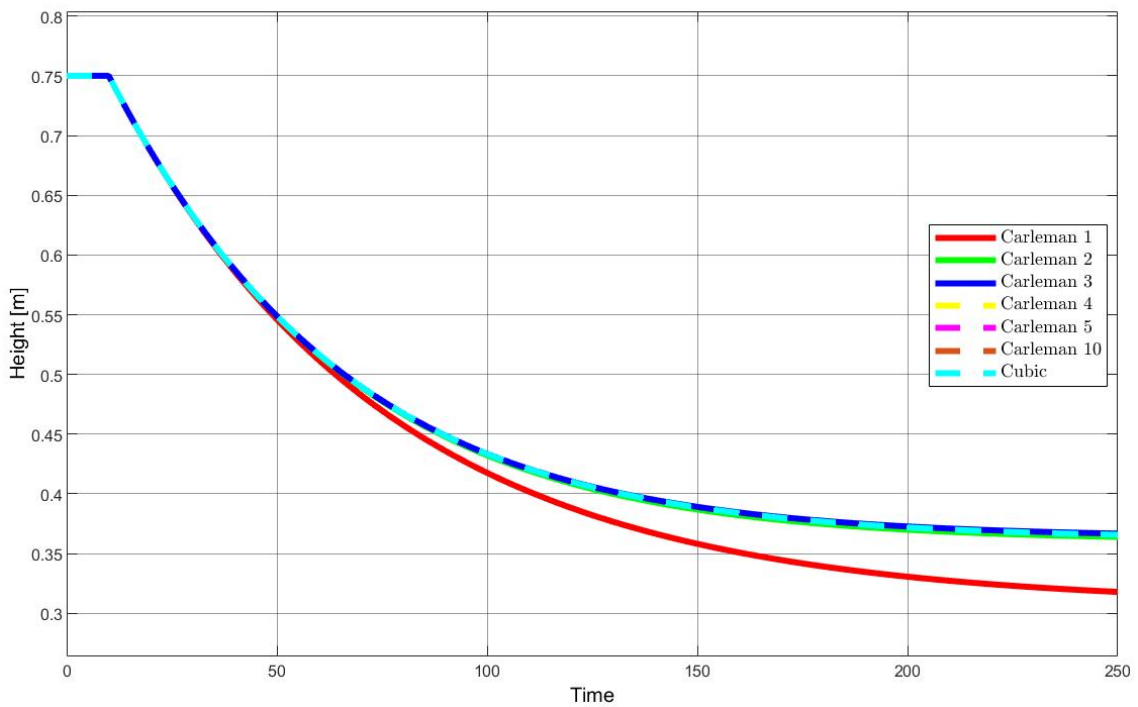


Figure B.4: Simulation of the quadratic Carleman approximations.



Note that the direction of the step is now positive, otherwise, the system would saturate.

Figure B.5: Simulation of the quadratic Carleman approximations with a larger step.

Appendix C

Controller of the quadratic Carleman approximation for Scenario 2

Controller gain for the 4th order quadratic Carleman approximation with one input variable ($\delta u_{LV001}(t)$):

$$\mathcal{K} = [0.3321 \quad -0.0131 \quad 0.0004 \quad -0.0004] \quad (\text{C.1})$$

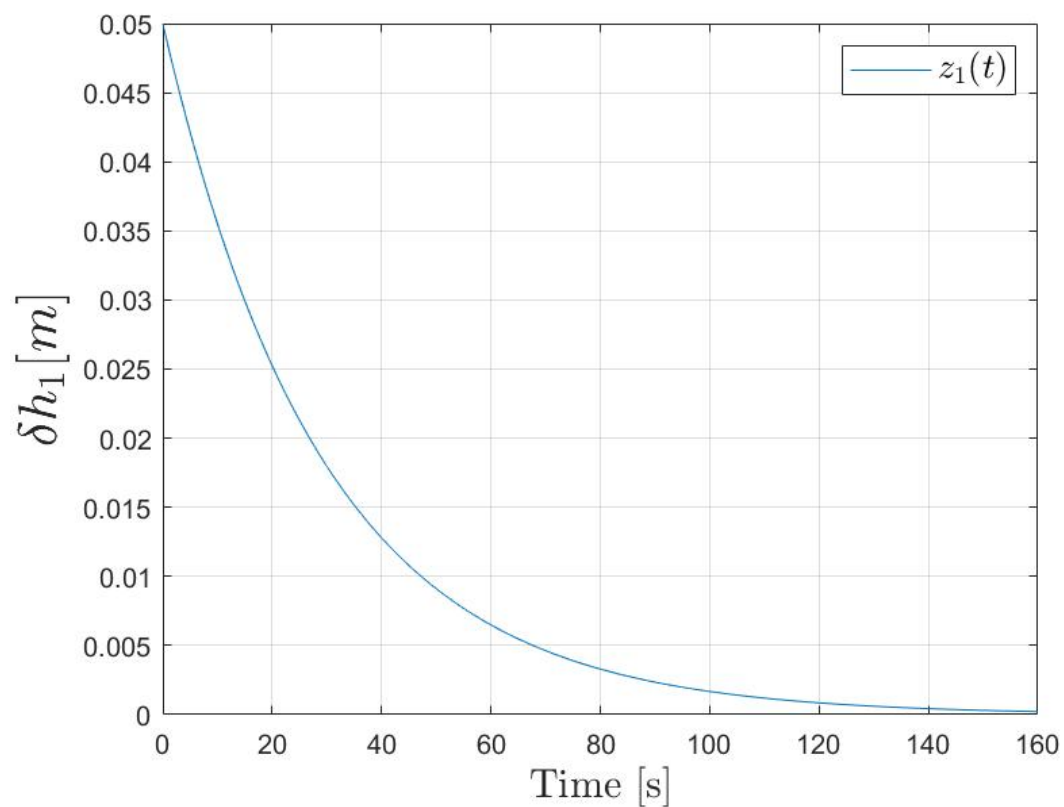


Figure C.1: Simulation of Eq. (6.29), with initial condition equal to $0.05m$.

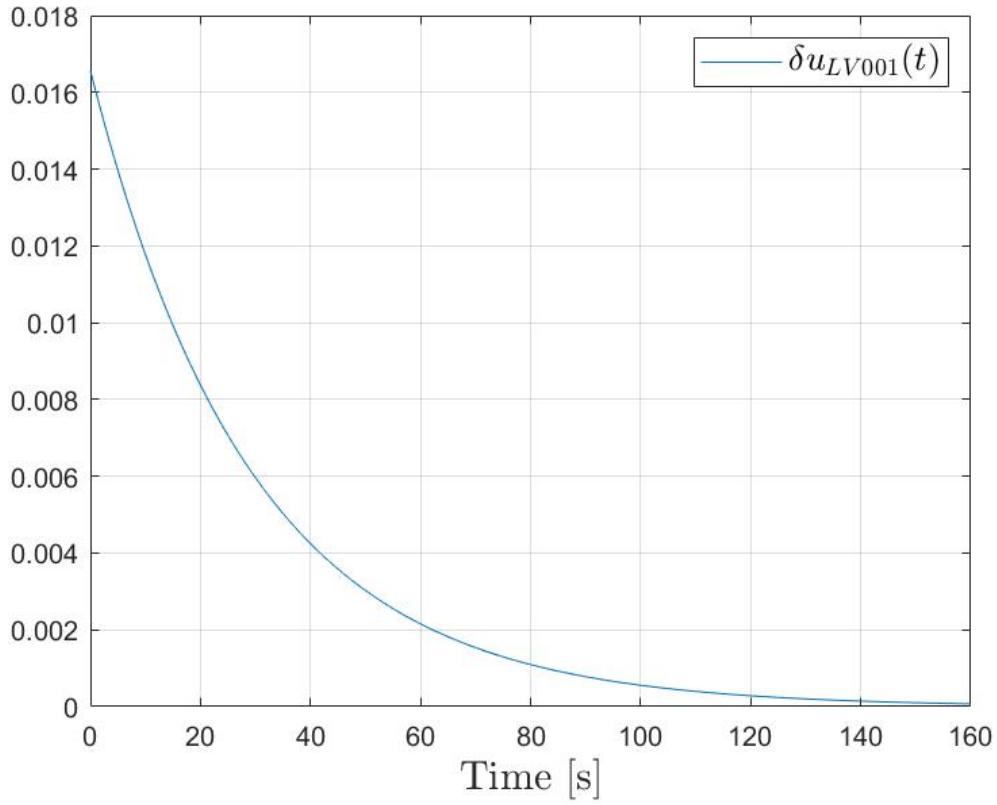


Figure C.2: Signal $\delta u_{LV001}(t)$, calculated by $\mathcal{K}z(t)$.

Controller gain for the 4th order quadratic Carleman approximation with two input variables ($\delta u_{LV001}(t)$, $\delta u_{PA001}(t)$):

$$\mathcal{K} = \begin{bmatrix} 0.3234 & -0.0309 & 0.0004 & 0.0004 \\ -0.1176 & -0.0194 & -0.0024 & 0.0011 \end{bmatrix} \quad (\text{C.2})$$

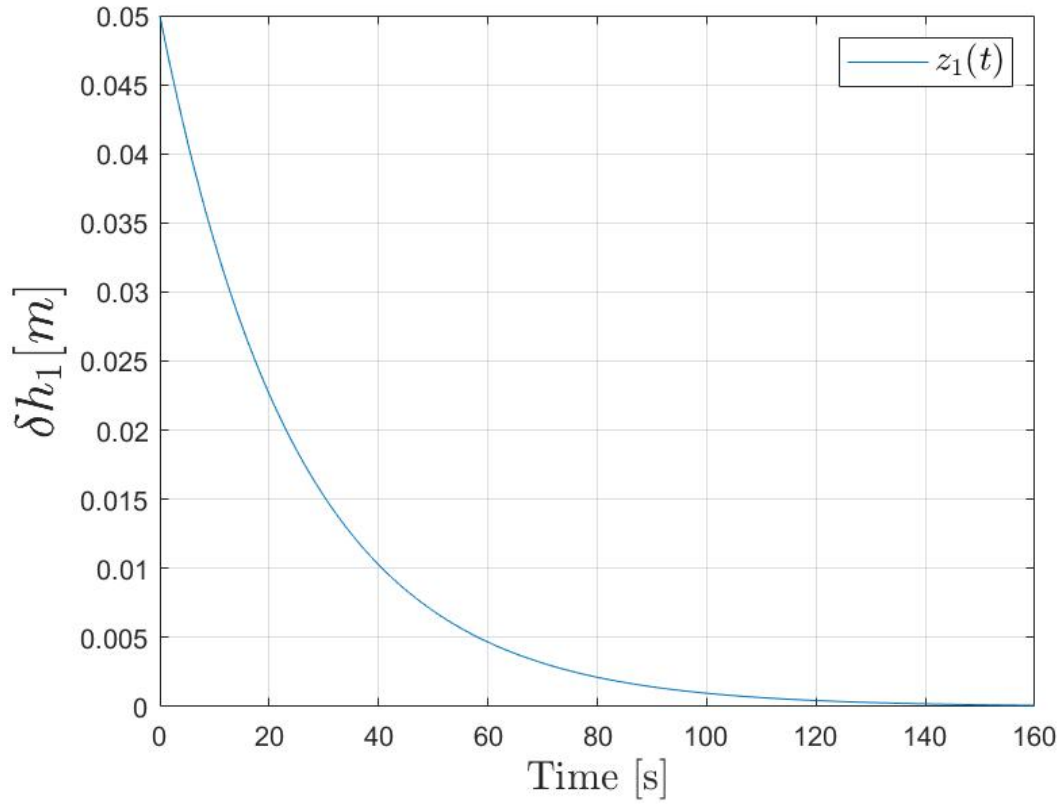


Figure C.3: 4th order quadratic Carleman approximation with two actuator.

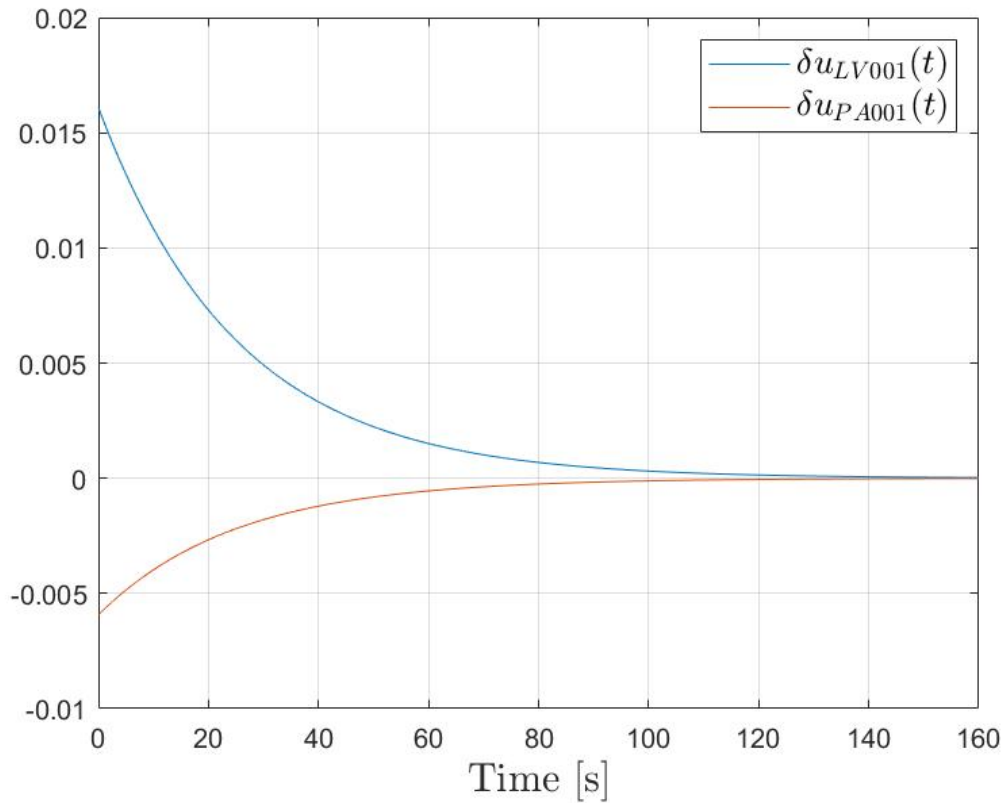


Figure C.4: Signal $u(t)$, calculated by $\mathcal{K}z(t)$.

Controller gain for the 4th order quadratic Carleman approximation with two input variables ($\delta u_{LV001}(t)$, $\delta u_{PA001}(t)$), and the inclusion of the convergence rate α :

$$\mathcal{K} = \begin{bmatrix} 1.9147 & -1.6602 & 0.6684 & 1.6311 \\ 0.2835 & 0.0583 & -0.4472 & -0.4170 \end{bmatrix} \quad (\text{C.3})$$

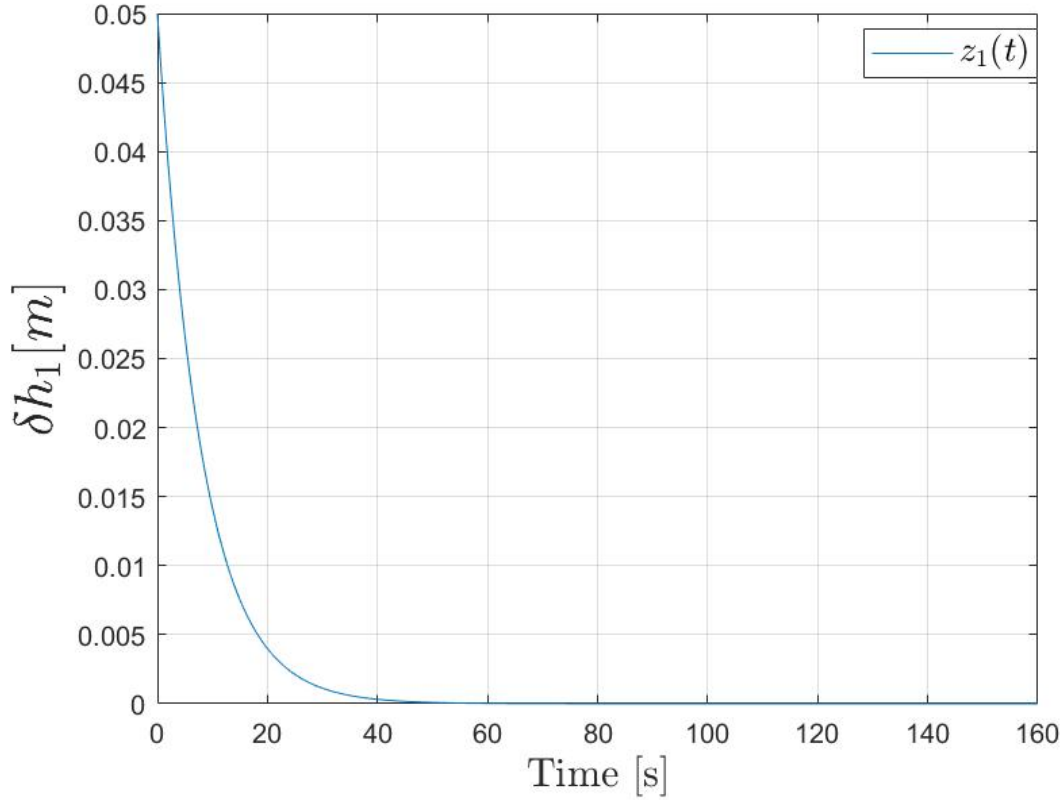


Figure C.5: 4th order quadratic Carleman approximation with two actuator and implemented convergence rate.

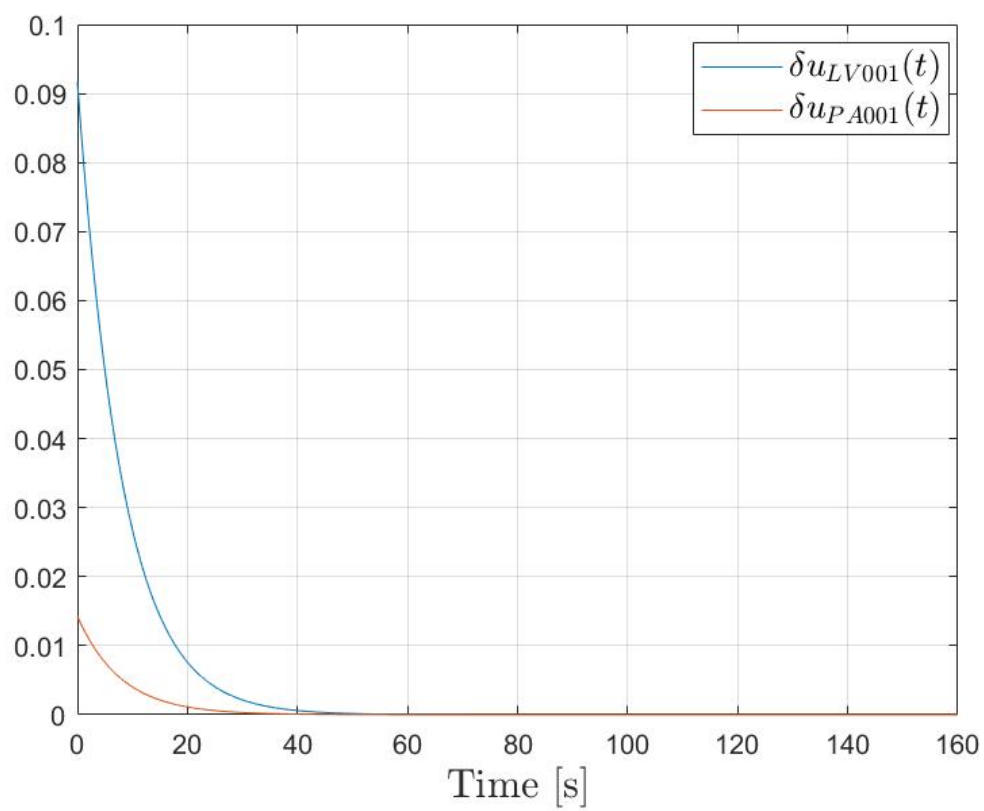


Figure C.6: Signal $u(t)$, calculated by $\mathcal{K}z(t)$ with implemented convergence rate.

Appendix D

Experimental results for Scenario 2

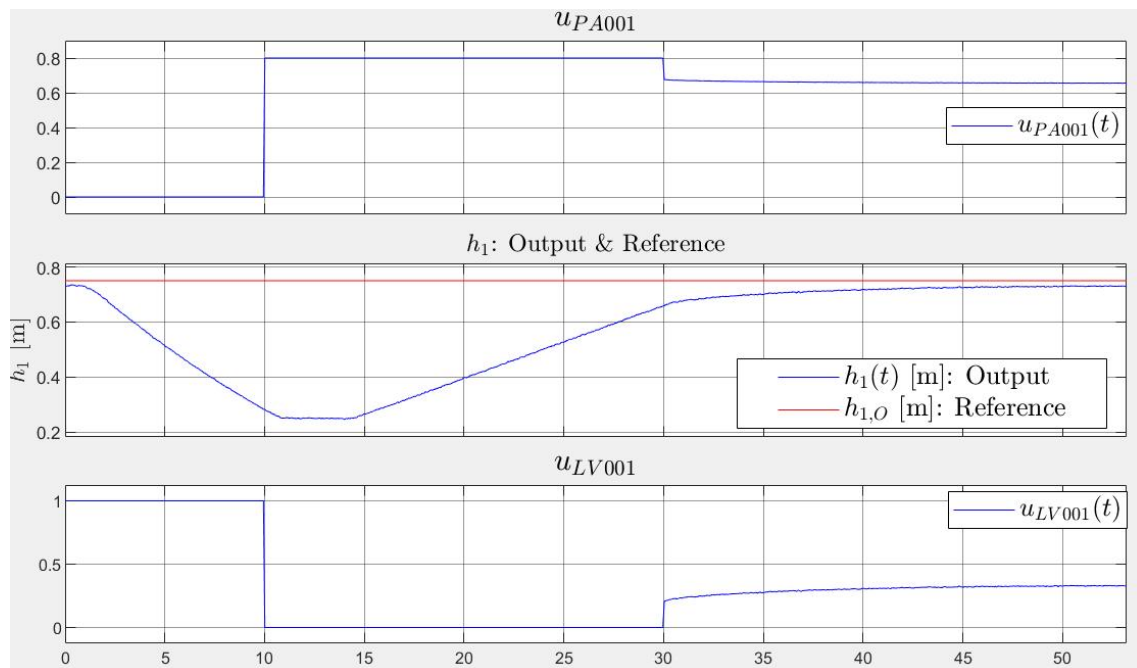


Figure D.1: Experimental results from the quadratic controller.

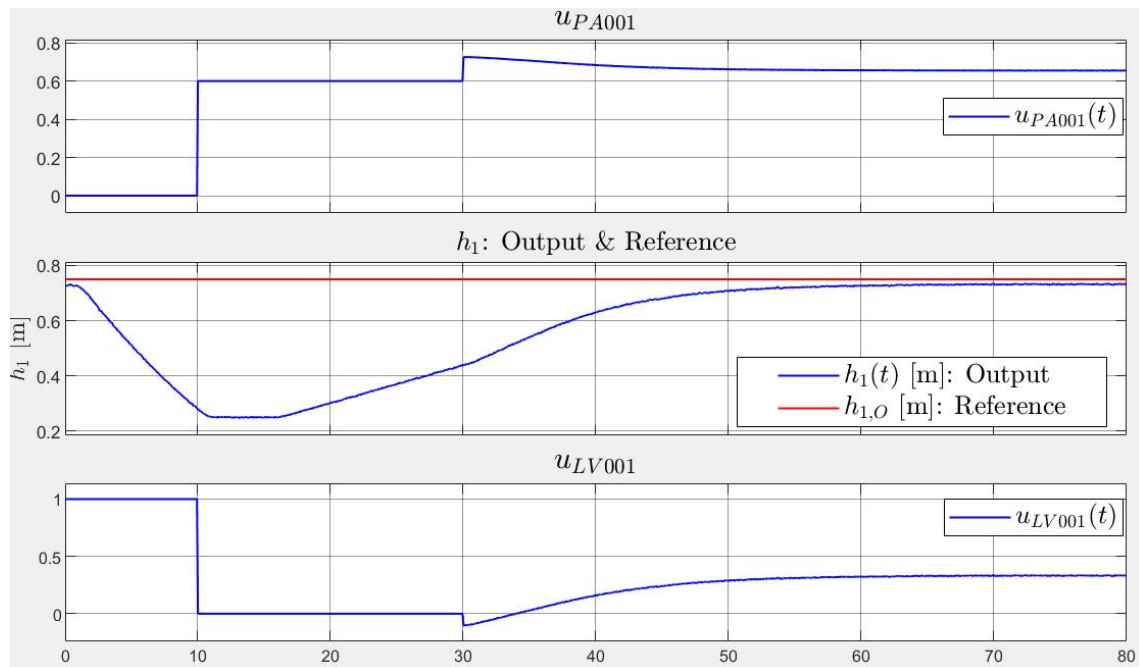


Figure D.2: Experimental results from the quadratic controller.

Appendix E

Simulation of the controller designed with a reduced polytope

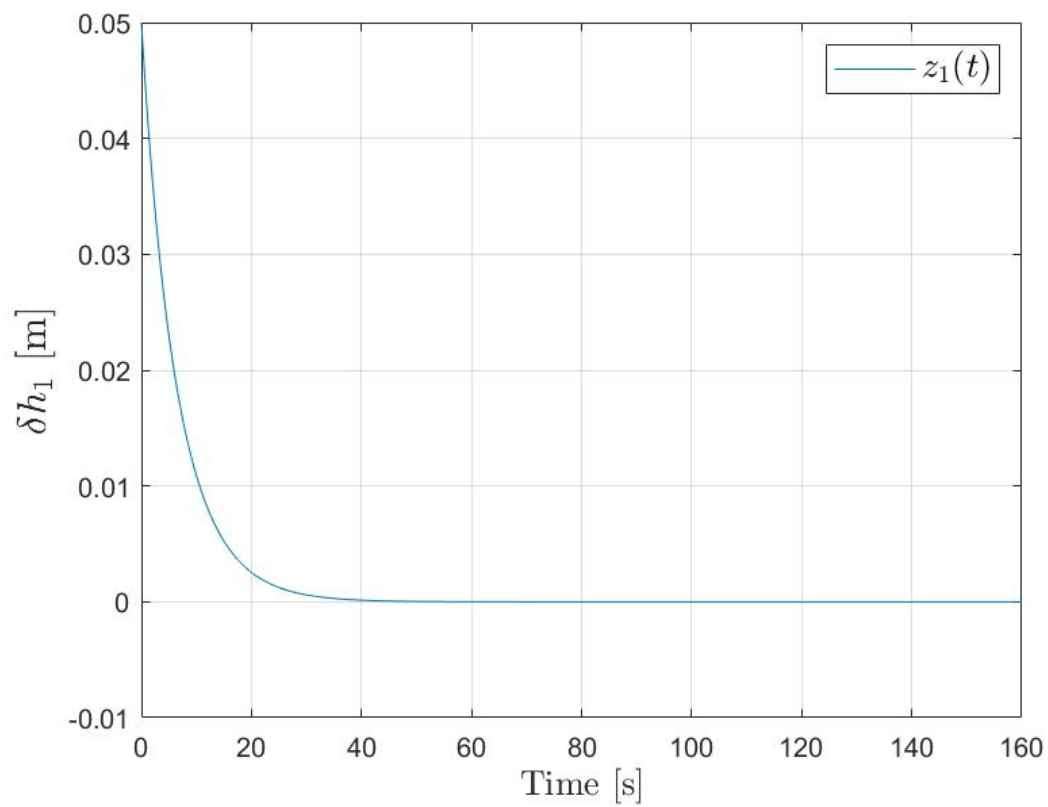


Figure E.1: Simulation of the state $z_1(t)$ for the reduced polytope.

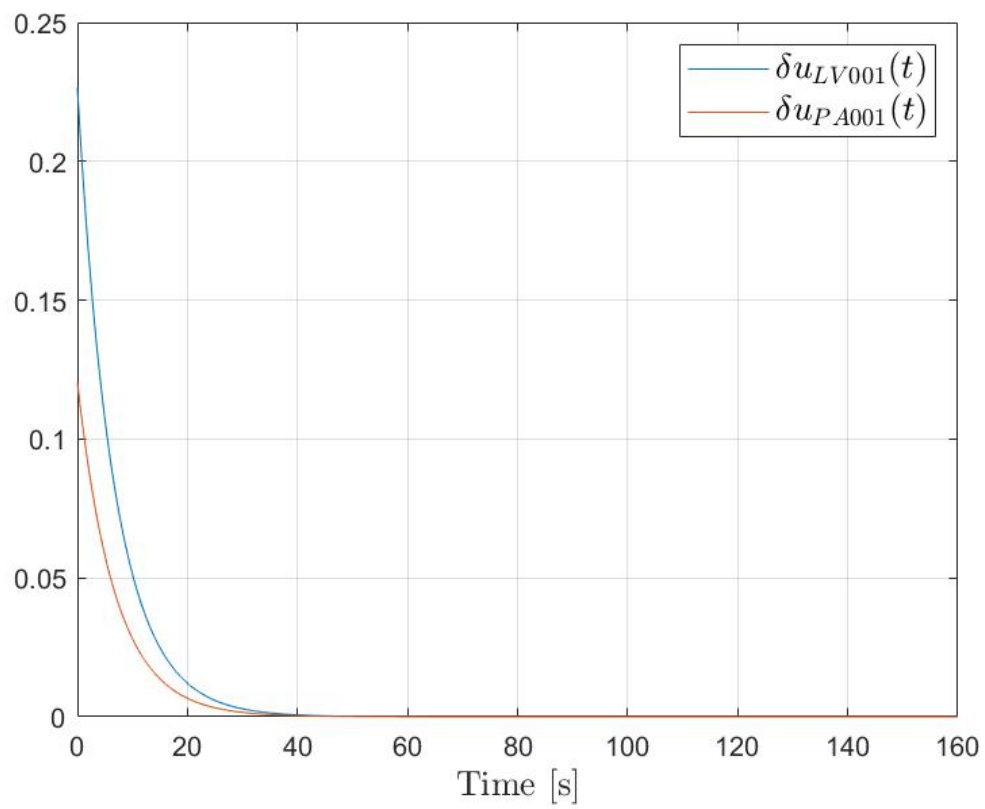


Figure E.2: Simulation of the input variables $\delta u_{LV001}(t)$ and $\delta u_{PA001}(t)$ for the reduced polytope.

Appendix F

MATLAB code and Simulink schemes

F.1 *totank_main.m*

```
1 %% Variable definitions
2 clear all
3 close all
4
5 syms A1 f3 Kv_LV001 f1 rho g h1 h_LV001
6
7 %The dynamic model for tank 1
8 dynamic_model_tank1 = (1/A1)*(f3 - ((Kv_LV001*f1)/3600)*sqrt((rho*g*(h1+h_LV001))
9 /100000));
10
11 % Calculating the partial derivatives (symbolic)
12 par_der_h1 = diff(dynamic_model_tank1, h1); % df/dh1
13 par_der_f1 = diff(dynamic_model_tank1, f1); % df/df1
14 par_der_f3 = diff(dynamic_model_tank1, f3); % df/df3
15 par_der_h1_h1 = diff(par_der_h1, h1); % d^2f/dh1^2
16 par_der_f1_f1 = diff(par_der_f1, f1); % d^2f/df1^2
17 par_der_f3_f3 = diff(par_der_f3, f3); % d^2f/df3^2
18 par_der_h1_f1 = diff(par_der_h1, f1); % d^2f/dh1df1
19 par_der_h1_f3 = diff(par_der_h1, f3); % d^2f/dh1df3
20 par_der_f1_f3 = diff(par_der_f1, f3); % d^2f/df1df3
21
22 par_der_h1_h1_h1 = diff(par_der_h1_h1, h1); % d^3f/dh1^3
23 par_der_h1_h1_f1 = diff(par_der_h1_h1, f1); % d^3f/dh1^2df1
24
25 par_der_h1_h1_h1_h1 = diff(par_der_h1_h1_h1, h1); % d^4f/dh1^4
26 par_der_h1_h1_h1_f1 = diff(par_der_h1_h1_h1, f1); % d^4f/dh1^3df1
27
28 par_der_h1_h1_h1_h1_h1 = diff(par_der_h1_h1_h1_h1, h1); % d^5f/dh1^5
29 par_der_h1_h1_h1_h1_f1 = diff(par_der_h1_h1_h1_h1, f1); % d^5f/dh1^4df1
30
31 scenario = 1;
32 if scenario == 1
33     % Setting the working point for h1 and f3
34     h1_arb = 0.25;
35     f3_arb = 0.0001783;
36
37     % Inserting every known variable in equation dynamic_model_tank1
38     a = subs(dynamic_model_tank1, [A1 Kv_LV001 rho g h_LV001 h1 f3],...
39         [0.01 11.25 1000 9.81 0.05 h1_arb f3_arb]);
40
41     % Solving equation 'a' wrt f1. This gives f1_arb
42     f1_arb = double(solve(a, f1));
43
44     % Since f3_arb is chosen, we can find upa_arb from the pump-characteristics
```

```

45     upa_arb = 0.65;
46     % We have found f1_arb. Using this value in the valve-characteristics gives us
47     ulv_arb = 0.5159;
48
49     df1_duLV001 = 0.98; % Manually calculated in simulink. delta_f1 /
50     delta_ulv
51     df3_dPA001 = 0.00052; % Manually calculated in simulink. delta_f3 /
52     delta_upa
53
54 elseif scenario == 2
55     % Setting the working point for h1 and f3
56     h1_arb = 0.75;
57     f3_arb = 0.0001783;
58
59     % Inserting every known variable in equation dynamic_model_tank1
60     a = subs(dynamic_model_tank1, [A1 Kv_LV001 rho g h_LV001 h1 f3],...
61         [0.01 11.25 1000 9.81 0.05 h1_arb f3_arb]);
62
63     % Solving equation 'a' wrt f1. This gives f1_arb
64     f1_arb = double(solve(a,f1));
65
66     % Since f3_arb is chosen, we can find upa_arb from the pump-characteristics
67     upa_arb = 0.65;
68     % We have found f1_arb. Using this value in the valve-characteristics gives us
69     ulv_arb = 0.3666;
70
71     df1_duLV001 = 0.78; % Manually calculated in simulink. delta_f1 /
72     delta_ulv
73     df3_dPA001 = 0.00052; % Manually calculated in simulink. delta_f3 /
74     delta_upa
75 end
76
77 % Calculating the partial derivatives used in the Taylor series expansion
78 % (Value at working point!)
79 par_der_h1_verdi = double((subs(par_der_h1,...
80     [A1 Kv_LV001 rho g h_LV001 h1 f1 f3],...
81     [0.01 11.25 1000 9.81 0.05 h1_arb f1_arb f3_arb]]));
82
83 par_der_uLV001_verdi = double(subs(par_der_f1 * df1_duLV001,...
84     [A1 Kv_LV001 rho g h_LV001 h1 f1 f3],...
85     [0.01 11.25 1000 9.81 0.05 h1_arb f1_arb f3_arb]]));
86
87 par_der_uPA001_verdi = double(subs(par_der_f3 * df3_dPA001,...
88     [A1 Kv_LV001 rho g h_LV001 h1 f1 f3],...
89     [0.01 11.25 1000 9.81 0.05 h1_arb f1_arb f3_arb]]));
90
91 par_der_h1_h1_verdi = double(subs(par_der_h1_h1,...
92     [A1 Kv_LV001 rho g h_LV001 h1 f1 f3],...
93     [0.01 11.25 1000 9.81 0.05 h1_arb f1_arb f3_arb]]));
94
95 par_der_uLV001_uLV001_verdi = double(subs(par_der_f1_f1 * df1_duLV001^2,...
96     [A1 Kv_LV001 rho g h_LV001 h1 f1 f3],...
97     [0.01 11.25 1000 9.81 0.05 h1_arb f1_arb f3_arb]]));
98
99 par_der_uPA001_uPA001_verdi = double(subs(par_der_f3_f3 * df3_dPA001^2,...
100     [A1 Kv_LV001 rho g h_LV001 h1 f1 f3],...
101     [0.01 11.25 1000 9.81 0.05 h1_arb f1_arb f3_arb]]));
102
103 par_der_h1_uLV001_verdi = double(subs(par_der_h1_f1 * df1_duLV001,...
104     [A1 Kv_LV001 rho g h_LV001 h1 f1 f3],...
105     [0.01 11.25 1000 9.81 0.05 h1_arb f1_arb f3_arb]]));
106
107 par_der_h1_uPA001_verdi = double(subs(par_der_h1_f3 * df3_dPA001,...
108     [A1 Kv_LV001 rho g h_LV001 h1 f1 f3],...
109     [0.01 11.25 1000 9.81 0.05 h1_arb f1_arb f3_arb]]));
110
111 par_der_uLV001_uPA001_verdi = double(subs(par_der_f1_f3 * df1_duLV001 * df3_dPA001
112     ,...
113     [A1 Kv_LV001 rho g h_LV001 h1 f1 f3],...
114     [0.01 11.25 1000 9.81 0.05 h1_arb f1_arb f3_arb]]));

```

```

111 par_der_h1_h1_h1_verdi = double((subs(par_der_h1_h1_h1,...
112 [A1 Kv_LV001 rho g h_LV001 h1 f1 f3],...
113 [0.01 11.25 1000 9.81 0.05 h1_arb f1_arb f3_arb]]));
114
115 par_der_h1_h1_uLV001_verdi = double((subs(par_der_h1_h1_f1 * df1_duLV001,...
116 [A1 Kv_LV001 rho g h_LV001 h1 f1 f3],...
117 [0.01 11.25 1000 9.81 0.05 h1_arb f1_arb f3_arb]]));
118
119 par_der_h1_h1_h1_h1_verdi = double((subs(par_der_h1_h1_h1_h1,...
120 [A1 Kv_LV001 rho g h_LV001 h1 f1 f3],...
121 [0.01 11.25 1000 9.81 0.05 h1_arb f1_arb f3_arb]]));
122
123 par_der_h1_h1_h1_uLV001_verdi = double((subs(par_der_h1_h1_h1_f1 * df1_duLV001,...
124 [A1 Kv_LV001 rho g h_LV001 h1 f1 f3],...
125 [0.01 11.25 1000 9.81 0.05 h1_arb f1_arb f3_arb]]));
126
127 par_der_h1_h1_h1_h1_h1_verdi = double((subs(par_der_h1_h1_h1_h1_h1,...
128 [A1 Kv_LV001 rho g h_LV001 h1 f1 f3],...
129 [0.01 11.25 1000 9.81 0.05 h1_arb f1_arb f3_arb]]));
130
131 par_der_h1_h1_h1_h1_uLV001_verdi = double((subs(par_der_h1_h1_h1_h1_f1 *
132 df1_duLV001,...
133 [A1 Kv_LV001 rho g h_LV001 h1 f1 f3],...
134 [0.01 11.25 1000 9.81 0.05 h1_arb f1_arb f3_arb]]));
135
136
137 % The following is a standard code that imports the characteristics of the
138 % pump and valve. This code also defines some constants. (From Reguleringsteknikk)
139
140 %%%%%%%%%%%%%%%%%%%%%%%%%%%%%%%%%%%%%%%%%%%%%%%%%%%%%%%%%%%%%%%
141 % data om vann og tyngdekraft
142 %%%%%%%%%%%%%%%%%%%%%%%%%%%%%%%%%%%%%%%%%%%%%%%%%%%%%%%%%%%%%%%
143 rho = 1000; % tetthet vann [kg/m^3]
144 g = 9.81; % tyngdens akselerasjon [m/s^2]
145 c_p = 4200; % varmekapasitet vann [j/kg*K]
146
147 %%%%%%%%%%%%%%%%%%%%%%%%%%%%%%%%%%%%%%%%%%%%%%%%%%%%%%%%%%%%%%%
148 % Tank 1
149 %%%%%%%%%%%%%%%%%%%%%%%%%%%%%%%%%%%%%%%%%%%%%%%%%%%%%%%%%%%%%%%
150 Kv_LV001 = 11.25; % ventilkonstant LV001 [m^3/h] ved 1 bar trykkfall
151 h_LV001 = 0.05; % h yde til LV001 [m]
152 h1_max = 1; % maks h yde tank 1 [m]
153 h1_min = 0.13; % min h yde tank 1 [m]
154 A1 = 0.01; % areal tank 1 [m^2]
155
156 %%%%%%%%%%%%%%%%%%%%%%%%%%%%%%%%%%%%%%%%%%%%%%%%%%%%%%%%%%%%%%%
157 % Tank 2
158 %%%%%%%%%%%%%%%%%%%%%%%%%%%%%%%%%%%%%%%%%%%%%%%%%%%%%%%%%%%%%%%
159 Kv_LV002 = 11.25; % ventilkonstant LV002 [m3/h]
160 h_LV002 = 0.25; % h yde fra bunn av tank 2 til LV002
161 h2_max = 0.4; % maks h yde tank 2 [m]
162 h2_min = 0.02; % min h yde tank 2 [m]
163
164 %%%%%%%%%%%%%%%%%%%%%%%%%%%%%%%%%%%%%%%%%%%%%%%%%%%%%%%%%%%%%%%
165 % Last inn p drag og m linger
166 %%%%%%%%%%%%%%%%%%%%%%%%%%%%%%%%%%%%%%%%%%%%%%%%%%%%%%%%%%%%%%%
167 load tankData_1 % det finnes ogs et datasett som heter tankData_2
168 load tankData_2
169
170 %%%%%%%%%%%%%%%%%%%%%%%%%%%%%%%%%%%%%%%%%%%%%%%%%%%%%%%%%%%%%%%
171 % Pumpekarakteristikk
172 %%%%%%%%%%%%%%%%%%%%%%%%%%%%%%%%%%%%%%%%%%%%%%%%%%%%%%%%%%%%%%%
173 u_PA001 = [0.00 0.45 0.46 0.47 0.48 0.49 0.50 0.55...
174 0.60 0.65 0.70 0.75 0.80 0.85 0.90 0.95 1.00];
175 q_PA001 = [0.00 0.00 1.25 2.25 3.15 3.75 4.40 6.75...
176 8.75 10.70 12.25 13.75 15.15 16.50 18.00 19.20 20.00];
177
178 q_PA001 = q_PA001/60000; % liter/time -> m3/s
179
180 close all
181 figure
182 plot(u_PA001, q_PA001, '*-')

```

```

183 title('Pump characteristic')
184 xlabel('Control signal u_{PA001}(t) to pump PA001')
185 ylabel('Volume flow q_{PA001}(t) through PA001 [m^3/s]')
186
187
188 %%%%%%%%%%%%%%%%%%%%%%%%%%%%%%%%%%%%%%%%%%%%%%%%%%%%%%%%%%%%%%%%%%%%%%%%%
189 % Ventilkararakteristikk
190 %%%%%%%%%%%%%%%%%%%%%%%%%%%%%%%%%%%%%%%%%%%%%%%%%%%%%%%%%%%%%%%%%%%%%%%%%
191 u_LV001 = 0:0.03:1;
192 f_LV001 = (exp(u_LV001.^1.2)-1)/(exp(1)-1);
193 u_LV002 = u_LV001;
194 f_LV002 = f_LV001;
195
196 figure
197 plot(u_LV001,f_LV001,'*-')
198 title('Valve characteristic for LV001 og LV002')
199 xlabel('Control signal u_{LV001}(t)')
200 ylabel('f(u_{LV001}(t))')
201
202 %End of the standard code from Reguleringsteknikk
203
204 %% NonLinear Model 3d-Plot
205
206 close all
207 figure
208 [ulv,h1]=meshgrid(0:0.005:1,[0:0.005:1]); %0.005
209
210 %We want to mesh ulv and h1, but the nonlinear model uses f1 in it's
211 %calculation. The following finds the corresponding values for f1.
212 resultat = sim('f1_invers', 3000);
213 f1 = resultat.f1_sim.Data;
214
215 % Calculates the NonLinear model
216 ydot = 1/A1*(f3_arb - 1/3600 *Kv_LV001.*f1.*sqrt(rho*g.*(h1+0.05)/100000));
217
218 NonLinear = surf(ulv,h1,ydot,'FaceColor','r'); % Draws the NonLinear model
219 rotate3d
220 xlabel('$u_{LV}$', 'Interpreter','latex','fontsize',16)
221 ylabel('$h_1$', 'Interpreter','latex','fontsize',16)
222 zlabel('$\dot{h}_1$', 'Interpreter','latex','fontsize',16)
223 title('NonLinear Model 3D-Plot')
224 legend(NonLinear, ['NonLinear' newline 'Model'])
225 hold on
226
227 Zero_Plane = surf(ulv,h1,-zeros(size(ulv)),'FaceColor','black');
228 legend([NonLinear Zero_Plane], {'NonLinear' newline 'Model'}, ['h_{1}-u_{LV001}'
    'plane']})
229
230 %% Quadratic Model 3d-Plot
231
232 close all
233 figure
234
235 NonLinear = surf(ulv,h1,ydot,'FaceColor','r'); % Draws the NonLinear model
236 rotate3d
237 xlabel('$u_{LV}$', 'Interpreter','latex','fontsize',16)
238 ylabel('$h_1$', 'Interpreter','latex','fontsize',16)
239 zlabel('$\dot{h}_1$', 'Interpreter','latex','fontsize',16)
240 title('Quadratic Model @0.25m 3D-Plot')
241 hold on
242
243 y_quadratic = par_der_h1_verdi.*(h1-h1_arb)...
244 + par_der_uLV001_verdi.*(ulv - ulv_arb) ...
245 + par_der_h1_h1_verdi.*0.5.*(h1-h1_arb).^2 ...
246 + par_der_h1_uLV001_verdi.*(h1-h1_arb).*(ulv-ulv_arb); % Calculates the
    Quadratic model
247
248 Quadratic = surf(ulv,h1,y_quadratic, 'FaceColor', 'g'); % Draws the Quadratic
    model
249 legend([Quadratic NonLinear], {'Quadratic' newline 'Model'}, ['NonLinear' newline
    'Model']})
250
251 %% Linear 3d-Plot

```

```

252
253 close all
254 figure
255
256 NonLinear = surf(ulv,h1,ydot,'FaceColor','r'); % Draws the NonLinear model
257 rotate3d
258 xlabel('$u_{LV}$', 'Interpreter','latex','fontsize',16)
259 ylabel('$h_1$', 'Interpreter','latex','fontsize',16)
260 zlabel('$\dot{h}_1$', 'Interpreter','latex','fontsize',16)
261 title('Linear Model @0.25m 3D-Plot')
262 hold on
263
264 y_linear = par_der_h1_verdi.*(h1-h1_arb)...
265           + par_der_uLV001_verdi.*(ulv-ulv_arb); % Calculates the Linear model
266
267 Linear = surf(ulv,h1,y_linear, 'FaceColor', 'b'); % Draws the Linear model
268 legend([Linear NonLinear], {'Linear' newline 'Model'}, ['NonLinear' newline '
Model']})
269
270 %% Partially Quadratic (h1xh1) Model 3d-Plot
271
272 close all
273 figure
274
275 NonLinear = surf(ulv,h1,ydot,'FaceColor','r'); % Draws the NonLinear model
276 rotate3d
277 xlabel('$u_{LV}$', 'Interpreter','latex','fontsize',16)
278 ylabel('$h_1$', 'Interpreter','latex','fontsize',16)
279 zlabel('$\dot{h}_1$', 'Interpreter','latex','fontsize',16)
280 title('Partially Quadratic(h1xh1) Model @0.25m 3D-Plot')
281 hold on
282
283 y_parQuad_h1xh1 = par_der_h1_verdi.*(h1-h1_arb)...
284                 + par_der_uLV001_verdi.*(ulv-ulv_arb)...
285                 + par_der_h1_h1_verdi.*0.5.*(h1-h1_arb).^2; %Calculates the Partially Quadratic
(h1xh1) model
286
287 %Draws the Partially Quadratic (h1xh1) model
288 PartQuad_h1xh1 = surf(ulv,h1,y_parQuad_h1xh1, 'FaceColor', 'y');
289 legend([PartQuad_h1xh1 NonLinear],...
290        {'Partially' newline 'Quadratic' newline '(h1xh1) Model'},...
291        ['NonLinear' newline 'Model']})
292
293 %% Partially Quadratic (h1xulv) Model 3d-Plot
294
295 close all
296 figure
297
298 NonLinear = surf(ulv,h1,ydot,'FaceColor','r'); % Draws the NonLinear model
299 rotate3d
300 xlabel('$u_{LV}$', 'Interpreter','latex','fontsize',16)
301 ylabel('$h_1$', 'Interpreter','latex','fontsize',16)
302 zlabel('$\dot{h}_1$', 'Interpreter','latex','fontsize',16)
303 title('Partially Quadratic (h1xulv) Model @0.25m 3D-Plot')
304 hold on
305
306 %Calculates the Partially Quadratic (h1xulv) model
307 y_parQuad_h1xulv = par_der_h1_verdi.*(h1-h1_arb)...
308                  + par_der_uLV001_verdi.*(ulv-ulv_arb)...
309                  + par_der_h1_uLV001_verdi.*(h1-h1_arb).*(ulv-ulv_arb);
310
311 %Draws the Partially Quadratic (h1xulv) model
312 PartQuad_h1xulv = surf(ulv,h1,y_parQuad_h1xulv, 'FaceColor', 'm');
313 legend([PartQuad_h1xulv NonLinear],...
314        {'Partially' newline 'Quadratic' newline '(h1xulv) Model'},...
315        ['NonLinear' newline 'Model']})
316
317 %% Cubic Model 3d-Plot
318
319 close all
320 figure
321
322 NonLinear = surf(ulv,h1,ydot,'FaceColor','r'); % Draws the NonLinear model

```

```

323 rotate3d
324 xlabel('$u_{LV}$', 'Interpreter','latex','fontsize',16)
325 ylabel('$h_1$', 'Interpreter','latex','fontsize',16)
326 zlabel('$\dot{h}_1$', 'Interpreter','latex','fontsize',16)
327 title('Cubic Model @0.25m 3D-Plot')
328 hold on
329
330 y_cubic = par_der_h1_verdi.*(h1-h1_arb)...
331     + par_der_uLV001_verdi.*(ulv - ulv_arb) ...
332     + par_der_h1_h1_verdi.*0.5.*(h1-h1_arb).^2 ...
333     + par_der_h1_uLV001_verdi.*(h1-h1_arb).*(ulv-ulv_arb)...
334     + (1/6).*par_der_h1_h1_h1_verdi.*(h1-h1_arb).^3 ...
335     + (1/2).*par_der_h1_h1_uLV001_verdi.*(h1-h1_arb).^2.*(ulv-ulv_arb); %
    Calculates the Cubic model
336
337 Cubic = surf(ulv,h1,y_cubic, 'FaceColor', 'cyan'); % Draws the Cubic model
338 legend([Cubic NonLinear], {'Cubic' newline 'Model'}, ['NonLinear' newline 'Model'
    ]})
339
340 %% 5th order T.S Model 3d-Plot
341
342 close all
343 figure
344
345 NonLinear = surf(ulv,h1,ydot, 'FaceColor','r'); % Draws the NonLinear model
346 rotate3d
347 xlabel('$u_{LV}$', 'Interpreter','latex','fontsize',16)
348 ylabel('$h_1$', 'Interpreter','latex','fontsize',16)
349 zlabel('$\dot{h}_1$', 'Interpreter','latex','fontsize',16)
350 title('5th Order Model @0.25m 3D-Plot')
351 hold on
352
353 % Calculates the 5th order model
354 y_fifth_order = par_der_h1_verdi.*(h1-h1_arb)...
355     + par_der_uLV001_verdi.*(ulv - ulv_arb) ...
356     + par_der_h1_h1_verdi.*0.5.*(h1-h1_arb).^2 ...
357     + par_der_h1_uLV001_verdi.*(h1-h1_arb).*(ulv-ulv_arb)...
358     + (1/6).*par_der_h1_h1_h1_verdi.*(h1-h1_arb).^3 ...
359     + (1/2).*par_der_h1_h1_uLV001_verdi.*(h1-h1_arb).^2.*(ulv-ulv_arb)...
360     + (1/24).*par_der_h1_h1_h1_h1_verdi.*(h1-h1_arb).^4 ...
361     + (1/6).*par_der_h1_h1_h1_uLV001_verdi.*(h1-h1_arb).^3.*(ulv-ulv_arb) ...
362     + (1/120).*par_der_h1_h1_h1_h1_h1_verdi.*(h1-h1_arb).^5 ...
363     + (1/24).*par_der_h1_h1_h1_h1_uLV001_verdi.*(h1-h1_arb).^4.*(ulv-ulv_arb);
364
365 fifth_Order = surf(ulv,h1,y_fifth_order, 'FaceColor', 'k'); % Draws the 5th
    order model
366 legend([fifth_Order NonLinear], {'5th Order' newline 'Model'}, ['NonLinear'
    newline 'Model']})
367
368 %% Mix 3d-Plot
369
370 close all
371 figure
372
373 NonLinear = surf(ulv,h1,-ydot, 'FaceColor','r'); % Draws the NonLinear model
374 rotate3d
375 xlabel('$u_{LV}$', 'Interpreter','latex','fontsize',16)
376 ylabel('$h_1$', 'Interpreter','latex','fontsize',16)
377 zlabel('$\dot{h}_1$', 'Interpreter','latex','fontsize',16)
378 title('Mix @0.25m 3D-Plot')
379 hold on
380
381 % Draws the Linear model
382 Linear = surf(ulv,h1,-y_linear, 'FaceColor', 'b');
383
384 % Draws the Quadratic model
385 Quadratic = surf(ulv,h1,-y_quadratic, 'FaceColor', 'g');
386
387 % Draws the Partially Quadratic (h1xh1) model
388 PartQuad_h1xh1 = surf(ulv,h1,-y_parQuad_h1xh1, 'FaceColor', 'y');
389
390 % Draws the Partially Quadratic (h1xulv) model
391 PartQuad_h1xulv = surf(ulv,h1,-y_parQuad_h1xulv, 'FaceColor', 'm');

```



```

392
393 % Draws the Cubic model
394 Cubic = surf(ulv,h1,-y_cubic, 'FaceColor', 'cyan');
395
396 % Draws the 5th order model
397 fifth_Order = surf(ulv,h1,-y_fifth_order, 'FaceColor', 'k');
398
399 legend([NonLinear Quadratic Linear PartQuad_h1xh1 PartQuad_h1xulv Cubic fifth_Order
400 ],...
401 {'NonLinear' newline 'Model'},...
402 {'Quadratic' newline 'Model'},...
403 {'Linear' newline 'Model'},...
404 {'Partially' newline 'Quadratic' newline '(h1xh1) Model'},...
405 {'Partially' newline 'Quadratic' newline '(h1xulv) Model'},...
406 {'Cubic' newline 'Model'}, ...
407 {'5th Order' newline 'Model'}})
408
409 %% Linear VS Other Models Contour-Plot
410 % This section plots the Contour-Plot of the comparison between our Linear
411 % Model, and all of the other models
412
413 close all
414
415 %Here, we can choose which section we want to plot.
416 h1_low = 1; %Minimum is 1
417 h1_hi = 201; %Maximum is 201
418 ulv_low = 1; %Minimum is 1
419 ulv_hi = 201; %Maximum is 201
420 colorbar_range_min = 0;
421 colorbar_range_max = 0.015;
422 if scenario == 1
423
424     H1_min = 20*2;
425     H1_max = 30*2;
426     ULV_min = 41*2;
427     ULV_max = 61*2;
428 elseif scenario == 2
429     H1_min = 70*2;
430     H1_max = 80*2;
431     ULV_min = 26*2;
432     ULV_max = 46*2;
433 end
434 %Makes a custom colormap
435 map = [ 0 0.7 0; %Green
436         0.359 1 0.402; %Light green
437         0.535 0.808 0.9375; %Light blue
438         0 0 1; %Blue
439         1 0 0]; %Red
440
441 % Calculates the error between the NonLinear system and our model
442 NL_Quad_error = abs((ydot - y_quadratic)); %Error between
443 % NonLinear model and Quadratic model
444 NL_Lin_error = abs((ydot - y_linear)); %Error between
445 % NonLinear model and Linear model
446 NL_ParQuad_h1xh1_error = abs((ydot - y_parQuad_h1xh1)); %Error between
447 % NonLinear model and Partially Quadratic (h1xh1) model
448 NL_ParQuad_h1xulv_error = abs((ydot - y_parQuad_h1xulv)); %Error between
449 % NonLinear model and Partially Quadratic (h1xulv) model
450 NL_Cubic_error = abs(ydot-y_cubic); %Error between
451 % NonLinear model and Cubic model
452 NL_fifth_error = abs(ydot-y_fifth_order); %Error between
453 % NonLinear model and 5th order model
454
455 % Calculates the error between the Linear model and our other models
456 Lin_Quad_diff= NL_Lin_error - NL_Quad_error; %Error between
457 % Linear model and Quadratic model
458 Lin_ParQuad_h1xh1_diff = NL_Lin_error - NL_ParQuad_h1xh1_error; %Error between
459 % Linear model and Partially Quadratic (h1xh1) model
460 Lin_ParQuad_h1xulv_diff = NL_Lin_error - NL_ParQuad_h1xulv_error; %Error between
461 % Linear model and Partially Quadratic (h1xulv) model
462 Lin_Cubic_diff = NL_Lin_error - NL_Cubic_error; %Error between
463 % Linear model and Cubic model

```

```

454 Lin_fifth_diff = NL_Lin_error - NL_fifth_error; %Error between
      Linear model and 5th order model
455 Cubic_fifth_diff = NL_Cubic_error - NL_fifth_error; %Error between
      Cubic model and 5th order model
456 Cubic_quadratic_diff = NL_Quad_error - NL_Cubic_error;
457 figure
458 %Plots the contour of the difference between Linear and Quadratic model
459 contourf(ulv_low:ulv_hi, h1_low:h1_hi,...
460     Lin_Quad_diff(h1_low:h1_hi, ulv_low:ulv_hi), 40)
461 hold on
462 plot(200*ulv_arb,200*h1_arb,'kx','MarkerSize',30)
463 c = colorbar;
464 c.Label.String = 'Delta';
465 c.Label.FontSize = 16;
466 caxis([colorbar_range_min, colorbar_range_max])
467 title('Linear VS Quadratic @0.25m Contour-Plot')
468 xlabel('$u_{LV}$', 'Interpreter','latex','fontsize',16)
469 ylabel('$h_1$', 'Interpreter','latex','fontsize',16)
470 colormap(jet(20))
471 xt = get(gca, 'XTick');
472 set(gca, 'XTick', xt, 'XTickLabel', xt/200)
473 yt = get(gca, 'YTick');
474 set(gca, 'YTick', yt, 'YTickLabel', yt/200)
475
476 figure
477 %Plots the contour of the difference between Linear and Partially Quadratic (h1xh1)
      model
478 contourf(ulv_low:ulv_hi, h1_low:h1_hi,...
479     Lin_ParQuad_h1xh1_diff(h1_low:h1_hi, ulv_low:ulv_hi), 40)
480 hold on
481 plot(200*ulv_arb,200*h1_arb,'kx','MarkerSize',30)
482 c = colorbar;
483 c.Label.String = 'Delta';
484 c.Label.FontSize = 16;
485 caxis([colorbar_range_min, colorbar_range_max])
486 title('Linear VS Partially Quadratic (h1xh1) @0.25m Contour-Plot')
487 xlabel('$u_{LV}$', 'Interpreter','latex','fontsize',16)
488 ylabel('$h_1$', 'Interpreter','latex','fontsize',16)
489 colormap(jet(20))
490 xt = get(gca, 'XTick');
491 set(gca, 'XTick', xt, 'XTickLabel', xt/200)
492 yt = get(gca, 'YTick');
493 set(gca, 'YTick', yt, 'YTickLabel', yt/200)
494
495 figure
496 %Plots the contour of the difference between Linear and Partially Quadratic (h1xulv
      ) model
497 contourf(ulv_low:ulv_hi, h1_low:h1_hi,...
498     Lin_ParQuad_h1xulv_diff(h1_low:h1_hi, ulv_low:ulv_hi), 40)
499 hold on
500 plot(200*ulv_arb,200*h1_arb,'kx','MarkerSize',30)
501 c = colorbar;
502 c.Label.String = 'Delta';
503 c.Label.FontSize = 16;
504 caxis([colorbar_range_min, colorbar_range_max])
505 title('Linear VS Partially Quadratic (h1xulv) @0.25m Contour-Plot')
506 xlabel('$u_{LV}$', 'Interpreter','latex','fontsize',16)
507 ylabel('$h_1$', 'Interpreter','latex','fontsize',16)
508 colormap(jet(20))
509 xt = get(gca, 'XTick');
510 set(gca, 'XTick', xt, 'XTickLabel', xt/200)
511 yt = get(gca, 'YTick');
512 set(gca, 'YTick', yt, 'YTickLabel', yt/200)
513
514 figure
515 %Plots the contour of the difference between Linear and Cubic model
516 contourf(ulv_low:ulv_hi, h1_low:h1_hi,...
517     Lin_Cubic_diff(h1_low:h1_hi, ulv_low:ulv_hi), 40)
518 hold on
519 plot(200*ulv_arb,200*h1_arb,'kx','MarkerSize',30)
520 c = colorbar;
521 c.Label.String = 'Delta';
522 c.Label.FontSize = 16;

```

```

523 caxis([colorbar_range_min, colorbar_range_max])
524 title('Linear VS Cubic @0.25m Contour-Plot')
525 xlabel('$u_{LV}$', 'Interpreter','latex','fontsize',16)
526 ylabel('$h_1$', 'Interpreter','latex','fontsize',16)
527 colormap(jet(20))
528 xt = get(gca, 'XTick');
529 set(gca, 'XTick', xt, 'XTickLabel', xt/200)
530 yt = get(gca, 'YTick');
531 set(gca, 'YTick', yt, 'YTickLabel', yt/200)
532
533 figure
534 %Plots the contour of the difference between Linear and 5th order model
535 contourf(ulv_low:ulv_hi, h1_low:h1_hi,...
536         Lin_fifth_diff(h1_low:h1_hi, ulv_low:ulv_hi), 40)
537 hold on
538 plot(200*ulv_arb,200*h1_arb,'kx','MarkerSize',30)
539 c = colorbar;
540 c.Label.String = 'Delta';
541 c.Label.FontSize = 16;
542 caxis([colorbar_range_min, colorbar_range_max])
543 title('Linear VS 5th Order @0.25m Contour-Plot')
544 xlabel('$u_{LV}$', 'Interpreter','latex','fontsize',16)
545 ylabel('$h_1$', 'Interpreter','latex','fontsize',16)
546 colormap(jet(20))
547 xt = get(gca, 'XTick');
548 set(gca, 'XTick', xt, 'XTickLabel', xt/200)
549 yt = get(gca, 'YTick');
550 set(gca, 'YTick', yt, 'YTickLabel', yt/200)
551
552 figure
553 %Plots the contour of the difference between Cubic and 5th order model
554 contourf(ulv_low:ulv_hi, h1_low:h1_hi,...
555         Cubic_fifth_diff(h1_low:h1_hi, ulv_low:ulv_hi), 40)
556 hold on
557 plot(200*ulv_arb,200*h1_arb,'kx','MarkerSize',30)
558 c = colorbar;
559 c.Label.String = 'Delta';
560 c.Label.FontSize = 16;
561 caxis([colorbar_range_min, colorbar_range_max])
562 title('Cubic VS 5th Order @0.25m Contour-Plot')
563 xlabel('$u_{LV}$', 'Interpreter','latex','fontsize',16)
564 ylabel('$h_1$', 'Interpreter','latex','fontsize',16)
565 colormap(jet(20))
566 xt = get(gca, 'XTick');
567 set(gca, 'XTick', xt, 'XTickLabel', xt/200)
568 yt = get(gca, 'YTick');
569 set(gca, 'YTick', yt, 'YTickLabel', yt/200)
570
571 %% Non-Linear VS Other Models Contour-Plot
572
573 % This section plots the Contour-Plot of the comparison between the NonLinear
574 % Model, and all of the other models
575
576 close all
577 figure
578 %Plots the contour of the error for the Quadratic model
579 contourf(ulv_low:ulv_hi, h1_low:h1_hi,...
580         NL_Quad_error(h1_low:h1_hi, ulv_low:ulv_hi), 40)
581 hold on
582 plot(200*ulv_arb,200*h1_arb,'kx','MarkerSize',30)
583 c = colorbar;
584 c.Label.String = 'Delta';
585 c.Label.FontSize = 16;
586 caxis([colorbar_range_min, colorbar_range_max])
587 title('Nonlinear VS Quadratic @0.25m Contour-Plot')
588 xlabel('$u_{LV}$', 'Interpreter','latex','fontsize',16)
589 ylabel('$h_1$', 'Interpreter','latex','fontsize',16)
590 colormap(jet(20))
591 xt = get(gca, 'XTick');
592 set(gca, 'XTick', xt, 'XTickLabel', xt/200)
593 yt = get(gca, 'YTick');
594 set(gca, 'YTick', yt, 'YTickLabel', yt/200)
595

```

```

596 figure
597 %Plots the contour of the error for the Linear model
598 contourf(ulv_low:ulv_hi, h1_low:h1_hi,...
599         NL_Lin_error(h1_low:h1_hi, ulv_low:ulv_hi), 40)
600 hold on
601 plot(200*ulv_arb,200*h1_arb,'kx','MarkerSize',30)
602 c = colorbar;
603 c.Label.String = 'Delta';
604 c.Label.FontSize = 16;
605 caxis([colorbar_range_min, colorbar_range_max])
606 title('NonLinear VS Linear @0.25m Contour-Plot')
607 xlabel('$u_{LV}$', 'Interpreter','latex','fontsize',16)
608 ylabel('$h_1$', 'Interpreter','latex','fontsize',16)
609 colormap(jet(20))
610 xt = get(gca, 'XTick');
611 set(gca, 'XTick', xt, 'XTickLabel', xt/200)
612 yt = get(gca, 'YTick');
613 set(gca, 'YTick', yt, 'YTickLabel', yt/200)
614
615 figure
616 %Plots the contour of the error for the Partially Quadratic (h1xh1) model
617 contourf(ulv_low:ulv_hi, h1_low:h1_hi,...
618         NL_ParQuad_h1xh1_error(h1_low:h1_hi, ulv_low:ulv_hi), 40)
619 hold on
620 plot(200*ulv_arb,200*h1_arb,'kx','MarkerSize',30)
621 c = colorbar;
622 c.Label.String = 'Delta';
623 c.Label.FontSize = 16;
624 caxis([colorbar_range_min, colorbar_range_max])
625 title('NonLinear VS Partially Quadratic (h1xh1) @0.25m Contour-Plot')
626 xlabel('$u_{LV}$', 'Interpreter','latex','fontsize',16)
627 ylabel('$h_1$', 'Interpreter','latex','fontsize',16)
628 colormap(jet(20))
629 xt = get(gca, 'XTick');
630 set(gca, 'XTick', xt, 'XTickLabel', xt/200)
631 yt = get(gca, 'YTick');
632 set(gca, 'YTick', yt, 'YTickLabel', yt/200)
633
634 figure
635 %Plots the contour of the error for the Partially Quadratic (h1xulv) model
636 contourf(ulv_low:ulv_hi, h1_low:h1_hi,...
637         NL_ParQuad_h1xulv_error(h1_low:h1_hi, ulv_low:ulv_hi), 40)
638 hold on
639 plot(200*ulv_arb,200*h1_arb,'kx','MarkerSize',30)
640 c = colorbar;
641 c.Label.String = 'Delta';
642 c.Label.FontSize = 16;
643 caxis([colorbar_range_min, colorbar_range_max])
644 title('NonLinear VS Partially Quadratic (h1xulV) @0.25m Contour-Plot')
645 xlabel('$u_{LV}$', 'Interpreter','latex','fontsize',16)
646 ylabel('$h_1$', 'Interpreter','latex','fontsize',16)
647 colormap(jet(20))
648 xt = get(gca, 'XTick');
649 set(gca, 'XTick', xt, 'XTickLabel', xt/200)
650 yt = get(gca, 'YTick');
651 set(gca, 'YTick', yt, 'YTickLabel', yt/200)
652
653 figure
654 %Plots the contour of the error for the Cubic model
655 contourf(ulv_low:ulv_hi, h1_low:h1_hi,...
656         NL_Cubic_error(h1_low:h1_hi, ulv_low:ulv_hi), 40)
657 hold on
658 plot(200*ulv_arb,200*h1_arb,'kx','MarkerSize',30)
659 c = colorbar;
660 c.Label.String = 'Delta';
661 c.Label.FontSize = 16;
662 caxis([colorbar_range_min, colorbar_range_max])
663 title('NonLinear VS Cubic @0.25m Contour-Plot')
664 xlabel('$u_{LV}$', 'Interpreter','latex','fontsize',16)
665 ylabel('$h_1$', 'Interpreter','latex','fontsize',16)
666 colormap(jet(20))
667 xt = get(gca, 'XTick');
668 set(gca, 'XTick', xt, 'XTickLabel', xt/200)

```

```

669 yt = get(gca, 'YTick');
670 set(gca, 'YTick', yt, 'YTickLabel', yt/200)
671
672 figure
673 %Plots the contour of the error for the 5th order model
674 contourf(ulv_low:ulv_hi, h1_low:h1_hi,...
675         NL_fifth_error(h1_low:h1_hi, ulv_low:ulv_hi),40)
676 hold on
677 plot(200*ulv_arb,200*h1_arb,'kx','MarkerSize',30)
678 c = colorbar;
679 c.Label.String = 'Delta';
680 c.Label.FontSize = 16;
681 caxis([colorbar_range_min, colorbar_range_max])
682 title('NonLinear VS 5th Order @0.25m Contour-Plot')
683 xlabel('\$u_{LV}\$', 'Interpreter','latex','fontsize',16)
684 ylabel('\$h_1\$', 'Interpreter','latex','fontsize',16)
685 colormap(jet(20))
686 xt = get(gca, 'XTick');
687 set(gca, 'XTick', xt, 'XTickLabel', xt/200)
688 yt = get(gca, 'YTick');
689 set(gca, 'YTick', yt, 'YTickLabel', yt/200)
690
691 %% Linear VS Quadratic Colormap
692
693 close all
694
695 %We want to make a matrix that tells us where the models differ from each
696 %other. Call this h
697 h = ones(201);
698
699 %Sorting algorithm
700 %Here we define a arbitrary value that tells us if the models differ. In
701 %this example, we chose 0.0005
702 for i = 1:201
703     for j = 1:201
704         if Lin_Quad_diff(i,j) == 0
705             h(i,j) = 5; %Quad
706         elseif Lin_Quad_diff(i,j) > 0 && Lin_Quad_diff(i,j) < 0.0005 %
707             Quad>
708             h(i,j) = 1;
709         elseif Lin_Quad_diff(i,j) > 0.0005 % Quad>>
710             h(i,j) = 0;
711         elseif Lin_Quad_diff(i,j) < 0 && Lin_Quad_diff(i,j) > -0.0005 % Lin>
712             h(i,j) = 2;
713         elseif Lin_Quad_diff(i,j) < -0.0005 % Lin>>
714             h(i,j) = 3;
715         end
716     end
717 end
718
719 %Now we have the marix h, which tells us where the models differ, but it
720 %does not tell us if the models are a good approximation to the NonLinear
721 %system.
722 %Sorting algorithm which gives us a 'red flag' if both models are a bad
723 %approximation at a certain point. Here, if both differ more than 0.0005
724 %from the NonLinear model, they are defined as a bad approximation.
725 for i = 1:201
726     for j = 1:201
727         if abs(NL_Lin_error(i,j)) > 0.005 && abs(NL_Quad_error(i,j)) > 0.005
728             h(i,j) = 4;
729         end
730     end
731 end
732
733
734 C = h(H1_min:H1_max, ULV_min:ULV_max);
735 [ii, jj] = find(C == 5)
736
737
738 figure
739 %Plots the contour of the data-matrix h

```

```

740 contourf(h, 100, 'EdgeColor', 'None')
741 hold on
742 plot(200*ulv_arb,200*h1_arb,'kx','MarkerSize',30)
743 hold on
744 plot([ULV_min ULV_min], [H1_min H1_max],'k','LineWidth',2)
745 plot([ULV_max ULV_max], [H1_min H1_max],'k','LineWidth',2)
746 plot([ULV_min ULV_max], [H1_min H1_min],'k','LineWidth',2)
747 plot([ULV_min ULV_max], [H1_max H1_max],'k','LineWidth',2)
748
749
750 colorbar('Ticks', [0, 1, 2, 3, 4], 'TickLabels', {'Quad>>', 'Quad>', 'Lin>', 'Lin>>'
, 'N/A'})
751 colormap(map)
752 caxis([0, 4])
753 title('Linear VS Quadratic @0.25m Contour-Plot')
754 xlabel('$u_{LV}$', 'Interpreter','latex','fontsize',16)
755 ylabel('$h_1$', 'Interpreter','latex','fontsize',16)
756 xt = get(gca, 'XTick');
757 set(gca, 'XTick', xt, 'XTickLabel', xt/200)
758 yt = get(gca, 'YTick');
759 set(gca, 'YTick', yt, 'YTickLabel', yt/200)
760
761 %% Linear VS Partially Quadratic (h1xh1) Colormap
762
763 close all
764
765 %Data-matrix
766 h = ones(201);
767
768 %Sorting algorithm
769 for i = 1:201
770     for j = 1:201
771         if Lin_ParQuad_h1xh1_diff(i,j) > 0 && Lin_ParQuad_h1xh1_diff(i,j) < 0.0005
772             %ParQuad_h1xh1>
773             h(i,j) = 1;
774             elseif Lin_ParQuad_h1xh1_diff(i,j) > 0.0005 %ParQuad_h1xh1>>
775                 h(i,j) = 0;
776             elseif Lin_ParQuad_h1xh1_diff(i,j) < 0 && Lin_ParQuad_h1xh1_diff(i,j) >
777                 -0.0005 %Lin>
778                 h(i,j) = 2;
779             elseif Lin_ParQuad_h1xh1_diff(i,j) < -0.0005 %Lin>>
780                 h(i,j) = 3;
781         end
782     end
783 end
784
785 %'red flag' algorithm
786 for i = 1:201
787     for j = 1:201
788         if abs(NL_Lin_error(i,j)) > 0.005 && abs(NL_ParQuad_h1xh1_error(i,j)) >
789             0.005
790             h(i,j) = 4;
791         end
792     end
793 end
794 figure
795 %Plots the contour of the data-matrix h
796 contourf(h, 100, 'EdgeColor', 'None')
797 hold on
798 plot(200*ulv_arb,200*h1_arb,'kx','MarkerSize',30)
799 colorbar('Ticks', [0, 1, 2, 3, 4], 'TickLabels', {'ParQuad>>', 'ParQuad>', 'Lin>', '
Lin>>', 'N/A'})
800 colormap(map)
801 caxis([0, 4])
802 title('Linear VS Partially Quadratic (h1xh1) @0.25m Contour-Plot')
803 xlabel('$u_{LV}$', 'Interpreter','latex','fontsize',16)
804 ylabel('$h_1$', 'Interpreter','latex','fontsize',16)
805 xt = get(gca, 'XTick');
806 set(gca, 'XTick', xt, 'XTickLabel', xt/200)
807 yt = get(gca, 'YTick');

```

```

808 set(gca, 'YTick', yt, 'YTickLabel', yt/200)
809
810 %% Linear VS Partially Quadratic (h1xulV) Colormap
811
812 close all
813
814 %Data-matrix
815 h = ones(201);
816
817 %Sorting algorithm
818 for i = 1:201
819     for j = 1:201
820         if Lin_ParQuad_h1xulv_diff(i,j) > 0 && Lin_ParQuad_h1xulv_diff(i,j) <
0.0005 %ParQuad_h1xulv>
821             h(i,j) = 1;
822         elseif Lin_ParQuad_h1xulv_diff(i,j) > 0.0005 %ParQuad_h1xulv>>
823             h(i,j) = 0;
824         elseif Lin_ParQuad_h1xulv_diff(i,j) < 0 && Lin_ParQuad_h1xulv_diff(i,j) >
-0.0005 %Lin>
825             h(i,j) = 2;
826         elseif Lin_ParQuad_h1xulv_diff(i,j) < -0.0005 %Lin>>
827             h(i,j) = 3;
828
829         end
830     end
831 end
832
833 %'red flag' algorithm
834 for i = 1:201
835     for j = 1:201
836         if abs(NL_Lin_error(i,j)) > 0.005 && abs(NL_ParQuad_h1xulv_error(i,j)) >
0.005
837             h(i,j) = 4;
838         end
839     end
840 end
841
842 figure
843 contourf(h, 100, 'EdgeColor', 'None') %Plots the contour of the data-matrix h
844 hold on
845 plot(200*ulv_arb,200*h1_arb,'kx','MarkerSize',30)
846 colorbar('Ticks', [0, 1, 2, 3, 4], 'TickLabels', {'ParQuad>>', 'ParQuad>', 'Lin>', '
Lin>>', 'N/A'})
847 colormap(map)
848 caxis([0, 4])
849 title('Linear VS Partially Quadratic (h1xulv) @0.25m Contour-Plot')
850 xlabel('\$u_{LV}\$', 'Interpreter','latex','fontSize',16)
851 ylabel('\$h_1\$', 'Interpreter','latex','fontSize',16)
852 xt = get(gca, 'XTick');
853 set(gca, 'XTick', xt, 'XTickLabel', xt/200)
854 yt = get(gca, 'YTick');
855 set(gca, 'YTick', yt, 'YTickLabel', yt/200)
856
857 %% Linear VS Cubic Colormap
858
859 close all
860
861 %Data-matrix
862 h = ones(201);
863
864 %Sorting algorithm
865 for i = 1:201
866     for j = 1:201
867         if Lin_Cubic_diff(i,j) > 0 && Lin_Cubic_diff(i,j) < 0.0005 %Cubic>
868             h(i,j) = 1;
869         elseif Lin_Cubic_diff(i,j) > 0.0005 %Cubic>>
870             h(i,j) = 0;
871         elseif Lin_Cubic_diff(i,j) < 0 && Lin_Cubic_diff(i,j) > -0.0005 %Lin>
872             h(i,j) = 2;
873         elseif Lin_Cubic_diff(i,j) < -0.0005 %Lin>>
874             h(i,j) = 3;
875
876     end
877 end

```

```

877     end
878 end
879
880 %'red flag' algorithm
881 for i = 1:201
882     for j = 1:201
883         if abs(NL_Lin_error(i,j)) > 0.005 && abs(NL_Cubic_error(i,j)) > 0.005
884             h(i,j) = 4;
885         end
886     end
887 end
888
889 figure
890 %Plots the contour of the data-matrix h
891 contourf(h, 100, 'EdgeColor', 'None')
892 hold on
893 plot(200*ulv_arb,200*h1_arb,'kx','MarkerSize',30)
894 colorbar('Ticks', [0, 1, 2, 3, 4], 'TickLabels', {'Cubic>>', 'Cubic>', 'Lin>', 'Lin
    >>', 'N/A'})
895 colormap(map)
896 caxis([0, 4])
897 title('Linear VS Cubic @0.25m Contour-Plot')
898 xlabel('$u_{LV}$', 'Interpreter','latex','fontsize',16)
899 ylabel('$h_1$', 'Interpreter','latex','fontsize',16)
900 xt = get(gca, 'XTick');
901 set(gca, 'XTick', xt, 'XTickLabel', xt/200)
902 yt = get(gca, 'YTick');
903 set(gca, 'YTick', yt, 'YTickLabel', yt/200)
904
905 %% Linear VS Fifth order Colormap
906
907 close all
908
909 %Data-matrix
910 h = ones(201);
911
912 %Sorting algorithm
913 for i = 1:201
914     for j = 1:201
915         if Lin_fifth_diff(i,j) > 0 && Lin_fifth_diff(i,j) < 0.0005           %Fifth>
916             h(i,j) = 1;
917         elseif Lin_fifth_diff(i,j) > 0.0005                               %Fifth>>
918             h(i,j) = 0;
919         elseif Lin_fifth_diff(i,j) < 0 && Lin_fifth_diff(i,j) > -0.0005    %Linear>
920             h(i,j) = 2;
921         elseif Lin_fifth_diff(i,j) < -0.0005                               %Linear>>
922             h(i,j) = 3;
923     end
924 end
925 end
926
927 %'red flag' algorithm
928 for i = 1:201
929     for j = 1:201
930         if abs(NL_Lin_error(i,j)) > 0.005 && abs(NL_fifth_error(i,j)) > 0.005
931             h(i,j) = 4;
932         end
933     end
934 end
935 end
936
937 figure
938 %Plots the contour of the data-matrix h
939 contourf(h, 100, 'EdgeColor', 'None')
940 hold on
941 plot(200*ulv_arb,200*h1_arb,'kx','MarkerSize',30)
942 colorbar('Ticks', [0, 1, 2, 3, 4], 'TickLabels', {'5th order>>', '5th order>', '
    Linear>', 'Linear>>', 'N/A'})
943 colormap(map)
944 caxis([0, 4])
945 title('Linear VS 5th Order @0.25m Contour-Plot')
946 xlabel('$u_{LV}$', 'Interpreter','latex','fontsize',16)
947 ylabel('$h_1$', 'Interpreter','latex','fontsize',16)

```



```

948 xt = get(gca, 'XTick');
949 set(gca, 'XTick', xt, 'XTickLabel', xt/200)
950 yt = get(gca, 'YTick');
951 set(gca, 'YTick', yt, 'YTickLabel', yt/200)
952
953 %% Cubic VS Fifth order Colormap
954
955 %close all
956
957 %Data-matrix
958 h = ones(201);
959
960 %Sorting algorithm
961 for i = 1:201
962     for j = 1:201
963         if Cubic_fifth_diff(i,j) == 0
964             h(i,j) = 5; %Cubic
965             == Fifth
966             elseif Cubic_fifth_diff(i,j) > 0 && Cubic_fifth_diff(i,j) < 0.0005 %
967                 Fifth>
968                 h(i,j) = 1;
969                 elseif Cubic_fifth_diff(i,j) > 0.0005 %Fifth>>
970                     h(i,j) = 0;
971                     elseif Cubic_fifth_diff(i,j) < 0 && Cubic_fifth_diff(i,j) > -0.0005 %
972                         Cubic>
973                         h(i,j) = 2;
974                         elseif Cubic_fifth_diff(i,j) < -0.0005 %Cubic>>
975                             h(i,j) = 3;
976
977                     end
978                 end
979             end
980         end
981     end
982 end
983
984 %'red flag' algorithm
985 for i = 1:201
986     for j = 1:201
987         if abs(NL_Cubic_error(i,j)) > 0.005 && abs(NL_fifth_error(i,j)) > 0.005
988             h(i,j) = 4;
989         end
990     end
991 end
992
993 C = h(H1_min:H1_max, ULV_min:ULV_max);
994 [ii, jj] = find(C == 2)
995
996 figure
997 %Plots the contour of the data-matrix h
998 contourf(h, 100, 'EdgeColor', 'None')
999 hold on
1000 plot(200*ulv_arb,200*h1_arb,'kx','MarkerSize',30)
1001 hold on
1002 plot([ULV_min ULV_min], [H1_min H1_max],'k','LineWidth',2)
1003 plot([ULV_max ULV_max], [H1_min H1_max],'k','LineWidth',2)
1004 plot([ULV_min ULV_max], [H1_min H1_min],'k','LineWidth',2)
1005 plot([ULV_min ULV_max], [H1_max H1_max],'k','LineWidth',2)
1006 colorbar('Ticks', [0, 1, 2, 3, 4], 'TickLabels', {'5th order>>', '5th order>>',
1007     Cubic>', 'Cubic>>', 'N/A'})
1008 colormap(map)
1009 caxis([0, 4])
1010 title('5th VS Cubic @0.25m Contour-Plot')
1011 xlabel('$u_{LV}$', 'Interpreter','latex','fontSize',16)
1012 ylabel('$h_1$', 'Interpreter','latex','fontSize',16)
1013 xt = get(gca, 'XTick');
1014 set(gca, 'XTick', xt, 'XTickLabel', xt/200)
1015 yt = get(gca, 'YTick');
1016 set(gca, 'YTick', yt, 'YTickLabel', yt/200)
1017
1018 %% Cubic VS Quadratic Colormap
1019 close all
1020
1021 %Data-matrix
1022 h = ones(201);
1023

```

```

1017 %Sorting algorithm
1018 for i = 1:201
1019     for j = 1:201
1020         if Cubic_quadratic_diff(i,j) == 0
1021             h(i,j) = 5; %Quad
1022             == cubic
1023                 elseif Cubic_quadratic_diff(i,j) > 0 && Cubic_quadratic_diff(i,j) < 0.0005
1024                     %Cubic>
1025                     h(i,j) = 1;
1026                 elseif Cubic_quadratic_diff(i,j) > 0.0005 %
1027                     Cubic>>
1028                     h(i,j) = 0;
1029                 elseif Cubic_quadratic_diff(i,j) < 0 && Cubic_quadratic_diff(i,j) > -0.0005
1030                     %Quad>
1031                     h(i,j) = 2;
1032                 elseif Cubic_quadratic_diff(i,j) < -0.0005 %
1033                     Quad>>
1034                     h(i,j) = 3;
1035             end
1036         end
1037     end
1038 end
1039
1040 %'red flag' algorithm
1041 for i = 1:201
1042     for j = 1:201
1043         if abs(NL_Cubic_error(i,j)) > 0.005 && abs(NL_Quad_error(i,j)) > 0.005
1044             h(i,j) = 4;
1045         end
1046     end
1047 end
1048
1049 C = h(H1_min:H1_max, ULV_min:ULV_max);
1050 [ii, jj] = find(C == 2)
1051
1052 figure
1053 %Plots the contour of the data-matrix h
1054 contourf(ulv_low:ulv_hi, h1_low:h1_hi,...
1055     h(h1_low:h1_hi, ulv_low:ulv_hi), 100, 'EdgeColor', 'None')
1056 hold on
1057 plot(200*ulv_arb,200*h1_arb,'kx','MarkerSize',30)
1058 hold on
1059 plot([ULV_min ULV_min], [H1_min H1_max],'k','LineWidth',2)
1060 plot([ULV_max ULV_max], [H1_min H1_max],'k','LineWidth',2)
1061 plot([ULV_min ULV_max], [H1_min H1_min],'k','LineWidth',2)
1062 plot([ULV_min ULV_max], [H1_max H1_max],'k','LineWidth',2)
1063 colorbar('Ticks', [0, 1, 2, 3, 4], 'TickLabels', {'Cubic>>', 'Cubic>', 'Quadratic>',
1064     'Quadratic>>', 'N/A'})
1065 colormap(map)
1066 caxis([0, 4])
1067 title('Quadratic VS Cubic @0.25m Contour-Plot')
1068 xlabel('$u_{LV}$', 'Interpreter','latex','fontSize',16)
1069 ylabel('$h_1$', 'Interpreter','latex','fontSize',16)
1070 xt = get(gca, 'XTick');
1071 set(gca, 'XTick', xt, 'XTickLabel', xt/200)
1072 yt = get(gca, 'YTick');
1073 set(gca, 'YTick', yt, 'YTickLabel', yt/200)
1074 %% Carleman Linearization
1075 close all
1076
1077 n = 1;
1078 Initial_level = 0;
1079
1080 [A_matrix_1, B_matrix_1, C_matrix_1, D_matrix_1, Initial_vector_1] =
1081     Carleman_Linearized_func(...
1082         par_der_h1_verdi,...
1083         par_der_uLV001_verdi,...
1084         par_der_uPA001_verdi,...
1085         par_der_h1_uLV001_verdi,...
1086         par_der_h1_h1_verdi,...
1087         par_der_h1_h1_h1_verdi,...
1088         par_der_h1_h1_uLV001_verdi,...
1089         Initial_level,...

```

```

1083         n);
1084 n = 2;
1085 [A_matrix_2, B_matrix_2, C_matrix_2, D_matrix_2, Initial_vector_2] =
1086     Carleman_Linearized_func(...
1087         par_der_h1_verdi,...
1088         par_der_uLV001_verdi,...
1089         par_der_uPA001_verdi,...
1090         par_der_h1_uLV001_verdi,...
1091         par_der_h1_h1_verdi,...
1092         par_der_h1_h1_h1_verdi,...
1093         par_der_h1_h1_uLV001_verdi,...
1094         Initial_level,...
1095         n);
1096 n = 3;
1097 [A_matrix_3, B_matrix_3, C_matrix_3, D_matrix_3, Initial_vector_3] =
1098     Carleman_Linearized_func(...
1099         par_der_h1_verdi,...
1100         par_der_uLV001_verdi,...
1101         par_der_uPA001_verdi,...
1102         par_der_h1_uLV001_verdi,...
1103         par_der_h1_h1_verdi,...
1104         par_der_h1_h1_h1_verdi,...
1105         par_der_h1_h1_uLV001_verdi,...
1106         Initial_level,...
1107         n);
1108 n = 4;
1109 [A_matrix_4, B_matrix_4, C_matrix_4, D_matrix_4, Initial_vector_4] =
1110     Carleman_Linearized_func(...
1111         par_der_h1_verdi,...
1112         par_der_uLV001_verdi,...
1113         par_der_uPA001_verdi,...
1114         par_der_h1_uLV001_verdi,...
1115         par_der_h1_h1_verdi,...
1116         par_der_h1_h1_h1_verdi,...
1117         par_der_h1_h1_uLV001_verdi,...
1118         Initial_level,...
1119         n);
1120 n = 5;
1121 [A_matrix_5, B_matrix_5, C_matrix_5, D_matrix_5, Initial_vector_5] =
1122     Carleman_Linearized_func(...
1123         par_der_h1_verdi,...
1124         par_der_uLV001_verdi,...
1125         par_der_uPA001_verdi,...
1126         par_der_h1_uLV001_verdi,...
1127         par_der_h1_h1_verdi,...
1128         par_der_h1_h1_h1_verdi,...
1129         par_der_h1_h1_uLV001_verdi,...
1130         Initial_level,...
1131         n);
1132 n = 10;
1133 [A_matrix_10, B_matrix_10, C_matrix_10, D_matrix_10, Initial_vector_10] =
1134     Carleman_Linearized_func(...
1135         par_der_h1_verdi,...
1136         par_der_uLV001_verdi,...
1137         par_der_uPA001_verdi,...
1138         par_der_h1_uLV001_verdi,...
1139         par_der_h1_h1_verdi,...
1140         par_der_h1_h1_h1_verdi,...
1141         par_der_h1_h1_uLV001_verdi,...
1142         Initial_level,...
1143         n);
1144 n = 6;
1145 [A_matrix_6, B_matrix_6, C_matrix_6, D_matrix_6, Initial_vector_6, E_matrix_6] =...
1146     Carleman_NonLinearized_func(...
1147         par_der_h1_verdi,...
1148         par_der_uLV001_verdi,...
1149         par_der_uPA001_verdi,...
1150         par_der_h1_uLV001_verdi,...
1151         par_der_h1_h1_verdi,...
1152         par_der_h1_h1_h1_verdi,...

```

```

1151         par_der_h1_h1_uLV001_verdi,...
1152         Initial_level,...
1153         n);
1154
1155
1156         %Non linear Carleman approximations
1157         n = 1;
1158 [A_matrix_NL_1, B_matrix_NL_1, C_matrix_NL_1, D_matrix_NL_1, Initial_vector_NL_1,
        E_matrix_NL_1] =...
1159         Carleman_NonLinearized_func(...
1160         par_der_h1_verdi,...
1161         par_der_uLV001_verdi,...
1162         par_der_uPA001_verdi,...
1163         par_der_h1_uLV001_verdi,...
1164         par_der_h1_h1_verdi,...
1165         par_der_h1_h1_h1_verdi,...
1166         par_der_h1_h1_uLV001_verdi,...
1167         Initial_level,...
1168         n);
1169
1170 E_matrix_matrix_1 = [];
1171
1172 for i = 1:n
1173     E_matrix_matrix_1(:,i) = E_matrix_NL_1{i};
1174 end
1175
1176         n = 2;
1177 [A_matrix_NL_2, B_matrix_NL_2, C_matrix_NL_2, D_matrix_NL_2, Initial_vector_NL_2,
        E_matrix_NL_2] =...
1178         Carleman_NonLinearized_func(...
1179         par_der_h1_verdi,...
1180         par_der_uLV001_verdi,...
1181         par_der_uPA001_verdi,...
1182         par_der_h1_uLV001_verdi,...
1183         par_der_h1_h1_verdi,...
1184         par_der_h1_h1_h1_verdi,...
1185         par_der_h1_h1_uLV001_verdi,...
1186         Initial_level,...
1187         n);
1188
1189         E_matrix_matrix_2 = [];
1190
1191 for i = 1:n
1192     E_matrix_matrix_2(:,i) = E_matrix_NL_2{i};
1193 end
1194
1195         n = 3;
1196 [A_matrix_NL_3, B_matrix_NL_3, C_matrix_NL_3, D_matrix_NL_3, Initial_vector_NL_3,
        E_matrix_NL_3] =...
1197         Carleman_NonLinearized_func(...
1198         par_der_h1_verdi,...
1199         par_der_uLV001_verdi,...
1200         par_der_uPA001_verdi,...
1201         par_der_h1_uLV001_verdi,...
1202         par_der_h1_h1_verdi,...
1203         par_der_h1_h1_h1_verdi,...
1204         par_der_h1_h1_uLV001_verdi,...
1205         Initial_level,...
1206         n);
1207 E_matrix_matrix_3 = [];
1208
1209 for i = 1:n
1210     E_matrix_matrix_3(:,i) = E_matrix_NL_3{i};
1211 end
1212
1213
1214         n = 4;
1215 [A_matrix_NL_4, B_matrix_NL_4, C_matrix_NL_4, D_matrix_NL_4, Initial_vector_NL_4,
        E_matrix_NL_4] =...
1216         Carleman_NonLinearized_func(...
1217         par_der_h1_verdi,...
1218         par_der_uLV001_verdi,...
1219         par_der_uPA001_verdi,...

```

```

1220         par_der_h1_uLV001_verdi,...
1221         par_der_h1_h1_verdi,...
1222         par_der_h1_h1_h1_verdi,...
1223         par_der_h1_h1_uLV001_verdi,...
1224         Initial_level,...
1225         n);
1226
1227 E_matrix_matrix_4 = [];
1228
1229 for i = 1:n
1230     E_matrix_matrix_4(:,i) = E_matrix_NL_4{i};
1231 end
1232
1233         n = 5;
1234 [A_matrix_NL_5, B_matrix_NL_5, C_matrix_NL_5, D_matrix_NL_5, Initial_vector_NL_5,
1235     E_matrix_NL_5] =...
1236         Carleman_NonLinearized_func(...
1237         par_der_h1_verdi,...
1238         par_der_uLV001_verdi,...
1239         par_der_uPA001_verdi,...
1240         par_der_h1_uLV001_verdi,...
1241         par_der_h1_h1_verdi,...
1242         par_der_h1_h1_h1_verdi,...
1243         par_der_h1_h1_uLV001_verdi,...
1244         Initial_level,...
1245         n);
1246 E_matrix_matrix_5 = [];
1247
1248 for i = 1:n
1249     E_matrix_matrix_5(:,i) = E_matrix_NL_5{i};
1250 end
1251
1252         n = 10;
1253 [A_matrix_NL_10, B_matrix_NL_10, C_matrix_NL_10, D_matrix_NL_10,
1254     Initial_vector_NL_10, E_matrix_NL_10] =...
1255         Carleman_NonLinearized_func(...
1256         par_der_h1_verdi,...
1257         par_der_uLV001_verdi,...
1258         par_der_uPA001_verdi,...
1259         par_der_h1_uLV001_verdi,...
1260         par_der_h1_h1_verdi,...
1261         par_der_h1_h1_h1_verdi,...
1262         par_der_h1_h1_uLV001_verdi,...
1263         Initial_level,...
1264         n);
1265 E_matrix_matrix_10 = [];
1266
1267 for i = 1:n
1268     E_matrix_matrix_10(:,i) = E_matrix_NL_10{i};
1269 end
1270
1271 [NUM,DEN] = ss2tf(A_matrix_1,B_matrix_1,C_matrix_1,D_matrix_1,1);
1272 system = tf(NUM,DEN);
1273 stability = isstable(system)
1274 figure
1275 pzmap(system)
1276 figure
1277 step(system)
1278
1279 %% Quadratic controller NY test
1280 n = 4;
1281 Initial_level = 0.05;
1282
1283 Alpha = 0.0; %Scenario 1: 0.096   Scenario 2: Grense 0.036
1284 %Scenario 1():0.221   Scenario 2(): Grense 0.077
1285
1286 %Senario 1: Ivar = 0.094
1287
1288 gamma = 0.1; %7e-1
1289
1290 %ulv_arb = 0.5159, dulv_max = 0.48
1291 %upa_arb = 0.65, dupa_max = 0.2

```

```

1291 dupa_max = 0.2; % var 0.2
1292 dulv_max = 0.45; %
1293 a = -0.05%-0.05; %delta_h1 min
1294 b = 0.05; %delta_h1 max
1295 x1 = [a b];
1296 Vertex = x1;
1297
1298 punkt_cell = cell(n,1);
1299
1300 if n >= 2
1301     for i = 2:n
1302         if mod(i,2) ~= 0
1303             punkt_cell{i} = x1.^i;
1304         end
1305         if mod(i,2) == 0
1306             punkt_cell{i} = [-max(a^i, b^i)/10,max(a^i, b^i)];
1307         end
1308         Vertex = combvec(Vertex, punkt_cell{i});
1309     end
1310 else
1311     Vertex = Vertex';
1312 end
1313
1314 %%%%%%%%%%%%%%%
1315 %Vertex_shifted = Vertex;
1316 [A_test,B_test] = vert2con(Vertex');
1317 z = B_test; %
1318
1319 ak_T = A_test./z;
1320 ak = ak_T';
1321
1322 %%%%%%%%%%%%%%%
1323 [A_matrix_1var, B_matrix_1var, C_matrix_1var, D_matrix_1var, Initial_vector_1var,
    E_matrix_1var] = Carleman_NonLinearized_func(...
1324     par_der_h1_verdi,...
1325     par_der_uLV001_verdi,...
1326     par_der_uPA001_verdi,...
1327     par_der_h1_uLV001_verdi,...
1328     par_der_h1_h1_verdi,...
1329     par_der_h1_h1_h1_verdi,...
1330     par_der_h1_h1_uLV001_verdi,...
1331     Initial_level,...
1332     n);
1333 %dupa_max = 0.2, dulv_max = 0.48
1334 B_matrix_1var(:,2) = 0;
1335
1336 for i = 1:n
1337     E_matrix_1var{i}(:,2) = 0;
1338 end
1339
1340 [K_1var, P_1var] = Quadratic_controller(A_matrix_1var, B_matrix_1var, E_matrix_1var
    , Vertex, Alpha, gamma,dupa_max,dulv_max,ak);
1341
1342 strucK.A = A_matrix_1var;
1343 strucK.B = B_matrix_1var;
1344 strucK.K = K_1var;
1345 strucK.E = E_matrix_1var;
1346
1347 [T1,X] = ode45(@(t,x)Quadratic_system(t, x, strucK),0:0.001:160,Initial_vector_1var
    ');
1348
1349 close all
1350 figure(1)
1351 hold on
1352 for i = 1:n
1353     plot(T1,X(:,i))
1354 end
1355 xlabel ('Time [s]')
1356 ylabel ('Delta height [m]')
1357 grid on
1358 hold off
1359
1360 figure(2)

```

```

1361 plot(T1,X(:,1))
1362 xlabel('Time [s]')
1363 ylabel('Delta height [m]')
1364 grid on
1365
1366 E_matrix_matrix_1var = [];
1367 for i = 1:n
1368     [r,k] = size(E_matrix_matrix_1var);
1369     E_matrix_matrix_1var(:,k+1:k+2) = E_matrix_1var{i};
1370 end
1371 [r,k] = size(X);
1372 U = [];
1373 for i = 1:r
1374     U(i,:) = (K_1var*X(i,:))';
1375 end
1376
1377 figure(3)
1378 ulv = plot(T1,U(:,1))
1379 hold on
1380 %upa = plot(T1,U(:,2))
1381 xlabel('Time [s]')
1382 ylabel('Delta upa/ulv')
1383 grid on
1384 legend([ulv],'ulv')
1385
1386 %% Quadratic controller 2Var
1387 n = 4;
1388 Initial_level = 0.05;
1389
1390 Alpha = 0.096; %Scenario 1: 0.096   Scenario 2: 0.036
1391 %Scenario 1():0.221   Scenario 2(): Grense 0.077
1392 gamma = 0.1; %7e-1
1393
1394 %ulv_arb = 0.5159, dulv_max = 0.48
1395 %upa_arb = 0.65, dupa_max = 0.2
1396 dupa_max = 0.2; % var 0.2
1397 dulv_max = 0.45; %
1398 a = -0.05%-0.05; %delta_h1 min
1399 b = 0.05; %delta_h1 max
1400 x1 = [a b];
1401 Vertex = x1;
1402
1403 punkt_cell = cell(n,1);
1404
1405 if n >= 2
1406     for i = 2:n
1407         if mod(i,2) ~= 0
1408             punkt_cell{i} = x1.^i;
1409         end
1410         if mod(i,2) == 0
1411             punkt_cell{i} = [-max(a^i, b^i)/10,max(a^i, b^i)];
1412         end
1413         Vertex = combvec(Vertex, punkt_cell{i});
1414     end
1415 else
1416     Vertex = Vertex';
1417 end
1418
1419 %Vertex = [-0.01 0.05 0.05;
1420 %          -0.01 -0.01 (0.05^2)]; %Dette er en test!! Fjern etterp .
1421
1422 %%%%%%%%%%%%%%%%%%%%%%%%%%%%%%%%%%%%%%%%%%%%%%%%%%%%%%%%%%%%%%%%%%%%%%%%%
1423 %Vertex_shifted = Vertex;
1424 [A_test,B_test] = vert2con(Vertex');
1425 z = B_test; %
1426
1427 ak_T = A_test./z;
1428 ak = ak_T';
1429 %ak = [];
1430 %[r,k] = size(ak)
1431
1432 % for i = 1:r
1433 %     for j = 1:k

```

```

1434 %         tall = ak(i,j)
1435 %         if tall < 1 && tall > -1
1436 %             ak(i,j) = 0
1437 %         end
1438 %     end
1439 % end
1440 %
1441 % ak = [20,-20,0,0,0,0,0,0;
1442 %      0,0,0,0,0,0,400,-1000;
1443 %      0,0,0,0,1000,-1000,0,0;
1444 %      0,0,-1000,1000,0,0,0,0];
1445 %
1446 %%%%%%%%%%
1447 [A_matrix_2var, B_matrix_2var, C_matrix_2var, D_matrix_2var, Initial_vector_2var,
    E_matrix_2var] = Carleman_NonLinearized_func_2Var(...
1448     par_der_h1_verdi,...
1449     par_der_uLV001_verdi,...
1450     par_der_uPA001_verdi,...
1451     par_der_h1_uLV001_verdi,...
1452     par_der_h1_h1_verdi,...
1453     par_der_h1_h1_h1_verdi,...
1454     par_der_h1_h1_uLV001_verdi,...
1455     Initial_level,...
1456     n);
1457 %dupa_max = 0.2, dulv_max = 0.48
1458 %
1459 [K_2var, P_2var] = Quadratic_controller(A_matrix_2var, B_matrix_2var, E_matrix_2var
    , Vertex, Alpha, gamma, dupa_max, dulv_max, ak);
1460 %
1461 strucK.A = A_matrix_2var;
1462 strucK.B = B_matrix_2var;
1463 strucK.K = K_2var;
1464 strucK.E = E_matrix_2var;
1465 %
1466 [T1,X] = ode45(@(t,x)Quadratic_system(t, x, strucK),0:0.001:160,Initial_vector_2var
    ');
1467 %
1468 close all
1469 figure(1)
1470 hold on
1471 for i = 1:n
1472     plot(T1,X(:,i))
1473 end
1474 xlabel ('Time [s]')
1475 ylabel ('Delta height [m]')
1476 grid on
1477 hold off
1478 %
1479 figure(2)
1480 z1 = plot(T1,X(:,1))
1481 xlabel ('Time [s]')
1482 ylabel ('Delta height [m]')
1483 grid on
1484 legend([z1], 'z1')
1485 %
1486 E_matrix_matrix_2var = [];
1487 for i = 1:n
1488     [r,k] = size(E_matrix_matrix_2var);
1489     E_matrix_matrix_2var(:,k+1:k+2) = E_matrix_2var{i};
1490 end
1491 [r,k] = size(X);
1492 U = [];
1493 for i = 1:r
1494     U(i,:) = (K_2var*X(i,:))';
1495 end
1496 %
1497 figure(3)
1498 ulv = plot(T1,U(:,1))
1499 hold on
1500 upa = plot(T1,U(:,2))
1501 xlabel ('Time [s]')
1502 %ylabel ('Delta upa/ulv')
1503 grid on

```



```

1504 legend([ulv, upa], 'ulv', 'upa')
1505 %% Error Values for Taylor
1506 clc
1507 %The Following code displays the Error Value for every model, wrt the
1508 %Nonlinear model.
1509 sim('Taylor_Simulations', 250);
1510
1511 disp('IAE Error: ')
1512 disp(['Quadratic:      ' num2str(IAE_Quadratic.Data(end))])
1513 disp(['Linear:         ' num2str(IAE_Linear.Data(end))])
1514 disp(['ParQuad_h1xh1:  ' num2str(IAE_ParQuad_h1xh1.Data(end))])
1515 disp(['ParQuad_h1xulv: ' num2str(IAE_ParQuad_h1xulv.Data(end))])
1516 disp(['Cubic:          ' num2str(IAE_Cubic.Data(end))])
1517 disp(['Fifth order:    ' num2str(IAE_Fifth.Data(end))])
1518
1519 fprintf('\n')
1520
1521 disp('ISE Error: ')
1522 disp(['Quadratic:      ' num2str(ISE_Quadratic.Data(end))])
1523 disp(['Linear:         ' num2str(ISE_Linear.Data(end))])
1524 disp(['ParQuad_h1xh1:  ' num2str(ISE_ParQuad_h1xh1.Data(end))])
1525 disp(['ParQuad_h1xulv: ' num2str(ISE_ParQuad_h1xulv.Data(end))])
1526 disp(['Cubic:          ' num2str(ISE_Cubic.Data(end))])
1527 disp(['Fifth:          ' num2str(ISE_Fifth.Data(end))])
1528
1529 fprintf('\n')
1530
1531 disp('ITAE Error: ')
1532 disp(['Quadratic:      ' num2str(ITAE_Quadratic.Data(end))])
1533 disp(['Linear:         ' num2str(ITAE_Linear.Data(end))])
1534 disp(['ParQuad_h1xh1:  ' num2str(ITAE_ParQuad_h1xh1.Data(end))])
1535 disp(['ParQuad_h1xulv: ' num2str(ITAE_ParQuad_h1xulv.Data(end))])
1536 disp(['Cubic:          ' num2str(ITAE_Cubic.Data(end))])
1537 disp(['Fifth order:    ' num2str(ITAE_Fifth.Data(end))])
1538
1539 fprintf('\n')
1540
1541 disp('ITSE Error: ')
1542 disp(['Quadratic:      ' num2str(ITSE_Quadratic.Data(end))])
1543 disp(['Linear:         ' num2str(ITSE_Linear.Data(end))])
1544 disp(['ParQuad_h1xh1:  ' num2str(ITSE_ParQuad_h1xh1.Data(end))])
1545 disp(['ParQuad_h1xulv: ' num2str(ITSE_ParQuad_h1xulv.Data(end))])
1546 disp(['Cubic:          ' num2str(ITSE_Cubic.Data(end))])
1547 disp(['Fifth order:    ' num2str(ITSE_Fifth.Data(end))])
1548
1549 fprintf('\n')
1550
1551 disp('ISTE Error: ')
1552 disp(['Quadratic:      ' num2str(ISTE_Quadratic.Data(end))])
1553 disp(['Linear:         ' num2str(ISTE_Linear.Data(end))])
1554 disp(['ParQuad_h1xh1:  ' num2str(ISTE_ParQuad_h1xh1.Data(end))])
1555 disp(['ParQuad_h1xulv: ' num2str(ISTE_ParQuad_h1xulv.Data(end))])
1556 disp(['Cubic:          ' num2str(ISTE_Cubic.Data(end))])
1557 disp(['Fifth order:    ' num2str(ISTE_Fifth.Data(end))])
1558 %% Error Values for Carleman
1559
1560 clc
1561 %The Following code displays the Error Value for every model, wrt the
1562 %Nonlinear model.
1563 sim('Taylor_Simulations', 250);
1564
1565 disp('IAE Error: ')
1566 disp(['Carleman n = 1:      ' num2str(IAE_Carleman_n_1.Data(end))])
1567 disp(['Carleman n = 2:      ' num2str(IAE_Carleman_n_2.Data(end))])
1568 disp(['Carleman n = 3:      ' num2str(IAE_Carleman_n_3.Data(end))])
1569 disp(['Carleman n = 4:      ' num2str(IAE_Carleman_n_4.Data(end))])
1570 disp(['Carleman n = 5:      ' num2str(IAE_Carleman_n_5.Data(end))])
1571 disp(['Carleman n = 10:     ' num2str(IAE_Carleman_n_10.Data(end))])
1572
1573 fprintf('\n')
1574
1575 disp('ISE Error: ')
1576 disp(['Carleman n = 1:      ' num2str(ISE_Carleman_n_1.Data(end))])

```

```

1577 disp(['Carleman n = 2:          ' num2str(ISE_Carleman_n_2.Data(end))])
1578 disp(['Carleman n = 3:          ' num2str(ISE_Carleman_n_3.Data(end))])
1579 disp(['Carleman n = 4:          ' num2str(ISE_Carleman_n_4.Data(end))])
1580 disp(['Carleman n = 5:          ' num2str(ISE_Carleman_n_5.Data(end))])
1581 disp(['Carleman n = 10:         ' num2str(ISE_Carleman_n_10.Data(end))])
1582
1583 fprintf('\n')
1584
1585 disp('ITAE Error: ')
1586 disp(['Carleman n = 1:          ' num2str(ITAE_Carleman_n_1.Data(end))])
1587 disp(['Carleman n = 2:          ' num2str(ITAE_Carleman_n_2.Data(end))])
1588 disp(['Carleman n = 3:          ' num2str(ITAE_Carleman_n_3.Data(end))])
1589 disp(['Carleman n = 4:          ' num2str(ITAE_Carleman_n_4.Data(end))])
1590 disp(['Carleman n = 5:          ' num2str(ITAE_Carleman_n_5.Data(end))])
1591 disp(['Carleman n = 10:         ' num2str(ITAE_Carleman_n_10.Data(end))])
1592
1593 fprintf('\n')
1594
1595 disp('ITSE Error: ')
1596 disp(['Carleman n = 1:          ' num2str(ITSE_Carleman_n_1.Data(end))])
1597 disp(['Carleman n = 2:          ' num2str(ITSE_Carleman_n_2.Data(end))])
1598 disp(['Carleman n = 3:          ' num2str(ITSE_Carleman_n_3.Data(end))])
1599 disp(['Carleman n = 4:          ' num2str(ITSE_Carleman_n_4.Data(end))])
1600 disp(['Carleman n = 5:          ' num2str(ITSE_Carleman_n_5.Data(end))])
1601 disp(['Carleman n = 10:         ' num2str(ITSE_Carleman_n_10.Data(end))])
1602
1603 fprintf('\n')
1604
1605 disp('ISTE Error: ')
1606 disp(['Carleman n = 1:          ' num2str(ISTE_Carleman_n_1.Data(end))])
1607 disp(['Carleman n = 2:          ' num2str(ISTE_Carleman_n_2.Data(end))])
1608 disp(['Carleman n = 3:          ' num2str(ISTE_Carleman_n_3.Data(end))])
1609 disp(['Carleman n = 4:          ' num2str(ISTE_Carleman_n_4.Data(end))])
1610 disp(['Carleman n = 5:          ' num2str(ISTE_Carleman_n_5.Data(end))])
1611 disp(['Carleman n = 10:         ' num2str(ISTE_Carleman_n_10.Data(end))])

```

F.2 *Carleman_lin_ss.m*

```

1 % 19.Februar 2021
2 % John H vard Aarv g
3
4 %Carleman matrix
5
6 %%
7 close all
8
9 syms A1 f3 Kv_LV001 f1 rho g h1 h_LV001
10
11 dynamic_model_tank1 = (1/A1)*(f3 - ((Kv_LV001*f1)/3600)*sqrt((rho*g*(h1+h_LV001))
    /100000)); %The dynamic model for tank 1
12
13 % Calculating the partial derivatives (symbolic)
14 par_der_h1 = diff(dynamic_model_tank1, h1); % df/dh1
15 par_der_f1 = diff(dynamic_model_tank1, f1); % df/df1
16 par_der_f3 = diff(dynamic_model_tank1, f3); % df/df3
17 par_der_h1_h1 = diff(par_der_h1, h1); % d^2f/dh1^2
18 par_der_f1_f1 = diff(par_der_f1, f1); % d^2f/df1^2
19 par_der_f3_f3 = diff(par_der_f3, f3); % d^2f/df3^2
20 par_der_h1_f1 = diff(par_der_h1, f1); % d^2f/dh1df1
21 par_der_h1_f3 = diff(par_der_h1, f3); % d^2f/dh1df3
22 par_der_f1_f3 = diff(par_der_f1, f3); % d^2f/df1df3
23
24 par_der_h1_h1_h1 = diff(par_der_h1_h1, h1); % d^3f/dh1^3
25 par_der_h1_h1_f1 = diff(par_der_h1_h1, f1); % d^3f/dh1^2df1
26
27 par_der_h1_h1_h1_h1 = diff(par_der_h1_h1_h1, h1); % d^4f/dh1^4
28 par_der_h1_h1_h1_f1 = diff(par_der_h1_h1_h1, f1); % d^4f/dh1^3df1
29
30 par_der_h1_h1_h1_h1_h1 = diff(par_der_h1_h1_h1_h1, h1); % d^5f/dh1^5
31 par_der_h1_h1_h1_h1_f1 = diff(par_der_h1_h1_h1_h1, f1); % d^5f/dh1^4df1
32
33 % Setting the working point for h1 and f3

```

```

34 h1_arb = 0.25;
35 f3_arb = 0.0001783;
36
37 % Inserting every known variable in equation dynamic_model_tank1
38 a = subs(dynamic_model_tank1, [A1 Kv_LV001 rho g h_LV001 h1 f3], [0.01 11.25 1000
    9.81 0.05 h1_arb f3_arb]);
39 % Solving equation 'a' wrt f1. This gives f1_arb
40 f1_arb = double(solve(a,f1));
41
42 % Since f3_arb is chosen, we can find upa_arb from the pump-characteristics
43 upa_arb = 0.65;
44 % We have found f1_arb. Using this value in the valve-characteristics gives us
    ulv_arb
45 ulv_arb = 0.5159;
46
47
48
49 df1_duLV001 = 0.98; % Manually calculated in simulink. delta_f1 / delta_ulv
50 df3_dPA001 = 0.00052; % Manually calculated in simulink. delta_f3 / delta_upa
51
52 % Calculating the partial derivatives used in the Taylor series expansion
53 % (Value at working point!)
54 par_der_h1_verdi = double((subs(par_der_h1,...
55     [A1 Kv_LV001 rho g h_LV001 h1 f1 f3],...
56     [0.01 11.25 1000 9.81 0.05 h1_arb f1_arb f3_arb])));
57
58 par_der_uLV001_verdi = double(subs(par_der_f1 * df1_duLV001,...
59     [A1 Kv_LV001 rho g h_LV001 h1 f1 f3],...
60     [0.01 11.25 1000 9.81 0.05 h1_arb f1_arb f3_arb]));
61
62 par_der_uPA001_verdi = double(subs(par_der_f3 * df3_dPA001,...
63     [A1 Kv_LV001 rho g h_LV001 h1 f1 f3],...
64     [0.01 11.25 1000 9.81 0.05 h1_arb f1_arb f3_arb]));
65
66 par_der_h1_h1_verdi = double(subs(par_der_h1_h1,...
67     [A1 Kv_LV001 rho g h_LV001 h1 f1 f3],...
68     [0.01 11.25 1000 9.81 0.05 h1_arb f1_arb f3_arb]));
69
70 par_der_uLV001_uLV001_verdi = double(subs(par_der_f1_f1 * df1_duLV001^2,...
71     [A1 Kv_LV001 rho g h_LV001 h1 f1 f3],...
72     [0.01 11.25 1000 9.81 0.05 h1_arb f1_arb f3_arb]));
73
74 par_der_uPA001_uPA001_verdi = double(subs(par_der_f3_f3 * df3_dPA001^2,...
75     [A1 Kv_LV001 rho g h_LV001 h1 f1 f3],...
76     [0.01 11.25 1000 9.81 0.05 h1_arb f1_arb f3_arb]));
77
78 par_der_h1_uLV001_verdi = double(subs(par_der_h1_f1 * df1_duLV001,...
79     [A1 Kv_LV001 rho g h_LV001 h1 f1 f3],...
80     [0.01 11.25 1000 9.81 0.05 h1_arb f1_arb f3_arb]));
81
82 par_der_h1_uPa001_verdi = double(subs(par_der_h1_f3 * df3_dPA001,...
83     [A1 Kv_LV001 rho g h_LV001 h1 f1 f3],...
84     [0.01 11.25 1000 9.81 0.05 h1_arb f1_arb f3_arb]));
85
86 par_der_uLV001_uPA001_verdi = double(subs(par_der_f1_f3 * df1_duLV001 * df3_dPA001
87     ,...
88     [A1 Kv_LV001 rho g h_LV001 h1 f1 f3],...
89     [0.01 11.25 1000 9.81 0.05 h1_arb f1_arb f3_arb]));
90
91 par_der_h1_h1_h1_verdi = double((subs(par_der_h1_h1_h1,...
92     [A1 Kv_LV001 rho g h_LV001 h1 f1 f3],...
93     [0.01 11.25 1000 9.81 0.05 h1_arb f1_arb f3_arb])));
94
95 par_der_h1_h1_uLV001_verdi = double((subs(par_der_h1_h1_f1 * df1_duLV001,...
96     [A1 Kv_LV001 rho g h_LV001 h1 f1 f3],...
97     [0.01 11.25 1000 9.81 0.05 h1_arb f1_arb f3_arb])));
98
99 % The following is a standard code that imports the characteristics of the
100 % pump and valve. This code also defines some constants. (From Reguleringsteknikk)
101 %%%%%%%%%%%%%%%%%%%%%%%%%%%%%%%%%%%%%%%%%%%%%%%%%%%%%%%%%%%%%%%
102 % data om vann og tyngdekraft
103 %%%%%%%%%%%%%%%%%%%%%%%%%%%%%%%%%%%%%%%%%%%%%%%%%%%%%%%%%%%%%%%

```

```

104 rho = 1000;           % tetthet vann           [kg/m^3]
105 g = 9.81;           % tyngdens akselerasjon [m/s^2]
106 c_p = 4200;         % varmekapasitet vann   [j/kg*K]
107
108 %%%%%%%%%%%%%%%%%%%%%%%%%%%%%%%%%%%%%%%%%%%%%%%%%%%%%%%%%%%
109 % Tank 1
110 %%%%%%%%%%%%%%%%%%%%%%%%%%%%%%%%%%%%%%%%%%%%%%%%%%%%%%%%%%%
111 Kv_LV001 = 11.25;    % ventilkonstant LV001 [m^3/h] ved 1 bar trykkfall
112 h_LV001 = 0.05;     % h yde til LV001 [m]
113 h1_max = 1;         % maks h yde tank 1 [m]
114 h1_min = 0.13;     % min h yde tank 1 [m]
115 A1 = 0.01;         % areal tank 1 [m^2]
116
117 %%%%%%%%%%%%%%%%%%%%%%%%%%%%%%%%%%%%%%%%%%%%%%%%%%%%%%%%%%%
118 % Tank 2
119 %%%%%%%%%%%%%%%%%%%%%%%%%%%%%%%%%%%%%%%%%%%%%%%%%%%%%%%%%%%
120 Kv_LV002 = 11.25;    % ventilkonstant LV002 [m3/h]
121 h_LV002 = 0.25;     % h yde fra bunn av tank 2 til LV002
122 h2_max = 0.4;       % maks h yde tank 2 [m]
123 h2_min = 0.02;     % min h yde tank 2 [m]
124
125 %%%%%%%%%%%%%%%%%%%%%%%%%%%%%%%%%%%%%%%%%%%%%%%%%%%%%%%%%%%
126 % Last inn p drag og m linger
127 %%%%%%%%%%%%%%%%%%%%%%%%%%%%%%%%%%%%%%%%%%%%%%%%%%%%%%%%%%%
128 load tankData_1     % det finnes ogs et datasett som heter tankData_2
129 load tankData_2
130
131 %%%%%%%%%%%%%%%%%%%%%%%%%%%%%%%%%%%%%%%%%%%%%%%%%%%%%%%%%%%
132 % Pumpekarakteristikk
133 %%%%%%%%%%%%%%%%%%%%%%%%%%%%%%%%%%%%%%%%%%%%%%%%%%%%%%%%%%%
134 u_PA001 = [0.00 0.45 0.46 0.47 0.48 0.49 0.50 0.55...
135            0.60 0.65 0.70 0.75 0.80 0.85 0.90 0.95 1.00];
136 q_PA001 = [0.00 0.00 1.25 2.25 3.15 3.75 4.40 6.75...
137            8.75 10.70 12.25 13.75 15.15 16.50 18.00 19.20 20.00];
138
139 q_PA001 = q_PA001/60000; % liter/time -> m3/s
140
141 % figure
142 % plot(u_PA001, q_PA001,'*-')
143 % title('Pumpekarakteristikk')
144 % xlabel('P drag u_{PA001}(t) til pumpe PA001')
145 % ylabel('Volumstr m q_{PA001}(t) gjennom PA001 [m^3/s]')
146
147
148 %%%%%%%%%%%%%%%%%%%%%%%%%%%%%%%%%%%%%%%%%%%%%%%%%%%%%%%%%%%
149 % Ventilkarakteristikk
150 %%%%%%%%%%%%%%%%%%%%%%%%%%%%%%%%%%%%%%%%%%%%%%%%%%%%%%%%%%%
151 u_LV001 = 0:0.03:1;
152 f_LV001 = (exp(u_LV001.^1.2)-1)/(exp(1)-1);
153 u_LV002 = u_LV001;
154 f_LV002 = f_LV001;
155
156 % figure
157 % plot(u_LV001,f_LV001,'*-')
158 % title('Ventilkarakteristikk for LV001 og LV002')
159 % xlabel('Ventilp drag u_{LV001}(t)')
160 % ylabel('f(u_{LV001}(t))')
161
162 %End of the standard code from Reguleringsteknikk
163
164
165
166 %%
167 %%carleman matrix
168 %%this section creates the A matrix in the eqn xdot = Ax + Bu, y = Cx + Du
169 %%This "linearization" removes all the mixed, nonlinear parts of the
170 %%carleman embedding.
171 %%
172 %%simplified variable names
173 % a_c = par_der_h1_verdi;
174 % b_c = par_der_uLV001_verdi;
175 % c_c = par_der_uPA001_verdi;
176 % d_c = par_der_h1_uLV001_verdi;

```

```

177 % e_c = par_der_h1_h1_verdi/2;
178 % f_c = par_der_h1_h1_h1_verdi/6;
179 % g_c = par_der_h1_h1_uLV001_verdi/2;
180 %
181 % % Truncate terms beyond n, small mismatches up till n = 18. beyond that it
182 % % gets worse
183 % n = 4;
184 %
185 % A_matrix = zeros(n+2);
186 % B_matrix = zeros(n,1);
187 % C_matrix = zeros(1,n);
188 % D_matrix = (0);
189 % C_matrix(1) = 1;
190 % B_matrix(1) = b_c;
191 %
192 % A_matrix(1,1) = a_c + d_c*0.01; %x1
193 % A_matrix(1,2) = e_c + g_c*0.01; %x2
194 % A_matrix(1,3) = f_c; %x3
195 % Initial_level = 0.1;
196 %
197 % Initial_vector = zeros(n,1);
198 % for i=1:n
199 %     Initial_vector(i) = Initial_level^i;
200 % end
201 % %this pattern is clear after computing the first terms by hand.
202 % for i = 2:n
203 %     A_matrix(i,i-1) = i*b_c*0.01;
204 %     A_matrix(i,i) = i*a_c + i*d_c*0.01;
205 %     A_matrix(i,i+1) = i*e_c + i*g_c*0.01;
206 %     A_matrix(i,i+2) = i*f_c;
207 % end
208 %
209 % %Removes the truncated terms, that is for x = 10, all x 11, x12 etc are
210 % %removed.
211 % A_matrix(:,n+2) = [];
212 % A_matrix(:,n+1) = [];
213 % A_matrix(n+2,:) = [];
214 % A_matrix(n+1,:) = [];
215 %
216 % %Makes the statespace representation into a tf
217 % [NUM,DEN] = ss2tf(A_matrix,B_matrix,C_matrix,D_matrix,1);
218 % syste = tf(NUM,DEN)
219 % Gent = isstable(syste)
220 % pzmap(syste)
221
222
223 %%
224 %carleman matrix
225 %this section creates the A matrix in the eqn xdot = Ax + Bu, y = Cx + Du
226 %This "linearization" removes all the mixed, nonlinear parts of the
227 %carleman embedding.
228
229 %simplified variable names
230 a_c = par_der_h1_verdi;
231 b_c = par_der_uLV001_verdi;
232 c_c = par_der_uPA001_verdi;
233 d_c = par_der_h1_uLV001_verdi;
234 e_c = par_der_h1_h1_verdi/2;
235 f_c = par_der_h1_h1_h1_verdi/6;
236 g_c = par_der_h1_h1_uLV001_verdi/2;
237
238 % Truncate terms beyond n, small mismatches up till n = 18. beyond that it
239 % gets worse
240 n = 4;
241
242 A_matrix = zeros(n+2);
243 B_matrix = zeros(n,1);
244 C_matrix = zeros(1,n);
245 D_matrix = (0);
246 C_matrix(1) = 1;
247 B_matrix(1) = b_c;
248
249

```

```

250 Initial_level = 0.4;
251 %this pattern is clear after computing the first terms by hand.
252 for i = 1:n
253     A_matrix(i,i) = i*a_c;
254     A_matrix(i,i+1)= i*e_c;
255     A_matrix(i,i+2) = i*f_c;
256 end
257
258 Initial_vector = zeros(n,1);
259 for i=1:n
260     Initial_vector(i) = Initial_level^i;
261 end
262
263 %Removes the truncated terms, that is for x = 10, all x 11, x12 etc are
264 %removed.
265 A_matrix(:,n+2) = [];
266 A_matrix(:,n+1) = [];
267 A_matrix(n+2,:) = [];
268 A_matrix(n+1,:) = [];
269
270
271
272 %Makes the statespace representation into a tf
273 [NUM,DEN] = ss2tf(A_matrix,B_matrix,C_matrix,D_matrix,1);
274 syste = tf(NUM,DEN)
275 Gent = isstable(syste)
276 pzmap(syste)

```

F.3 Carleman_Linearized_func.m

```

1 function [A_matrix, B_matrix, C_matrix, D_matrix, Initial_vector] =...
2     Carleman_Linearized_func(h1, ulv, upa, h1_ulv, h1_h1, h1_h1_h1, h1_h1_ulv,
3     initC, n)
4
5     %Simplifies the notation of the partial derivatives
6     a_c = h1;
7     b_c = ulv;
8     c_c = upa;
9     d_c = h1_ulv;
10    e_c = h1_h1/2;
11    f_c = h1_h1_h1/6;
12    g_c = h1_h1_ulv/2;
13
14    %Defines the amount of terms to include in the Carleman linearization
15    n = n;
16
17    %Defines the initial condition of the water level
18    Initial_level = initC;
19
20    %Finds the initial condition for every x_dot
21    Initial_vector = zeros(n,1);
22    for i=1:n
23        Initial_vector(i) = Initial_level^i;
24    end
25
26    %
27    A_matrix = zeros(n+2);
28    B_matrix = zeros(n,1);
29    C_matrix = zeros(1,n);
30    D_matrix = (0);
31    C_matrix(1) = 1;
32    B_matrix(1) = b_c;
33
34    %Constructs the A_matrix.
35    %This pattern is clear after computing the first terms by hand.
36    for i = 1:n
37        A_matrix(i,i) = i*a_c;
38        A_matrix(i,i+1)= i*e_c;
39        A_matrix(i,i+2) = i*f_c;
40    end
41
42    %Removes the truncated terms

```

```

42 A_matrix(:,n+2) = [];
43 A_matrix(:,n+1) = [];
44 A_matrix(n+2,:) = [];
45 A_matrix(n+1,:) = [];
46 end

```

F.4 Carleman_NonLinearized_func_2Var.m

```

1 function [A_matrix, B_matrix, C_matrix, D_matrix, Initial_vector, E_matrix] =...
2 Carleman_NonLinearized_func_2Var(h1, ulv, upa, h1_ulv, h1_h1, h1_h1_h1,
3 h1_h1_ulv, initC, n)
4 %Simplifies the notation of the partial derivatives
5 a_c = h1;
6 b_c = ulv;
7 c_c = upa;
8 d_c = h1_ulv;
9 e_c = h1_h1/2;
10 f_c = h1_h1_h1/6;
11 g_c = h1_h1_ulv/2;
12
13 %Defines the amount of terms to include in the Carleman linearization
14 n = n;
15
16 %Defines the initial condition of the water level
17 Initial_level = initC;
18
19 %Finds the initial condition for every x_dot
20 Initial_vector = zeros(n,1);
21 for i=1:n
22     Initial_vector(i) = Initial_level^i;
23 end
24
25 %
26 A_matrix = zeros(n+2);
27 B_matrix = zeros(n,2);
28 C_matrix = zeros(1,n);
29 D_matrix = (0);
30 C_matrix(1) = 1;
31 B_matrix(1,1) = b_c;
32 B_matrix(1,2) = c_c;
33
34 %Constructs the A_matrix.
35 %This pattern is clear after computing the first terms by hand.
36 for i = 1:n
37     A_matrix(i,i) = i*a_c;
38     A_matrix(i,i+1) = i*e_c;
39     A_matrix(i,i+2) = i*f_c;
40 end
41
42 %Removes the truncated terms
43 A_matrix(:,n+2) = [];
44 A_matrix(:,n+1) = [];
45 A_matrix(n+2,:) = [];
46 A_matrix(n+1,:) = [];
47
48
49 E_matrix = cell(1,n);
50 E_matrix{1} = zeros(n,2);
51 E_matrix{1}(1,1) = d_c;
52 E_matrix{1}(2,1) = g_c;
53
54 for i = 2:n
55     E_matrix{i} = zeros(n,2);
56     E_matrix{i}(i-1,1) = i*b_c;
57     E_matrix{i}(i,1) = i*d_c;
58     E_matrix{i}(i+1,1) = i*g_c;
59     E_matrix{i}(i-1,2) = i*c_c;
60 end
61 E_matrix{n}(n+1,:) = [];
62
63 end

```

F.5 *Carleman_NonLinearized_func.m*

```

1 function [A_matrix, B_matrix, C_matrix, D_matrix, Initial_vector, E_matrix] =...
2   Carleman_NonLinearized_func(h1, ulv, upa, h1_ulv, h1_h1, h1_h1_h1, h1_h1_ulv,
3     initC, n)
4
5   %Simplifies the notation of the partial derivatives
6   a_c = h1;
7   b_c = ulv;
8   c_c = upa;
9   d_c = h1_ulv;
10  e_c = h1_h1/2;
11  f_c = h1_h1_h1/6;
12  g_c = h1_h1_ulv/2;
13
14  %Defines the amount of terms to include in the Carleman linearization
15  n = n;
16
17  %Defines the initial condition of the water level
18  Initial_level = initC;
19
20  %Finds the initial condition for every x_dot
21  Initial_vector = zeros(n,1);
22  for i=1:n
23    Initial_vector(i) = Initial_level^i;
24  end
25
26  %
27  A_matrix = zeros(n+2);
28  B_matrix = zeros(n,1);
29  C_matrix = zeros(1,n);
30  D_matrix = (0);
31  C_matrix(1) = 1;
32  B_matrix(1) = b_c;
33
34  %Constructs the A_matrix.
35  %This pattern is clear after computing the first terms by hand.
36  for i = 1:n
37    A_matrix(i,i) = i*a_c;
38    A_matrix(i,i+1) = i*e_c;
39    A_matrix(i,i+2) = i*f_c;
40  end
41
42  %Removes the truncated terms
43  A_matrix(:,n+2) = [];
44  A_matrix(:,n+1) = [];
45  A_matrix(n+2,:) = [];
46  A_matrix(n+1,:) = [];
47
48  E_matrix = cell(1,n);
49  E_matrix{1} = zeros(n,1);
50  E_matrix{1}(1) = d_c;
51  E_matrix{1}(2) = g_c;
52
53  for i = 2:n
54    E_matrix{i} = zeros(n,1);
55    E_matrix{i}(i-1) = i*b_c;
56    E_matrix{i}(i) = i*d_c;
57    E_matrix{i}(i+1) = i*g_c;
58  end
59  E_matrix{n}(n+1) = [];
60
61 end

```

F.6 *carleman_statespace_2Var.m*

```

1 %Carleman lin_part
2 clear
3 clc
4 n = 12;

```



```

5 syms a b c d e f g dh dulv dupa
6 syms x [1 n+3]
7
8 dhdot = a.*dh^1 + b.*dulv + c.*dupa + d.*dh^1.*dulv + e.*dh^2 + f.*dh^3 + g.*dh^2.*
    dulv;
9 %dhdot = a.*dh + e.*dh.^2 + f.*dh.^3;
10
11 C = cell(1,n);
12
13 %x2dot ->
14 for i = 2:n
15     C{i} = expand(i*dh^(i-1).*dhdot);
16     C{i} = subs(C{i},[dh^(i+3), dh^(i+2), dh^(i+1), dh^i, dh^(i-1), dh],[x(i+3), x(
    i+2), x(i+1),x(i),x(i-1), x1])
17 end

```

F.7 *carleman_statespace.m*

```

1 %Carleman lin_part
2 clear
3 clc
4 n = 12;
5 syms a b c d e f g dh dulv
6 syms x [1 n+3]
7
8 dhdot = a.*dh^1 + b.*dulv + d.*dh^1.*dulv + e.*dh^2 + f.*dh^3 + g.*dh^2.*dulv;
9 %dhdot = a.*dh + e.*dh.^2 + f.*dh.^3;
10
11 C = cell(1,n);
12
13 %x2dot ->
14 for i = 2:n
15     C{i} = expand(i*dh^(i-1).*dhdot);
16     C{i} = subs(C{i},[dh^(i+3), dh^(i+2), dh^(i+1), dh^i, dh^(i-1), dh],[x(i+3), x(
    i+2), x(i+1),x(i),x(i-1), x1])
17 end

```

F.8 *example_file_solver.m*

```

1 A = [1 3 4 ; 0 2 1 ; 1 7 6];
2 B = [1 0 0]';
3
4 eig(A)
5
6 % after installing YALMIP (toolbox) and SeDuMi (solver)
7
8 Q = sdpvar(3); %variable to find is a symmetric matrix 3x3
9 W = sdpvar(1,3,'full'); % variable to find a full (non-symmetric) matrix 1x3
10
11 alpha = 10;
12
13 inequality = Q >= 1e-9;
14 % inequality = [inequality,A'*Q+W'*B'*Q+Q*A+Q*B*W <= -1e-9]; % NO!
15 % BILINEAR MATRIX INEQUALITY (BMI)
16 inequality = [inequality,Q*A'+ W'*B'+ A*Q+ B*W+ 2*alpha*Q <= -1e-9]; %YES! LINEAR
    MATRIX INEQUALITY (LMI)
17
18 optimize(inequality)
19
20 Q = double(Q) %transform symbolic into numbers
21 W = double(W)
22
23 P = inv(Q)
24 K = W*inv(Q)

```

F.9 *Quadratic_controller.m*

```

1 function [K,P] = Quadratic_controller(A_matrix, B_matrix, E_cell, Vertex, Alpha,
2     gamma,dupa_max, dulv_max,ak)
3 [r, k] = size(B_matrix);
4
5 n = r;
6
7 Q = sdpvar(n); %variable to find is a symmetric matrix nxn
8 W = sdpvar(k,n,'full'); % variable to find a full (non-symmetric) matrix
9 inequality = [Q >= 1e-7*eye(n)]; %P>0
10 inequality = [inequality, [Q W(1,:)'; W(1,:) eye(1)*dulv_max^2]>=1e-9*eye(n+1)]; %
    limits ux
11 inequality = [inequality, [Q W(2,:)'; W(2,:) eye(1)*dupa_max^2]>=1e-9*eye(n+1)]; %
    limits ux2
12
13 % max_vertex = 0;
14 % for i = 1:2^n %finds the vertex furthest away from eq.
15 %     agent = norm(Vertex(1:end,i));
16 %     if agent >= max_vertex
17 %         max_vertex = agent;
18 %     end
19 % end
20
21 for i = 1:2^n
22     Z = [];
23     Y = [];
24     for j = 1:n
25         Z(j,:) = Vertex(1:end,i)'*E_cell{j}; %1xn Radvektor
26         Y(:,j) = E_cell{j}'*Vertex(1:end,i); %nx1 Kolonnevektor
27     end
28
29     if i == 2^n %max_vertex == max(norm(Vertex(1:end,i)))%if vertex number x is the
        same size as max
30         inequality = [inequality, gamma*(Q*A_matrix' + W'*B_matrix' + A_matrix*Q +
        B_matrix*W) + ...
31             W'*Y ...
32             + Z*W + gamma*Q*2*Alpha <= -1e-9*eye(n)];
33
34     else
35         inequality = [inequality, gamma*(Q*A_matrix' + W'*B_matrix' + A_matrix*Q +
        B_matrix*W) + ...
36             W'*Y ...
37             + Z*W <= -1e-9*eye(n)];
38     end
39     inequality = [inequality, [1 Vertex(1:end,i)'; Vertex(1:end,i) Q] >= 1e-9*eye(n
        +1)]; %6d
40 end
41
42 [ak_r,ak_k] = size(ak);
43 for k_ = 1:ak_k
44     inequality = [inequality, [1 gamma*ak(1:end, k_)'*Q; Q*ak(1:end, k_)*gamma Q]
        >= 1e-9*eye(n+1)];
45     disp('Test')
46 end
47
48 %[1 x'; x Q] x = 6d
49 %[1 vertex(1:end,i)'; vertex(1:end,i) Q] >=1e-7 x(i) = vertex(1:end,i)
50 %1x1 1xn nx1 nxn
51
52 optimize(inequality)
53
54 Q = double(Q); %transform symbolic into numbers
55 W = double(W);
56
57 P = Q;
58 K = W*inv(Q); %kxn
59 end

```

F.10 Quadratic_system.m

```

1 function dx = Quadratic_system(t, x, strucK)
2

```

```

3 A = strucK.A;
4 B = strucK.B;
5 E = strucK.E;
6 K = strucK.K;
7
8 SS = size(A);
9 n = SS(1);
10
11 resultat = [];
12 for i = 1:n
13     resultat(i,:) = x'*E{i}*K*x;
14 end
15
16 dx = (A+B*K)*x + resultat;
17 end

```

F.11 *Polytope_figures.m*

```

1 P = [-0.05 0; 0.05 0; -0.05 0.025; 0.05 0.025]
2
3 %[A,b] = vert2con(P);
4
5
6 k = convhull(P)
7
8 %plot(P(:,1),P(:,2))
9 %hold on
10 plot(P(k,1),P(k,2), 'b', 'LineWidth', 2, 'Marker', 'o')
11 hold on
12 fill(P(k,1), P(k,2), 'g', 'FaceAlpha', 0.5)
13 xlabel('z1')
14 ylabel('z2')
15 grid on
16 xlim([-0.06 0.06])
17 ylim([-0.02 0.03])

```

F.12 *vert2con.m* [11]

```

1 function [A,b] = vert2con(V)
2 % VERT2CON - convert a set of points to the set of inequality constraints
3 %           which most tightly contain the points; i.e., create
4 %           constraints to bound the convex hull of the given points
5 %
6 % [A,b] = vert2con(V)
7 %
8 % V = a set of points, each ROW of which is one point
9 % A,b = a set of constraints such that A*x <= b defines
10 %       the region of space enclosing the convex hull of
11 %       the given points
12 %
13 % For n dimensions:
14 % V = p x n matrix (p vertices, n dimensions)
15 % A = m x n matrix (m constraints, n dimensions)
16 % b = m x 1 vector (m constraints)
17 %
18 % NOTES: (1) In higher dimensions, duplicate constraints can
19 %           appear. This program detects duplicates at up to 6
20 %           digits of precision, then returns the unique constraints.
21 %           (2) See companion function CON2VERT.
22 %           (3) ver 1.0: initial version, June 2005.
23 %           (4) ver 1.1: enhanced redundancy checks, July 2005
24 %           (5) Written by Michael Kleder
25 %
26 % EXAMPLE:
27 %
28 % V=rand(20,2)*6-2;
29 % [A,b]=vert2con(V)
30 % figure('renderer','zbuffer')
31 % hold on

```

```

32 % plot(V(:,1),V(:,2),'r.')
33 % [x,y]=ndgrid(-3:.01:5);
34 % p=[x(:) y(:)]';
35 % p=(A*p <= repmat(b,[1 length(p)]));
36 % p = double(all(p));
37 % p=reshape(p,size(x));
38 % h=pcolor(x,y,p);
39 % set(h,'edgecolor','none')
40 % set(h,'zdata',get(h,'zdata')-1) % keep in back
41 % axis equal
42 % set(gca,'color','none')
43 % title('A*x <= b (1=True, 0=False)')
44 % colorbar
45 k = convhulln(V);
46 c = mean(V(unique(k),:));
47 V=V-repmat(c,[size(V,1) 1]);
48 A = NaN*zeros(size(k,1),size(V,2));
49 rc=0;
50 for ix = 1:size(k,1)
51     F = V(k(ix,:),:);
52     if rank(F,1e-5) == size(F,1)
53         rc=rc+1;
54         A(rc,:)=F\ones(size(F,1),1);
55     end
56 end
57 A=A(1:rc,:);
58 b=ones(size(A,1),1);
59 b=b+A*c';
60 % eliminate duplicate constraints:
61 [null,I]=unique(num2str([A b],6),'rows');
62 A=A(I,:); % rounding is NOT done for actual returned results
63 b=b(I);
64 return

```

F.13 EKSEMPEL_CARLEMAN.m

```

1 x = 0:0.01:1;
2
3 dx = x + x.^2+ x.^3
4
5 y = dx;
6
7 plt_n1 = plot(x,y,'b-','Linewidth',3)
8 %%
9 n = 3;
10
11 A = zeros(n+2);
12 B = zeros(n,1);
13 C = zeros(1,n);
14 D = (0);
15 C(1) = 1;
16
17 for i = 1:n
18     A(i,i:i+2) = i;
19 end
20
21 %Removes the truncated terms
22 A(:,n+2) = [];
23 A(:,n+1) = [];
24 A(n+2,:) = [];
25 A(n+1,:) = [];
26
27 [r,k] = size(x);
28 z_mat = zeros(k,1);
29
30 for j = 1:k
31     z_mat(1:end,j) = x.^j;
32 end
33
34 dz1 = zeros(1,k);
35 for l = 1:k
36     dz1(l,1:n) = A*z_mat(l,1:n,1)';

```

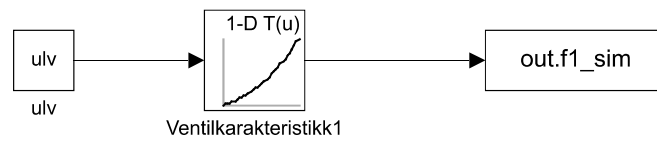
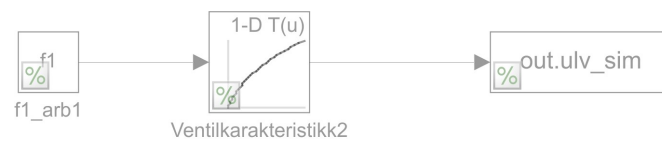
```

37 end
38
39 y1 = x + dz1;
40
41 hold on
42
43 plt_3 = plot(x,y1(1:end,1),'r--','Linewidth',2)
44
45 %%
46 n = 2;
47
48 A = zeros(n+2);
49 B = zeros(n,1);
50 C = zeros(1,n);
51 D = (0);
52 C(1) = 1;
53
54 for i = 1:n
55     A(i,i:i+2) = i;
56 end
57
58 %Removes the truncated terms
59 A(:,n+2) = [];
60 A(:,n+1) = [];
61 A(n+2,:) = [];
62 A(n+1,:) = [];
63
64 [r,k] = size(x);
65 z_mat = zeros(k,1);
66
67 for j = 1:k
68     z_mat(1:end,j) = x.^j;
69 end
70
71 dz1 = zeros(1,k);
72 for l = 1:k
73     dz1(1,1:n) = A*z_mat(l,1:n,1)';
74 end
75
76 y2 = x + dz1;
77
78 hold on
79
80 plt_2 = plot(x,y2(1:end,1),'y--','Linewidth',2)
81
82
83 %%
84 n = 1;
85
86 A = zeros(n+2);
87 B = zeros(n,1);
88 C = zeros(1,n);
89 D = (0);
90 C(1) = 1;
91
92 for i = 1:n
93     A(i,i:i+2) = i;
94 end
95
96 %Removes the truncated terms
97 A(:,n+2) = [];
98 A(:,n+1) = [];
99 A(n+2,:) = [];
100 A(n+1,:) = [];
101
102 [r,k] = size(x);
103 z_mat = zeros(k,1);
104
105 for j = 1:k
106     z_mat(1:end,j) = x.^j;
107 end
108
109 dz1 = zeros(1,k);

```

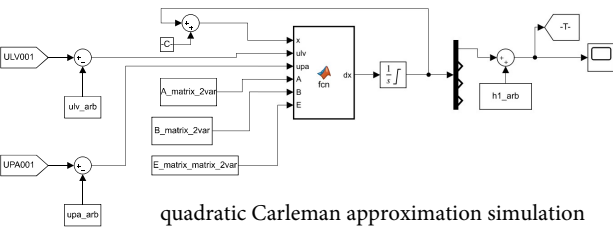
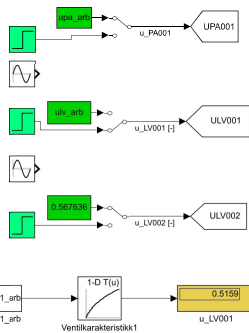
```
110 for l = 1:k
111     dz1(1,1:n) = A*z_mat(l,1:n,1)';
112 end
113
114 y3 = x + dz1;
115
116 hold on
117
118 plt_1 = plot(x,y3(1:end,1),'g--','Linewidth',2)
119
120 legend([plt_1, plt_2, plt_3, plt_n1], 'Carleman: n = 1', 'Carleman: n = 2', '
    Carleman: n = 3', 'Nonlinear system (4.4)')
121 xlabel('$z_1(t) = x(t)$','Interpreter','latex')
122 ylabel('$\dot{x}(t) = \dot{z}(t)$','Interpreter','latex')
123 grid on
```

F.14 Simulink schemes

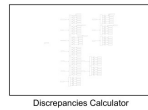
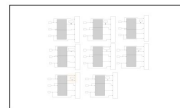


Finds the inverse of the valve characteristics.

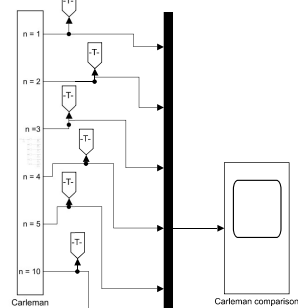
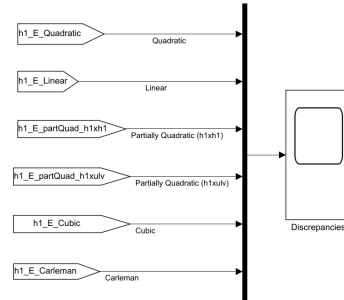
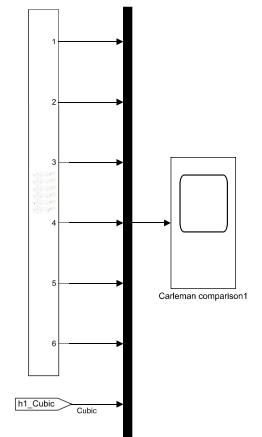
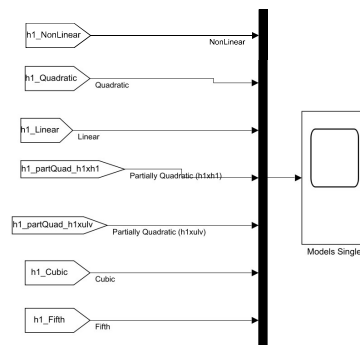
Step or operating values are set.



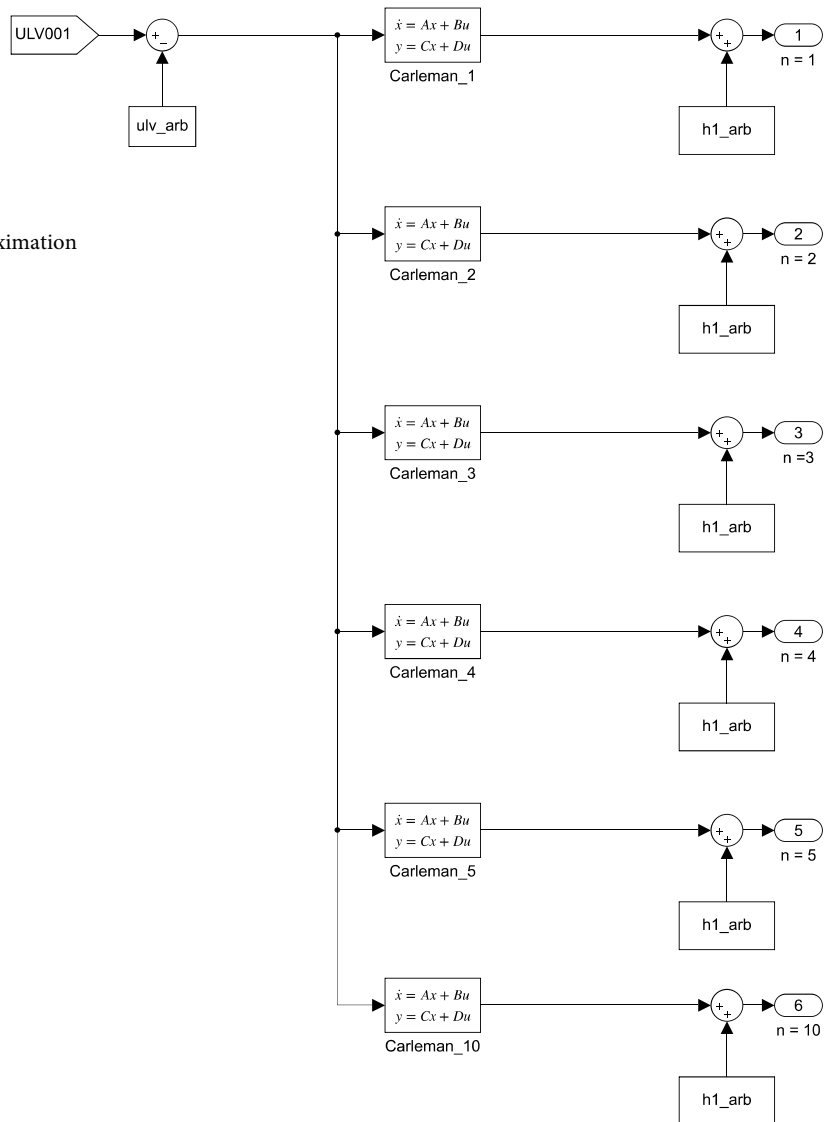
quadratic Carleman approximation simulation



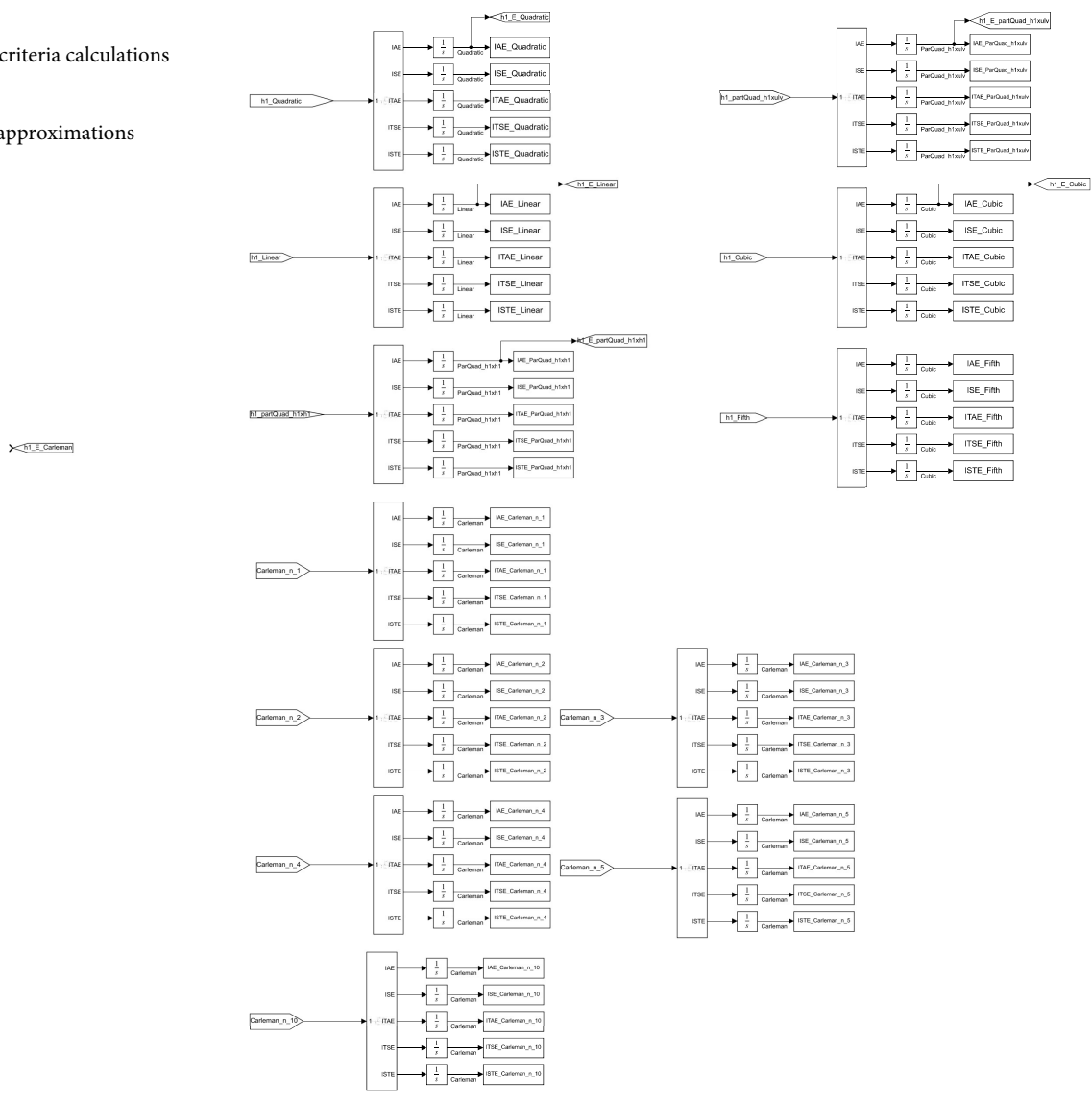
Scopes for comparison between models.



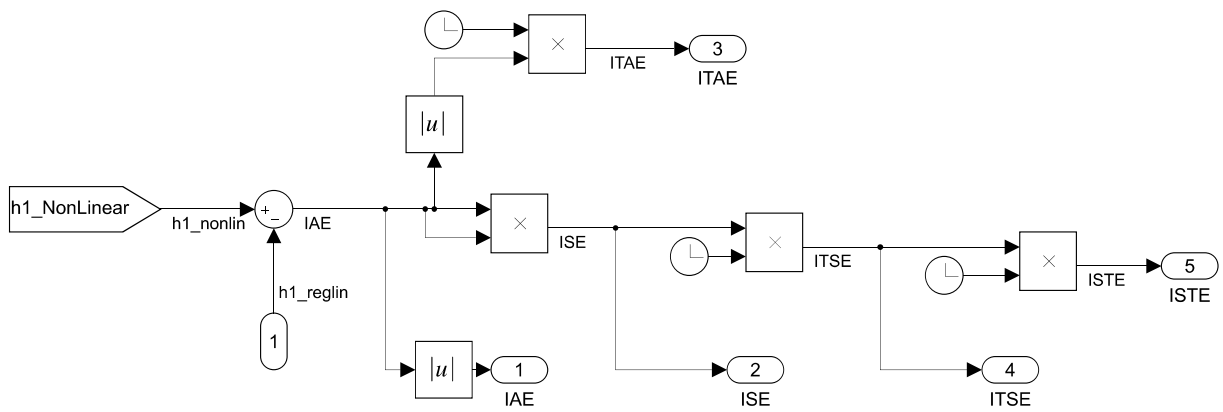
Linearized Carleman approximation
for different n.



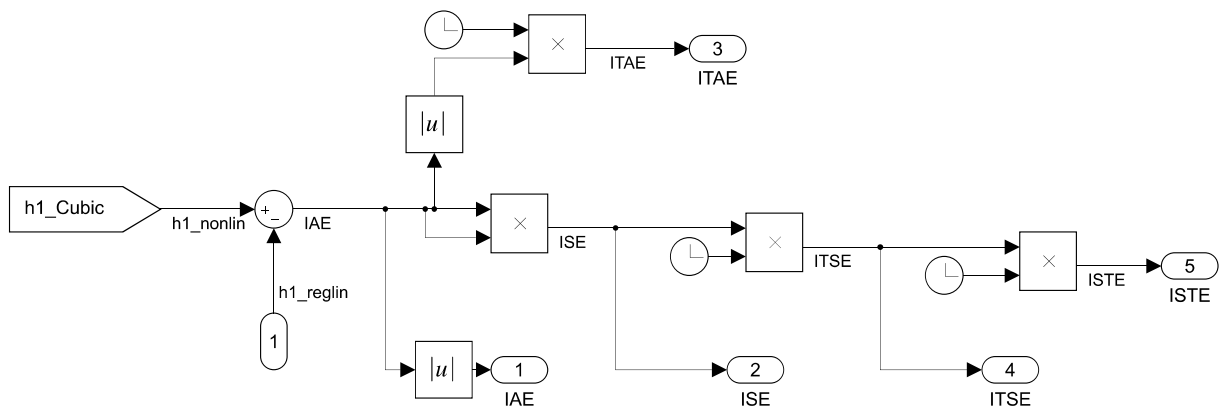
Integral performance criteria calculations for:
 Taylor models
 Linearized Carleman approximations



Integral performance criteria calculations
for: The nonlinear model.



Integral performance criteria calculations
for: The cubic model.



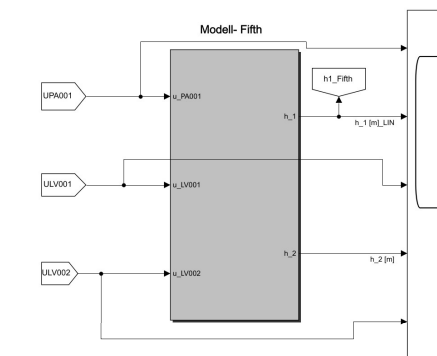
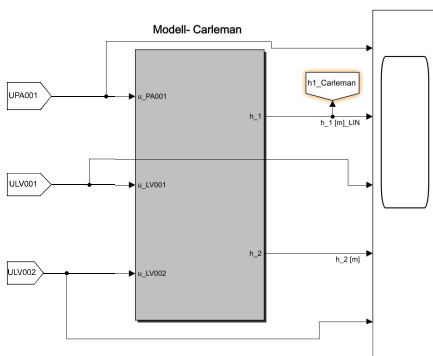
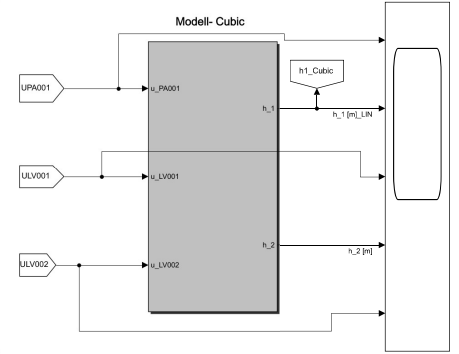
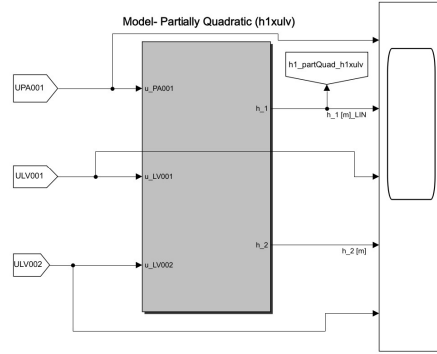
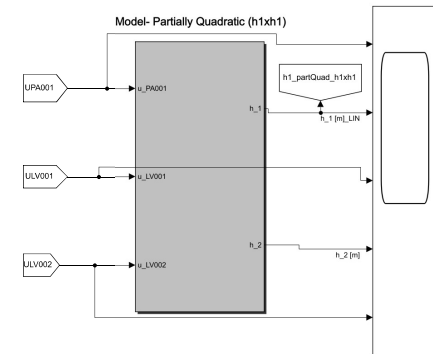
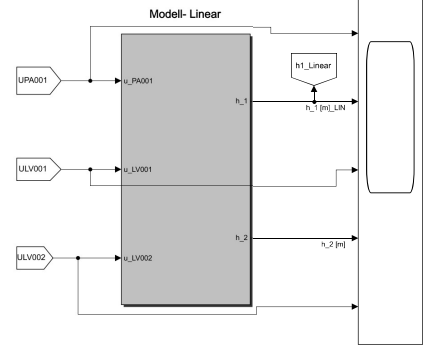
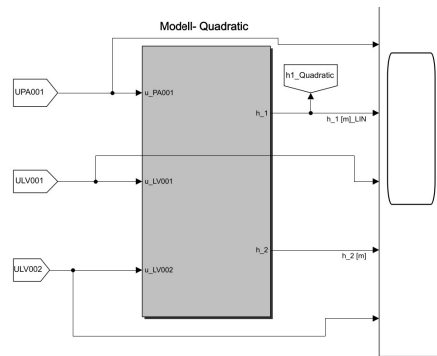
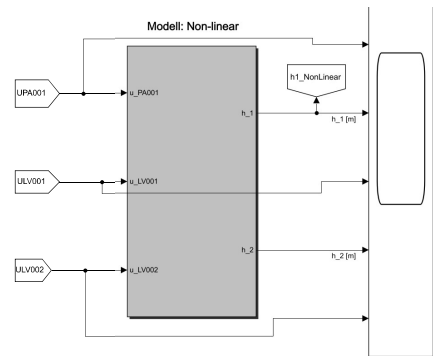
```
function dx = fcn(x,ulv,upa, A,B,E)
```

```
SS = size(A);  
n = SS(1);  
u = [ulv;upa];
```

```
resultat = zeros(n,1);  
r = 0;  
for i = 1:n  
    resultat(i,:) = x'*E(:, r+1:r+2)*u;  
    r = r+2;  
end
```

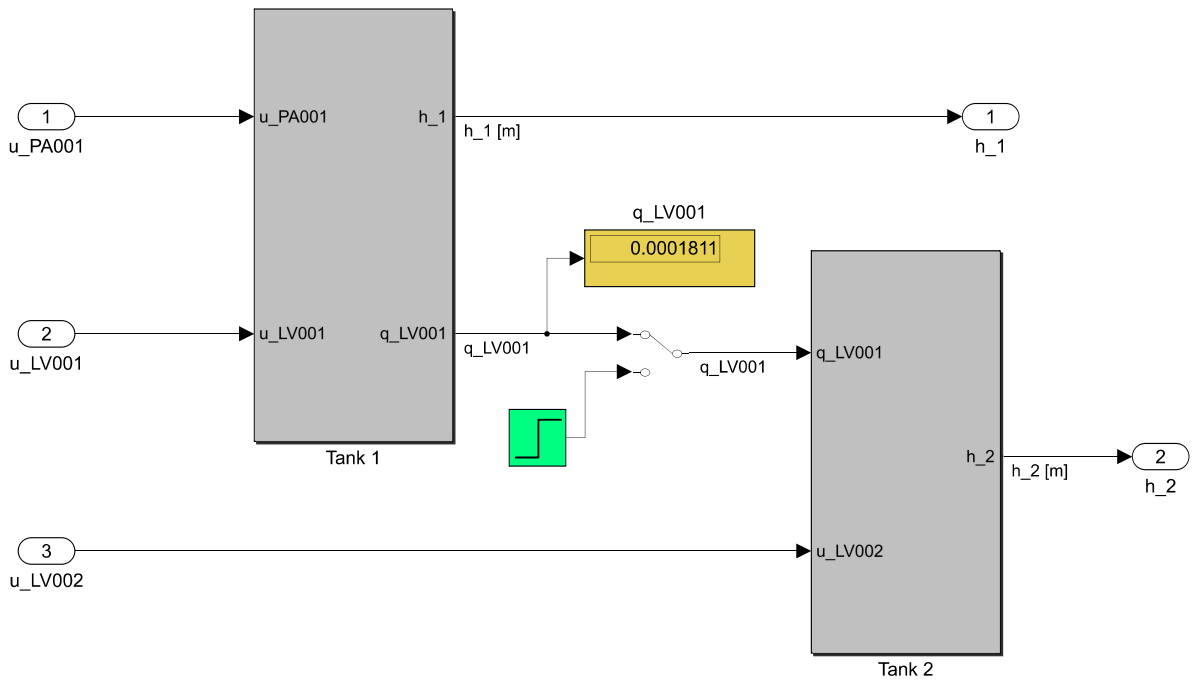
```
dx = A*x+B*u + resultat;  
end
```

Function calculating dx for the quadratic Carleman approximation using 2 variables.

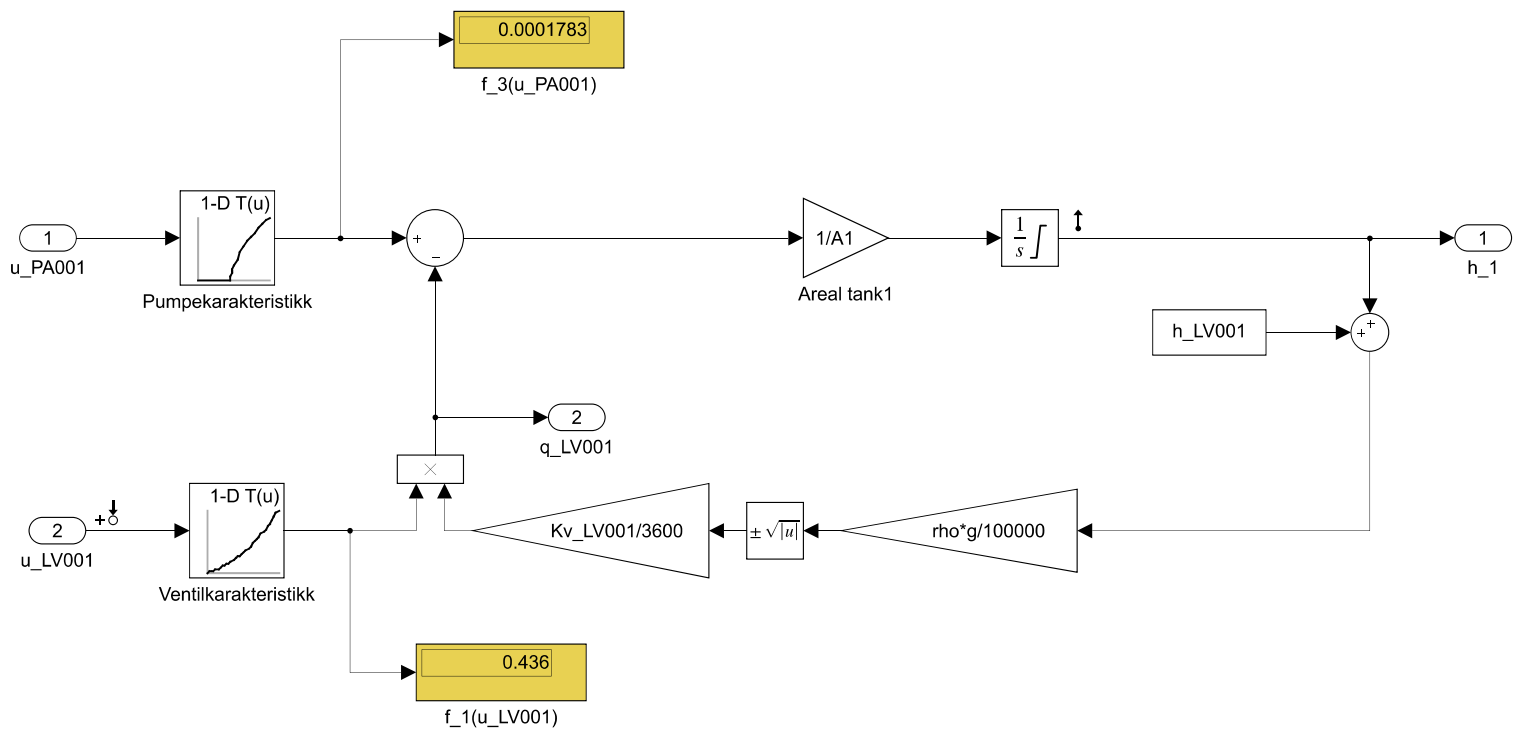


Model simulations schemes: level 0.

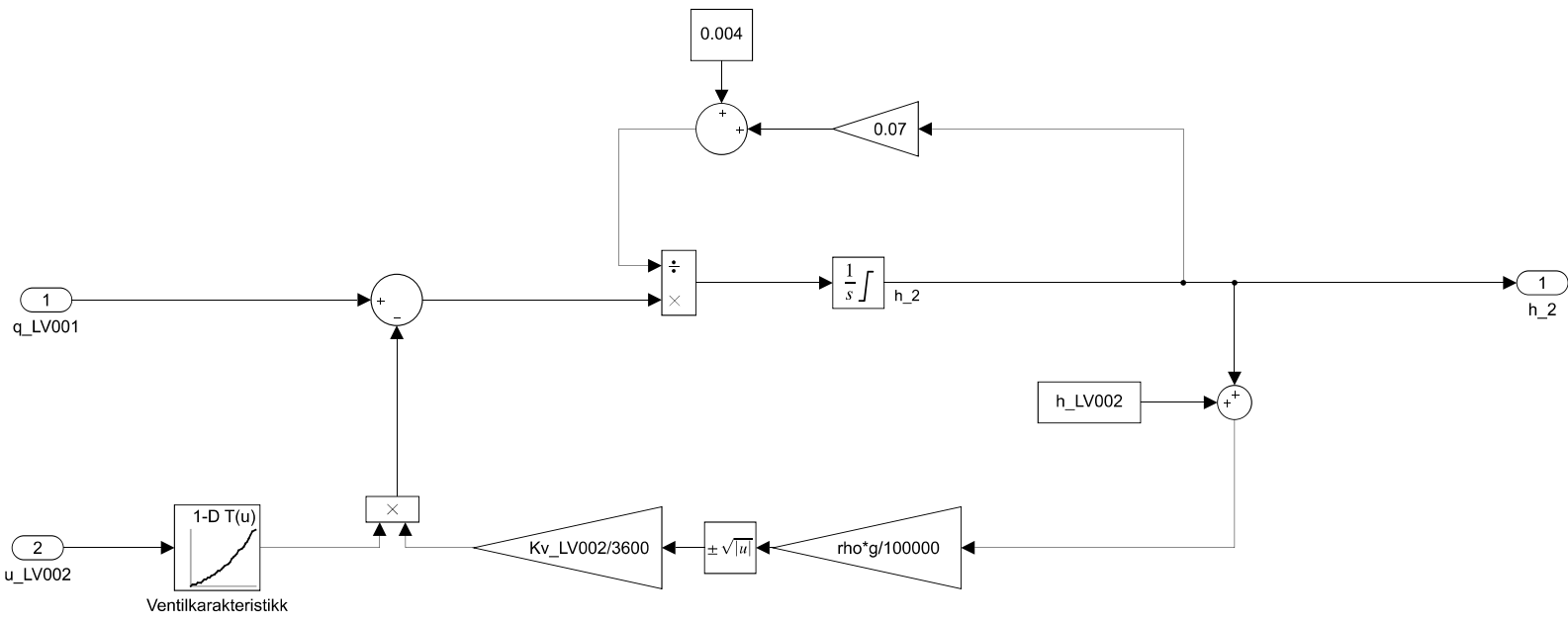
Inside a model scheme: level 1.



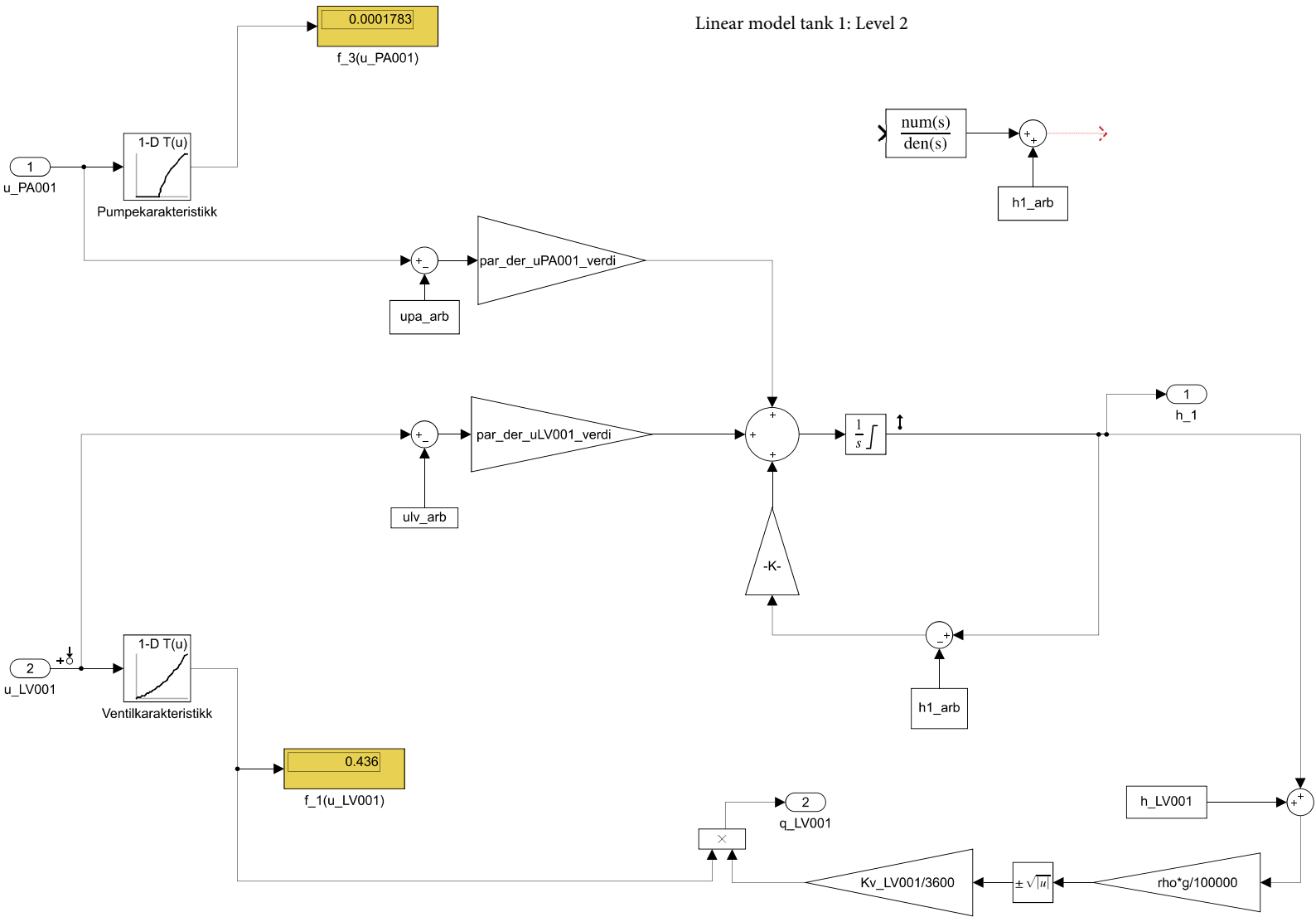
Nonlinear dynamical model model tank1: level 2.



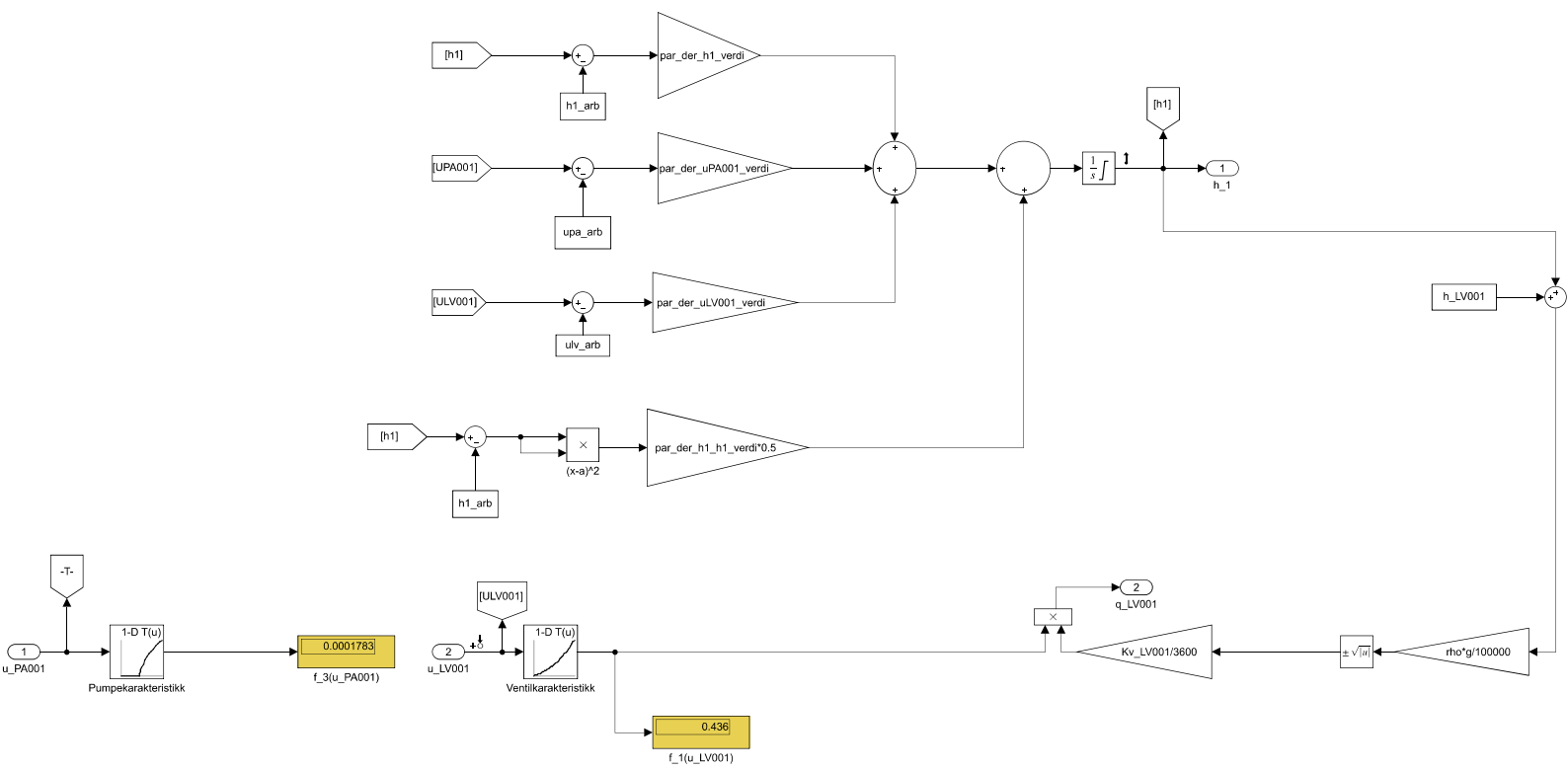
Nonlinear dynamical model tank 2: level2.



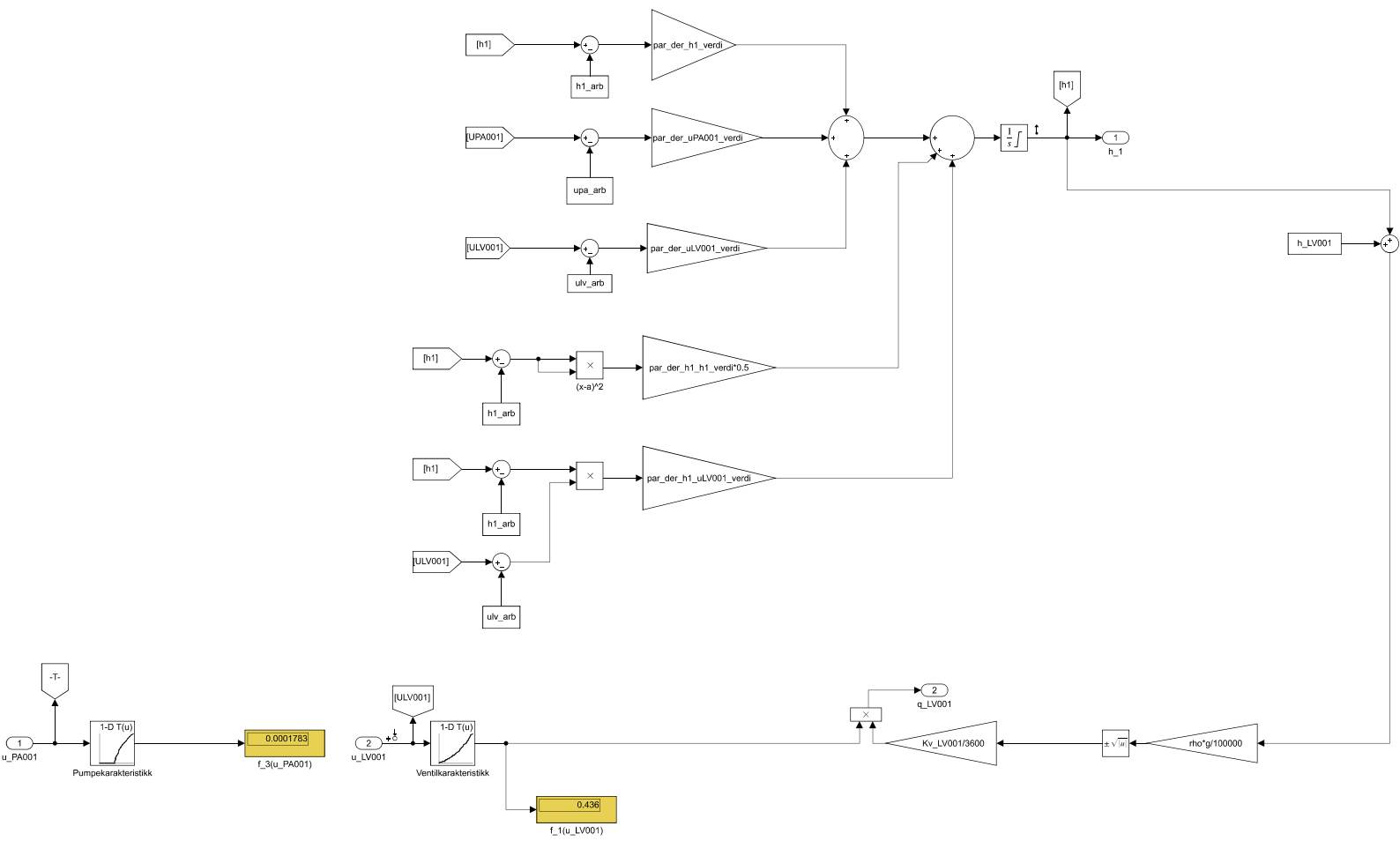
Linear model tank 1: Level 2



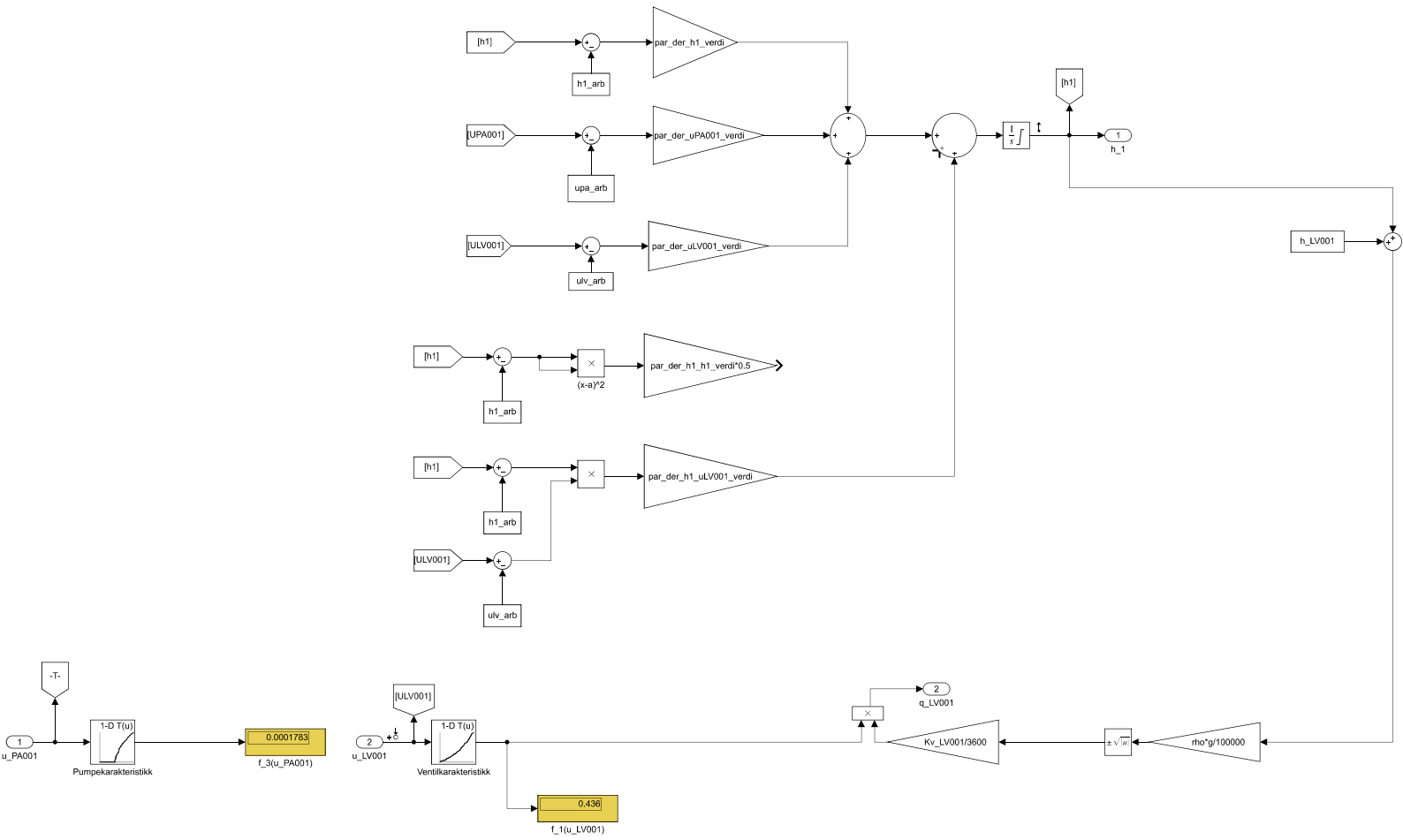
PQA: Level 2



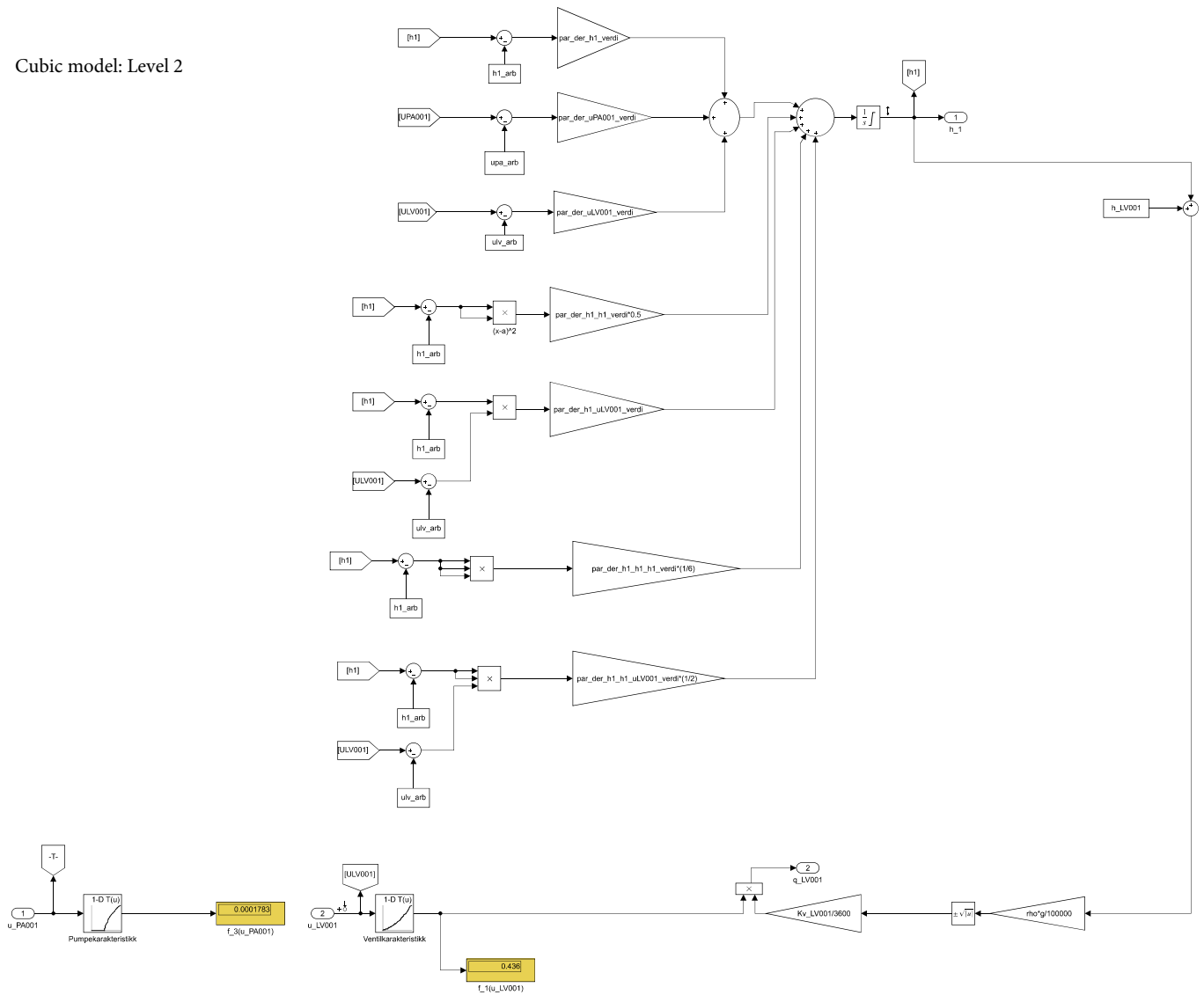
Quadratic model: Level 2



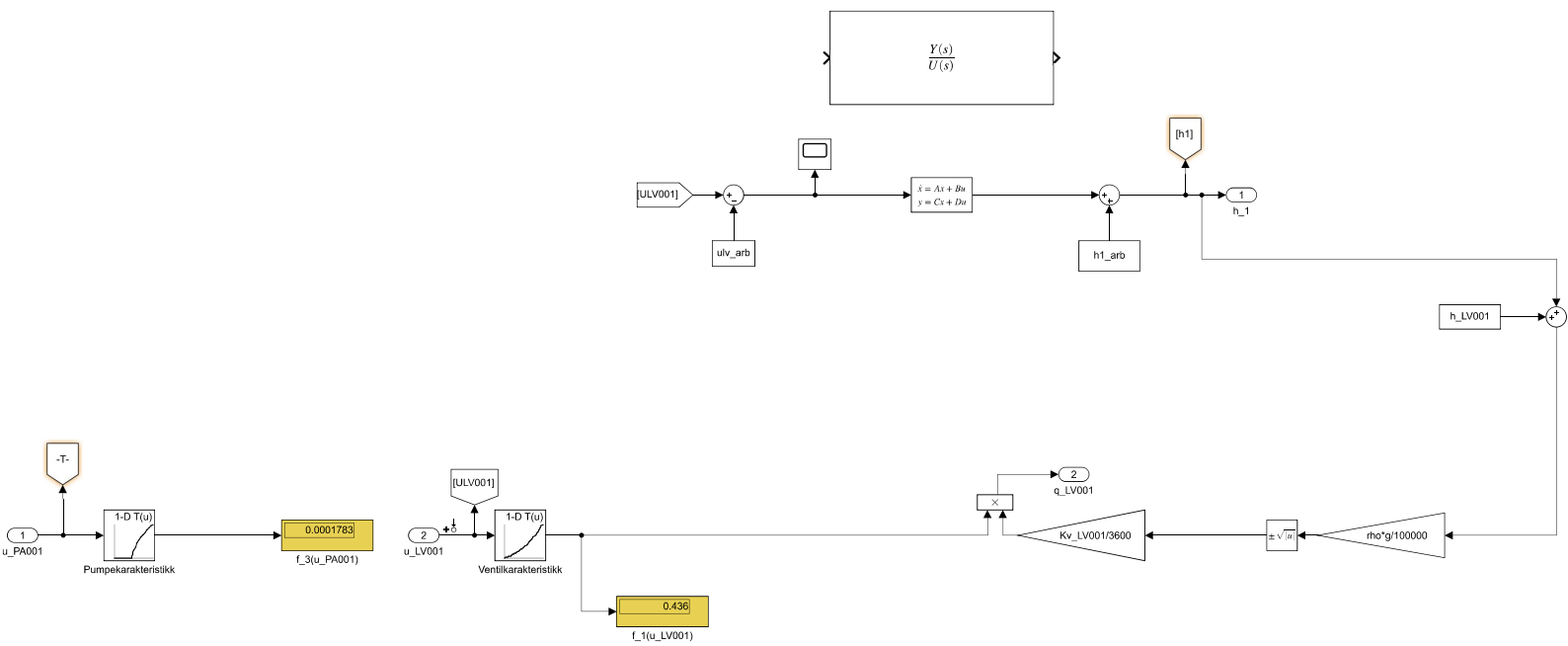
PQB: Level 2



Cubic model: Level 2



Linearized Carleman model: Level 2

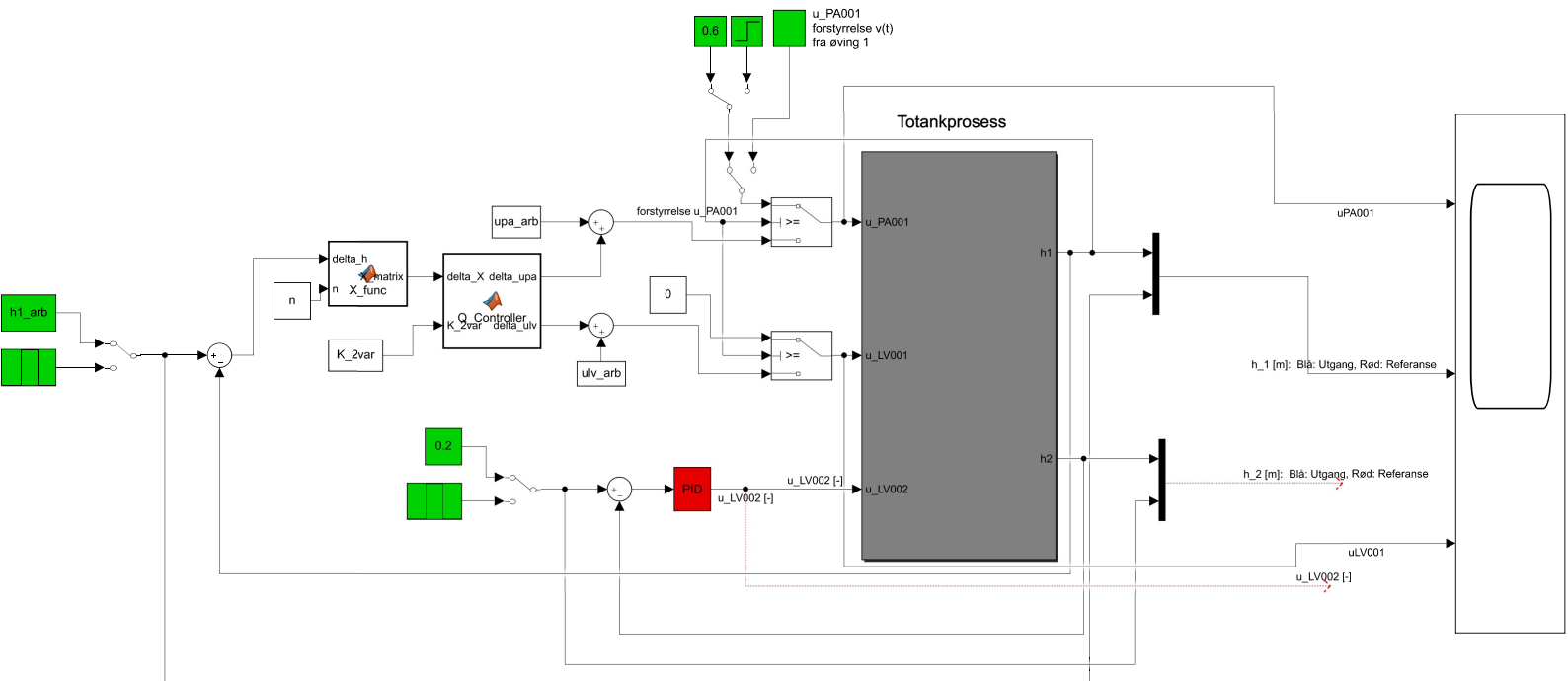



```
function dx = fcn(x,u, A,B,E)

SS = size(A);
n = SS(1);
resultat = zeros(n,1);
for i = 1:n
    resultat(i,:) = x'*E(:,i)*u;
end
dx = A*x+B*u + resultat;
end
```

Function calculating dx for the quadratic Carleman approximation using 1 variable.

Scheme of the implemented controller for the quadratic Carleman approximation.



```
function X_matrix = X_func(delta_h, n)
X_matrix = zeros(n,1);
for i = 1:n
    x = delta_h^i;
    X_matrix(i, 1) = x;
end
```

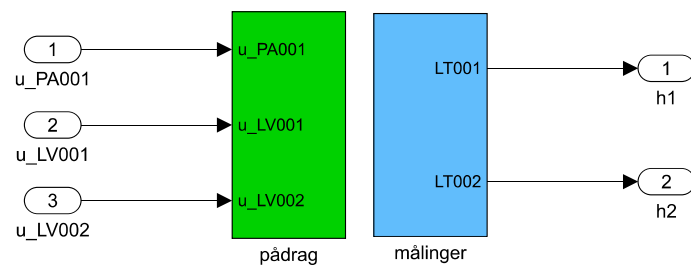
Function creating the $z(t)$ state vector.

```
function [delta_upa,delta_ulv]= Q_Controller(delta_X,K_2var)
U = K_2var.*delta_X;
delta_ulv = U(1, 1:end);
delta_upa = U(2, 1:end);
```

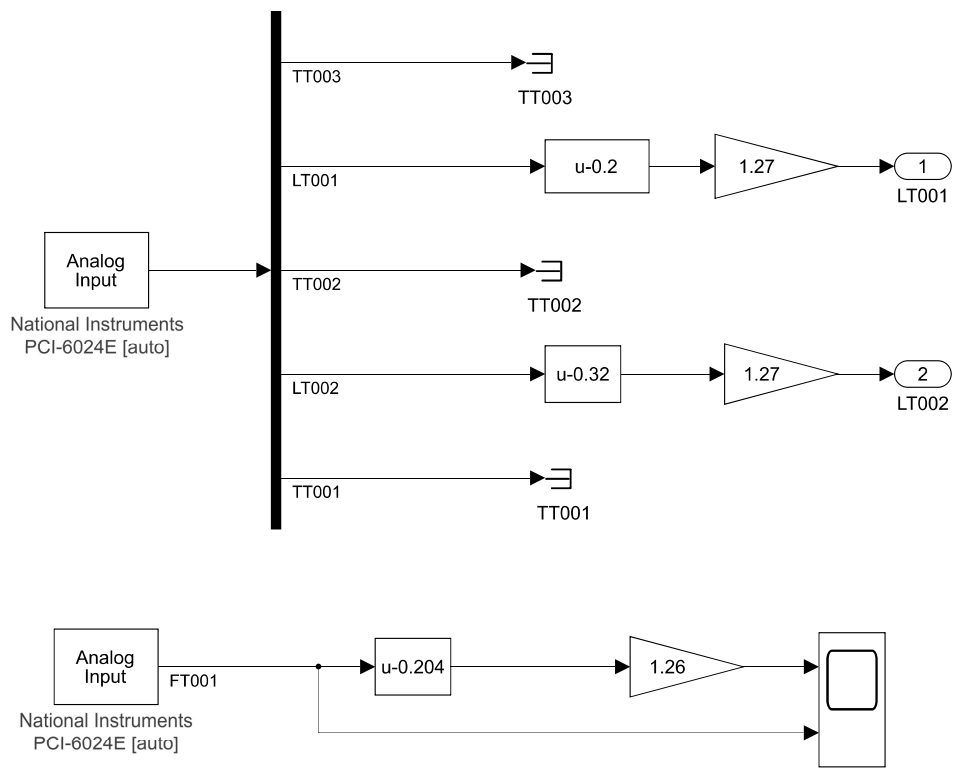
Function calculating the delta variables uLV001 and UPA001 using the controller gain.

The calculated uPA001, uLV001 and uLV002 signals are sent to the actuators.

The measurements from the two-tank system feeding into the controller.



Analog inputs.



Analog outputs.

